Exceptional Event Demonstration for Ozone Exceedances in Clark County, Nevada – August 18-21, 2020

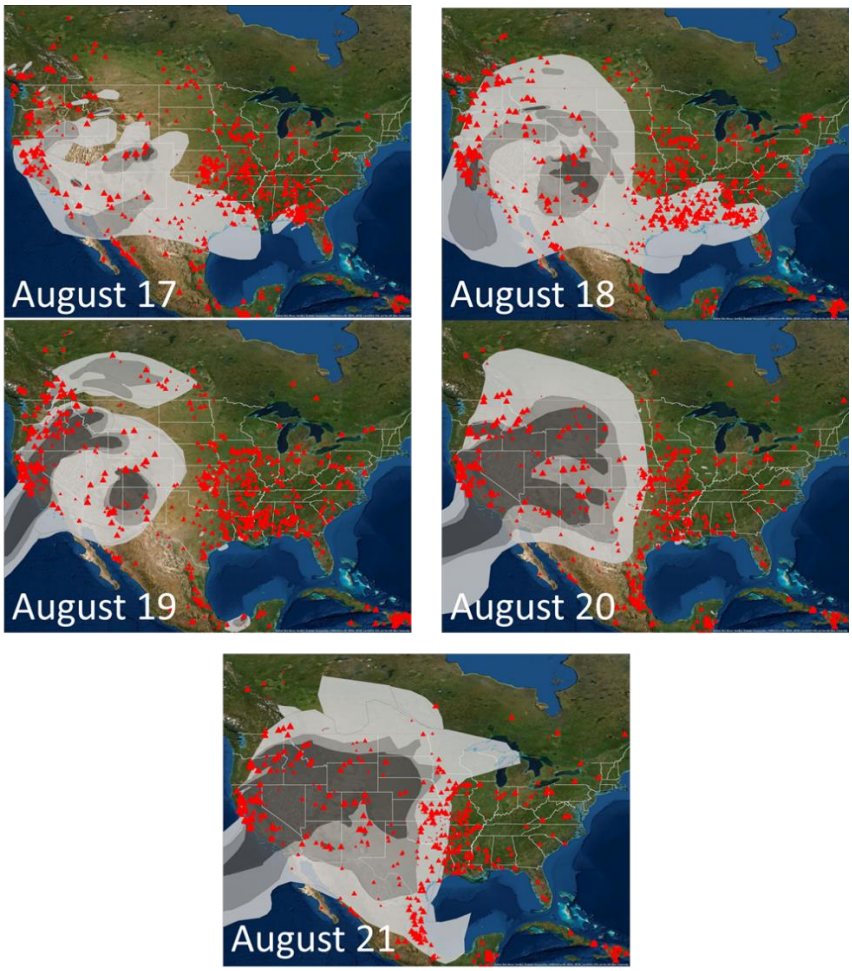

Final Report Prepared for

U.S. EPA Region 9
San Francisco, CA

September 2021

STi | Sonoma Technology

This document contains blank pages to accommodate two-sided printing.

Exceptional Event Demonstration for Ozone Exceedances in Clark County, Nevada – August 18-21, 2020

Prepared by

Steve Brown, PhD
Crystal McClure, PhD
Cari Gostic
David Miller, PhD
Nathan Pavlovic
Charles Scarborough
Ningxin Wang, PhD

Sonoma Technology
1450 N. McDowell Blvd., Suite 200
Petaluma, CA 94954
Ph 707.665.9900 | F 707.665.9800
sonomatech.com

Prepared for

Clark County Department of Environment and Sustainability
Division of Air Quality
4701 W. Russell Road, Suite 200
Las Vegas, NV 89118
Ph 702.455.3206
www.clarkcountynv.gov

Final Report

STI-920053-7477

September 1, 2021

Cover graphic illustrates daily HMS smoke over the United States for one day prior to and during the August 18-21 event. See Section 3.1.2 for more information.

Contents

Figures

Tables

Executive Summary

From August 18, 2020, through August 21, 2020, Clark County experienced atypical episodes of elevated ambient ozone. During these episodes, the 2015 8-hr ozone National Ambient Air Quality Standards (NAAQS) thresholds were exceeded at the Joe Neal, Paul Meyer, Walter Johnson, and Green Valley monitoring sites on at least one day from August 18-21, 2020. The exceedance at all four sites could lead to an ozone nonattainment designation for the Clark County area. Air trajectory analysis and air quality modeling results show that emissions from wildfires burning throughout California contributed to the transport to and formation of ozone in Clark County. The U.S. Environmental Protection Agency (EPA) Exceptional Event Rule (U.S. Environmental Protection Agency, 2016) allows air agencies to omit air quality data from the design value calculation if it can be demonstrated that the measurement in question was caused by an exceptional event. This report describes analyses that help to establish a clear causal relationship between wildfire smoke and the August 18-21, 2020, ozone exceedances at all monitoring sites.

The analyses we conducted provide evidence supportive of wildfire smoke and impacts on ozone concentrations in Clark County. We show that (1) smoke was transported from wildfires throughout California to the surface in the Clark County area in the hours and days leading up to and on the exceedance dates; (2) wildfire smoke impacted the typical diurnal profiles of ground-level pollution measurements, including $PM_{2.5}$, in the Clark County area on August 18-21; (3) byproducts and tracers of wildfire combustion were present and elevated at the surface in the Clark County area during and after the August 18-21 period; and (4) meteorological regression modeling and similar meteorological day analysis show that ozone observations on August 18-21 were unusual in the historical record given the meteorological conditions. Sources of evidence used in these analyses include (1) air quality monitor data to show that supporting pollutant trends at the surface were influenced by wildfire smoke; (2) air trajectory analysis to show transport of smoke-laden air to the Clark County area; (3) media coverage of wildfires and smoke impacts; and (4) meteorological regression modeling and meteorologically similar day analysis.

EPA guidance for exceptional event demonstrations (U.S. Environmental Protection Agency, 2016) provides a three-tiered approach; depending on the complexity of the event, increasingly involved information may be required to demonstrate a causal relationship between wildfire smoke and an exceedance. Here, we provide the results of analyses conducted to address Tier 1, Tier 2, and Tier 3 exceptional event demonstration requirements.

These analyses show that smoke was transported from a wildfire in southern California to the Clark County area over the hours leading up to August 18-21. Combined with additional evidence, such as meteorological regression modeling and meteorologically similar day analysis, our results provide key evidence to support smoke impacts on ozone concentrations during this potential exceptional event.

1. Overview

1.1 Introduction

The 2020 wildfire season in California was unprecedented, with five of the six largest wildfires in California history occurring in either August or September 2020 (https://www.fire.ca.gov/media/4jandlhh/top20_acres.pdf). Smoke emissions from California wildfires can affect downwind areas such as Clark County, Nevada. This was the case during August 18-21, 2020, as smoke emissions from multiple rapidly growing, lightning-initiated wildfires in California reached Clark County. During this period, 4 of the 14 ozone (O_3) monitoring locations around Clark County recorded an exceedance of the 2015 National Ambient Air Quality Standard (NAAQS) for 8-hour ozone (0.070 ppm).

Emissions from wildfires can affect concentrations of ozone downwind by direct transport of both ozone and precursor gases (i.e., nitrogen oxides [NO_x] and volatile organic compounds [VOCs]). Each mechanism can cause an enhancement in the overall ozone concentration and/or the amount of ozone that could be produced. For example, in an area where NO_x concentrations are high, such as an urban area like Las Vegas, Nevada, the transport of VOCs from wildfire emissions can enhance the amount of ozone that can be produced, potentially driving concentrations above the ozone standard. According to U.S. Environmental Protection Agency's (EPA) exceptional event (EE) guidance (U.S. Environmental Protection Agency, 2016), EEs such as wildfires that affect ozone concentrations can be subject to exclusion from calculations of NAAQS attainment if a clear causal relationship can be established between a specific event and the monitoring exceedance.

This report describes the clear causal relationship between multiple large complex, lightning-initiated wildfires in California (i.e., Red Salmon Complex, August Complex, LNU Lightning Complex, SCU Lightning Complex, CZU Lightning Complex, Lake Fire, Cold Springs Fire, River & Carmel fires, North Complex, Dolan Fire, North Range Fire, Dome Fire, and Loyalton Fire) and the exceedance of the maximum daily 8-hour ozone average (MDA8) at the four monitoring sites in Clark County during August 18-21, 2020. The evidence in this report includes all three tiers of analysis required by EPA's exceptional event guidance: for Tier 1, ground and satellite-based measurement of smoke emissions, transport of smoke from the wildfires in California to Clark County, and media coverage of the smoke event in Clark County; for Tier 2, emission vs. distance analysis, ground and satellite analysis of smoke-related pollutants, and comparison of event and non-event concentrations; and for Tier 3, vertical column analyses and statistical Generalized Additive Modeling (GAM) of the event. The wildfires that affected ozone concentrations in Clark County could not be reasonably controlled or prevented because they were caused by lightning and are unlikely to recur. Table 1-1 lists the sites affected during the August 18-21 event, as well as their locations and MDA8 ozone concentrations.

Table 1-1. August 18-21, 2020, EE information. All monitoring sites in Clark County that exceeded the 2015 NAAQS standard during August 18-21, 2020, are listed along with EPA Air Quality System (AQS) Site Codes, location information, and MDA8 ozone concentrations.

Date	AQS Site Code	Site Name	Latitude (degrees N)	Longitude (degrees W)	MDA8 O_3 Concentration (ppb)
8/18/2020	320030075	Joe Neal	36.271	-115.238	78
	320030043	Paul Meyer	36.106	-115.253	79
	320030071	Walter Johnson	36.170	-115.263	82
8/19/2020	320030043	Paul Meyer	36.106	-115.253	74
	320030071	Walter Johnson	36.170	-115.263	74
	320030075	Joe Neal	36.271	-115.238	73
	320030298	Green Valley	36.049	-115.053	71
8/20/2020	320030075	Joe Neal	36.271	-115.238	71
8/21/2020	320030043	Paul Meyer	36.106	-115.253	71

Concurrent with this document, Clark County is submitting documentation for other ozone EEs in 2018 and 2020 that were caused by wildfires and stratospheric intrusions. These events are mentioned throughout this report and are referred to as "proposed 2018 and 2020 exceptional events," recognizing that discussion with EPA is still pending. All proposed EEs for Clark County in 2018 and 2020 are listed in Tables 1-2 and 1-3. Wherever possible, we calculated statistics to provide context that both includes and excludes the proposed EEs from 2018 and 2020.

Table 1-2. Proposed Clark County 2018 EEs. For each site and date combination where the 2015 NAAQS standard was exceeded, the MDA8 ozone concentration is shown in parts per billion (ppb). Blank cells indicate that there was no exceedance on that site/date combination.

Date	Paul Meyer	Walter Johnson	Green Valley	Jerome Mack	Joe Neal	Palo Verde	Jean	Indian Springs	Apex	Boulder City
6/19/2018	72	72	77	75						
6/20/2018	71	74			72					
6/23/2018	72	76	75	72	72	71	77	73		
6/27/2018	75	76	78	76	72	72	81	78	74	72
7/14/2018	72		78	78						
7/15/2018		71	73	73	78					
7/16/2018	75	79	71	73	80	75				
7/17/2018	74	77				74				
7/25/2018	71	72	72							
7/26/2018	72	75	77	77					71	
7/27/2018	72	74			76					
7/30/2018			73	72						
7/31/2018		73			73					
8/6/2018	79	77	74	71	76	72			74	
8/7/2018	73	74	72	71	74				71	

Table 1-3. Proposed Clark County 2020 EEs. For each site and date combination where the 2015 NAAQS standard was exceeded, the MDA8 ozone concentration is shown in ppb. Blank cells indicate that there was no exceedance on that site/date combination.

Date	Walter Johnson	Paul Meyer	Joe Neal	Jerome Mack	Green Valley	Boulder City	Jean	Indian Springs	Apex
5/6/2020	78	77	76	73	72		75		76
5/9/2020	71	74							
5/28/2020	71	76							
6/22/2020	73	74	78						
6/26/2020		73							
8/3/2020	82	78	81		72	72	73	71	
8/7/2020	71		72					72	
8/18/2020	82	79	78						
8/19/2020	74	74	73		71				
8/20/2020			71						
8/21/2020		71							
9/2/2020	75	73							
9/26/2020	71		75						

1.2 Exceptional Event Rule Summary

The "EPA Guidance on the Preparation of Exceptional Events Demonstration for Wildfire Events that May Influence Ozone Concentrations" (U.S. Environmental Protection Agency, 2016) describes a three-tier analysis approach to determine a "clear causal relationship" for EEs demonstrations from an air agency. A summary of analysis requirements for each tier is listed in Table 1-4, and in the list below.

- Tier 1 analyses can be used when ozone exceedances are clearly influenced by a wildfire in areas of typically low ozone concentrations, are associated with ozone concentrations higher than non-event-related values, or occur outside of an area's usual ozone season.
- Tier 2 analyses are appropriate for wildfire emission cases where the impacts of the wildfire on ozone levels are less clear and require more supportive documentation than Tier 1 analyses.
- If a more complicated relationship between the wildfire and the ozone exceedance is observed, Tier 3 analyses with additional supportive documentation—such as statistical modeling of the ozone event, vertical profile analysis of smoke in the column, and meteorological analysis—should be used.

In this work, we conduct all the recommended Tier 1, Tier 2, and Tier 3 analyses.

Table 1-4. Tier 1, 2, and 3 EE analysis requirements for evaluating wildfire impacts on ozone exceedances.

Tier	Requirements
1	• Comparison of fire-influenced exceedance with historical concentrations • Key factor: Evidence that fire and monitor meet one of the following criteria: – Seasonality differs from typical season, or – Ozone concentrations are 5-10 ppb higher than non-event-related concentrations • Evidence of transport of fire emissions to monitor: – Trajectories of fire emissions (reaching ground level) – Satellite images and supporting evidence from surface measurements – Media coverage and photographic evidence of smoke
2	• All Tier 1 requirements • Key Factor #1: Fire emissions and distance of fires • Key Factor #2: Comparison of the event-related ozone concentration, with non-event-related high ozone concentrations (high percentile rank over five years/seasons) – Annual and seasonal comparison • Evidence that fire emissions affected the monitor (at least one of the following): – Visibility impacts – Changes in supporting measurements – Satellite enhancements of fire-related species (i.e., NO_x, carbon dioxide (CO), aerosol optical depth [AOD], etc.) – Fire-related enhancement ratios and/or tracer species – Differences in spatial/temporal patterns
3	• All Tier 2 requirements • Evidence of fire emissions effects on monitor: – Multiple analyses from those listed for Tier 2 • Evidence of fire emissions transport to the monitor: – Trajectory or satellite plume analysis, and – Additional discussion of meteorological conditions • Additional evidence such as: – Comparison to ozone concentrations on matching (meteorologically similar) days – Statistical regression modeling – Photochemical modeling of smoke contributions to ozone concentrations

1.3 Demonstration Outline

As discussed in Section 1.2, the "clear causal relationship" analyses involve first comparing the exceedance ozone concentrations to historical values, providing evidence that the event and monitors meet the tier's key factors, providing evidence of the transport of wildfire emissions to the

monitors, and additional analyses such as ground-level measurements and various forms of modeling depending on the complexity of the event. Table 1-5 summarizes the key factors and additional supporting evidence of the tiered approach and shows the corresponding sections in this report for each analysis.

Table 1-5. Locations of Tier 1, 2, and 3 elements in this report.

Tier	Element	Section of This Report (Analysis Type)
Tier 1	Key Factor: seasonality differs from typical season and/or ozone concentrations are 5-10 ppb higher than non-event-related concentrations	Section 3.1.1 (comparison of event with historical data)
	Evidence of transport of fire emissions to monitor	Sections 3.1.2 (maps of ozone, particulate matter with a diameter less than 2.5 micrometers ($PM_{2.5}$), fire, smoke, visible satellite imagery), and 3.1.3 (Hybrid Single-Particle Lagrangian Integrated Trajectory [HYSPLIT] trajectories)
	Media coverage and photographic evidence of smoke	Section 3.1.4 (Media coverage and Images)
Tier 2	Key Factor #1: fire emissions and distance of fires	Section 3.2.1 (analysis of the relationship between fire emissions and distance [Q/d])
	Key Factor #2: comparison of event concentrations with non-event-related high ozone concentrations	Section 3.2.2 (comparison of event concentrations with non-event concentrations)
	Evidence that the fire emissions affected the monitor	Sections 3.2.3 (Satellite Retrievals of Pollutant Concentrations) and 3.2.4 (changes in supporting measurements, differences in spatial/temporal patterns, and tracer measurements)
Tier 3	Evidence of fire emissions transport to the monitor	Section 3.3.1 (trajectory or satellite plume analysis, additional discussion of meteorological conditions, comparison to ozone concentrations on matching [meteorologically similar] days)
	Meteorologically similar matching day analysis	Section 3.3.2 (methodology and analysis for meteorologically similar days)
	Additional evidence	Section 3.3.3 (statistical regression modeling)

Tier 1 analyses are shown in Section 3.1. The key factor of Tier 1 analyses is the ozone concentration's uniqueness when compared to the typical seasonality and/or levels of ozone exceedance. The EPA guidance suggests providing a time series plot of 12 months of ozone

concentrations overlaying more than five years of monitored data and describing how typical seasonality differs from ozone in the demonstration (U.S. Environmental Protection Agency, 2016). In addition, trajectory analysis—produced by the Hybrid Single-Particle Lagrangian Integrated Trajectory (HYSPLIT) model, together with satellite plume imagery and ground-level measurements of plume components (e.g., $PM_{2.5}$, CO, or organic and elemental carbon)—should be used to provide evidence of wildfire emissions being transported to the monitoring sites. We demonstrate the Tier 1 analysis results for the August 18-21, 2020, event in Section 3.1. We address the key factors in Section 3.1.1, provide evidence of wildfire smoke transport to the Clark County monitoring sites in Sections 3.1.2 and 3.1.3, and discuss the media coverage and show ground images in Section 3.1.4.

Tier 2 analyses are shown in Section 3.2. The two key factors for Tier 2 analyses are (1) fire emissions and distance of fires to the impacted monitoring sites, and (2) comparison of event-related ozone concentrations with non-event-related high ozone values. We address the first factor in Section 3.2.1 by determining the emissions divided by distance (Q/d) relationship and address the second factor in Section 3.2.2 by comparing the six-year percentiles and yearly rank-order analysis of ozone concentrations. The Tier 2 analyses also require evidence of wildfire smoke transport to affected monitoring sites; we provide this evidence in Section 3.2.3 through satellite measurements of pollutant concentrations. In Section 3.2.4, we discuss supporting pollutant trends and diurnal patterns of $PM_{2.5}$, CO, NO_x, and total non-methane organic compounds (TNMOC) compared with ozone concentrations and wildfire tracer measurements.

Tier 3 analyses are shown in Section 3.3. We investigated total column information and event-related meteorological conditions (Section 3.3.1), analyzed meteorologically similar days to find typical ozone concentrations for the exceptional event's specific meteorological conditions (Section 3.3.2), and developed a Generalized Additive Statistical Model (GAM) to estimate the wildfire's contribution to ozone concentrations (Section 3.3.3).

Following the EPA's EE guidance, we performed Tier 1, Tier 2, and Tier 3 analyses to show the "clear causal relationship" between the wildfires in California and the exceedance event in Clark County during August 18-21, 2020. Focusing on the characterization of the meteorology, smoke, transport, and air quality on the days leading up to the event, we conducted the following specific analyses (results of these analyses are presented in Section 3):

- Developed time series plots that show the August 18-21 ozone concentrations at each affected monitoring site in historical context for 2020 and the past six years
- Compiled maps of (1) ozone and $PM_{2.5}$ concentrations in the area, (2) smoke plumes, and (3) fire locations from satellite data
- Showed the transport patterns via HYSPLIT modeling, and identified where the back trajectory air mass intersected with smoke plumes or passed over or near fires
- Discussed media coverage of the August 18-21 event and showed ground images
- Quantified total fire emissions and calculated emissions/distance ratio (Q/d) for the fire

- Performed statistical analysis to compare event ozone concentrations to non-event concentrations
- Provided maps showing satellite retrievals of NO_x, AOD, and CO
- Developed plots to show diurnal patterns of ozone and supporting pollutants such as $PM_{2.5}$, CO, NO_x, and TNMOC
- Examined wildfire tracer species and their background concentrations vs. event concentrations
- Assessed vertical transport of smoke using satellite-observed aerosol vertical profiles and ceilometer mixing height retrievals
- Performed meteorologically similar matching ozone day analysis to assess typical concentrations of ozone given meteorological parameters
- Created a GAM model of MDA8 ozone concentrations to assess the enhancement of ozone concentrations due to wildfire influence

1.4 Conceptual Model

The conceptual model for the exceptional event that led to the ozone exceedances at the Joe Neal, Paul Meyer, Walter Johnson, and Green Valley monitoring sites on at least one day from August 18-21, 2020, is outlined in Table 1-5, which provides the analysis techniques performed and evidence for each Tier. This establishes a weight of evidence for the clear causal relationship between the wildfire emissions in California and the August 18-21 exceptional ozone events. We assert that wildfire emissions from 13 fires burning in California from August 17-21 led to enhanced ozone concentrations in Clark County and the MDA8 ozone exceedances at the Joe Neal, Paul Meyer, Walter Johnson, and Green Valley monitoring sites on at least one day from August 18-21, 2020. In support of this assertion, the key points of evidence for the conceptual model are summarized below.

1) The August 18-21 ozone exceedances occurred during a typical ozone season, but event concentrations at the Joe Neal, Paul Meyer, Walter Johnson, and Green Valley exceedance sites were significantly higher than non-event concentrations. Ozone concentrations at all sites on the corresponding day of their exceedances showed a high percentile rank when compared with the past six years and ozone seasons.
2) HMS smoke and fire detections, CALIPSO aerosol profiles, visible satellite imagery, aerosol optical depth, and CO observations show a consistent picture of wildfire emission plumes at 1-4 km altitude from southern and northern California fires, including the Red Salmon Complex, August Complex, LNU Lightning Complex, SCU Lightning Complex, CZU Lightning Complex, Lake Fire, River and Carmel Fire, North Range Fire, and Dome Fire. These plumes extended south and eastward and impacted Clark County on August 18-21.

3) Back and forward trajectories from the near-surface boundary layer at the exceedance sites at the time of maximum ozone concentration show consistent transport patterns passing over the HMS smoke plumes originating from regional fires (Dome, Lake, and North Range fires in southern California, and the LNU Lightning Complex Fire in northern California). Dispersion modeling from all 13 fires in California also show amassed smoke from all fires being transported to the boundary layer in Clark County. The combination of trajectories intersecting the fire locations and the associated smoke plumes and a deep mixed layer over Clark County favoring vertical mixing demonstrate that wildfire emissions were transported to the surface in Clark County during the August 18-21 exceptional event period.

4) Meteorological conditions on August 18-21 did not favor enhanced local ozone production when compared with day-specific meteorologically similar ozone season days. Average MDA8 ozone across similar days was well below the ozone NAAQS and at least 10 ppb lower than the August 18-21 ozone exceedances.

5) GAM model predictions of MDA8 ozone for August 18 through 21 are all well below the 70-ppb ozone NAAQS for each EE-affected site.

6) Abnormal surface $PM_{2.5}$, concentration enhancements midday on August 17, 18, 19, and 21 with typical PM_{10}:$PM_{2.5}$ ratios (not a dust event), and enhancements of the wildfire tracer levoglucosan above background ozone season levels at two sites on August 19 and 22 indicate the presence of wildfire smoke and associated ozone precursors at the surface in Clark County coincident with multiple days of wildfire plumes that arrived during the August 17-21, 2020, exceptional event.

2. Historical and Non-Event Model

2.1 Regional Description

Clark County is located in the southern portion of Nevada and borders California and Arizona. It includes the City of Las Vegas, one of the fastest growing metropolitan areas in the United States with a population of approximately 2 million (U.S. Census Bureau, 2010). Surrounded by the Spring Mountains to the west (3,000 m elevation) and the Sheep Mountain Range to the north (2,500 m elevation), Las Vegas is located in a 1,600 km^2 desert valley basin at 500 to 900 m above sea level (Langford et al., 2015). . Three mountain ranges comprise the southern end of the valley. The valley floor slopes downward from west to east, which influences surface wind, temperature, precipitation, and runoff patterns. The Cajon Pass and I-15 corridor to the east are important atmospheric transport pathways from the Los Angeles Basin into the Las Vegas Valley (Langford et al., 2015). **Figures 2-1 and 2-2** show the topography of Clark County and the surrounding areas.

The Las Vegas Valley climatology features abundant sunshine and hot summertime temperatures (average summer month high temperatures of 34-40°C). The region experiences dry conditions year-round (~107 mm annual precipitation, 22% of which occurs during the summer monsoon season in July through September) due to mountain barriers to moisture inflow. The urban heat island effect during summer leads to large temperature gradients within the valley, with generally cooler temperatures on the eastern side. In the summer, monsoon moisture brings high humidity and thunderstorms to the region, typically in July and August (National Weather Service Forecast Office, 2020). Winds in the Las Vegas basin tend to come from the southwest during spring and summer (Los Angeles is upwind), while winds in the fall and winter tend to come from the northwest, while air is transported between neighboring mountain ranges and along the valley.

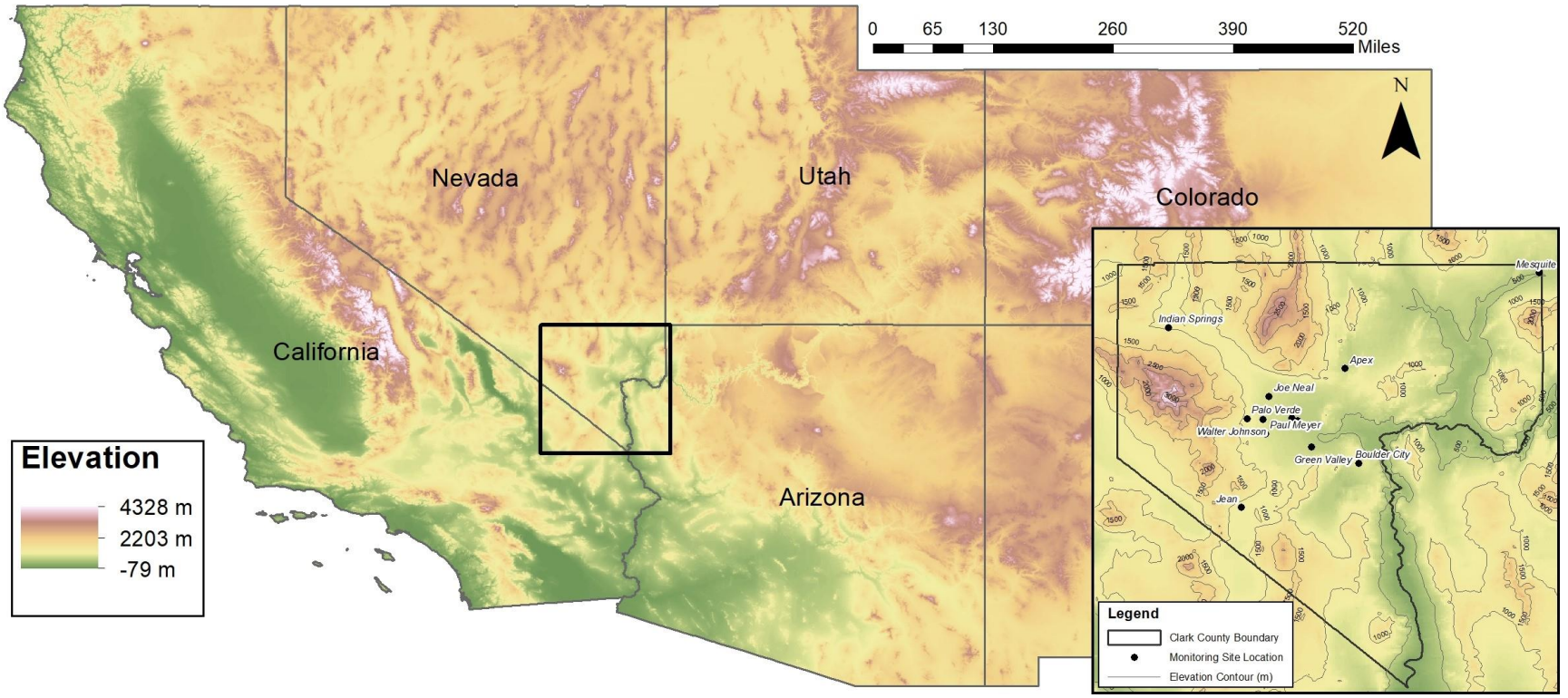

Figure 2-1. Regional topography around Clark County, with an inset showing county boundaries and the air quality monitoring sites analyzed in this report.

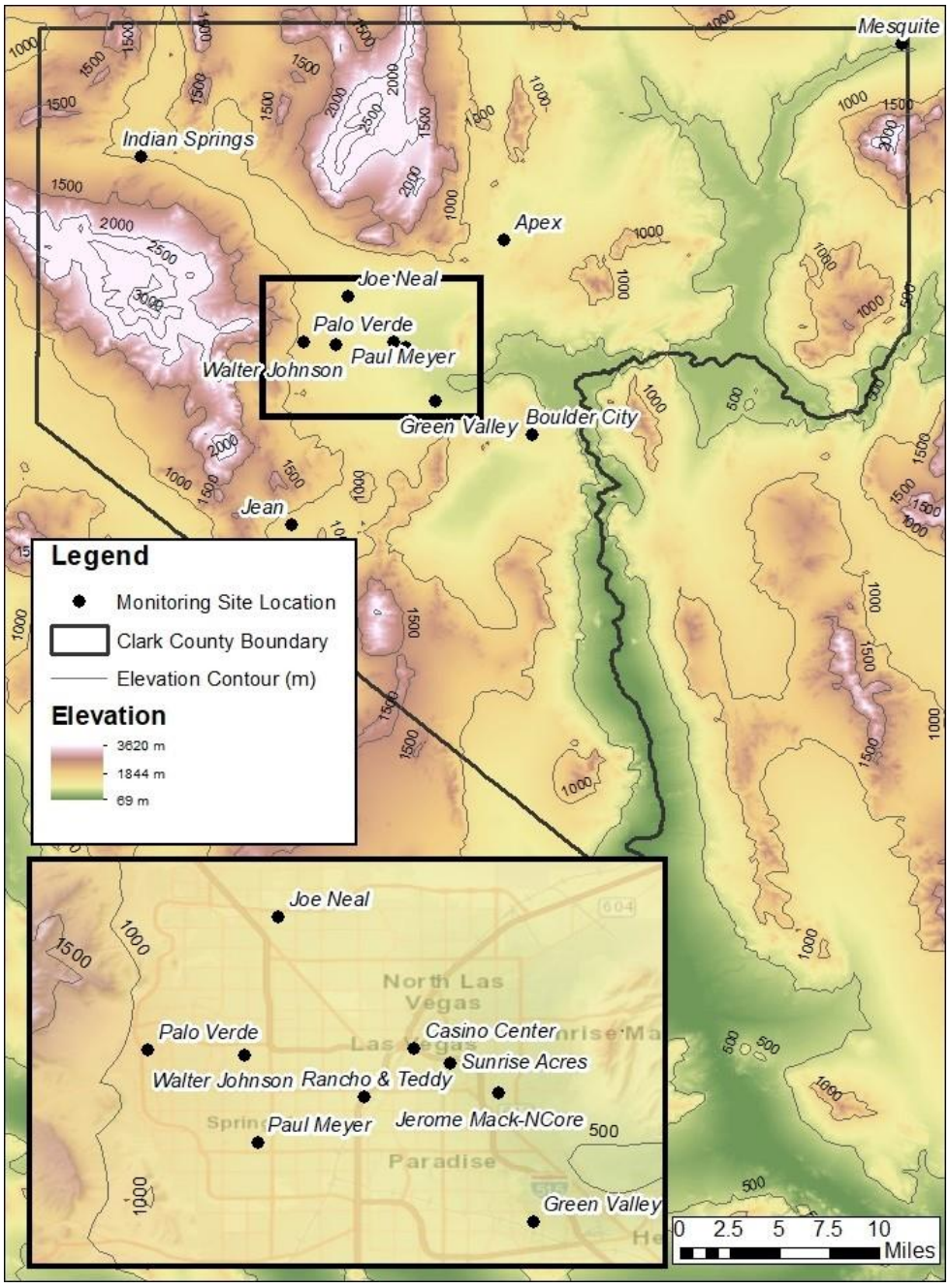

Figure 2-2. Clark County topography, with an inset showing air quality monitoring sites that measure ozone in the Clark County area.

2.2 Overview of Monitoring Network

The Clark County Department of Environment and Sustainability, Division of Air Quality (DAQ) operated 14 ambient air monitoring sites in the region during 2020 (Figure 2-2). These sites measure hourly ozone, $PM_{2.5}$, PM_{10}, NO_x, TNMOC, and CO concentrations as well as meteorological parameters. Table 2-1 presents the monitoring data coverage across time and space for criteria pollutants, surface meteorological parameters (barometric pressure, temperature, wind speed and direction), and mixing height. We examined ozone and other criteria pollutants at 11 sites around Clark County to investigate the high ozone event on August 18-21, 2020. DAQ's ambient air monitoring network meets the monitoring requirements for criteria pollutants (40 CFR Part 58, Appendix D). Data are quality-assured in accordance with 40 CFR 58 and submitted to the EPA's Air Quality System (AQS). The spatial distribution of monitoring sites characterizes Las Vegas's regional air quality as well as air quality upwind and downwind of the urban valley region (Figure 2-2). The Jean monitoring site along the I-15 corridor is generally upwind such that it captures atmospheric transport into the region and is least impacted by local sources (Figure 2-2).

Table 2-1. Clark County monitoring site data. The available date ranges of all parameters and monitoring sites used in this report for Clark County, Nevada, are shown. Casino Center and RT are near-road sites that are not used for the exceptional event analysis.

Site	AQS Sitecode	O_3	$PM_{2.5}$	CO	NO	NO_2	TNMOC	Temp.	Wind Speed	Wind Direction	Barom. Pressure	Mixing Height
Apex	320030022	2014-2020						2014-2020	2014-2020	2014-2020		
Boulder City	320030601	2014-2020									2014-2016	
Green Valley	320030298	2015-2020	2014-2020	2020				2016-2020	2014-2020	2014-2020	2014-2016	
Indian Springs	320037772	2014-2020										
Jean	320031019	2014-2020	2014-2020					2014-2020	2014-2020	2014-2020	2014-2016	
Jerome Mack	320030540	2014-2020	2014-2020	2015-2020[1,2]	2015-2020	2015-2020	2020	2014-2020	2014-2020	2014-2020	2014-2020	2020
Joe Neal	320030075	2020	2018-2020	2019-2020		2015-2020		2014-2020	2014-2020	2014-2020	2014-2016	
Mesquite	320030023	2014-2020						2014-2020	2014-2020	2014-2020		
Palo Verde	320030073	2014-2020	2020					2014-2020	2014-2020	2014-2020	2014-2016	
Paul Meyer	320030043	2014-2020	2017-2020					2014-2020	2014-2020	2014-2020	2014-2016	
Walter Johnson	320030071	2014-2020	2020					2015-2020	2015-2020	2015-2020	2014-2016	

[1] CO data invalid at Jerome Mack on Sep. 2, 2020

[2] CO data invalid at Jerome Mack Apr. 28, 2020 – May 20, 2020

2.3 Characteristics of Non-Event Historical O_3 Formation

During Clark County's ozone season (April–September), ozone concentrations are typically influenced by local formation, transport into the region, and, on occasion, by EEs such as wildfires and stratospheric intrusions. Transport from upwind source regions (e.g., Los Angeles Basin, Mojave Desert, Asia) occurs with southwesterly winds, and southerly transport dominates later in the season due to the summer monsoon (Langford et al., 2015; Zhang et al., 2020). Local precursor emissions in Clark County include mobile NO_x and VOCs sources, natural-gas fueled power generation NO_x sources, and biogenic VOC emissions. Based on 2017 Las Vegas emission inventories, on a typical ozone season weekday there are 98 tons of NO_x emissions per day and 238 tons of VOC emissions per day (Clark County Department of Environment and Sustainability, 2020). On-road mobile sources comprise 40% of NO_x emissions and total mobile emissions comprise 88% of total NO_x emissions during the ozone season. In contrast, 52% of VOC emissions originate from biogenic sources within Clark County. Local emissions and/or precursors transported into the region contribute to ozone formation within Clark County (Langford et al., 2015; Clark County Department of Air Quality, 2019).

In this demonstration, we discuss the impacts of wildfire smoke on ozone concentrations in Clark County on August 18-21, 2020. In order to fully discern the effect of wildfire smoke on ozone concentrations in Clark County on August 18-21, 2020, we examine the historical ozone record for all affected sites (Table 1-1). *Non-event days* refer to all days other than the August 18-21, 2020, event. Because percentile rankings are sensitive to including the relatively large number of potential EE days during 2018 and 2020, we also provide statistics *excluding potential EE days* (i.e., without including the 2018 and 2020 potential EE days as defined in Tables 1-2 and 1-3 in Section 1). The 8-hour ozone design value (DV) is the three-year running average of the fourth-highest daily maximum 8-hour (MDA8) ozone concentration (40 CFR Part 50, Appendix U). Within Clark County, Las Vegas is classified as an EPA Region 9 marginal nonattainment region with a 73 ppb ozone DV for 2017-2019 (U.S. Environmental Protection Agency, 2020). Ozone EE days are identified by having significant wildfire or stratospheric intrusion influence in addition to an MDA8 concentration greater than 70 ppb. By this criterion, we identified 15 possible EE days in 2018, 13 possible EE days in 2020, and no EE days in 2019.

The August 18-21, 2020, EE occurred late in the ozone season under hot, dry air, upper-level high pressure, and surface low-pressure meteorological conditions favoring subsidence and enhanced vertical mixing of wildfire smoke-influenced ozone and ozone precursors to the ground level (see Section 3.3.1). In comparison to a non-event conceptual model of local precursor emissions that contributed to ground-level ozone under similar conditions, the August 18-21 conditions indicate the transport of wildfire-influenced air parcels from regional smoke plumes over California, Nevada, and Colorado. These plumes were transported via upper-level winds that shifted from southeasterly to westerly/southwesterly during August 18-21.

Figures 2-3 through 2-10 depict the six-year historical record and seasonality of MDA8 ozone concentrations at each EE-affected monitoring site, along with the 99th percentile and NAAQS standard ozone concentrations. At least one day during the August 18-21 event ranks in the top 1% for daily maximum ozone concentration in the six-year historical record at three of the four EE-affected sites. August 18 and 19 rank in the top 1% for daily maximum ozone concentration in the six-year historical record at Walter Johnson and Paul Meyer monitoring sites. August 18 and 19 also rank in the top 5% for MDA8 ozone during the ozone season at all EE-affected sites. Figure 2-11 depicts a two-week ozone diurnal cycle of 1-hour ozone beginning one week before the first event day (August 18) and ending one week after the final event day (August 21). Daily maximum 1-hour ozone concentrations were the highest at all EE-affected sites on August 18 and 19 during this two-week period, and at least the second highest on August 20 and 21.

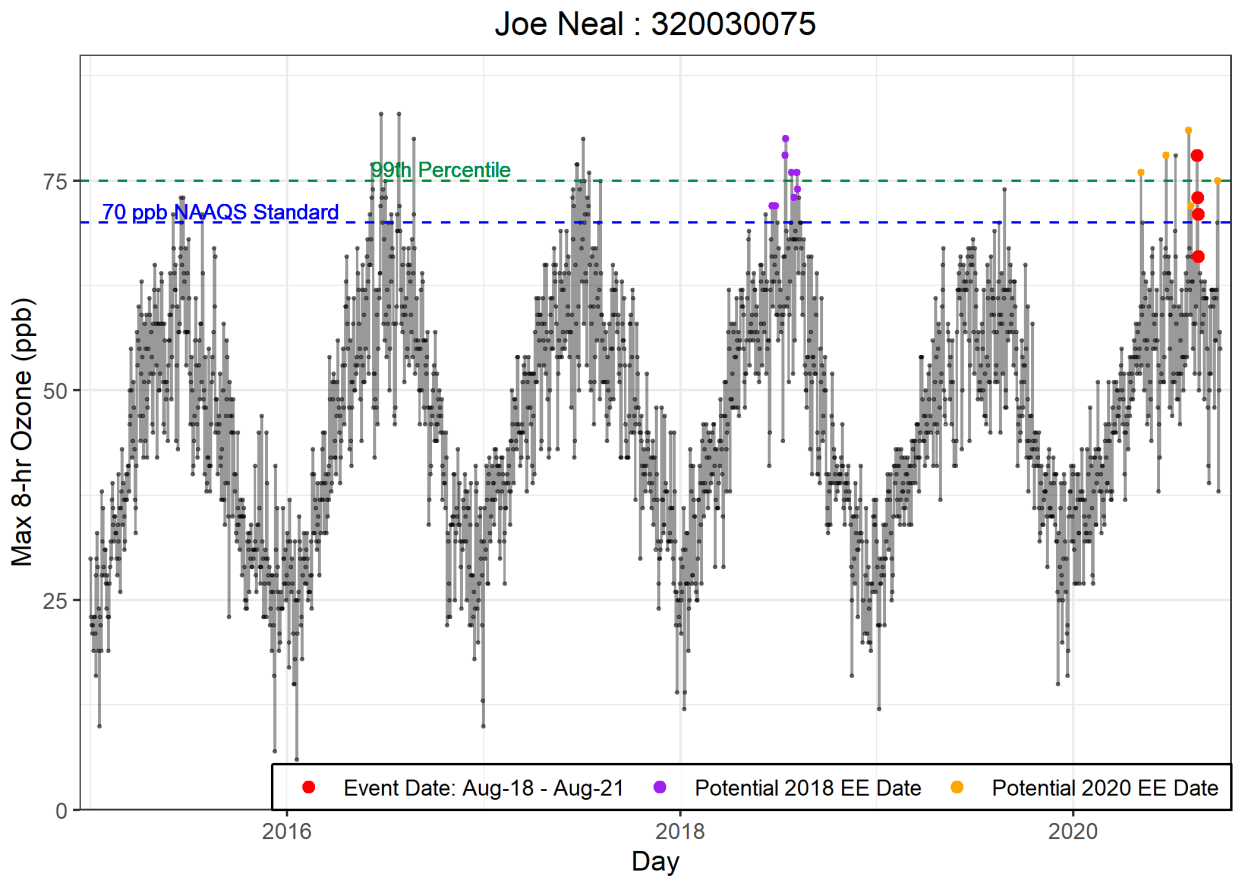

Figure 2-3. Time series of 2015-2020 ozone concentrations at Joe Neal.

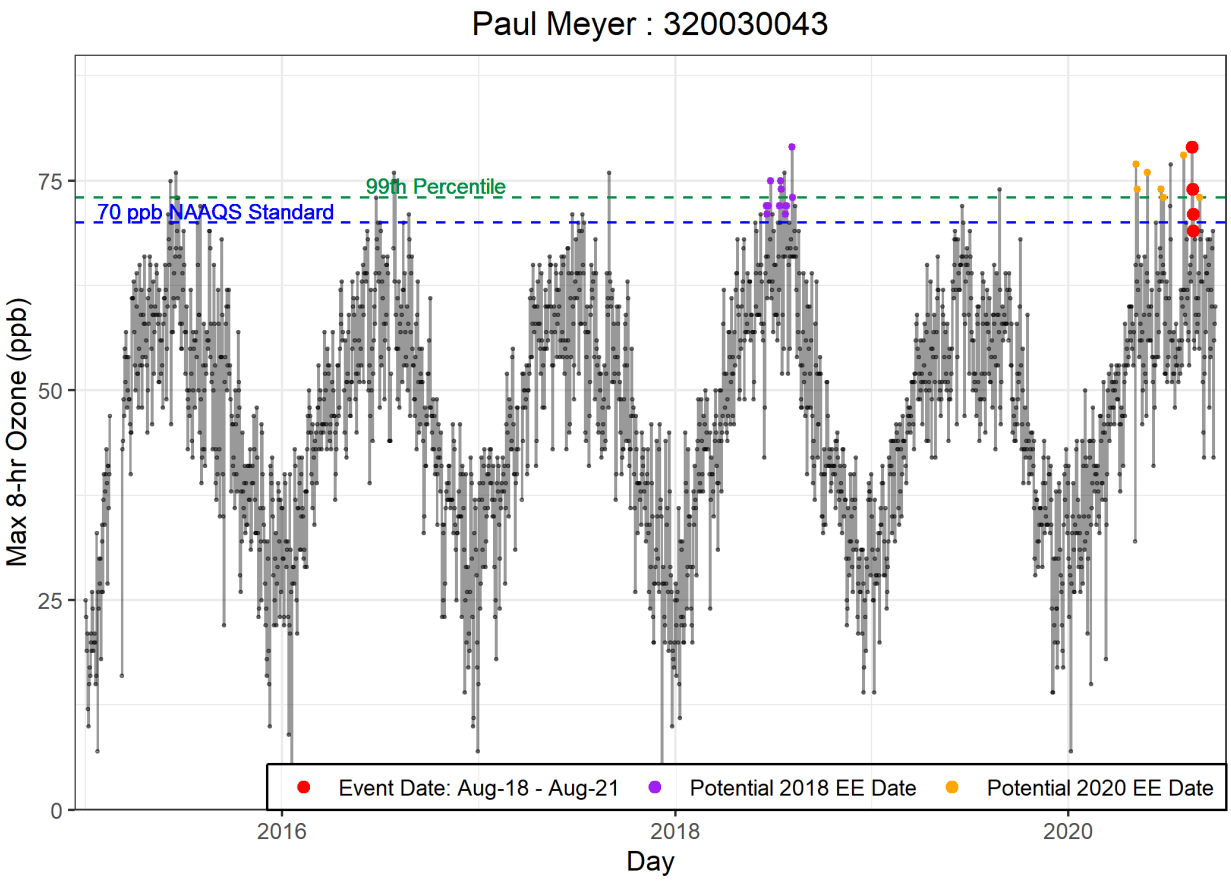

Figure 2-4. Time series of 2015-2020 ozone concentrations at Paul Meyer.

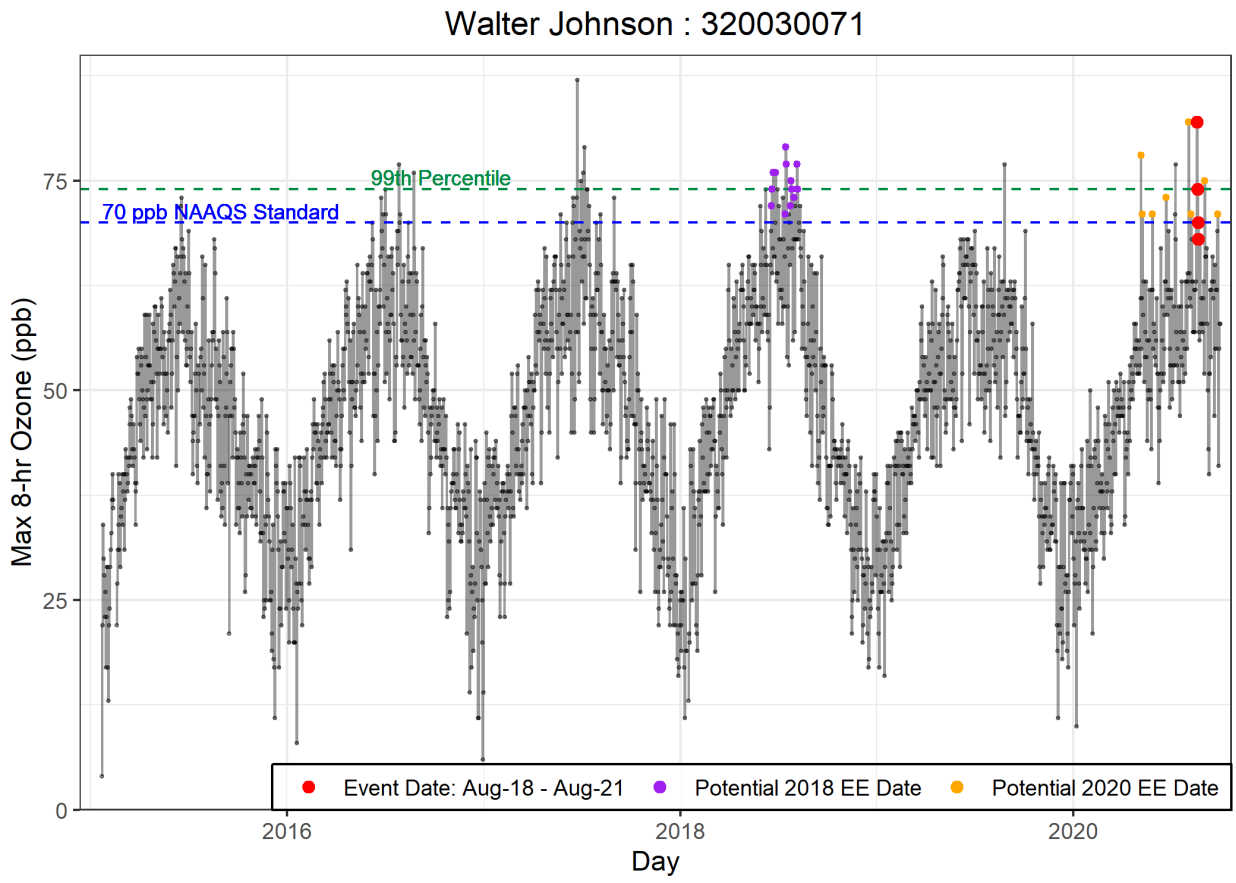

Figure 2-5. Time series of 2015-2020 ozone concentrations at Walter Johnson.

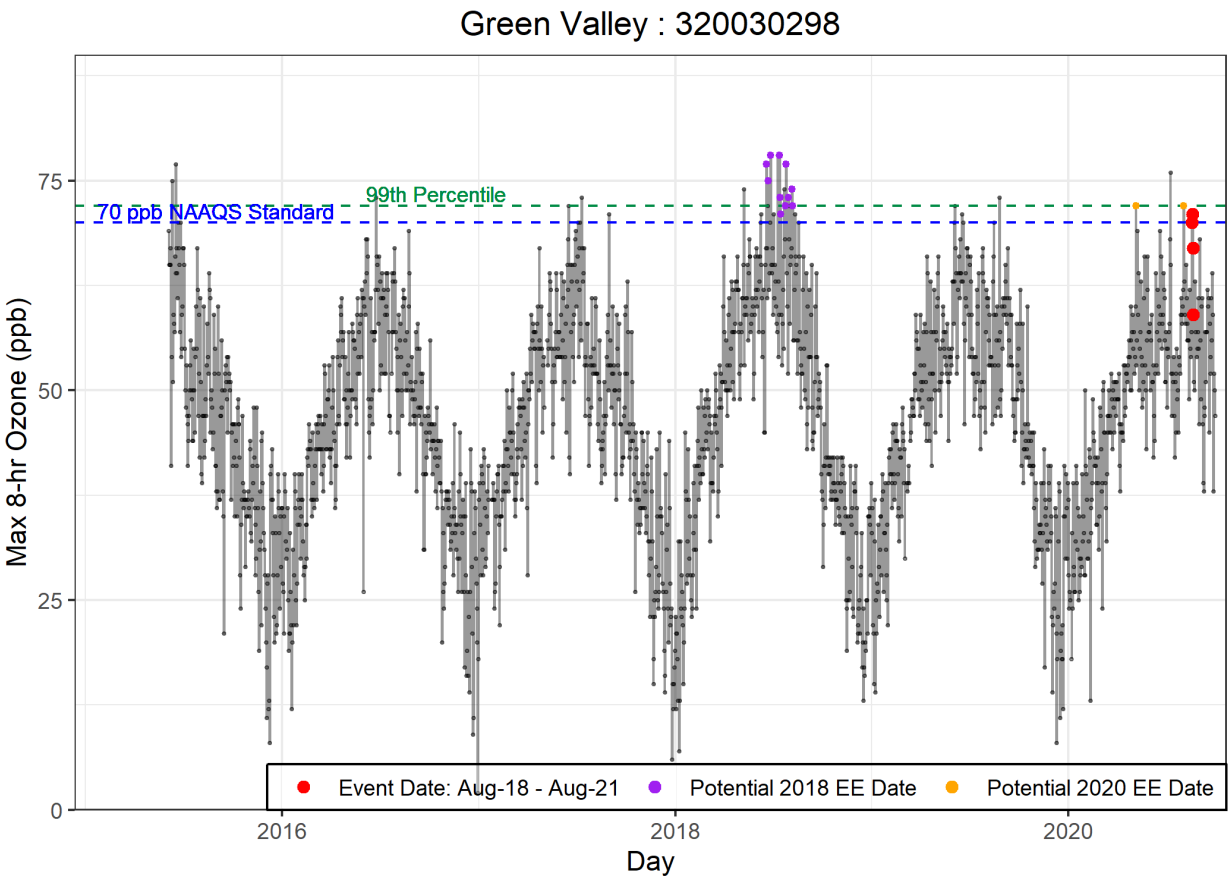

Figure 2-6. Time series of 2015-2020 ozone concentrations at Green Valley.

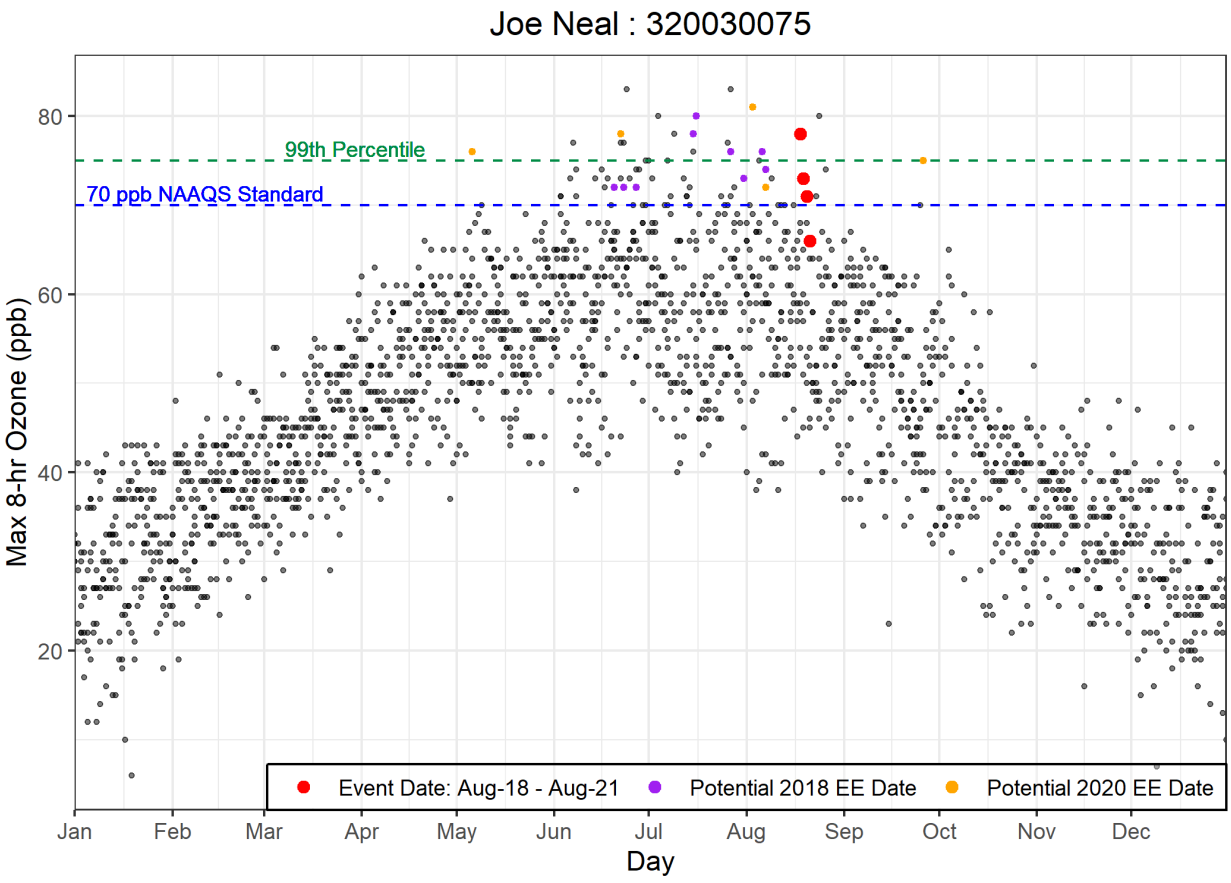

Figure 2-7. Seasonality of 2015-2020 ozone concentrations from Joe Neal.

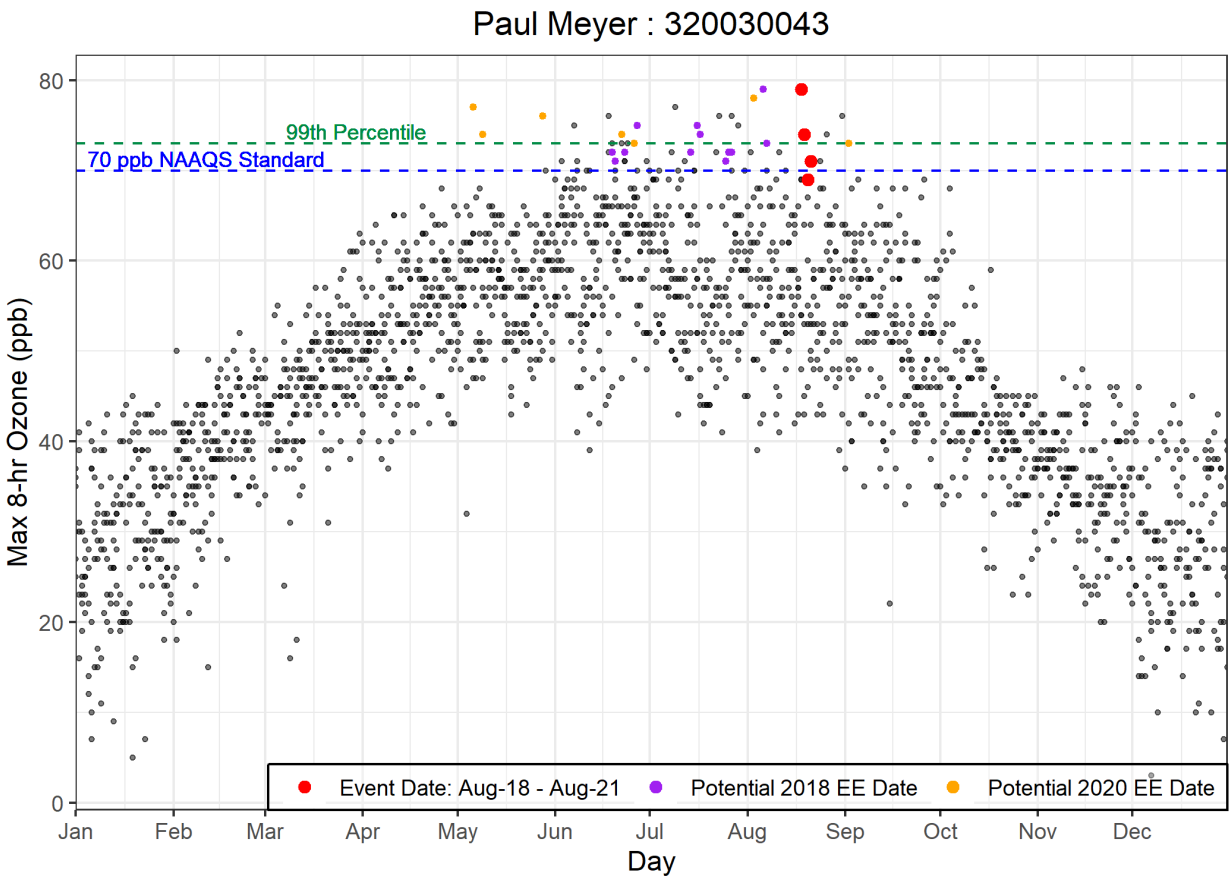

Figure 2-8. Seasonality of 2015-2020 ozone concentrations from Paul Meyer.

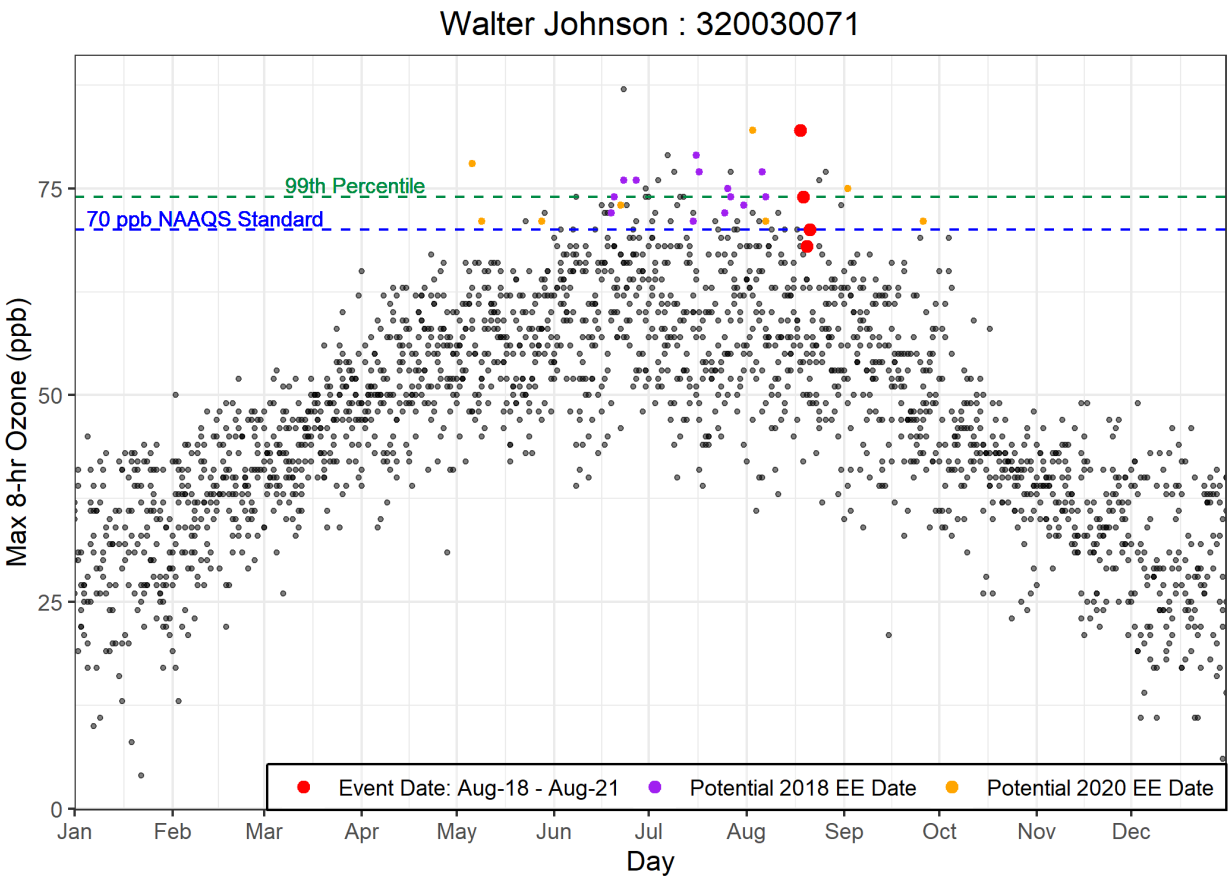

Figure 2-9. Seasonality of 2015-2020 ozone concentrations from Walter Johnson.

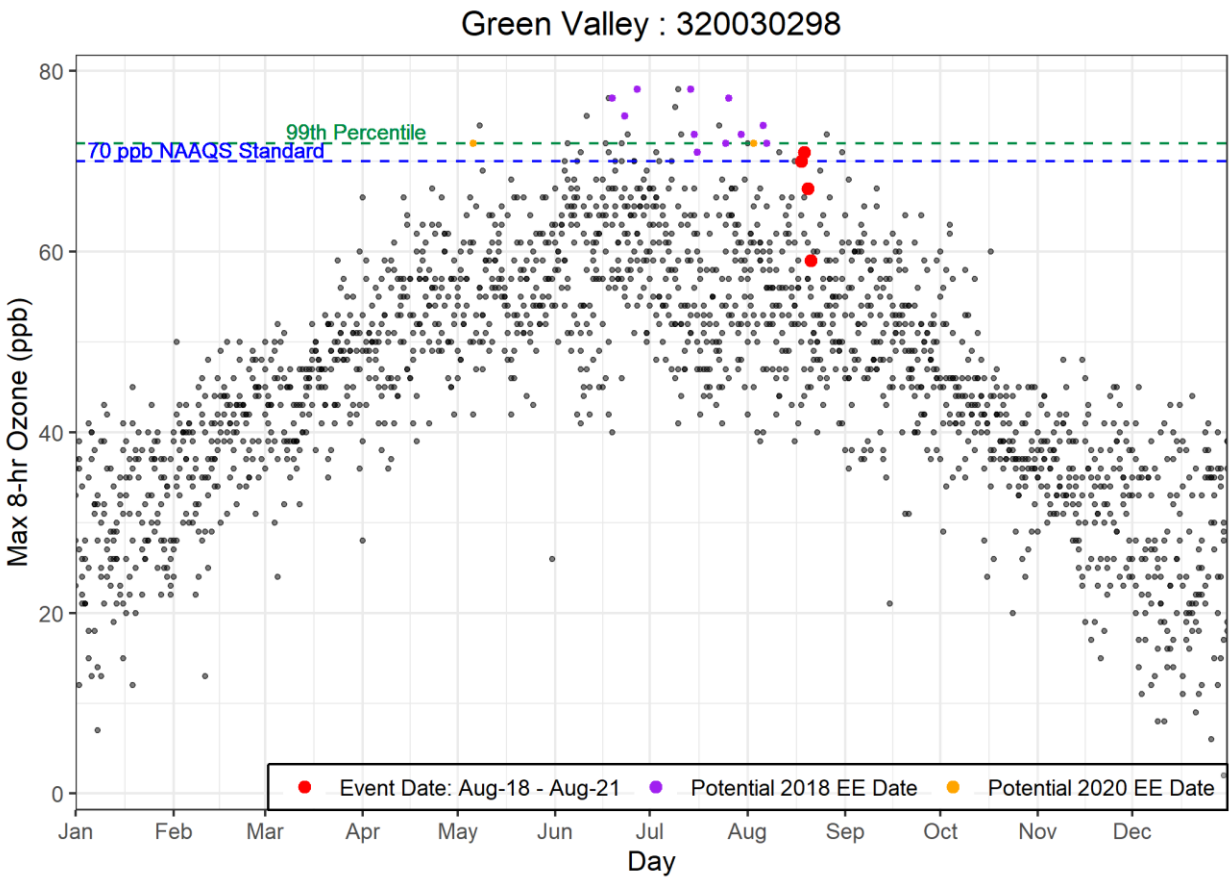

Figure 2-10. Seasonality of 2015-2020 ozone concentrations from Green Valley.

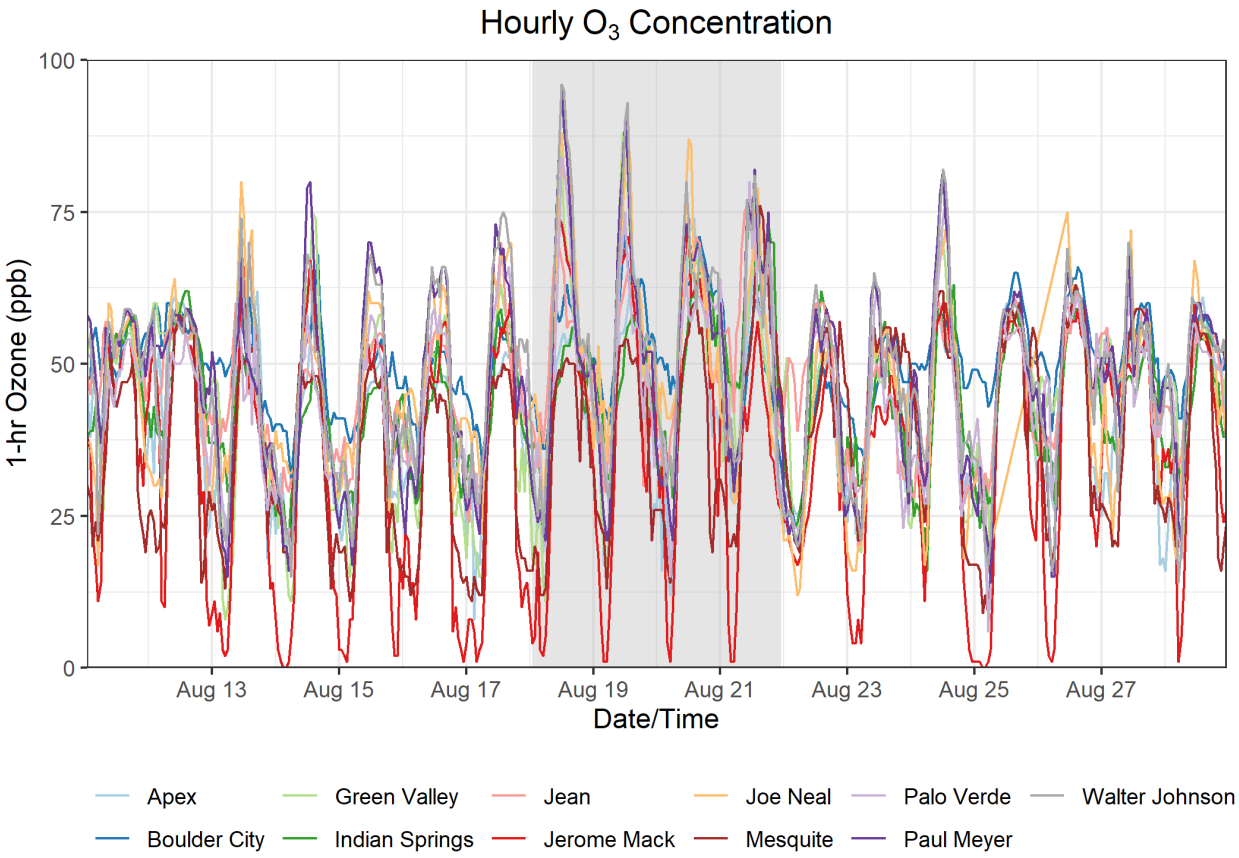

Figure 2-11. Ozone time series at all monitoring sites. Time series of hourly ozone concentrations at monitoring sites in Clark County for one week before and after the August 18-21 event are shown. August 18-21, 2020, is shaded for reference.

3. Clear Causal Relationship Analyses

3.1 Tier 1 Analyses

3.1.1 Comparison of Event with Historical Data

To address the Tier 1 EE criterion of comparison with historical ozone, we compared the August 18-21 EE ozone concentrations at each site with the 2020 ozone record, focusing mainly on the ozone season with highest ozone concentrations. **Figures 3-1 through 3-4** depict the 2020 daily maximum ozone record at each monitoring site, along with the 99th percentile of previous 5-year MDA8 ozone and NAAQS criteria ozone concentrations. During 2020, August 18 and 19 rank in the top 1% (and highest on August 18) for daily maximum ozone concentration in the past five years at the Paul Meyer and Walter Johnson monitoring sites. When compared with daily ozone rankings on August 18-21 over the six-year ozone record at all EE-affected sites (Figures 2-7 through 2-10), the 2020 rankings on August 18, 19, 20 and 21 indicate that this period was an extreme ozone event.

Although the exceedances occurred during a typical ozone season, the August 18-21 MDA8 ozone concentrations were the highest compared with daily ozone concentrations (excluding potential EE days) at three of four EE affected sites (Figures 3-1 through 3-4). **Table 3-1** provides historical monitoring statistics for each affected site on August 18-21, 2020, for May through September in 2015-2019; we do not exclude proposed 2018 EE ozone concentrations. The MDA8 ozone concentrations on August 18-20 were >10 ppb above the mean and median ozone concentrations for the historical ozone season at all EE affected sites (Table 3-1). Because August 18-21 falls during the normal ozone season and MDA8 ozone concentration at all EE affected sites were not clearly distinguishable from the 95th percentile ozone concentration during the non-event historical ozone season, the August 18-21, 2020, event does not satisfy the key factor for a Tier 1 EE. Section 3.2.2 describes Tier 2 comparison of the event-related ozone concentrations with non-event-related high ozone concentrations (>99th percentile over five years or top four highest daily ozone measurements).

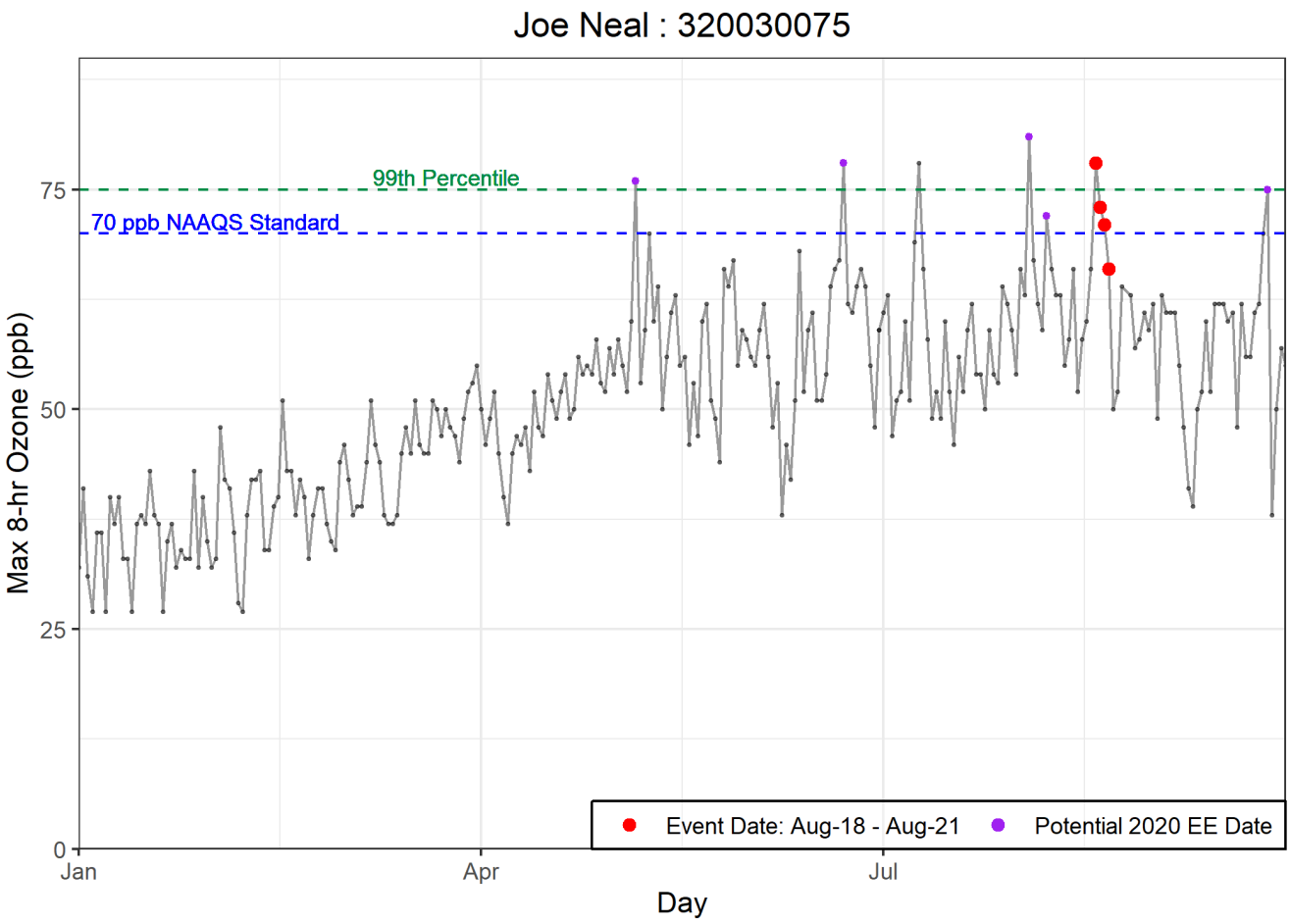

Figure 3-1. Time series of 2020 MDA8 ozone concentrations from Joe Neal.

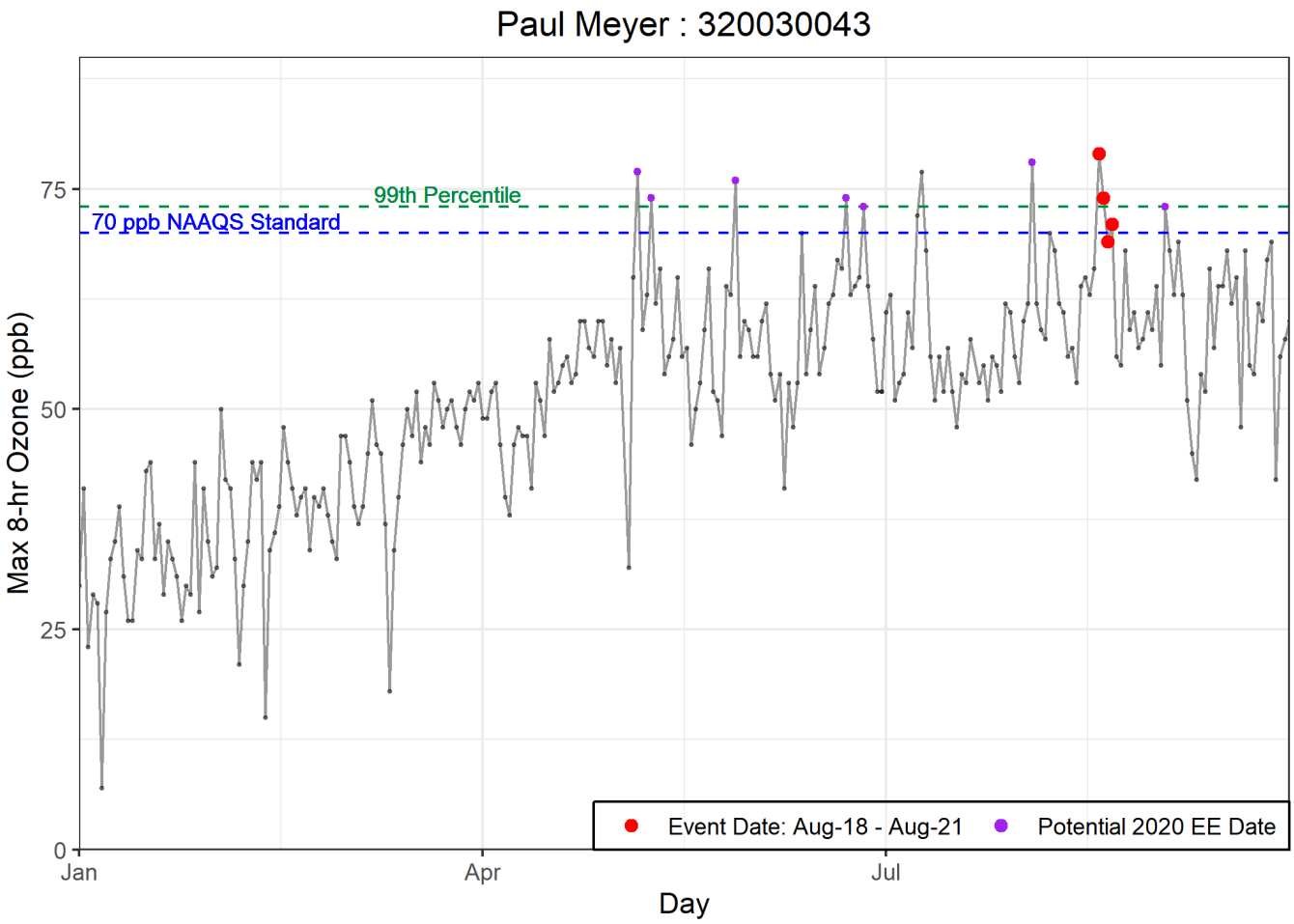

Figure 3-2. Time series of 2020 MDA8 ozone concentrations from Paul Meyer.

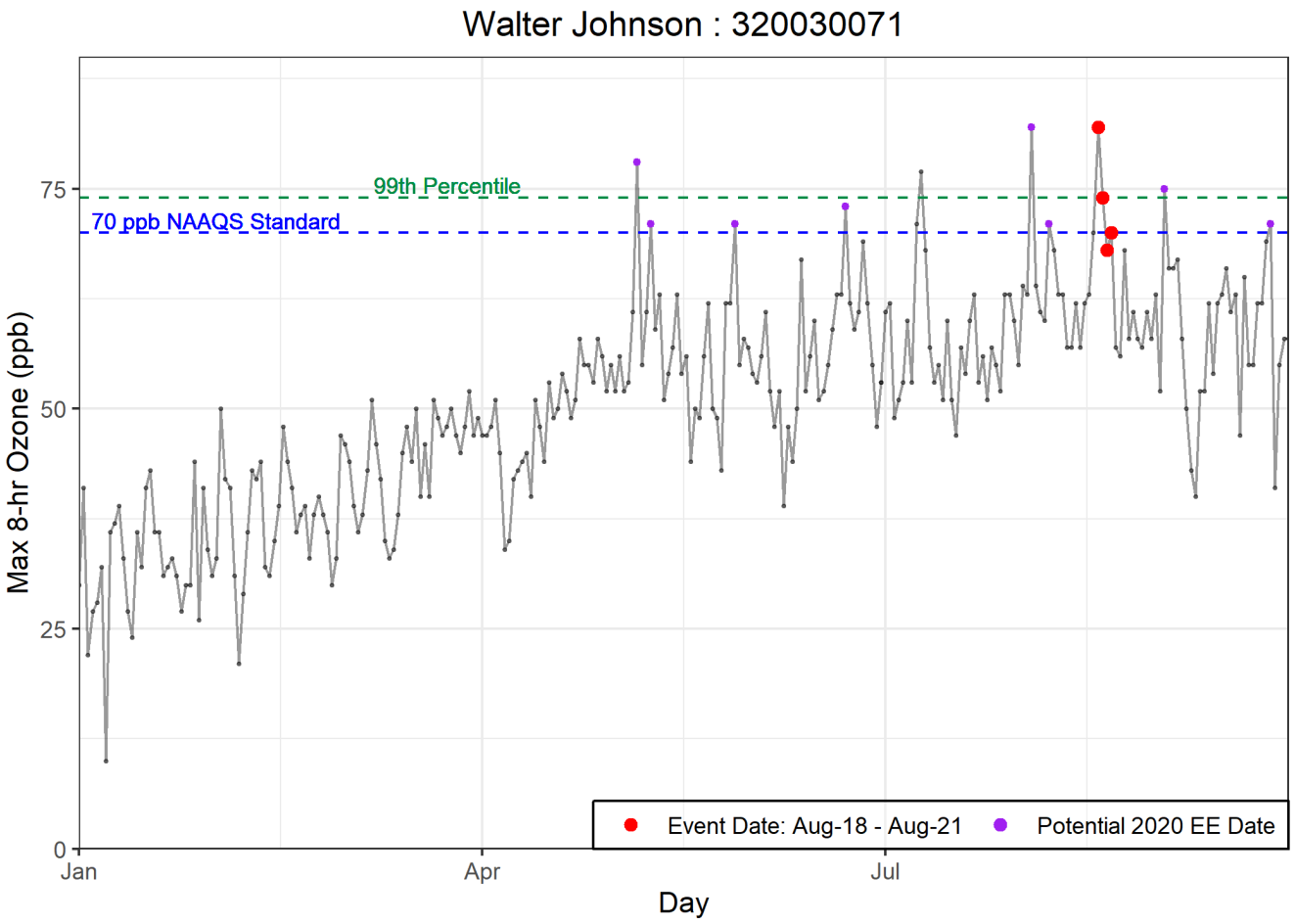

Figure 3-3. Time series of 2020 MDA8 ozone concentrations from Walter Johnson.

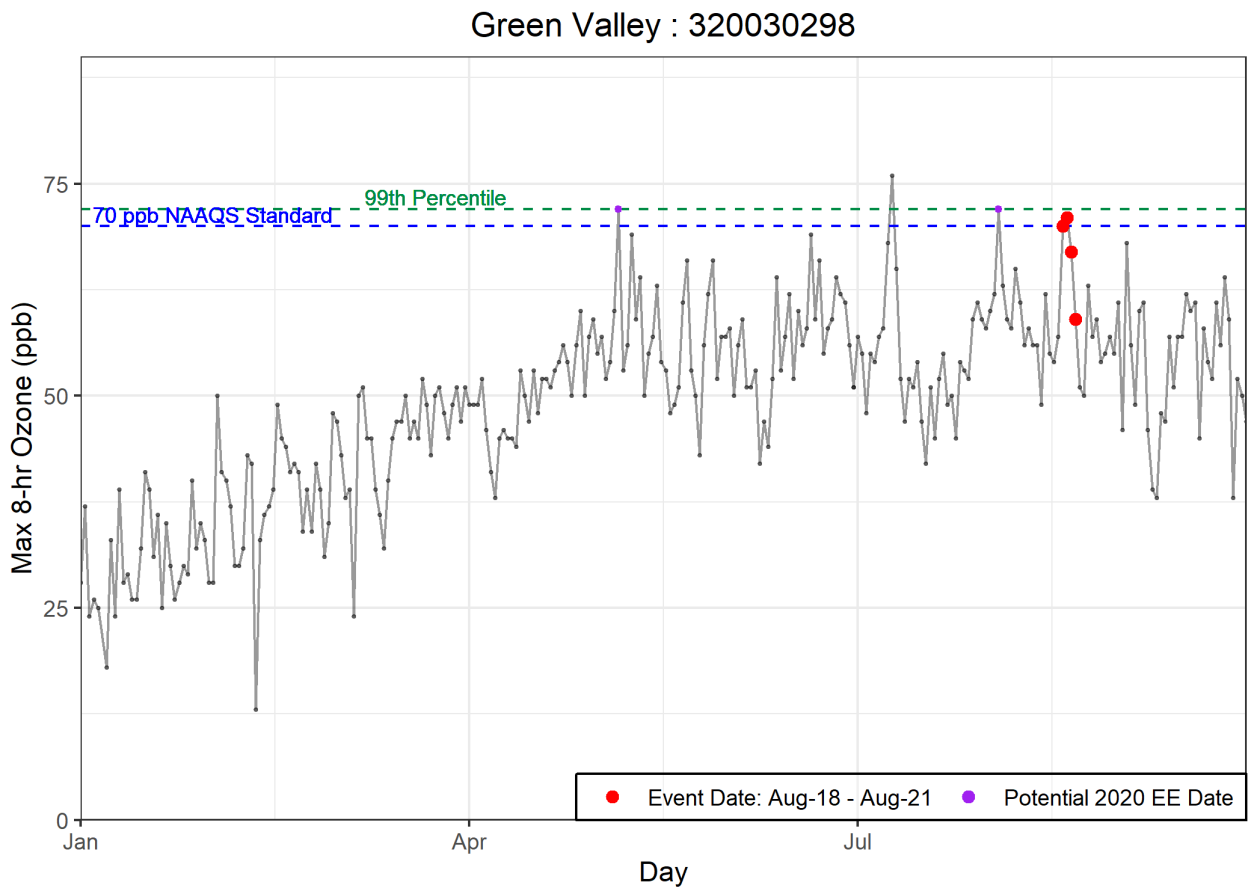

Figure 3-4. Time series of 2020 MDA8 ozone concentrations from Green Valley.

Table 3-1. Ozone season non-event comparison. August 18-21, 2020, MDA8 ozone concentrations for each affected site are shown in the top row. Five-year (2015-2019) average MDA8 ozone statistics for May through September ozone season are shown for each affected site around Clark County to compare with the event ozone concentrations.

	Green Valley 320030298	Joe Neal 320030075	Paul Meyer 320030043	Walter Johnson 320030071
August 18		78	79	82
August 19	71	73	74	74
August 20		71		
August 21			71	
Mean	56	57	57	57
Median	56	57	58	57
Mode	52	62	58	57
St. Dev	8	9	8	9
Minimum	21	23	22	21
95 %ile	69	72	70	71
99 %ile	74	78	76	77
Maximum	78	83	79	87
Range	57	60	57	66
Count	877	912	911	917

3.1.2 Ozone, Fire, and Smoke Maps

We produced maps of ozone Air Quality Index (AQI), $PM_{2.5}$ AQI, active fire and smoke detections from satellites, and visible satellite imagery that assessed the transport of wildfire-influenced air parcels to Las Vegas from California, on August 18-21, 2020.

O_3 and $PM_{2.5}$ Maps

Figure 3-5 shows daily ozone AQI maps from August 17-21, 2020. High ozone concentrations that corresponded with the presence of wildfire smoke occurred across multiple states. Locations with moderate and unhealthy ground-level ozone concentrations (yellow, orange, and red areas) were observed on August 17 through 21, 2020 across a large region from southern and central California to southern Nevada, Arizona, Utah, and Colorado. These elevated ozone AQI levels expanded to additional regions throughout the August 18-21 event. The ozone AQI values also increased in southern California and Arizona on August 19 and across a broader region to the north (southern Idaho, Utah, Colorado, and Wyoming). Elevated ozone AQI in Clark County persisted from August 17 through 21, 2020.

Figure 3-6 shows elevated daily ground-level $PM_{2.5}$ AQI in California, southern Nevada, and western Arizona that persisted from August 17 through 21, 2020. The highest $PM_{2.5}$ AQI was observed near California wildfire locations and in southern Idaho on August 19 through 21, 2020. The presence of elevated ground-level $PM_{2.5}$ in the Clark County region, along with regionally elevated ozone AQI, indicates wildfire smoke influenced ground-level air in Clark County.

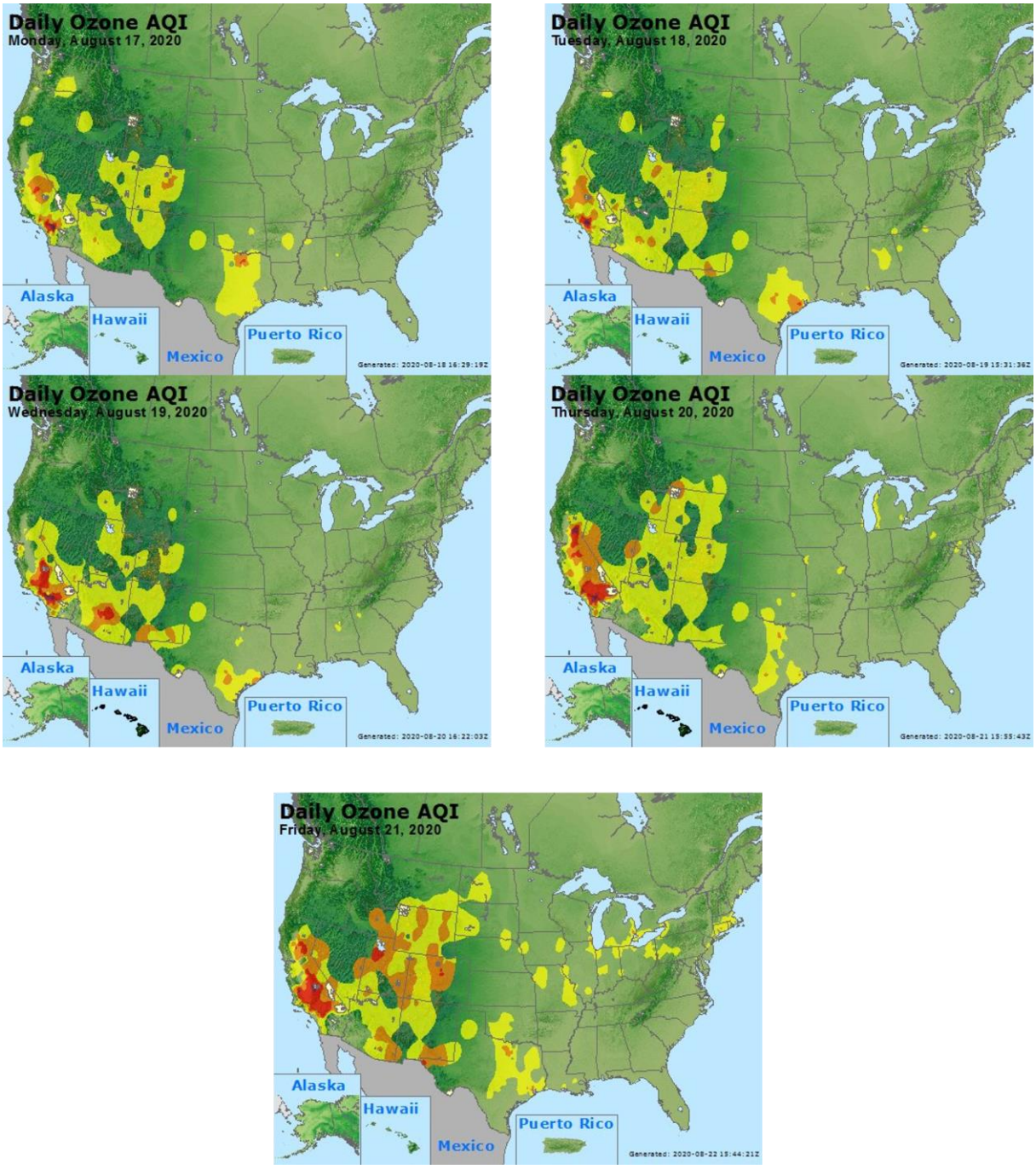

Figure 3-5. Daily ozone AQI one day prior to and during the August 18-21 event.

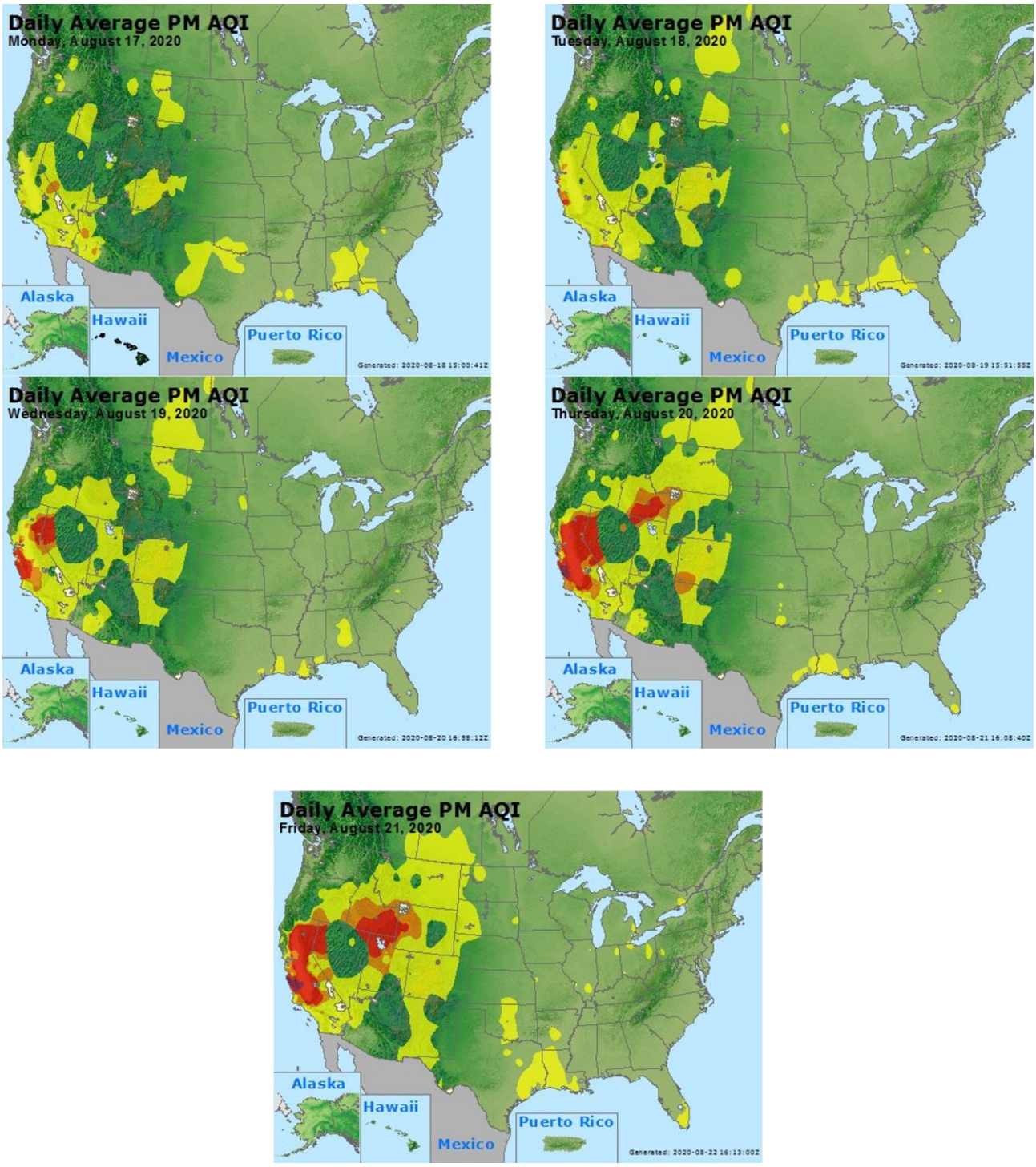

Figure 3-6. Daily $PM_{2.5}$ AQI one day prior to and during the August 18-21 event.

HMS Fire Detection Maps

According to EPA's guidance to Tier 1 analysis requirements (U.S. Environmental Protection Agency, 2016), the National Oceanic and Atmospheric Administration (NOAA) Hazard Mapping System (HMS) Fire and Smoke Product can be used to demonstrate the transport of fire emissions to impacted monitors. The HMS Fire and Smoke Product consists of

1. A daily fire detection product derived from three satellite data products[1] to spatially and temporally map fire locations at 1 km grid resolution, and
2. A daily smoke product derived from visible satellite imagery[2] that consists of polygons showing regions impacted by smoke in the atmospheric column.

The HMS smoke plume data are based on measurements from several environmental satellites and reviewed by trained NOAA analysts to identify cases where smoke is dispersed by transport. One can download real-time HMS fire detection and smoke products and a six-month archive of the products from the NOAA Satellite and Information Service website (ospo.noaa.gov/Products/land/hms.html).

Figure 3-7 shows the HMS smoke plume and fire detection data for August 17 to 21, 2020. These products indicate that elevated smoke plume levels were centered over and associated with fires in Colorado and northern New Mexico, as well as the Dome wildfire in Mojave National Preserve, close to Clark County. A second smoke plume region centered over and associated with multiple northern California fires was also detected on August 18 and 19. This plume expanded over a large region of the western U.S. on August 20 and 21, including Clark County, Nevada. These fire and smoke detections indicate that the Colorado, Dome wildfire, and northern California fires are candidates contributing to local and regional wildfire smoke plumes observed in the atmospheric column over Clark County, Nevada, during the August 18-21 event.

The HMS smoke plume data for the days prior to August 18-21 were obtained and combined with HYSPLIT back trajectories on high ozone concentration days to identify intersections and assess potential smoke impacts (Section 3.1.3). The following sections provide further evidence of smoke transport (based on HYSPLIT trajectories and satellite data) that traveled from southern and northern California fires to the Clark County area.

[1] The HMS fire detection product is developed using data from the Moderate Resolution Imaging Spectroradiometer (MODIS), Geostationary Operational Environmental Satellite system (GOES), Advanced Very High Resolution Radiometer (AVHRR) and Visible Infrared Imaging Radiometer Suite (VIIRS) satellite instruments.
[2] The HMS smoke product is derived from GOES-EAST and GOES-WEST visible satellite imagery.

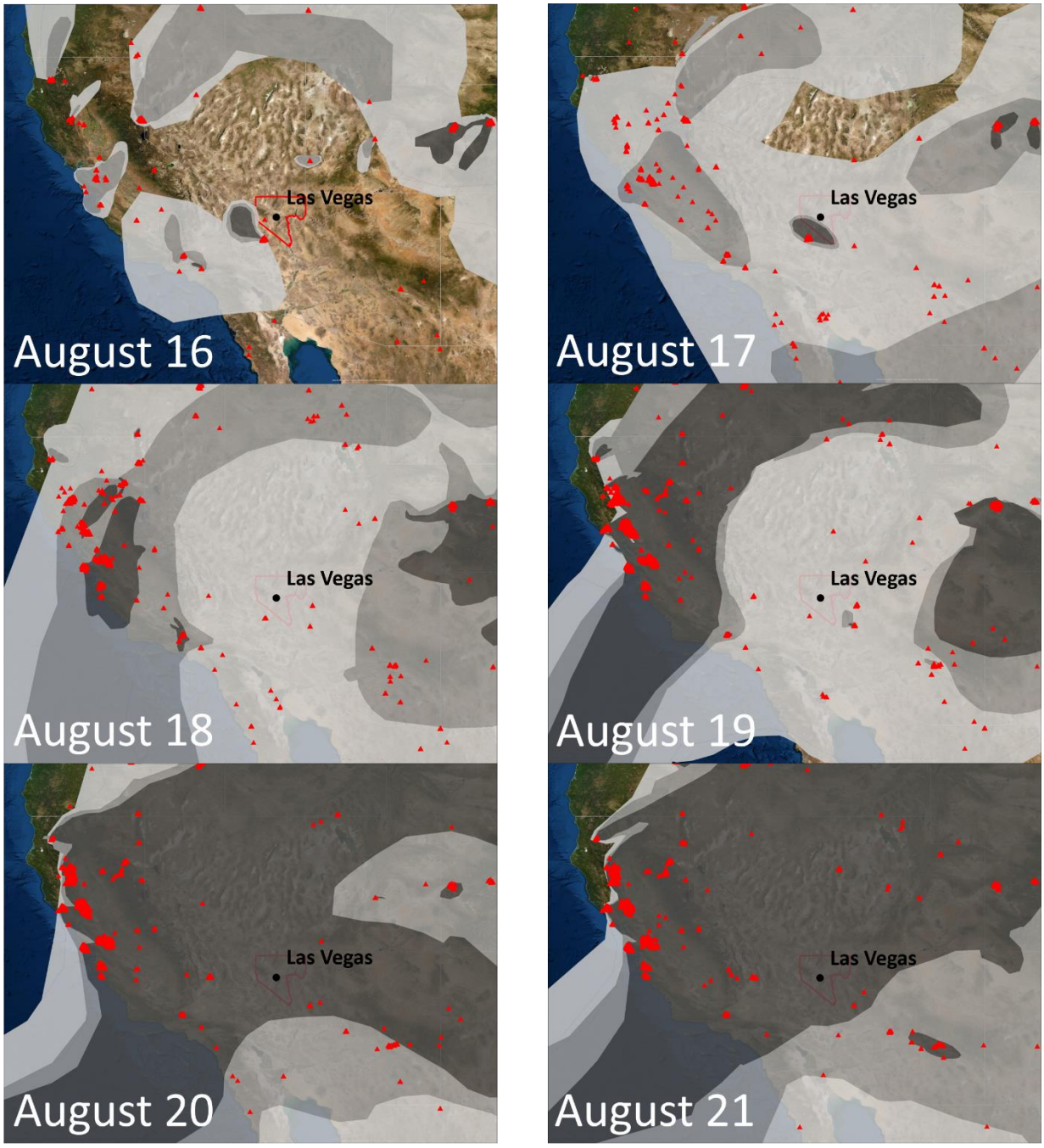

Figure 3-7. Daily HMS smoke over the United States for one day prior to and during the August 18-21 event. Fire detections are shown as red triangles, and smoke presence and intensity are shown in the gray shades.

Visible Satellite Imagery

Visible satellite imagery from the Moderate Resolution Imaging Spectroradiometer (MODIS) Aqua and Terra satellites (Figures 3-8 through 3-12) show the presence of smoke immediately east of multiple northern California fires burning on August 19-21, and a fire burning east of Sequoia National Forest on August 20. This is generally consistent with the evidence of smoke associated with fires in California demonstrated by the HMS maps above. The satellite imagery provides an additional granular picture of the eastward transport of smoke plumes from multiple California fires (especially on August 19-21) towards Clark County, Nevada. The arrival of these smoke plumes coincided with the high ozone observed in Clark County on August 18-21. Eastward smoke plume transport towards southern Nevada due to westerly and northwesterly winds is consistent with transport patterns observed in the HYSPLIT trajectory analysis presented in Section 3.1.3, as well as the satellite and ground-based measurements of smoke-associated species presented in Sections 3.2.3 and 3.2.4.

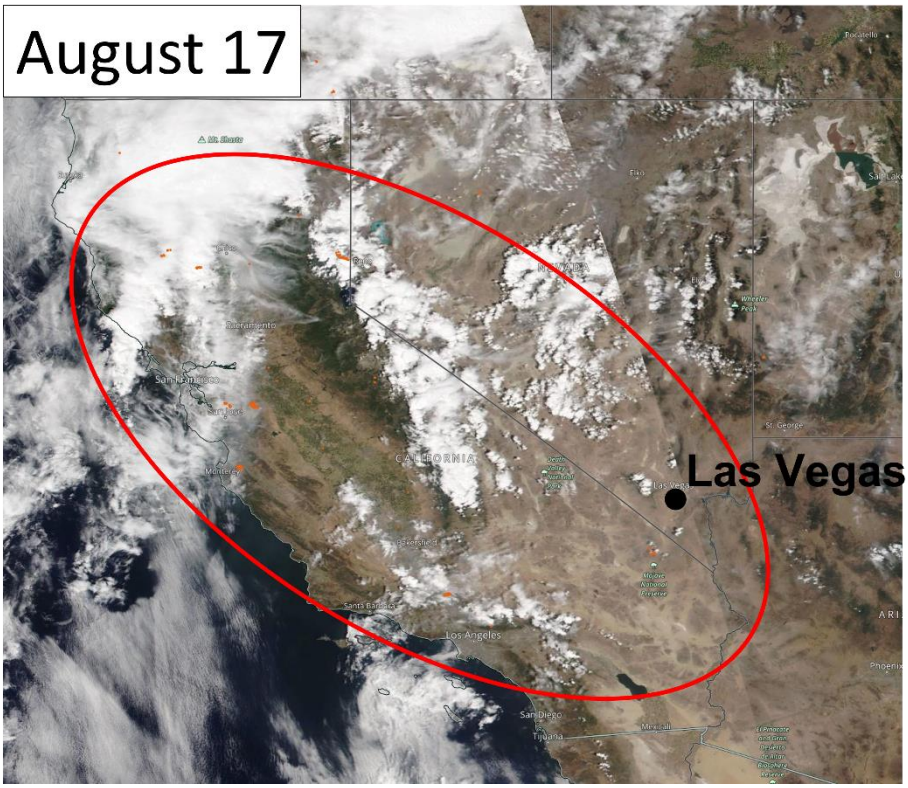

Figure 3-8. Visible satellite imagery from over California, Nevada, Arizona, and Utah on August 17, 2020. MODIS fire detection locations are indicated in orange. Large wildfires are circled in red. Source: NASA Worldview.

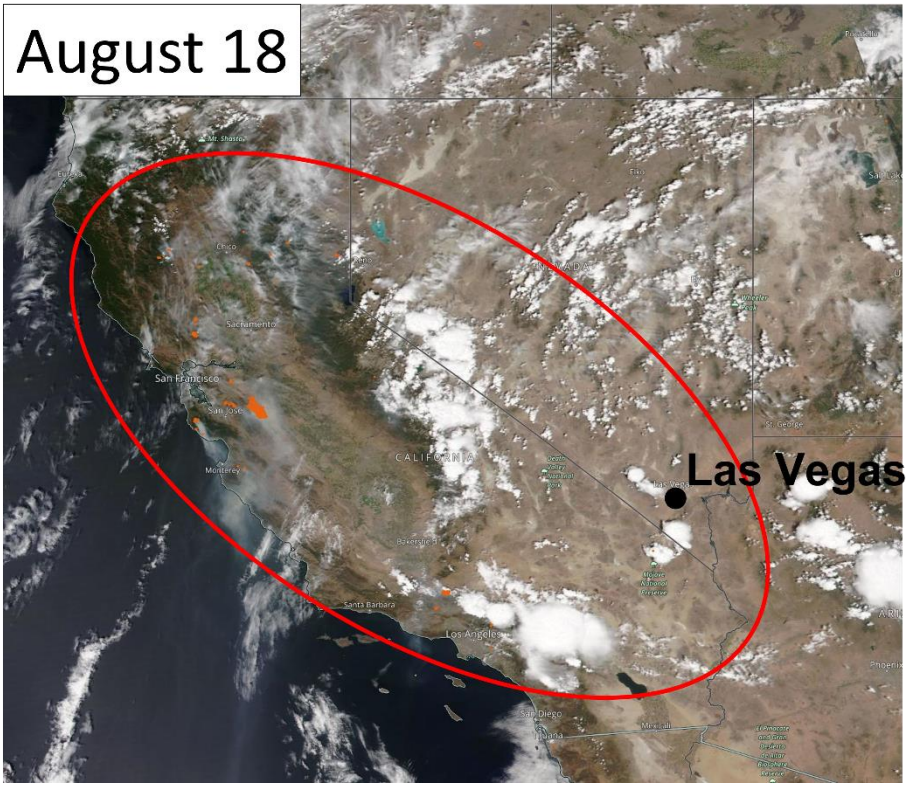

Figure 3-9. Visible satellite imagery from over California, Nevada, Arizona, and Utah on August 18, 2020. MODIS fire detection locations are indicated in orange. Large wildfires are circled in red. Source: NASA Worldview.

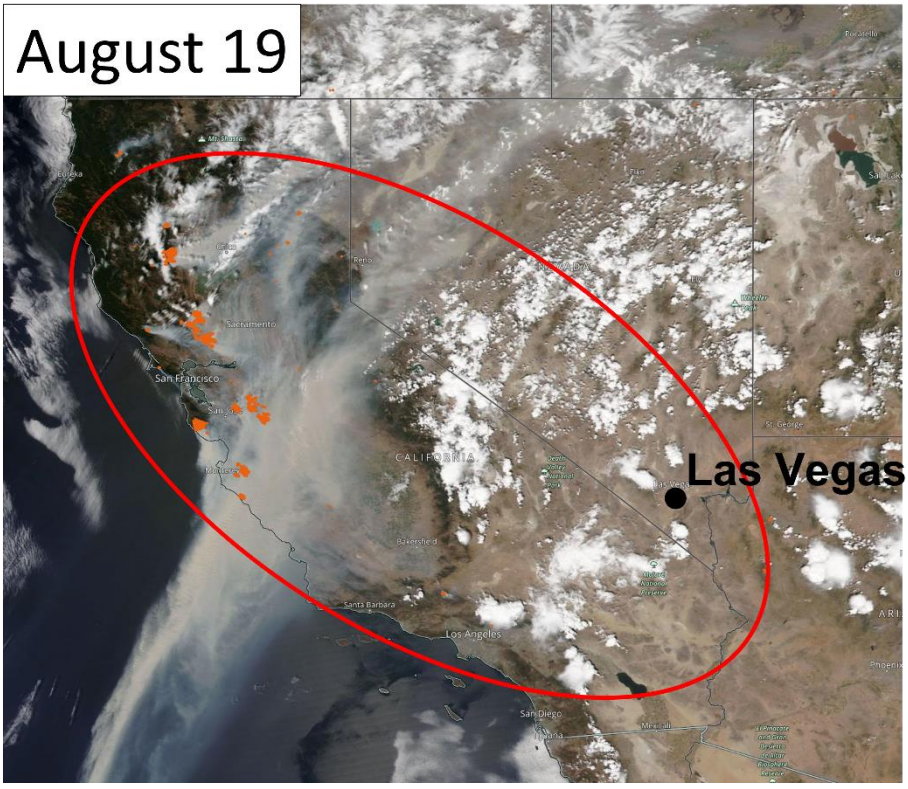

Figure 3-10. Visible satellite imagery from California, Nevada, Arizona, and Utah on August 19, 2020. MODIS fire detection locations are indicated in orange. Large wildfires are circled in red. Source: NASA Worldview.

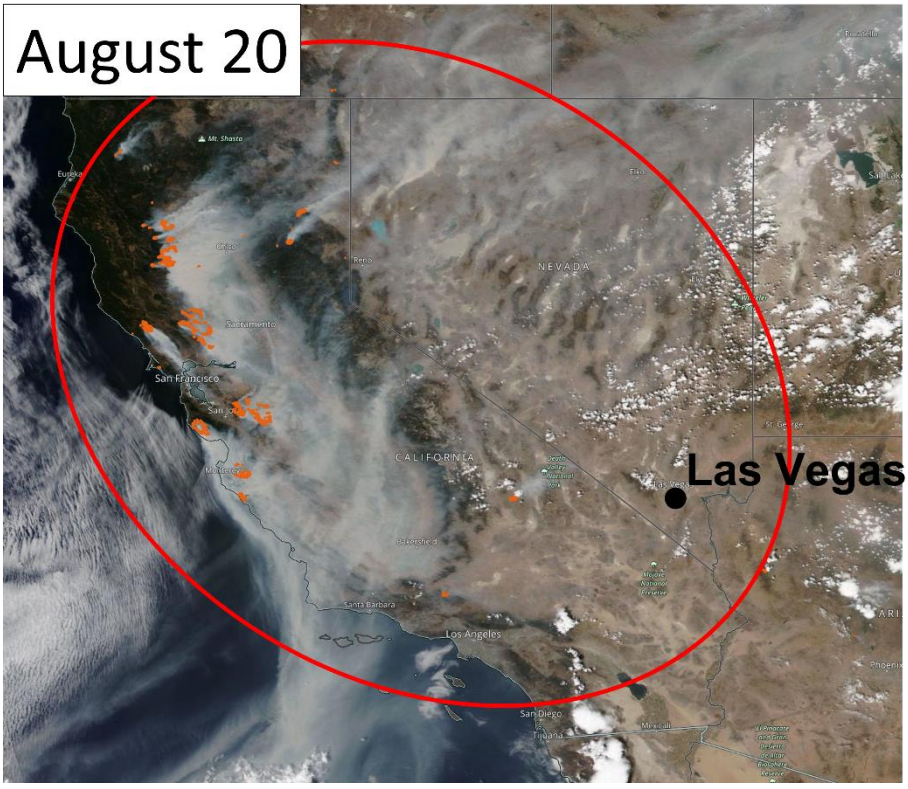

Figure 3-11. Visible satellite imagery from California, Nevada, Arizona, and Utah on August 20, 2020. MODIS fire detection locations are indicated in orange. Large wildfires are circled in red. Source: NASA Worldview.

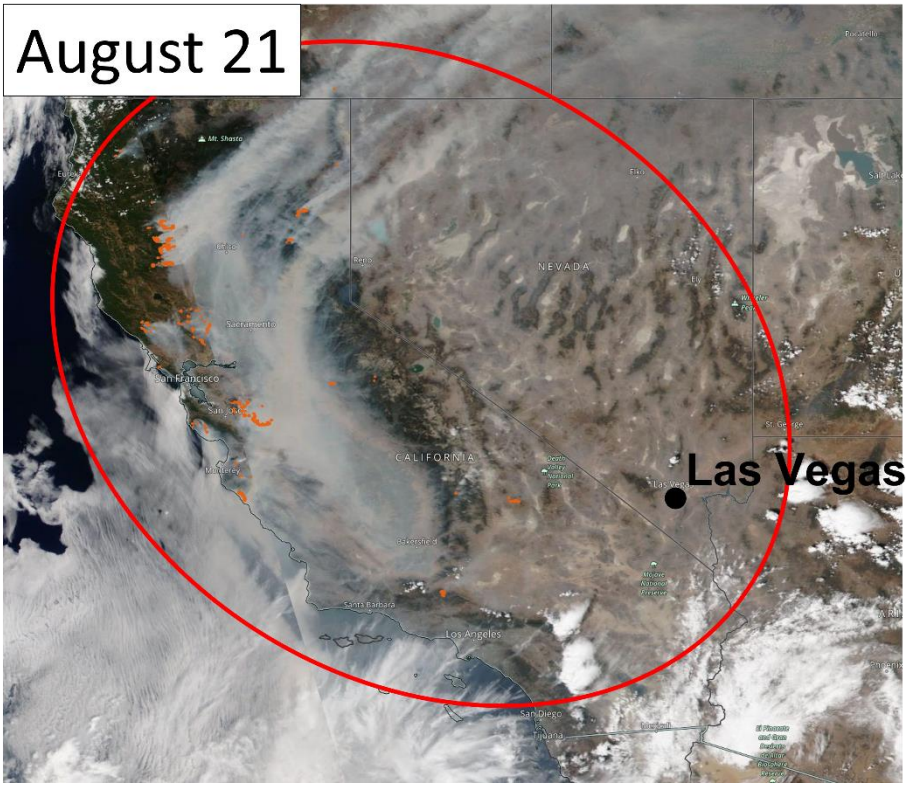

Figure 3-12. Visible satellite imagery from California, Nevada, Arizona, and Utah on August 21, 2020. MODIS fire detection locations are indicated in orange. Large wildfires are circled in red. Source: NASA Worldview.

3.1.3 HYSPLIT Trajectories

HYSPLIT trajectories were run to demonstrate the transport of air parcels to Las Vegas from upwind areas and to evaluate transport of smoke-containing air parcels from wildfires toward the affected monitors. These trajectories show that air was transported from the Dome, Lake, North Range, and northern California fires to the Clark County area during the period August 17-21, 2020. Combined with satellite observations described in Sections 3.1.2 and 3.2.3, the trajectories demonstrate that smoke was transported from both southern and northern California to Las Vegas, Nevada.

NOAA's online HYSPLIT model tool was used for the trajectory modeling (http://ready.arl.noaa.gov/HYSPLIT.php). HYSPLIT is a commonly used model that calculates the path of a single air parcel from a specific location and height above the ground over a period of time. This path is the modeled trajectory. HYSPLIT trajectories can be used as evidence that fire emissions were transported to an air quality monitor. This type of analysis is important for meeting Tier 1 requirements and is required under Tier 3.

Table 3-2 summarizes the model options used for this study. We used meteorological data from the North American Mesoscale Forecast System (NAM, 12-km resolution) and High-Resolution Rapid Refresh (HRRR, 3-km resolution) model (ready.noaa.gov/archives.php). These data are high in spatial resolution, readily available for HYSPLIT modeling over the desired lengths of time and expected to capture fine-scale meteorological variability. Backward trajectory times were selected to be the average hour of peak ozone concentration at all sites in a day. If one day had only one ozone exceedance site, the hour of maximum ozone concentration was selected to be the backward trajectory initiation time. As suggested in the EPA's exceptional event guidance (U.S. Environmental Protection Agency, 2016), a backward trajectory length of 72 hours was selected to assess whether smoke from the current day or from the previous two days may have been transported over a long distance to the monitoring sites. Trajectories were initiated at 50 m, 500 m, and 1,000 m above ground level to capture transport throughout the mixed boundary layer, as ozone precursors may be transported aloft and influence concentrations at the surface through vertical mixing. Three backward trajectory approaches available in the HYSPLIT model were used in this analysis, including site-specific trajectories, trajectory matrix, and trajectory frequency.

Site-specific back trajectories were run to show direct transport from the wildfire smoke to the affected site(s). This analysis is useful in linking smoke impacts at a single location (i.e., an air quality monitor) to wildfire smoke. Matrix back trajectories were run to show the general air parcel transport patterns from the Las Vegas area to the wildfire smoke plumes. Similarly, matrix forward trajectories were run to show air parcel transport patterns from the fires to the Las Vegas area. Matrix trajectories are useful in analyzing air transport over areas larger than a single air quality site. Trajectory frequency analysis show the frequency with which multiple trajectories initiated over multiple hours pass over a grid cell on a map. Trajectory frequencies are useful in estimating the temporal and spatial patterns of air transport from a source region to a specific air quality monitor. Based on the transport patterns, fire and smoke detections, and initial back trajectories, we ran additional forward trajectory matrices from representative fires (i.e., the LNU Lightning Complex, North Range, and Lake fires). To further model smoke from all fires contributing to the August 18-21 EE, we initialized forward dispersion modeling from all fires (i.e., August Complex, SCU Lightning Complex, CZU Lightning Complex, LNU Lightning Complex, Cold Springs Fire, River Fire, Carmel Fire, North Complex, Dolan Fire, North Range Fire, Dome Fire, Red Salmon Complex, Lake Fire, and Loyalton Fire). Dispersion modeling is useful for determining the extent and timing of smoke entering the Clark County area in relation to the August 18 through 21 event, especially when smoke from multiple wildfires is mixing throughout California from extensive burning. Together, these trajectory analyses indicate the transport patterns of emissions from multiple fire locations into Clark County on August 18-21, 2020.

Table 3-2. HYSPLIT run configurations for each analysis type, including meteorology data set, time period of run, starting location(s), trajectory time length, starting height(s), starting time(s), vertical motion methodology, and top of model height.

HYSPLIT Parameter	Backward Trajectory Analysis – Site-Specific	Back Trajectory Analysis – Matrix	Backward Trajectory Analysis – Frequency	Forward Trajectory Analysis – Matrix	Backward Trajectory Analysis – High Resolution	Forward Dispersion Modeling
Meteorology	12-km NAM	12-km NAM	12-km NAM	12-km NAM	3-km HRRR	12-km NAM
Time Period	August 18 – August 21, 2020	August 18 – August 21, 2020	August 16 – August 21, 2020	August 16 – August 21, 2020	August 18 – August 21, 2020	August 16-21, 2020
Starting Location	36.1822 N, 115.2516 W, 36.1489 N, 115.2019 W, Joe Neal, Paul Meyer	Evenly spaced grid covering Las Vegas, Nevada	Near downtown Las Vegas (36.1822 N, 115.2516 W)	Evenly spaced grid covering Lake, LNU Lightning Complex, or North Range Fire	Las Vegas Valley (36.1489 N, 115.2019 W)	Location of all 14 California fires listed in Section 3.2.1
Trajectory Time Length	72 hours	72 hours	72 hours	72 hours	72 hours	48-72 hours
Starting Heights (AGL)	50 m, 500 m, 1,000 m	500 m	500 m	100 m, 1,000 m	50 m, 500 m, 1,000 m	500 m
Starting Times	19:00 UTC, 20:00 UTC	19:00 UTC, 20:00 UTC	19:00 UTC, 20:00 UTC	19:00 UTC, 22:00 UTC	19:00 UTC, 20:00 UTC	00:00 UTC
Vertical Motion Method	Model Vertical Velocity	Model Vertical Velocity	Model Vertical Velocity	Model Vertical Velocity	Model Vertical Velocity	Model Vertical Velocity
Top of Model	10,000 m	10,000 m	10,000 m	10,000 m	10,000 m	10,000 m

Figures 3-13 through 3-16 show site-specific backward trajectories initiated on August 16-21 from the Las Vegas Valley, near downtown Las Vegas and the two EE affected sites (Joe Neal and Paul Meyer) at near surface and altitudes within the mixed layer. HMS fire and smoke detections are also overlaid for the previous two days. The average hour of maximum ozone concentrations between all exceedance sites for a given day was chosen as the start time. If a day had one site where an ozone exceedance occurred, the hour of maximum ozone for that site was chosen as the initiation time. Transport patterns evolved during the August 18-21 period. The trajectories indicate surface transport of air parcels on August 18 from the west (California) and longer distance boundary layer (1,000 m above ground level) transport from the east and north (Utah) (Figure 3-13). On August 19, circulating air transport patterns towards Clark County crossed California and Nevada and passed directly over the Dome and North Range fires at 1,000 m altitude (Figure 3-14). On August 20 and

21, 2020, boundary layer air was transported into Clark County from the west (Figure 3-15) and south (Figure 3-16). On both August 20 and 21, trajectories intersected with regional smoke plumes originating from northern California fires (e.g., LNU Lightning Complex Fire), including the Lake and North Range fires in southern California. (Figure 3-45 in Section 3.2.1 provides a map of the wildfires burning throughout California on August 18-21, 2020.) Single-site backward trajectories show that air parcels that reached the lower boundary layer over the Las Vegas area on August 18-21 passed through expansive and dense smoke plumes in the days leading up to each exceedance day.

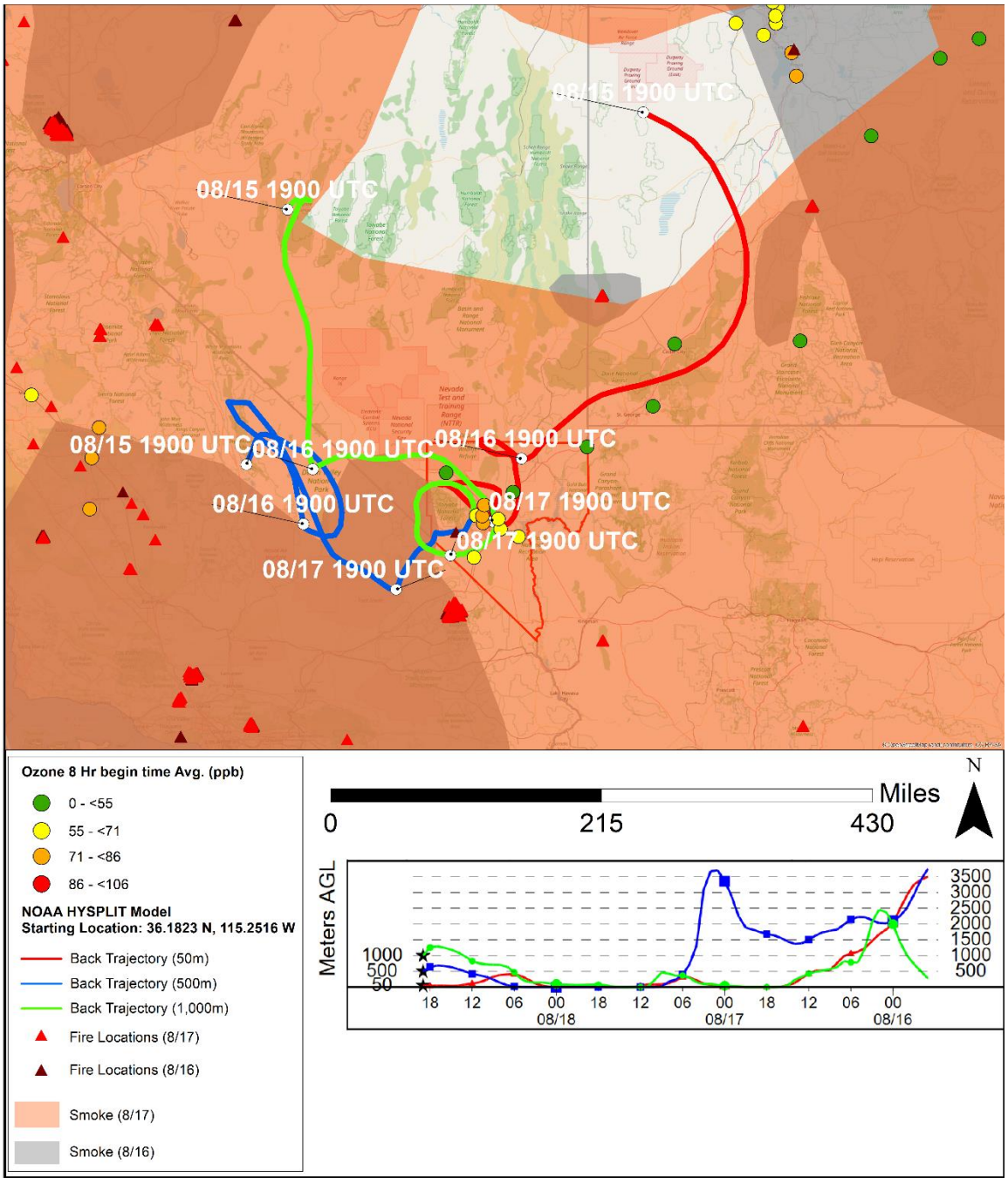

Figure 3-13. 72-hour HYSPLIT back trajectories with HMS smoke from August 16 and 17, 2020, initiated near downtown Las Vegas (average coordinates of Paul Meyer, Walter Johnson, and Joe Neal site locations), ending on August 18, 2020, at 19:00 UTC (11:00 a.m. Local Time [LT]). NAM back trajectories are shown for 50 m (red), 500 m (blue), and 1,000 m (green) above ground level.

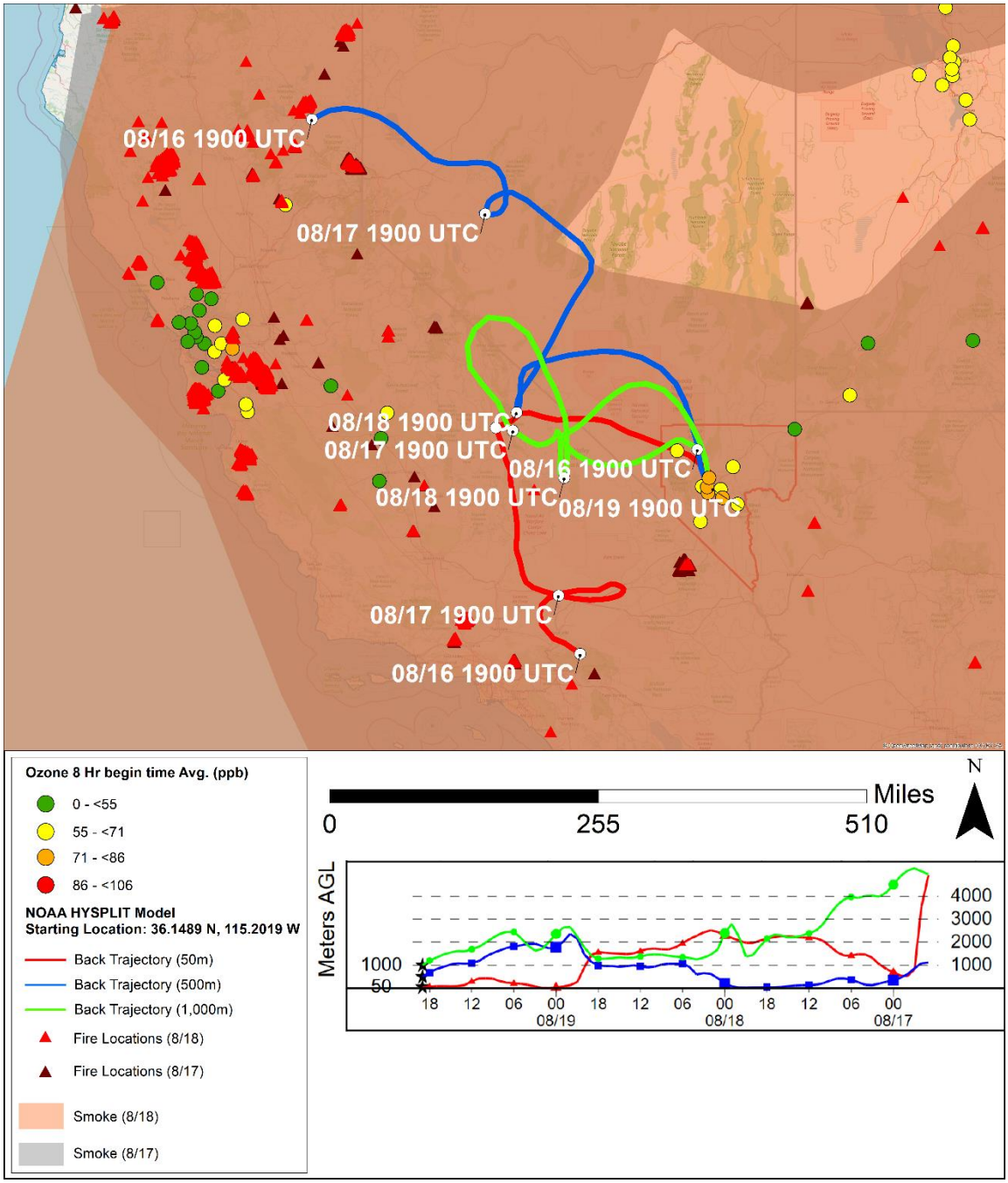

Figure 3-14. 72-hour HYSPLIT back trajectories with HMS smoke from August 17 and 18, 2020, initiated from the Las Vegas Valley (average coordinates of Paul Meyer, Walter Johnson, Joe Neal, and Green Valley site locations), ending on August 19, 2020, at 19:00 UTC (11:00 a.m. LT). NAM back trajectories are shown for 50 m (red), 500 m (blue), and 1,000 m (green) above ground level.

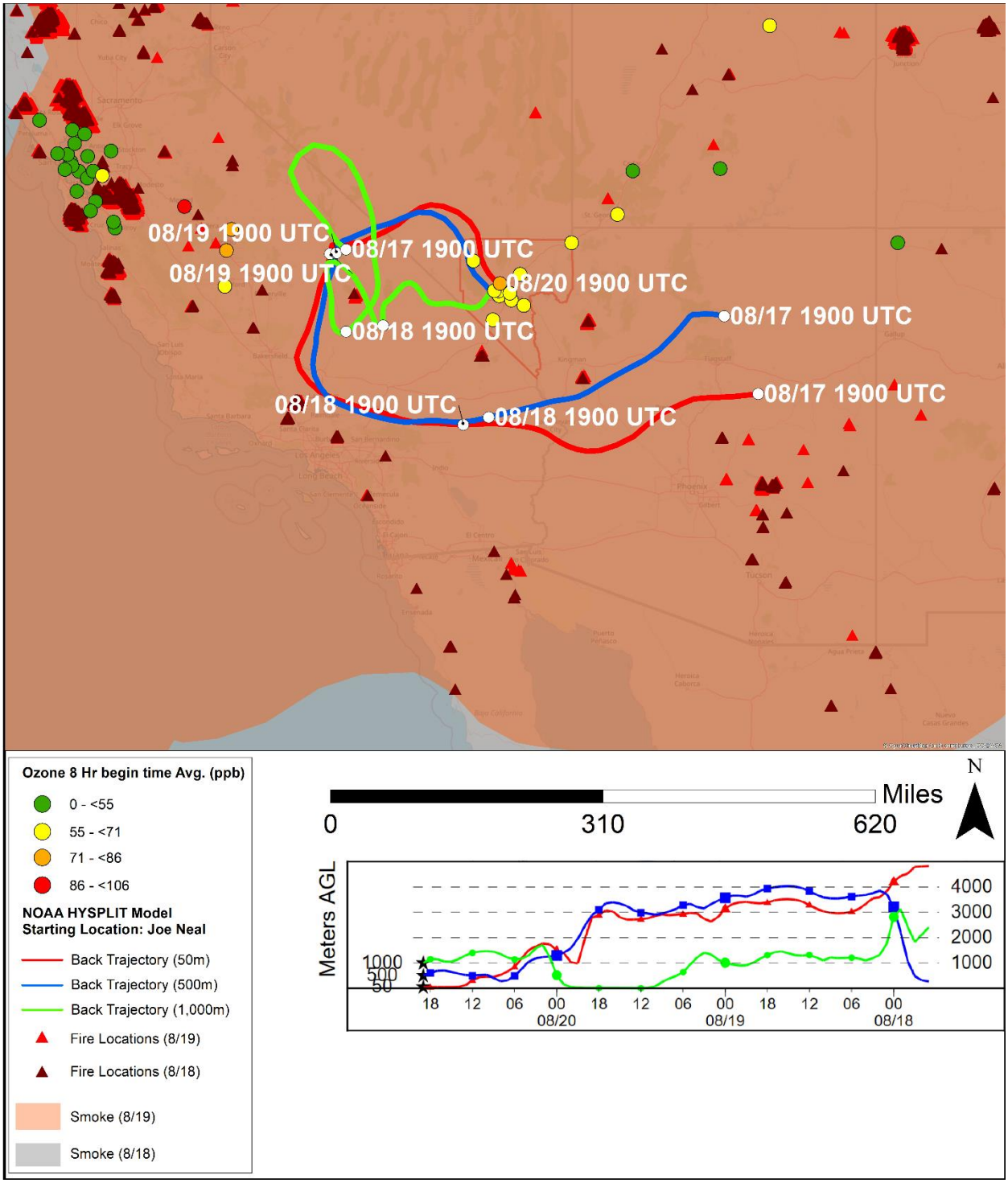

Figure 3-15. 72-hour HYSPLIT back trajectories with HMS smoke from August 18 and 19, 2020, initiated from the Joe Neal monitoring site, ending on August 20, 2020, at 19:00 UTC (11:00 a.m. LT). NAM back trajectories are shown for 50 m (red), 500 m (blue), and 1,000 m (green) above ground level.

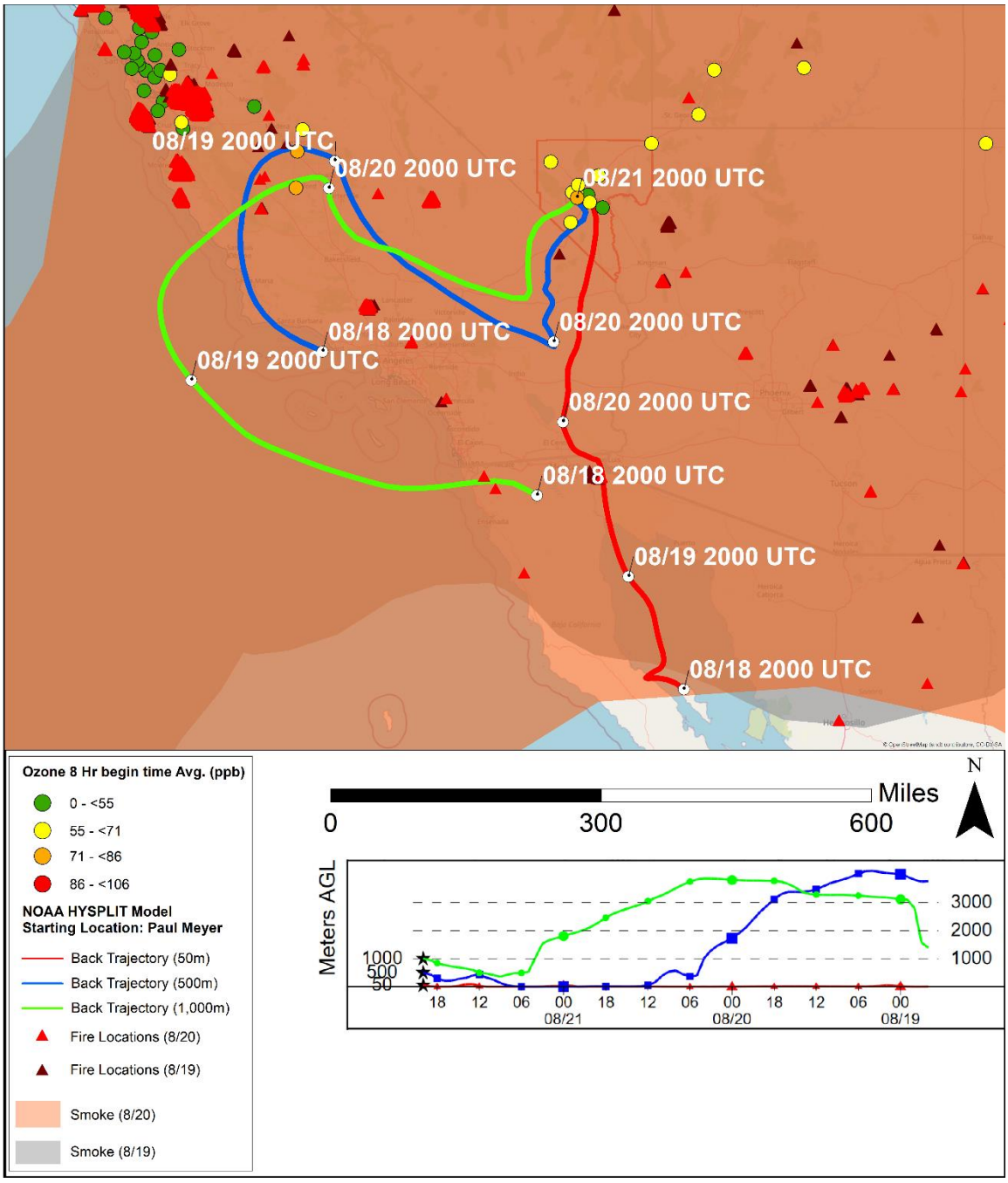

Figure 3-16. 72-hour HYSPLIT back trajectories with HMS smoke from August 19 and 20, 2020, initiated from the Paul Meyer monitoring site, ending on August 21, 2020, at 20:00 UTC (12:00 p.m. LT). NAM back trajectories are shown for 50 m (red), 500 m (blue), and 1,000 m (green) above ground level.

Figures 3-17 through 3-20 show high-resolution (3 km) backward trajectories driven by HRRR meteorological fields at the corresponding locations and initiation times as in Figures 3-13 through 3-16. The transport pattern directions using HRRR-driven trajectories are generally consistent with those driven by NAM meteorology (with August 18 and 19 showing some differences). Trajectories modeled with HRRR meteorology indicate air parcels arriving on August 18 from the south (50 m and 500 m trajectory) or in a circulating pattern (1,000 m trajectory). Trajectories modeled with HRRR meteorology arriving on August 19 indicate air parcels following a circular pattern (500 m and 1,000 m trajectory), passing through Colorado, New Mexico, Arizona, and southern California before descending into Clark County. Although the August 18 and 19 HRRR trajectories are different than the NAM trajectories shown in the previous figures, these trajectories still pass through smoke from the large complex California fires based on HMS smoke data presented previously.

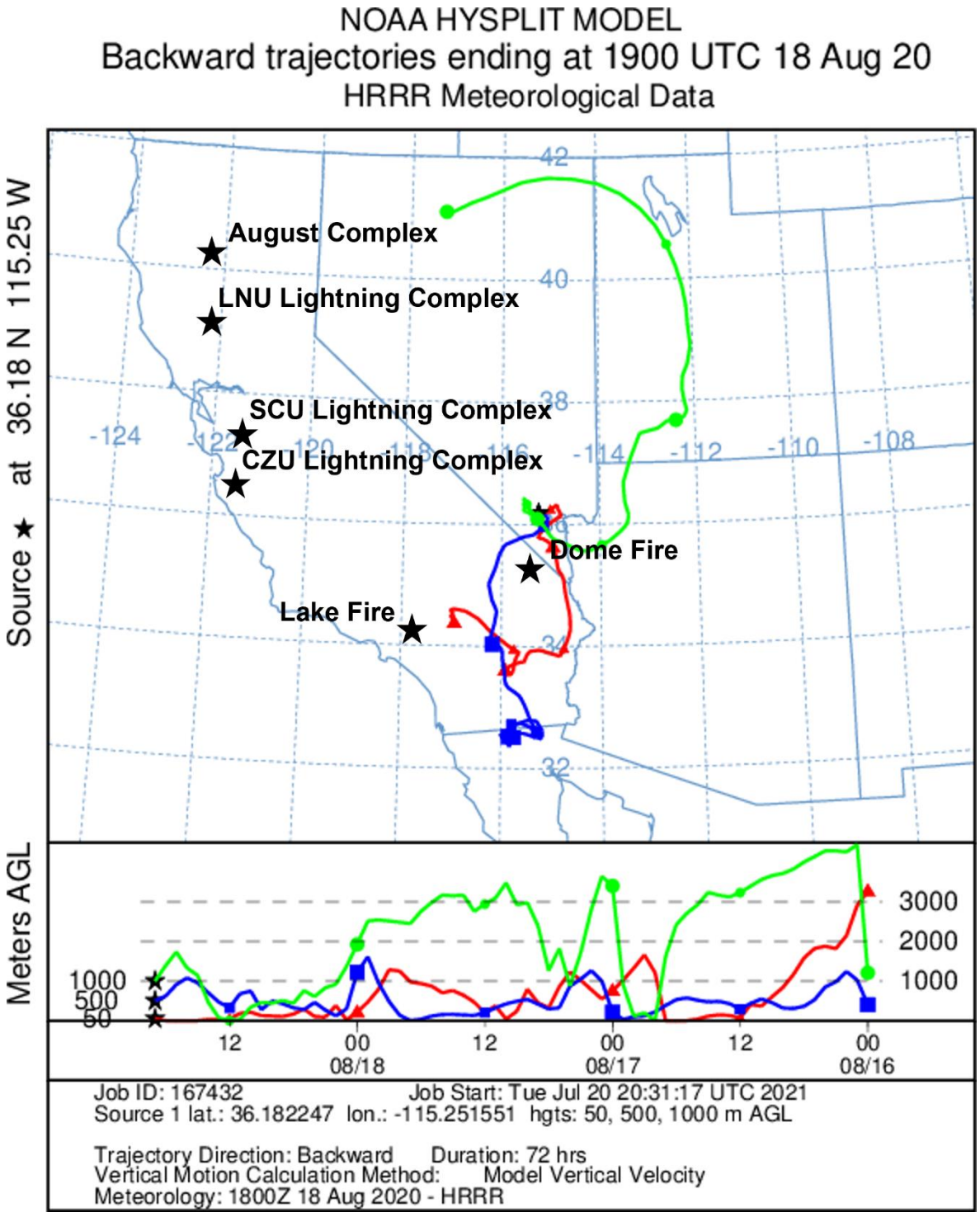

Figure 3-17. High-resolution HYSPLIT back trajectories. 72-hour, HRRR 3-km back trajectories initiated on August 18, 2020, at 19:00 UTC (11:00 a.m. LT) near downtown Las Vegas (average coordinates of Paul Meyer, Walter Johnson, and Joe Neal site locations) are shown for 50 m (red), 500 m (blue), and 1,000 m (green) above ground level.

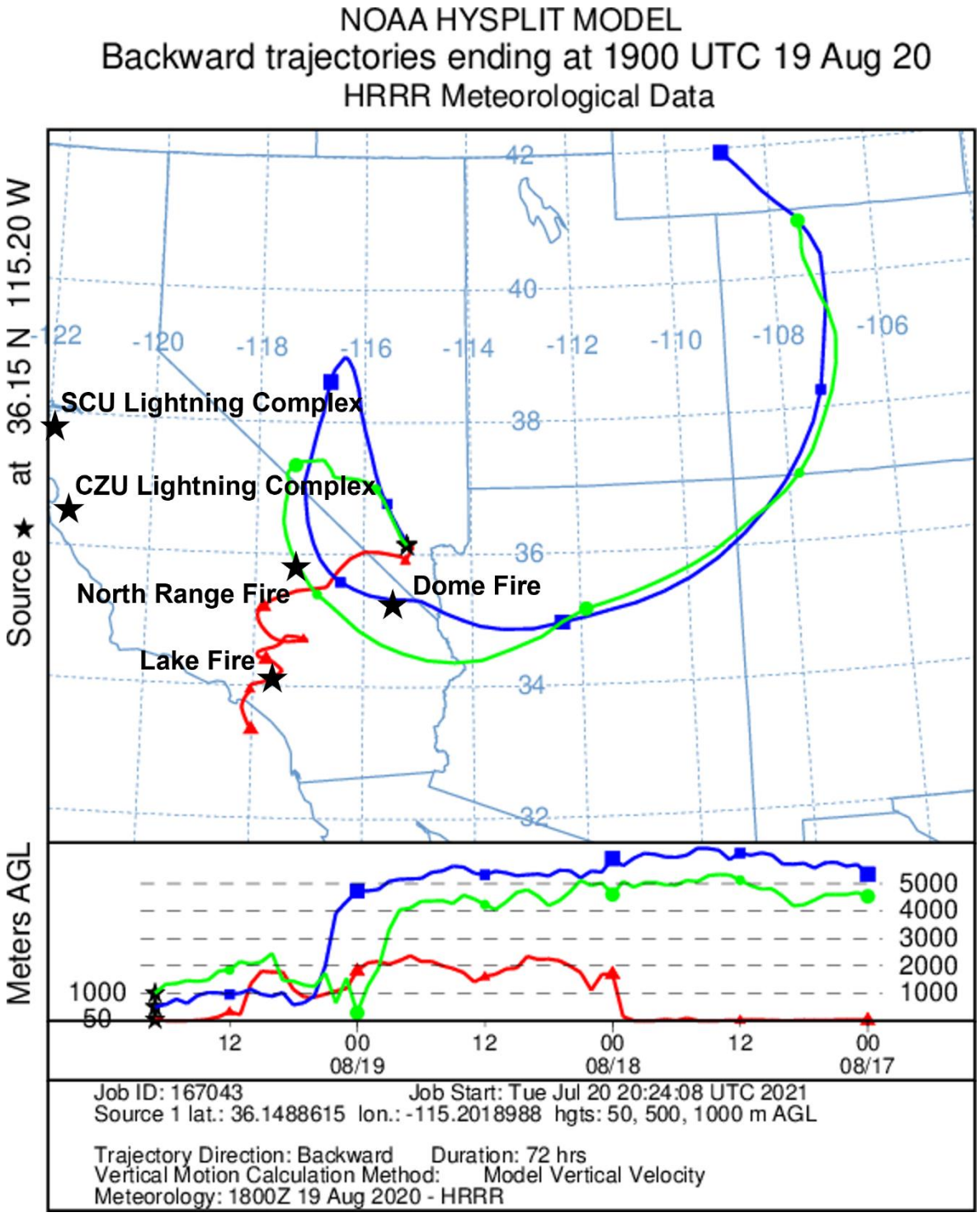

Figure 3-18. High-resolution HYSPLIT back trajectories. 72-hour, HRRR 3-km back trajectories initiated on August 19, 2020, at 19:00 UTC (11:00 a.m. LT) from the Las Vegas Valley (average coordinates of Paul Meyer, Walter Johnson, Joe Neal, and Green Valley site locations) are shown for 50 m (red), 500 m (blue), and 1,000 m (green) above ground level.

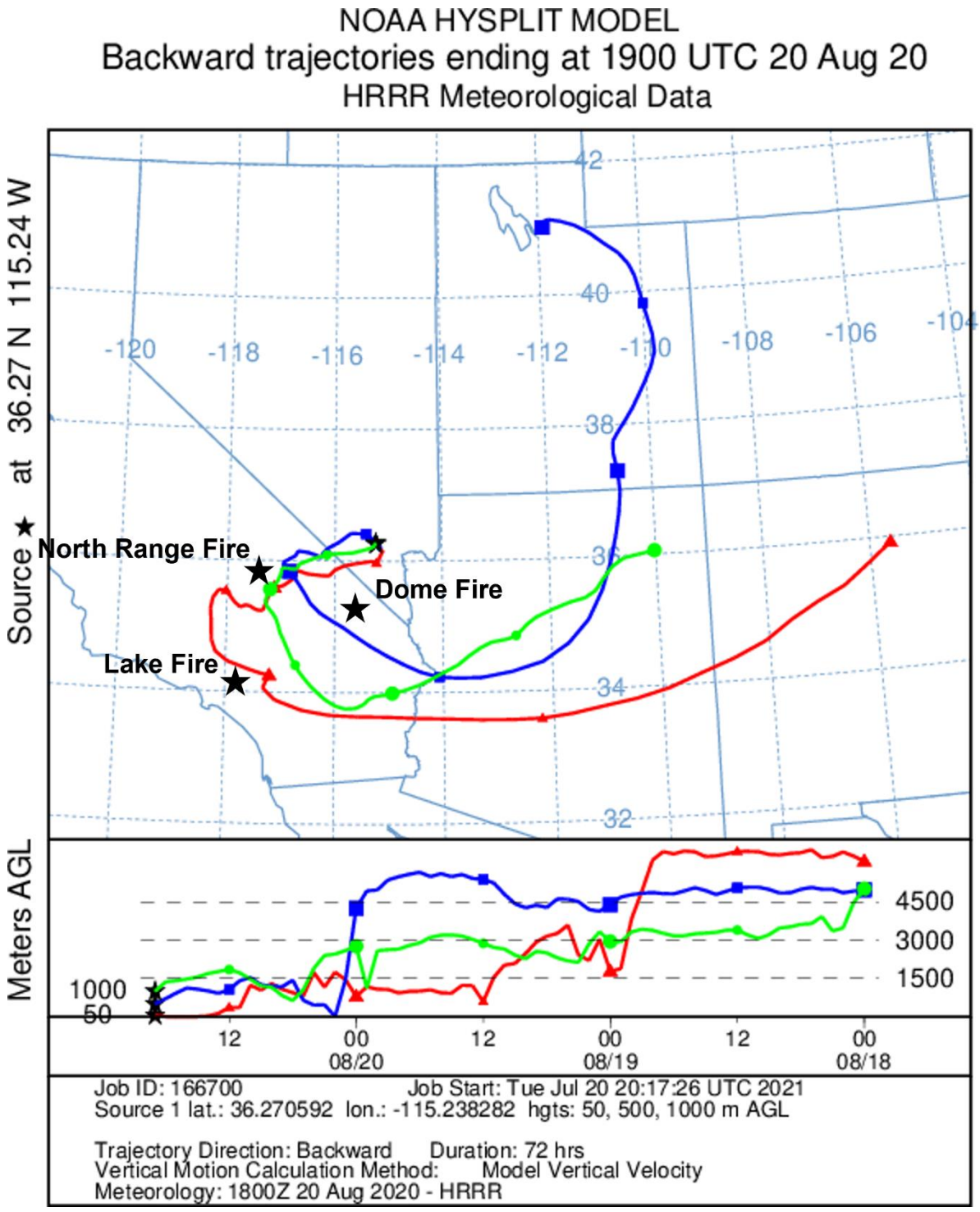

Figure 3-19. High-resolution HYSPLIT back trajectories. 72-hour, HRRR 3-km back trajectories initiated on August 20, 2020, at 19:00 UTC (11:00 a.m. LT) from the Joe Neal monitoring site are shown for 50 m (red), 500 m (blue), and 1,000 m (green) above ground level.

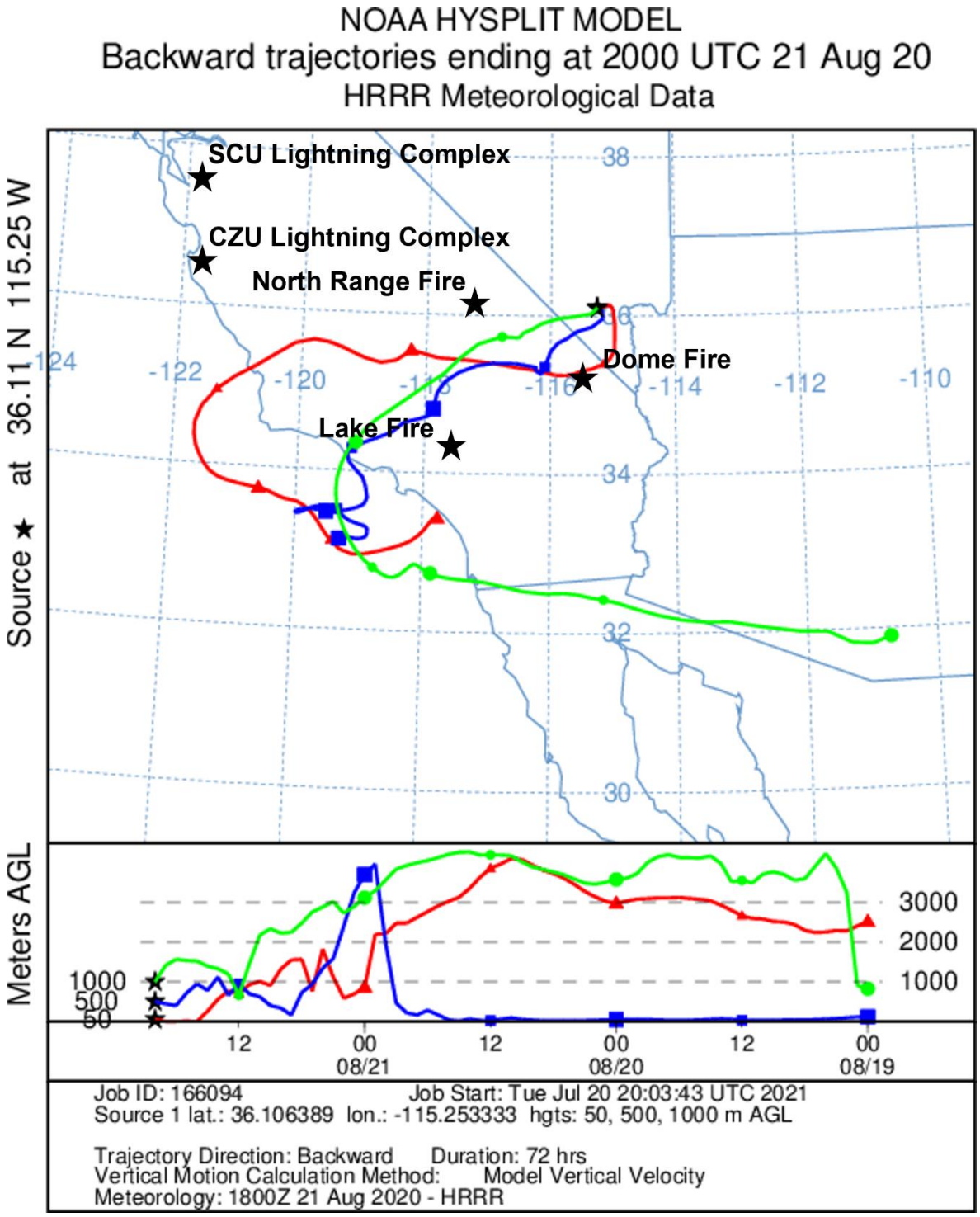

Figure 3-20. High-resolution HYSPLIT back trajectories. 72-hour, HRRR 3-km back trajectories initiated on August 21, 2020, at 20:00 UTC (12:00 p.m. LT) from the Paul Meyer monitoring site are shown for 50 m (red), 500 m (blue), and 1,000 m (green) above ground level.

Figures 3-21 through 3-24 show 72-hour backward trajectory matrices from an evenly spaced grid of source locations covering Las Vegas, Nevada, at 500 m AGL. The backward trajectories were initiated from the late mornings and early afternoons (11:00 a.m. PST/19:00 UTC and 12:00 p.m. PST/20:00 p.m. UTC) of August 18-21, 2020. Air parcels that reached the lower boundary layer (500 m AGL) in Las Vegas at 11:00 a.m. PST on August 18-20 and 12:00 p.m. PST on August 21 originated from both the boundary layer (<2,000 m AGL) and upper troposphere (>3,000 m AGL). The directions for regional transport from background trajectory matrices are consistent with those from the individual site locations in Figures 3-13 through 3-16 and the extent of HMS smoke from the wildfires in California. Specifically, a subset of August 18 initiated trajectories pass over the Dome fire, August 19 and 20 initiated trajectories pass over the Lake, Dome, and North Range fires, and August 21 initiated trajectories pass over the Dome, Lake, and SCU Lightning Complex fires.

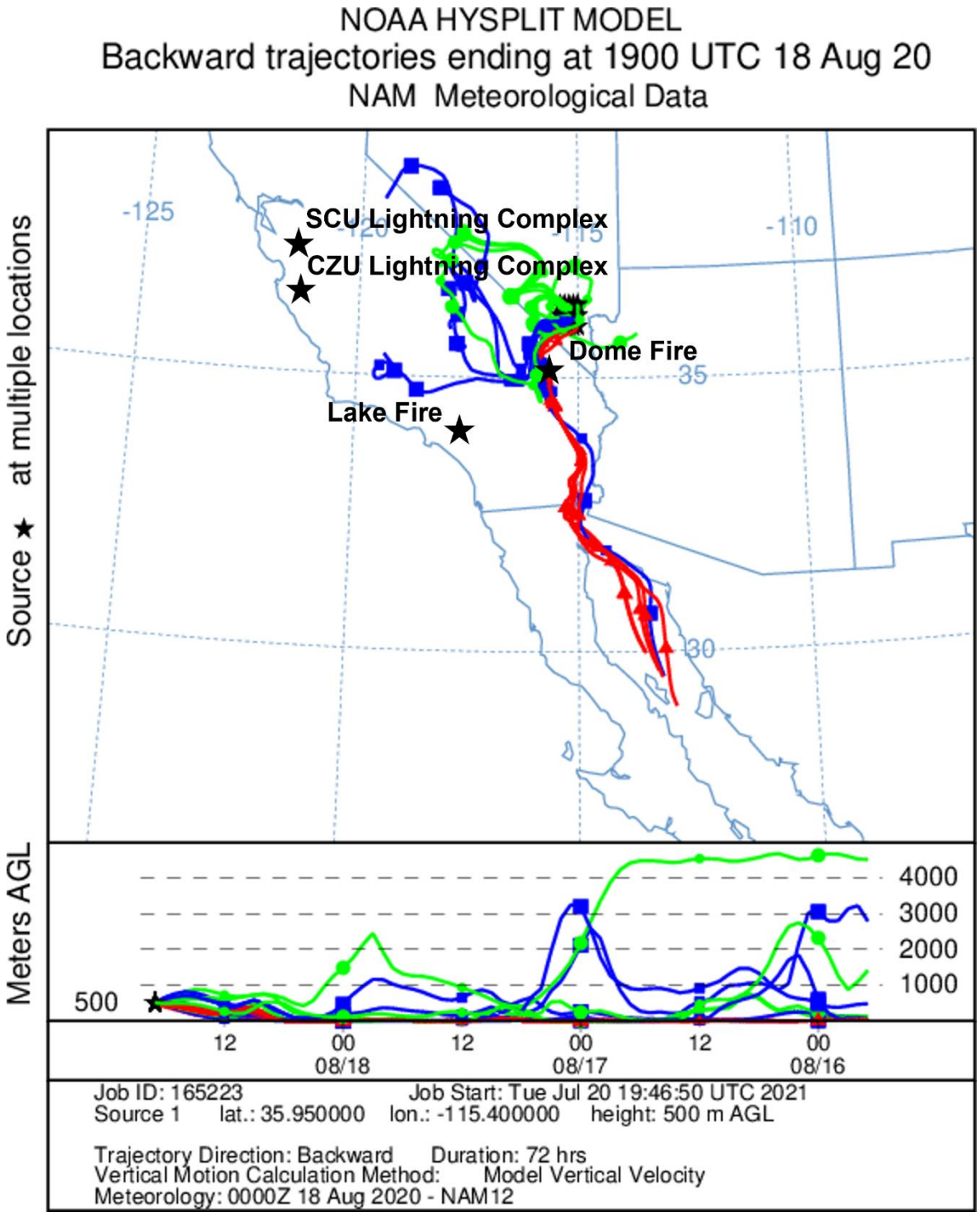

Figure 3-21. HYSPLIT back trajectory matrix. A 72-hour, NAM 12-km back trajectory matrix was initiated on August 18, 2020, at 19:00 UTC (11:00 a.m. LT) from an evenly spaced grid covering Las Vegas, Nevada, at 500 m above ground level.

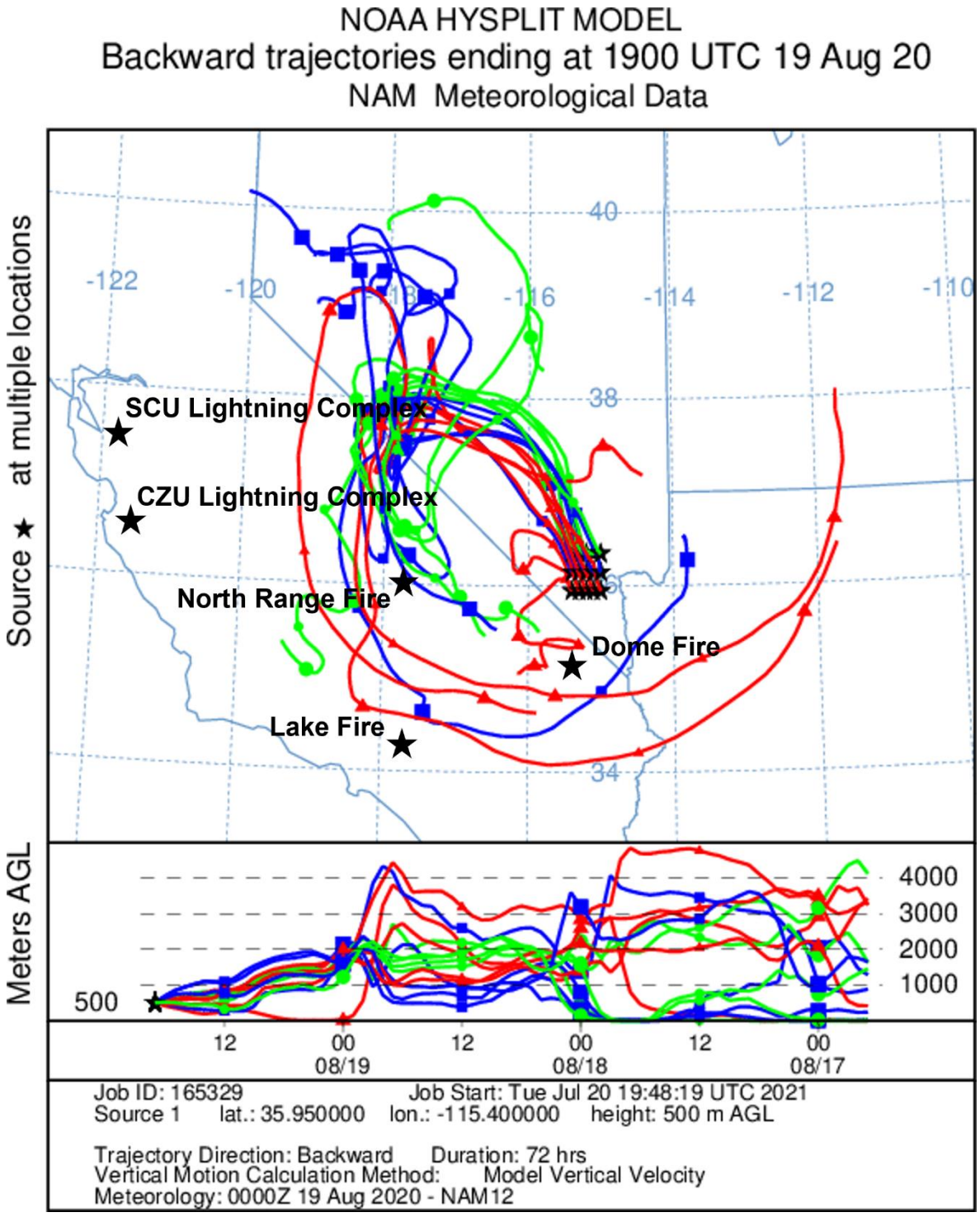

Figure 3-22. HYSPLIT back trajectory matrix. A 72-hour, NAM 12-km back trajectory matrix was initiated on August 19, 2020, at 19:00 UTC (11:00 a.m. LT) from an evenly spaced grid covering Las Vegas, Nevada, at 500 m above ground level.

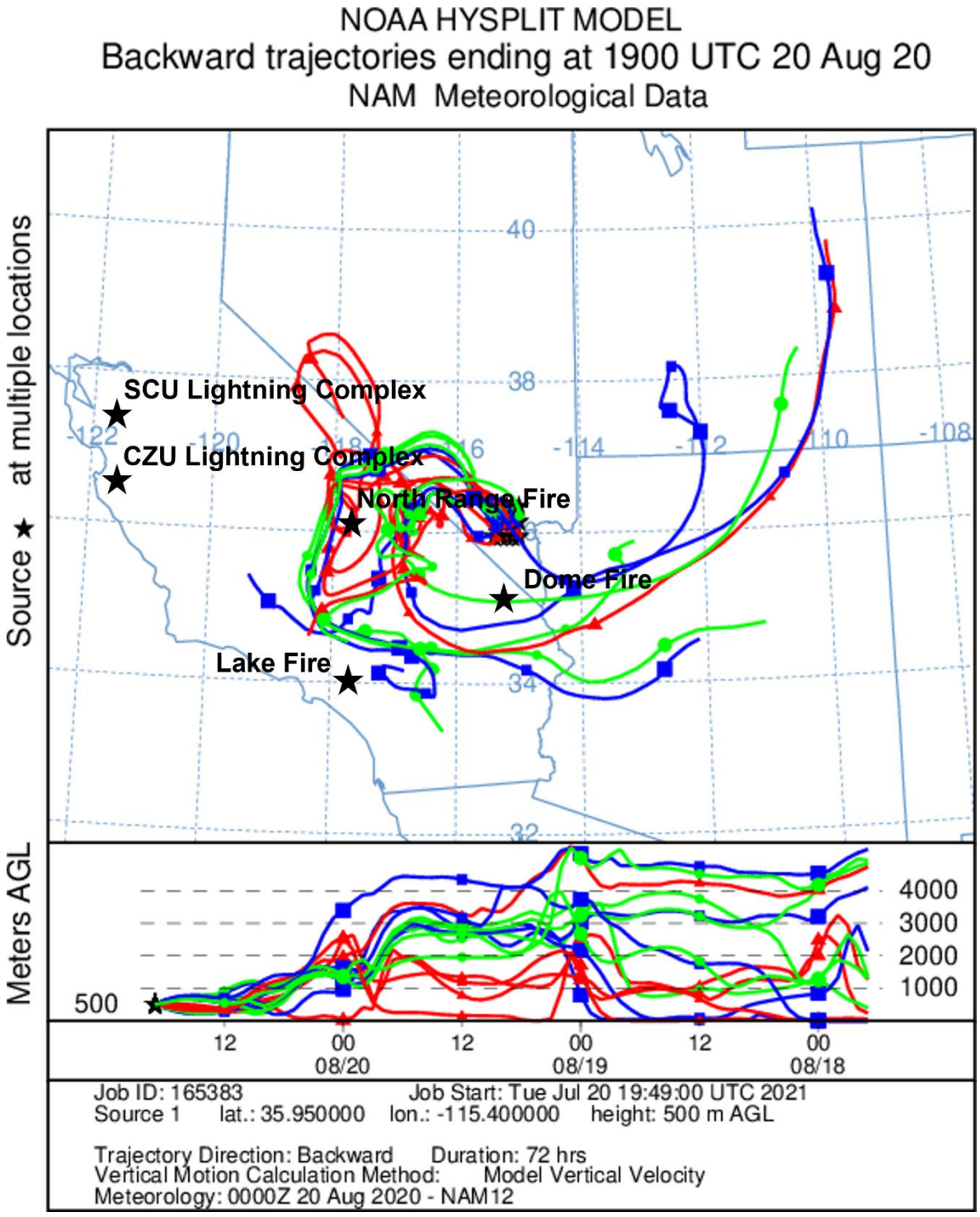

Figure 3-23. HYSPLIT back trajectory matrix. A 72-hour, NAM 12-km back trajectory matrix was initiated on August 20, 2020, at 19:00 UTC (11:00 a.m. LT) from an evenly spaced grid covering Las Vegas, Nevada, at 500 m above ground level.

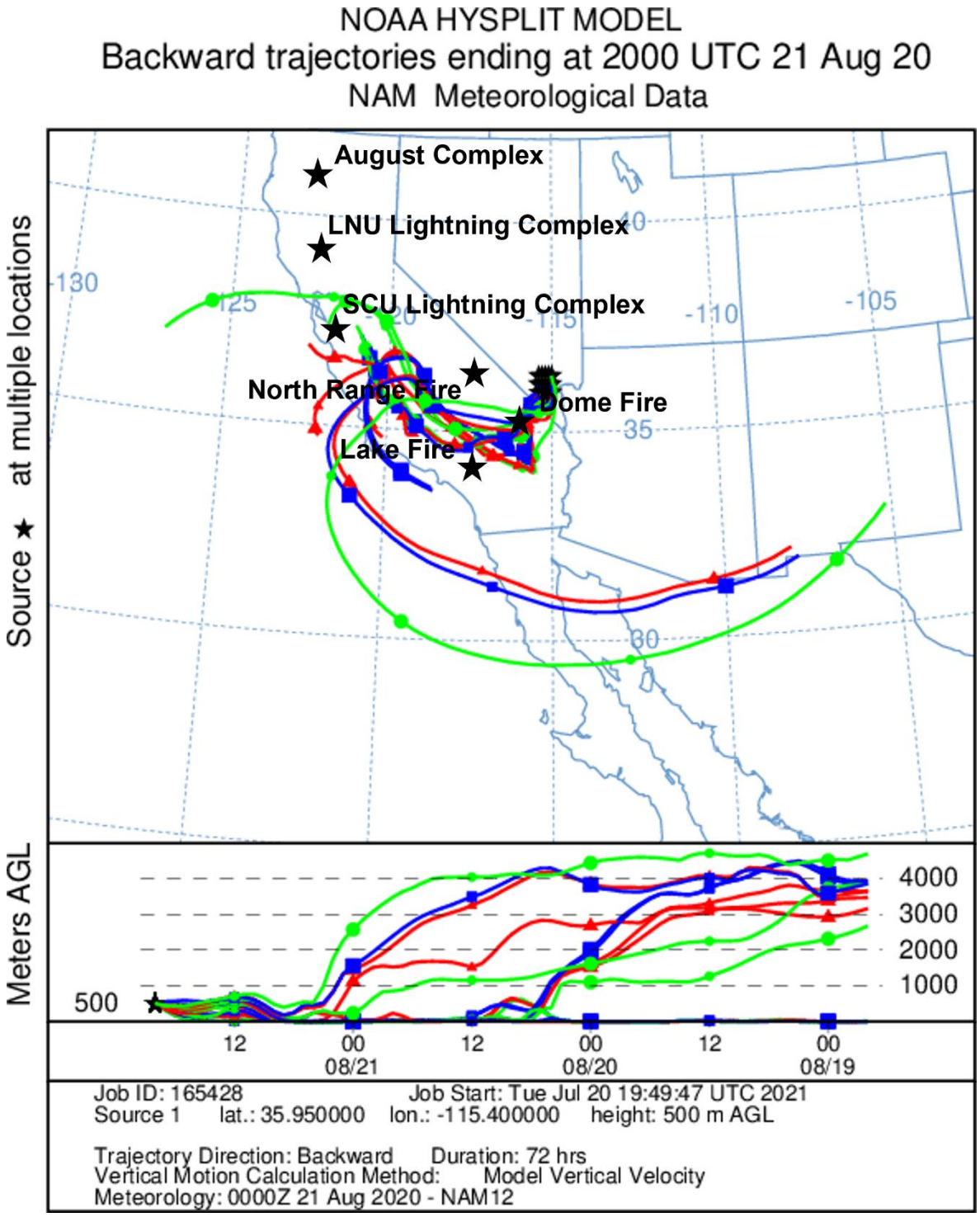

Figure 3-24. HYSPLIT back trajectory matrix. A 72-hour, NAM 12-km back trajectory matrix was initiated on August 21, 2020, at 20:00 UTC (12:00 p.m. LT) from an evenly spaced grid covering Las Vegas, Nevada, at 500 m above ground level.

Figures 3-25 through 3-28 show 72-hour back trajectory frequencies for multiple trajectories from near downtown Las Vegas at 500 m above ground level, initiated every 3 hours, starting on August 18-20, 2020, at 19:00 UTC (11:00 a.m. LT) and on August 21 at 20:00 UTC (12:00 p.m. LT). Between August 15 and 18, approximately 20% of the back trajectories starting near downtown Las Vegas passed over the Dome Fire (Figure 3-25). Between August 16 and 19, approximately 20%-30% of the back trajectories passed over the North Range Fire, and 1%-10% passed over the Lake Fire (Figure 3-26). Between August 17 and 20, approximately 10%-20% of the trajectories passed over the Dome Fire and near the Lake and North Range fires (Figure 3-27). Between August 18 and 21, approximately 30%-40% of the trajectories passed over the North Range Fire and 1%-10% passed over the Lake and Dome fires (Figure 3-28). The time evolution of transport directions observed in site-specific and matrix back trajectory model results are consistent with the trajectory results. Specifically, Figure 3-28 shows up to 40% of trajectories from the August 18-21 period passed over the Central Valley, coincident in time and location with the regional smoke plume from the northern California fires (Figures 3-13 through 3-16).

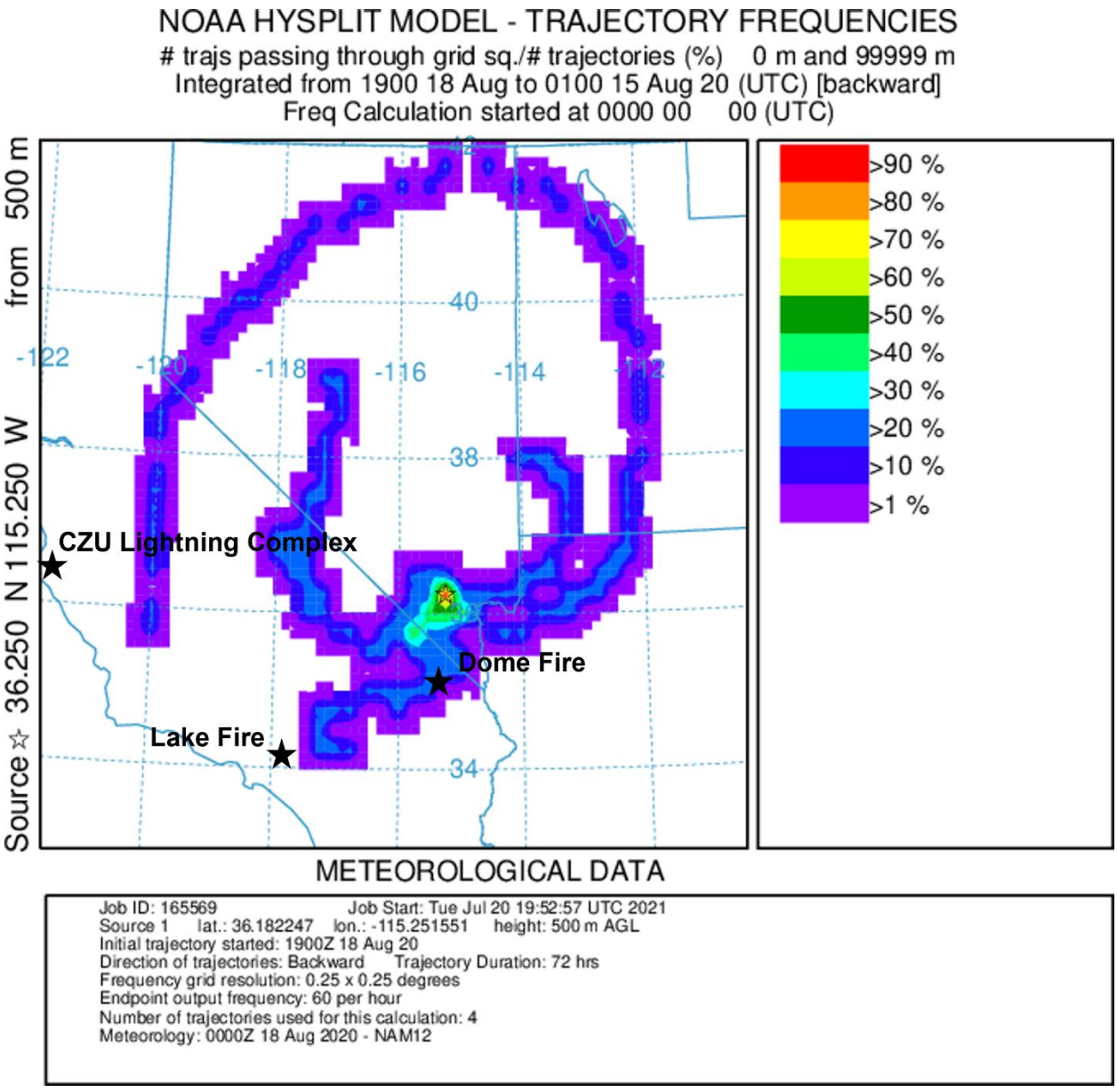

Figure 3-25. HYSPLIT back trajectory frequency. A 72-hour, NAM 12-km frequency of back trajectories was initiated on August 18, 2020, at 19:00 UTC (11:00 a.m. LT) from near downtown Las Vegas at 500 m above ground level. The colors within the frequency plot indicate the percent of trajectories that pass through a grid square.

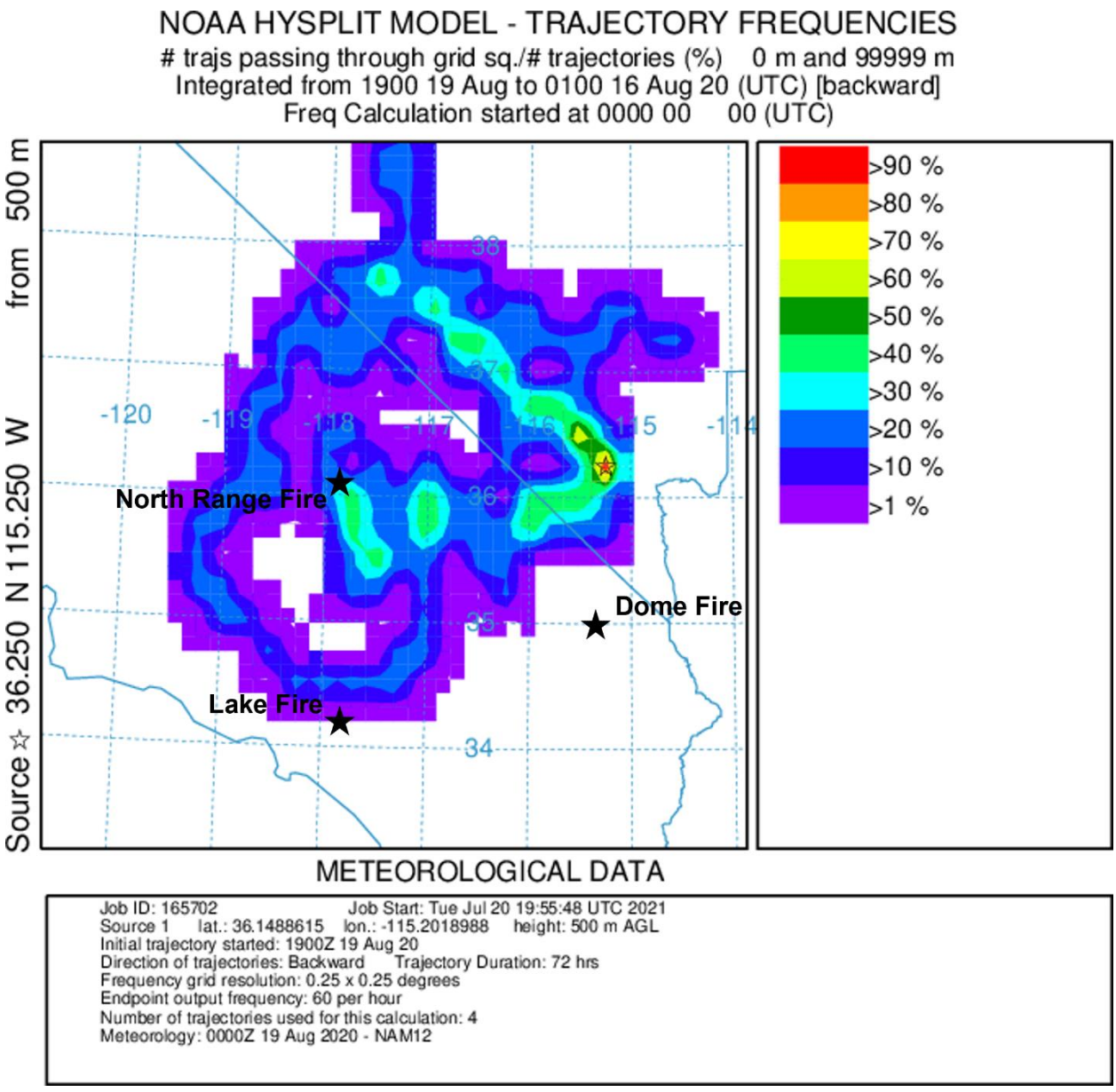

Figure 3-26. HYSPLIT back trajectory frequency. A 72-hour, NAM 12-km frequency of back trajectories was initiated on August 19, 2020, at 19:00 UTC (11:00 a.m. LT) from near downtown Las Vegas at 500 m above ground level. The colors within the frequency plot indicate the percent of trajectories that pass through a grid square.

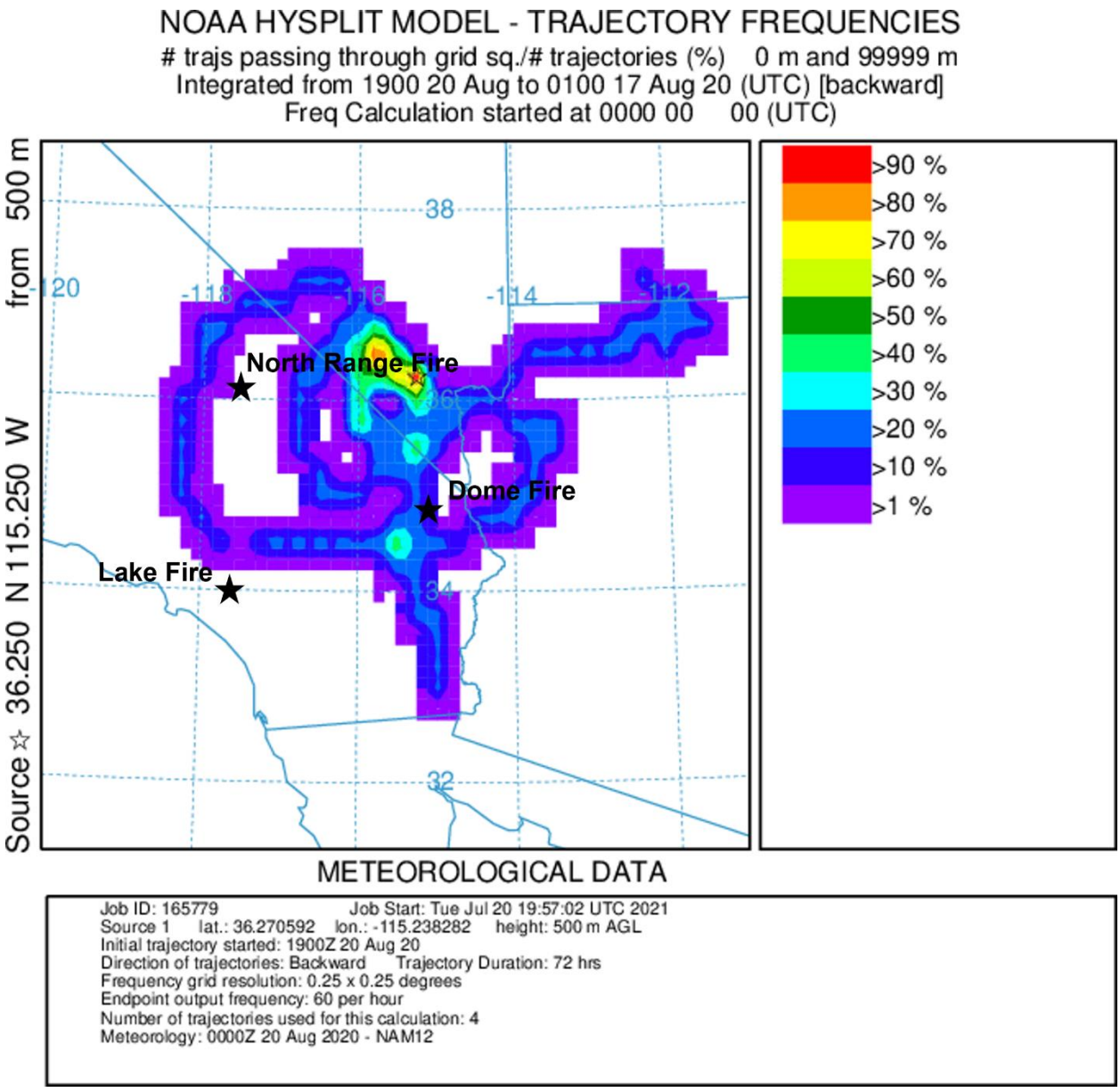

Figure 3-27. HYSPLIT back trajectory frequency. A 72-hour, NAM 12-km frequency of back trajectories was initiated on August 20, 2020, at 19:00 UTC (11:00 a.m. LT) from near downtown Las Vegas at 500 m above ground level. The colors within the frequency plot indicate the percent of trajectories that pass through a grid square.

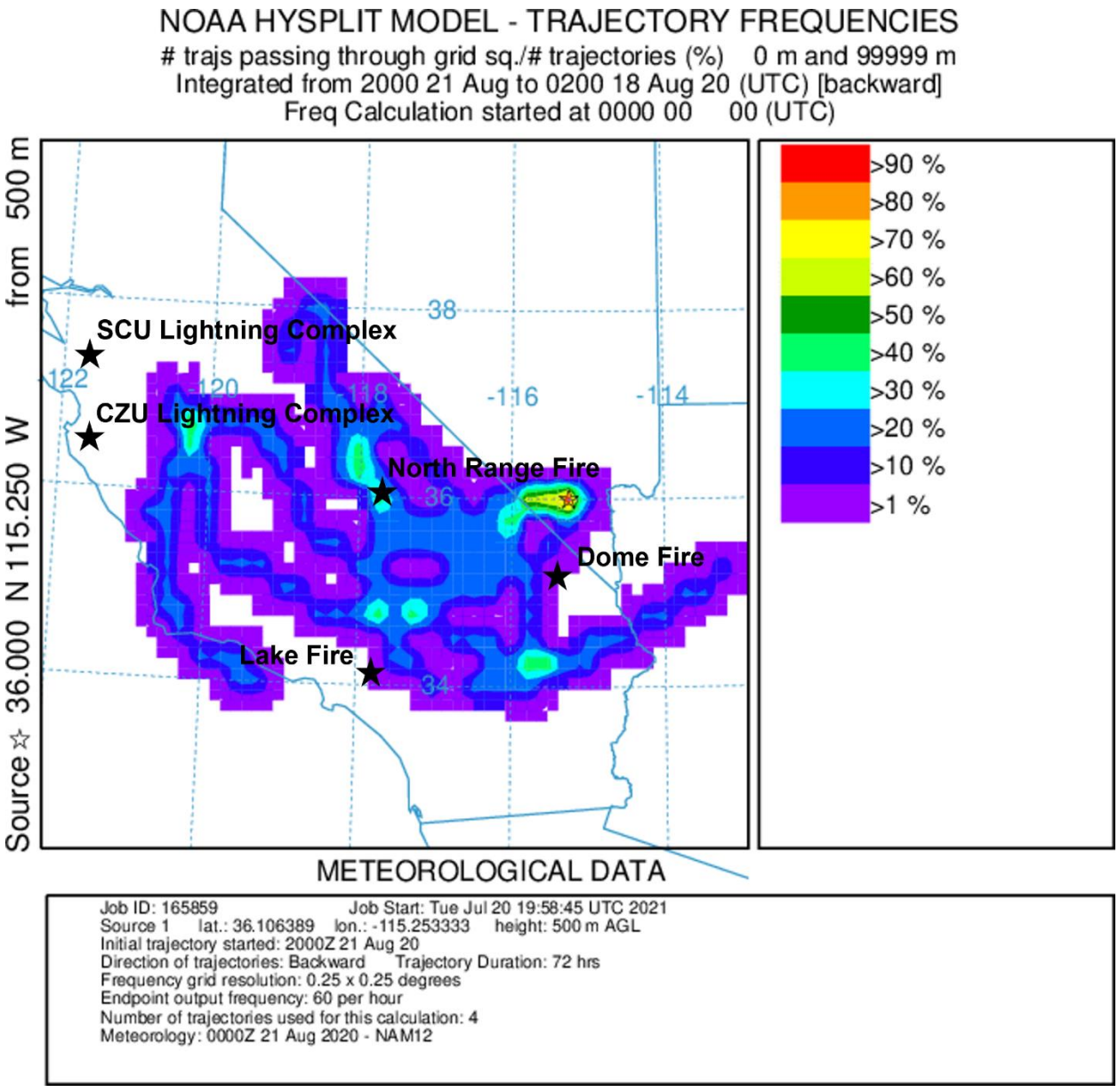

Figure 3-28. HYSPLIT back trajectory frequency. A 72-hour, NAM 12-km frequency of back trajectories was initiated on August 21, 2020, at 20:00 UTC (12:00 p.m. LT) from near downtown Las Vegas at 500 m above ground level. The colors within the frequency plot indicate the percent of trajectories that pass through a grid square.

Figures 3-29 through 3-35 show 72-hour forward trajectory matrices initiated at 100-1,000 m above ground level on August 16 through 21, 2020, from evenly spaced grids covering the Lake, North Range, or LNU Lightning Complex fires as representative locations covering the range of California fires contributing to the regional smoke plumes. First, these forward trajectories indicate that Lake Fire emissions were transported to Clark County from August 16-19, and a subset of forward trajectories reached the Clark County boundary layer on August 18-21 (Figures 3-29 through 3-32). Second, a subset of forward trajectories indicates that LNU Lightning Complex Fire emissions reached Clark County on August 20-22 (Figures 3-33 and 3-34). Third, a majority of forward trajectories indicate that North Range Fire emissions reached Clark County on August 20-22 (Figure 3-35).

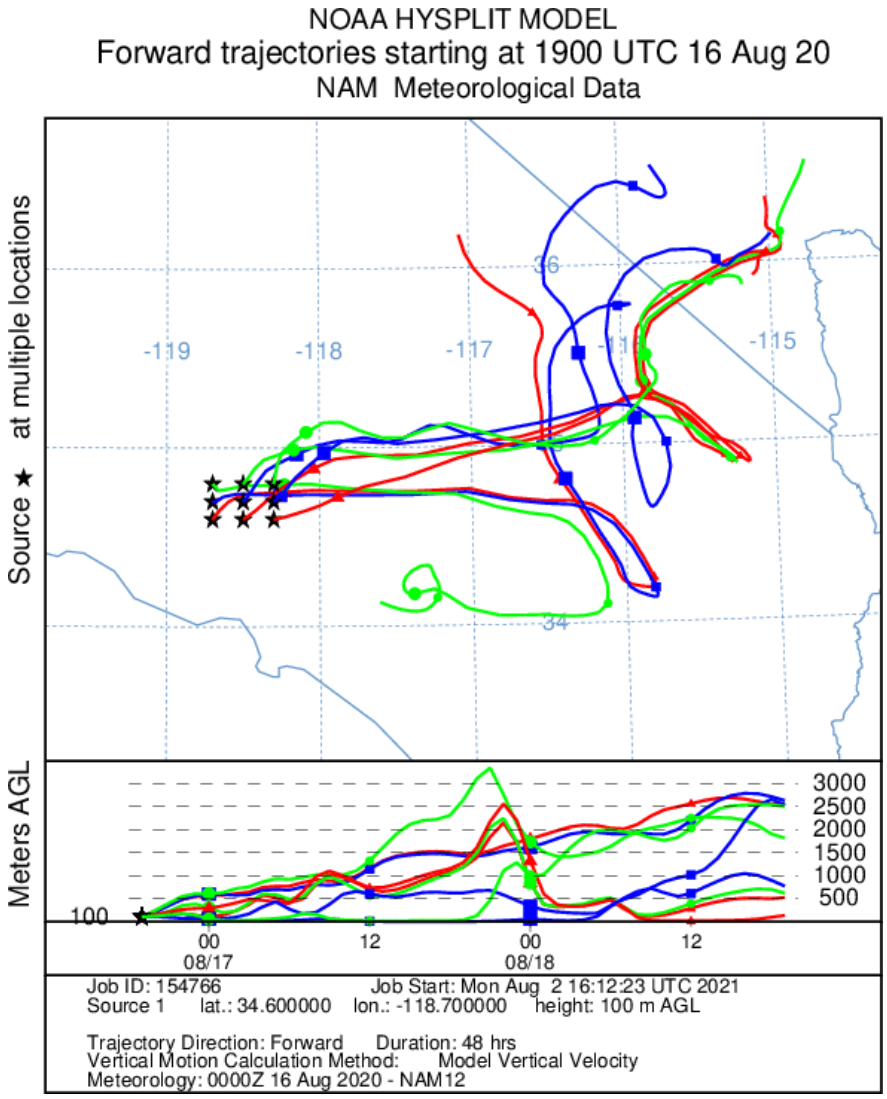

Figure 3-29. HYSPLIT forward trajectory matrix from the Lake Fire. A 72-hour, NAM 12-km forward trajectory matrix was initiated on August 16, 2020, at 19:00 UTC (11:00 a.m. LT) from an evenly spaced grid covering the Lake Fire at 100 m above ground level.

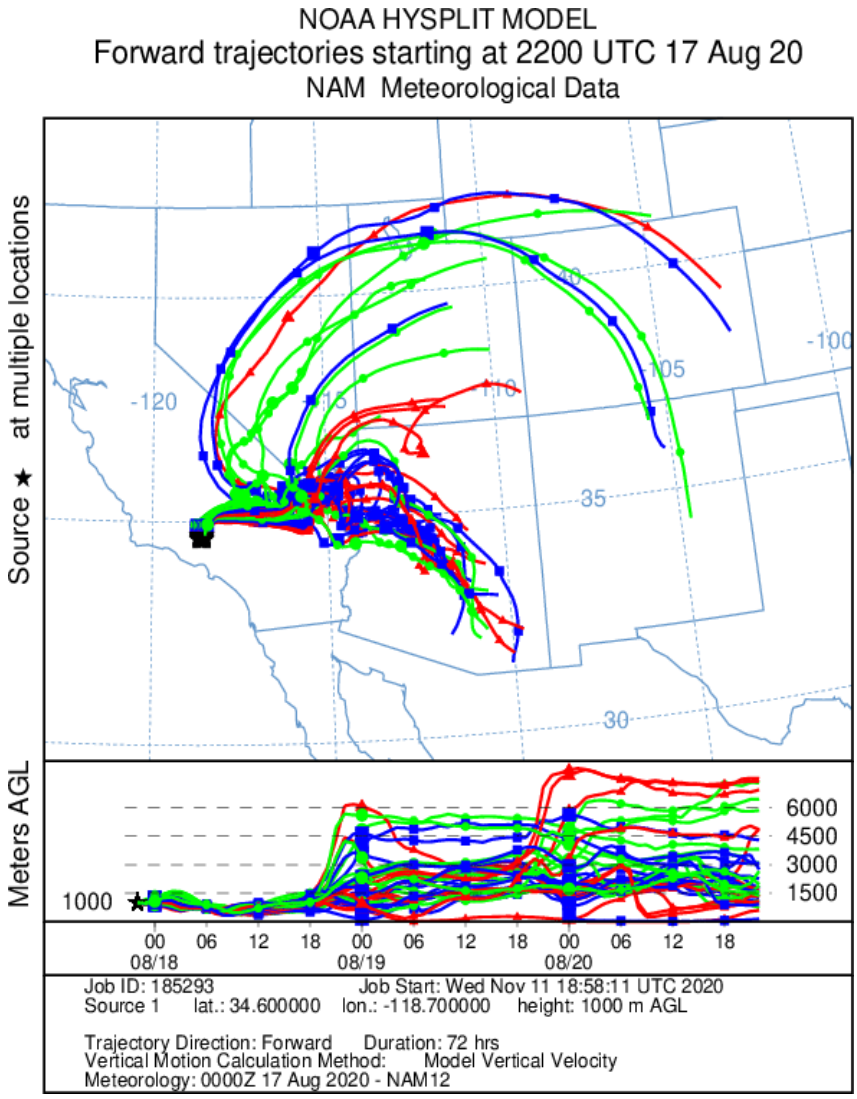

Figure 3-30. HYSPLIT forward trajectory matrix from the Lake Fire. A 72-hour, NAM 12-km forward trajectory matrix was initiated on August 17, 2020, at 22:00 UTC (2:00 p.m. LT) from an evenly spaced grid covering the Lake Fire at 1,000 m above ground level.

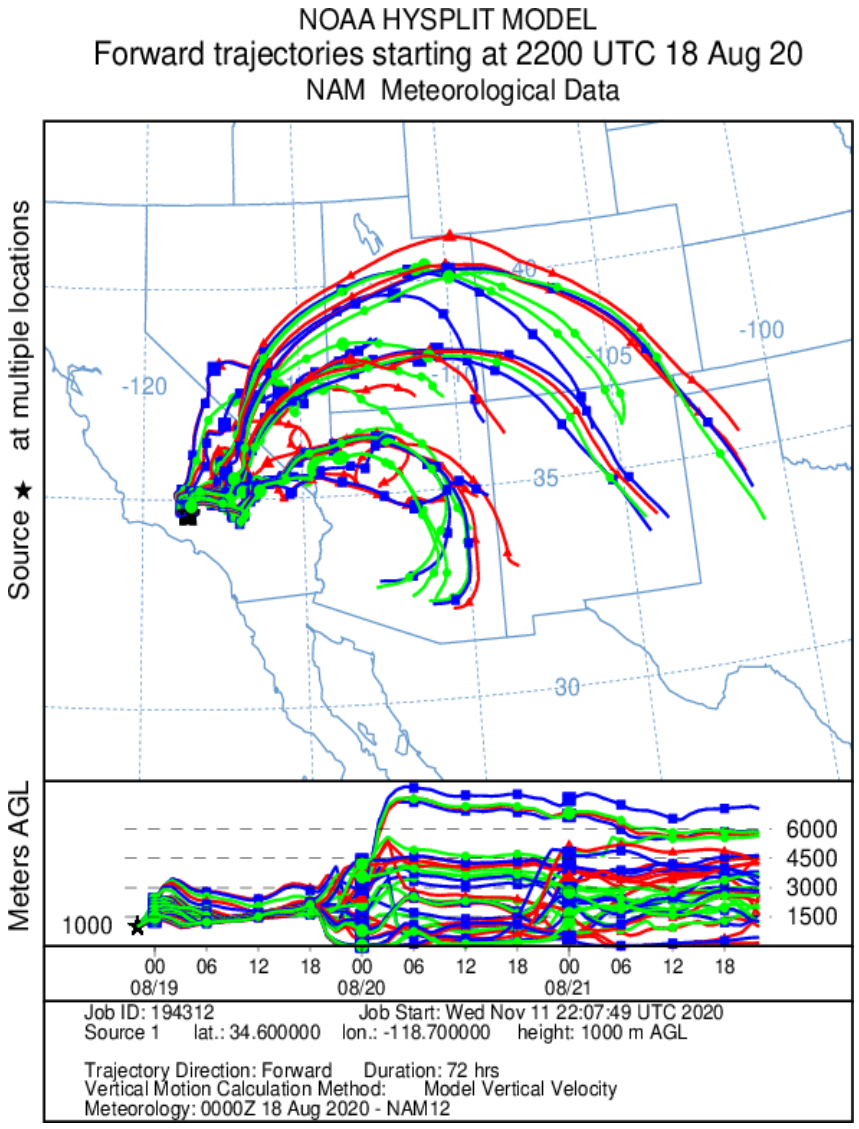

Figure 3-31. HYSPLIT forward trajectory matrix from the Lake Fire. A 72-hour, NAM 12-km forward trajectory matrix was initiated on August 18, 2020, at 22:00 UTC (2:00 p.m. LT) from an evenly spaced grid covering the Lake Fire at 1,000 m above ground level.

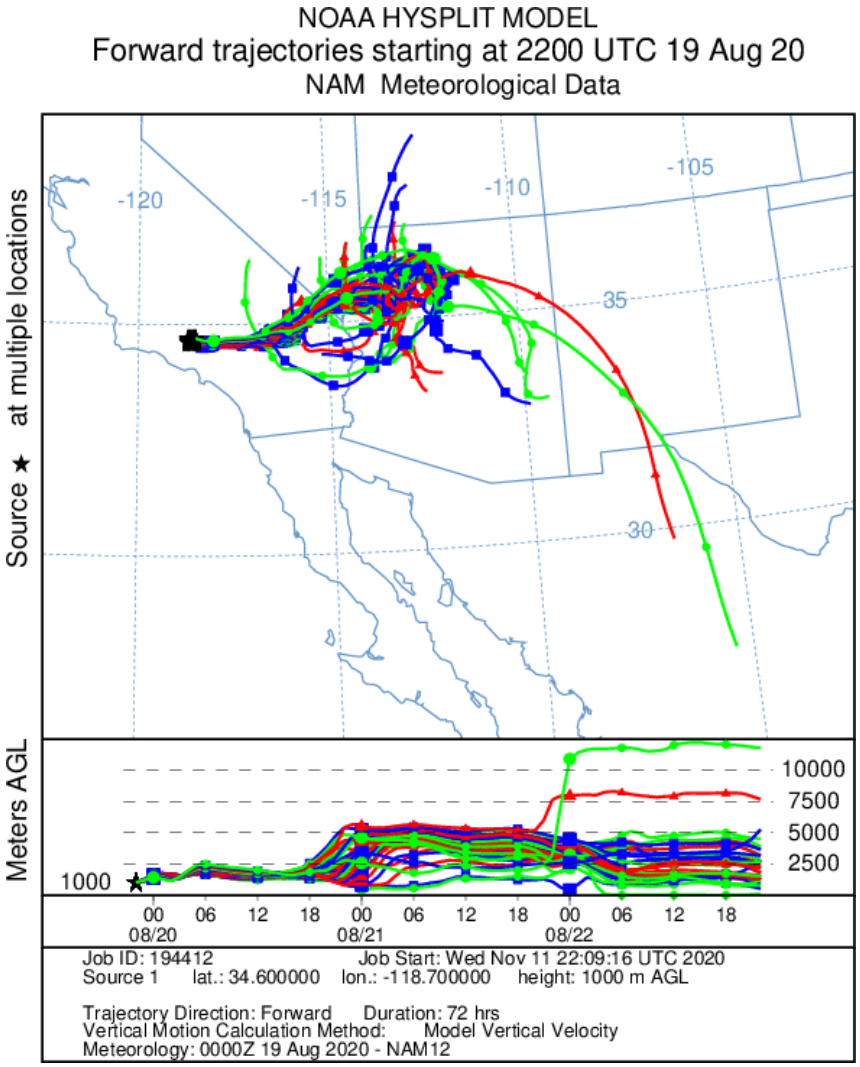

Figure 3-32. HYSPLIT forward trajectory matrix from the Lake Fire. A 72-hour, NAM 12-km forward trajectory matrix was initiated on August 19, 2020, at 22:00 UTC (2:00 p.m. LT) from an evenly spaced grid covering the Lake Fire at 1,000 m above ground level.

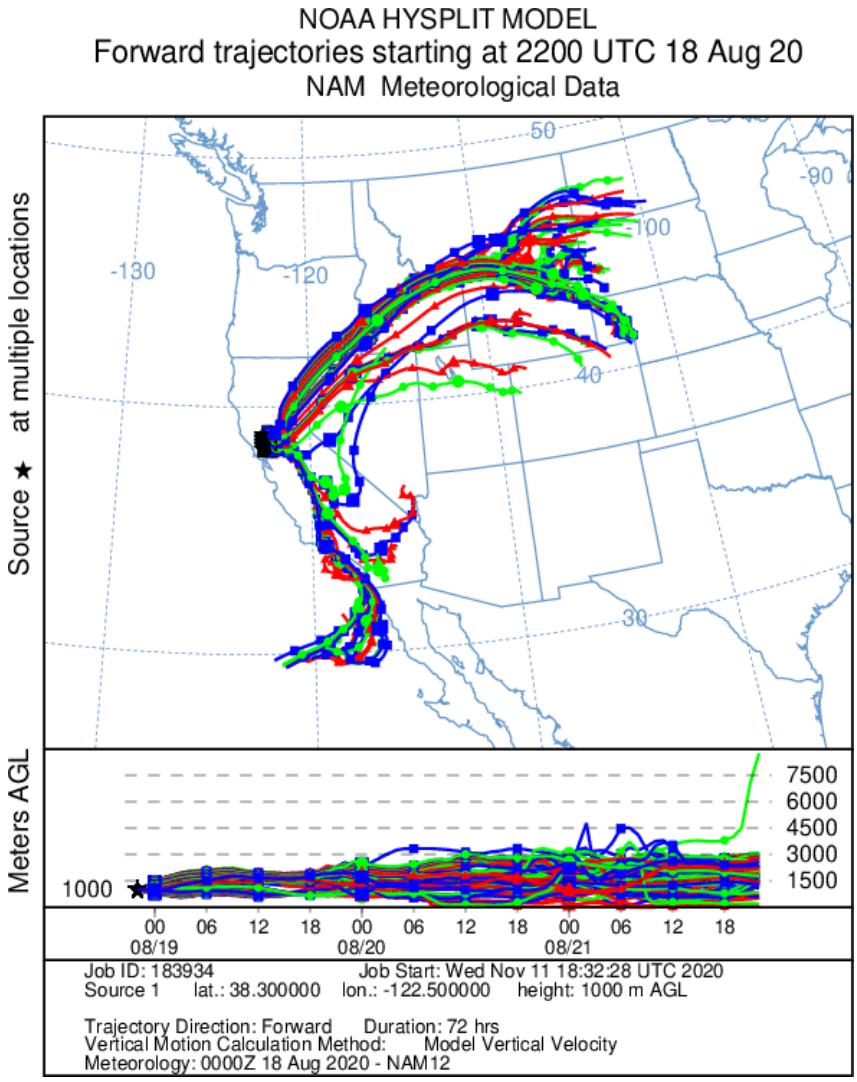

Figure 3-33. HYSPLIT forward trajectory matrix from the LNU Lightning Complex Fire. A 72-hour, NAM 12-km forward trajectory matrix was initiated on August 18, 2020, at 22:00 UTC (2:00 p.m. LT) from an evenly spaced grid covering the LNU Lightning Complex Fire at 1,000 m above ground level.

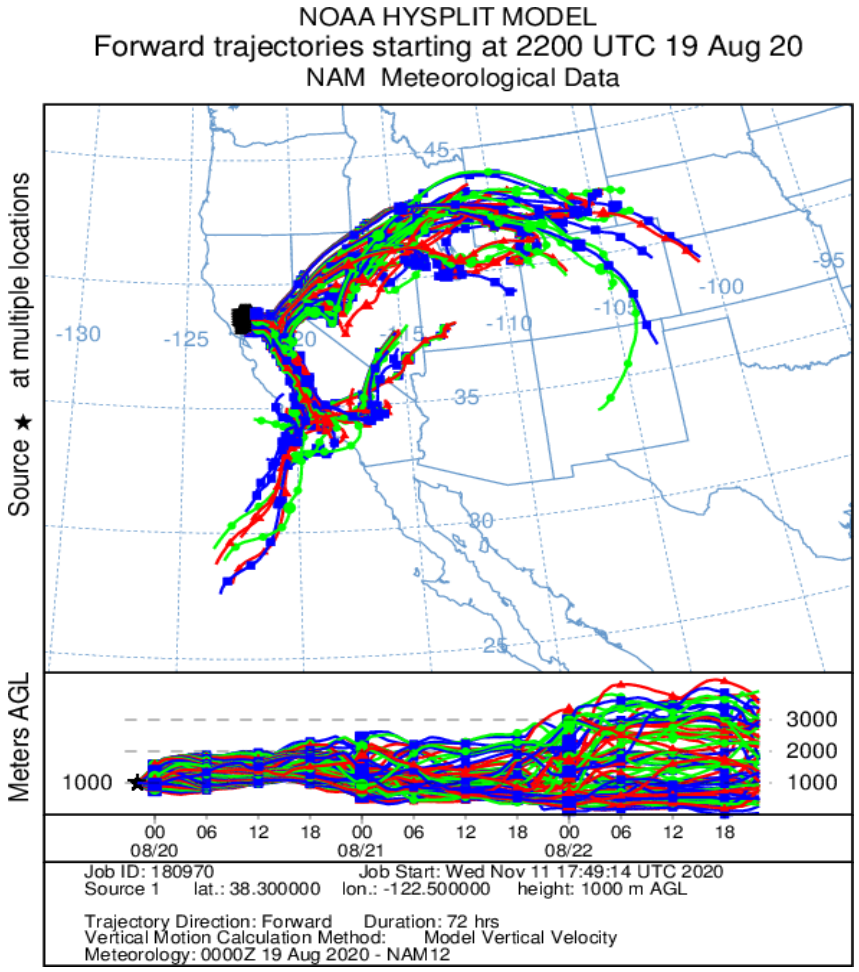

Figure 3-34. HYSPLIT forward trajectory matrix from the LNU Lightning Complex Fire. A 72-hour, NAM 12-km forward trajectory matrix was initiated on August 19, 2020, at 22:00 UTC (2:00 p.m. LT) from an evenly spaced grid covering the LNU Lightning Complex Fire at 1,000 m above ground level.

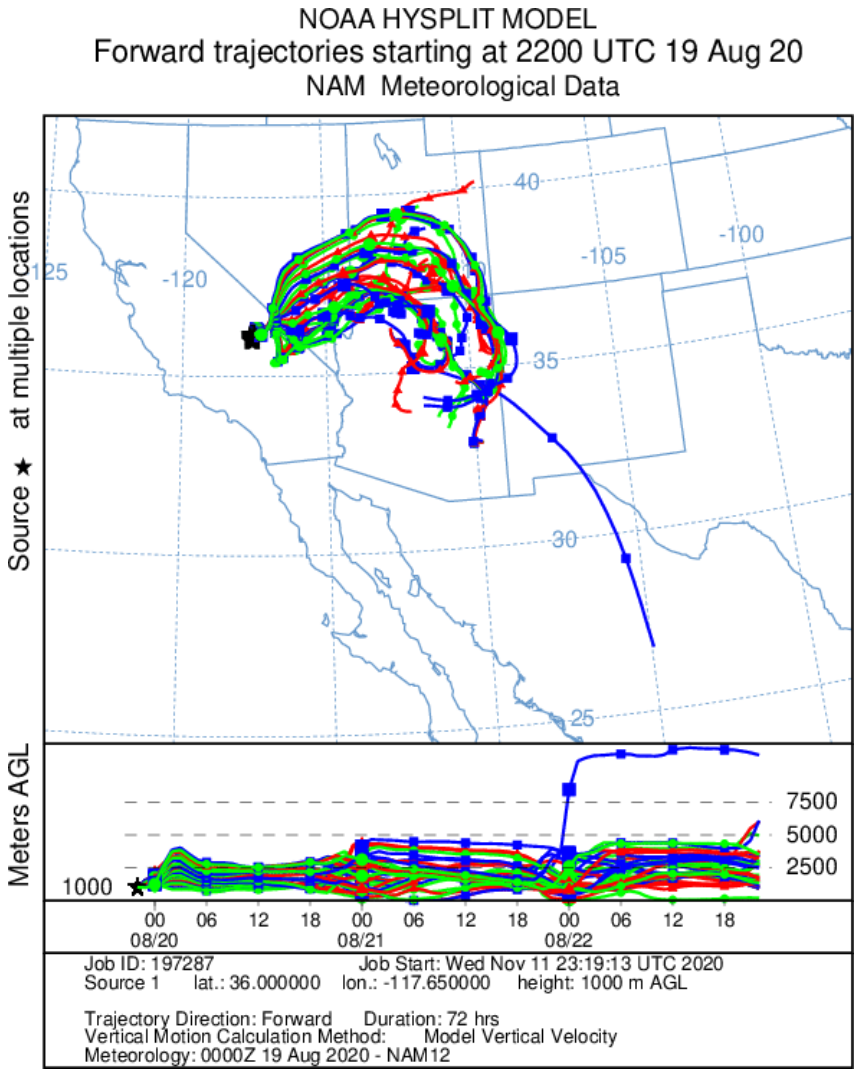

Figure 3-35. HYSPLIT forward trajectory matrix from the North Range Fire. A 72-hour, NAM 12-km forward trajectory matrix was initiated on August 19, 2020, at 22:00 UTC (2:00 p.m. LT) from an evenly spaced grid covering the North Range Fire at 1,000 m above ground level.

Forward dispersion modeling was initiated from all fires (i.e., August Complex, SCU Lightning Complex, CZU Lightning Complex, LNU Lightning Complex, Cold Springs Fire, River Fire, Carmel Fire, North Complex, Dolan Fire, North Range Fire, Dome Fire, Red Salmon Complex, Lake Fire, and Loyalton Fire [see Section 3.2.1 for a detailed fire map]) affecting the August 18-21 EE in Clark County using NAM 12-km meteorology. An equal number of tracer smoke particles were released from each fire based on the conceptual model timeline to help determine the timing and extent of smoke reaching Clark County by August 18, 19, 20, and 21. Because an equal number of smoke tracers are released from each fire, the tracer concentration is not relevant to actual smoke concentrations, only the absence or presence of the smoke tracer in a given area should be considered in this analysis. Particles were emitted at 500 m from each fire location hourly, and modeling was resolved to 0.05-degrees latitude and longitude grid spacing. Particles were allowed to

dry-deposit and leave the western U.S. domain, but were otherwise retained for five days, representing aged smoke. **Figure 3-36** shows the particulate tracer emissions and dispersion from all fires burning on August 17, 2020 (i.e., excluding the Dolan, North Range, and Cold Springs fires). Emissions and dispersion in this figure began on August 17 at 00:00 UTC and ended on August 19 00:00 UTC (or August 18 at 4:00 p.m. PST) for a total of 48 hours. This figure illustrates that smoke in the lower boundary layer from all fires burning on August 17 had spread north, east, and southward by the afternoon of August 18, creating widespread smoke coverage which encapsulated Clark County. **Figure 3-37** shows the particulate tracer emissions and dispersion from all fires burning on August 18, 2020, (i.e., excluding the North Range Fire) beginning on August 18 at 00:00 UTC and ending on August 20 at 00:00 UTC (or August 19 at 4:00 p.m. PST). Again, widespread smoke coverage from the fires burning on August 18 had reached Clark County by the afternoon of August 19. **Figures 3-38 and 3-39** show emissions and dispersion from all fires burning by August 19, 2020, (i.e., all 14 California fires identified previously) beginning on August 19 at 00:00 UTC and ending on August 21 at 00:00 UTC (or August 20 at 4:00 p.m. PST) and August 22 at 00:00 UTC (or August 21 at 4:00 p.m. PST), respectively. These figures show extensive smoke throughout the western U.S. from the large complex fires burning in California, with Clark County completely encapsulated by smoke on each day. The modeled smoke coverage is consistent with the visible and HMS smoke products from the same time period shown in Section 3.1.2. The presence of the smoke tracer in the lower boundary layer in Clark County on the EE date reinforces the other analyses presented in this section, and indicates that smoke (contributed by all fires listed) affected Clark County on the EE date.

Overall, the combination of backward trajectory, forward trajectory, and dispersion modeling results provides consistent evidence for the transport of wildfire smoke and ozone precursors from the large complex fires in California to Clark County, Nevada.

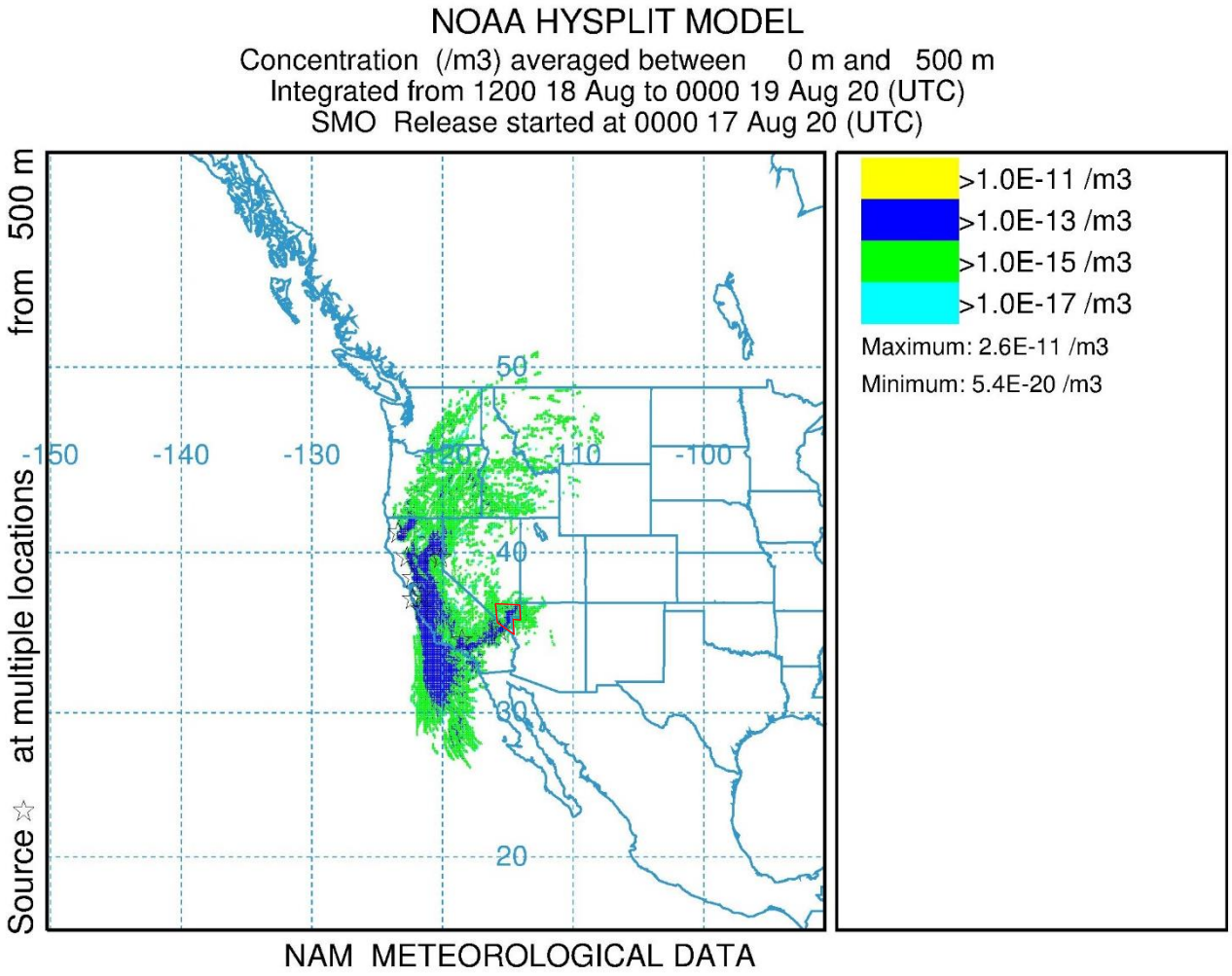

Figure 3-36. HYSPLIT forward dispersion modeling showing transport from all fires (shown as stars) burning on August 17, 2020. A 48-hour, NAM 12-km emissions and dispersion modeling of smoke tracer particles was initiated on August 17 at 00:00 UTC (4:00 p.m. PST on August 16) at 500 m above ground level. Hourly emission of tracers concluded on August 19 at 00:00 UTC (4:00 p.m. PST on August 18). The particulate smoke tracers shown here are integrated from August 18 at 12:00 UTC (4:00 a.m. PST on August 18) to August 19 at 00:00 UTC (4:00 p.m. PST on August 18) and from 0 to 500 m above ground level. The approximate outline of Clark County is shown in red.

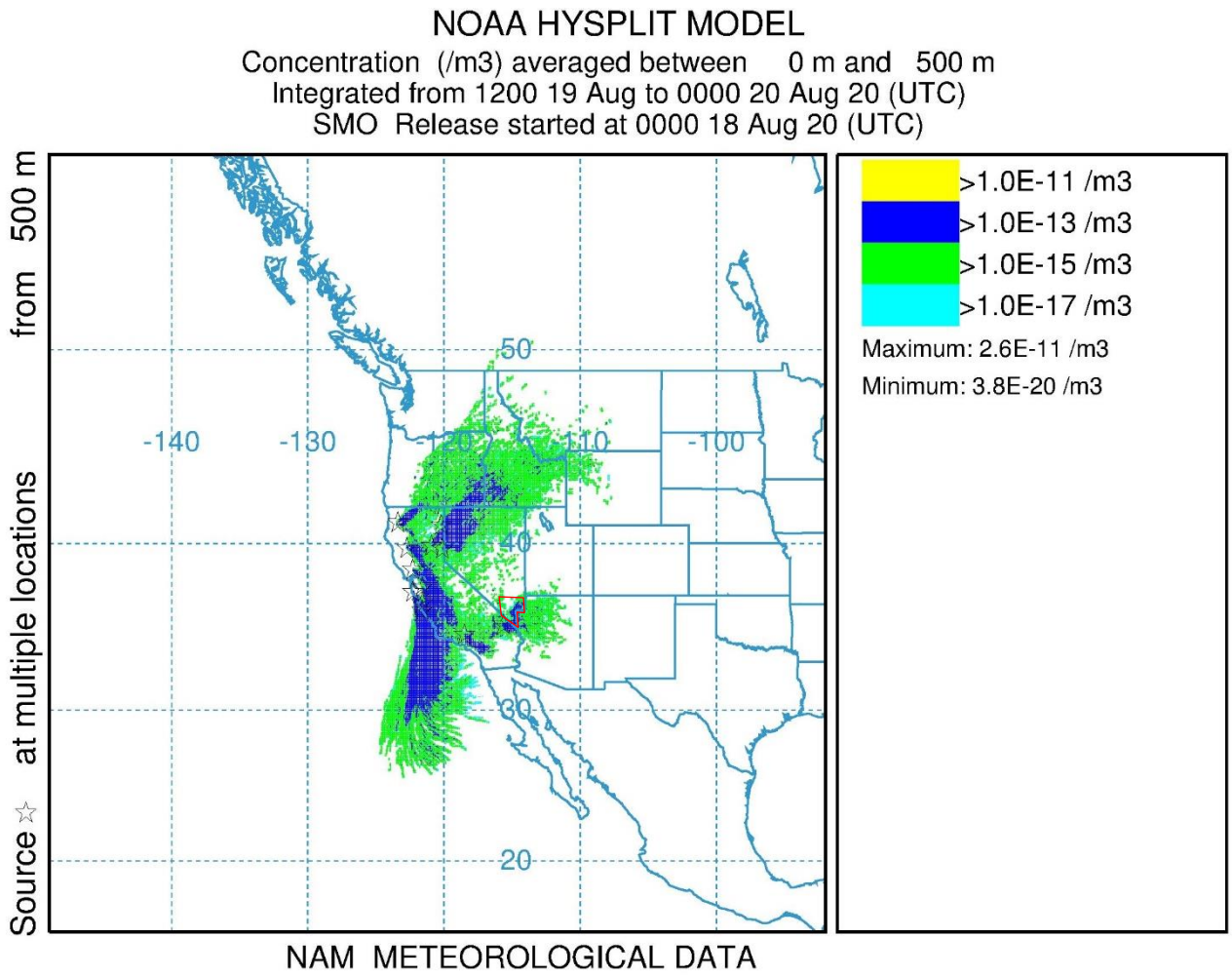

Figure 3-37. HYSPLIT forward dispersion modeling showing transport from all fires (shown as stars) burning on August 18, 2020. A 48-hour, NAM 12-km emissions and dispersion modeling of smoke tracer particles was initiated on August 18 at 00:00 UTC (4:00 p.m. PST on August 17) at 500 m above ground level. Hourly emission of tracers concluded on August 20 at 00:00 UTC (4:00 p.m. PST on August 19). The particulate smoke tracers shown here are integrated from August 19 at 12:00 UTC (4:00 a.m. PST on August 19) to August 20 at 00:00 UTC (4:00 p.m. PST on August 19) and from 0 to 500 m above ground level. The approximate outline of Clark County is shown in red.

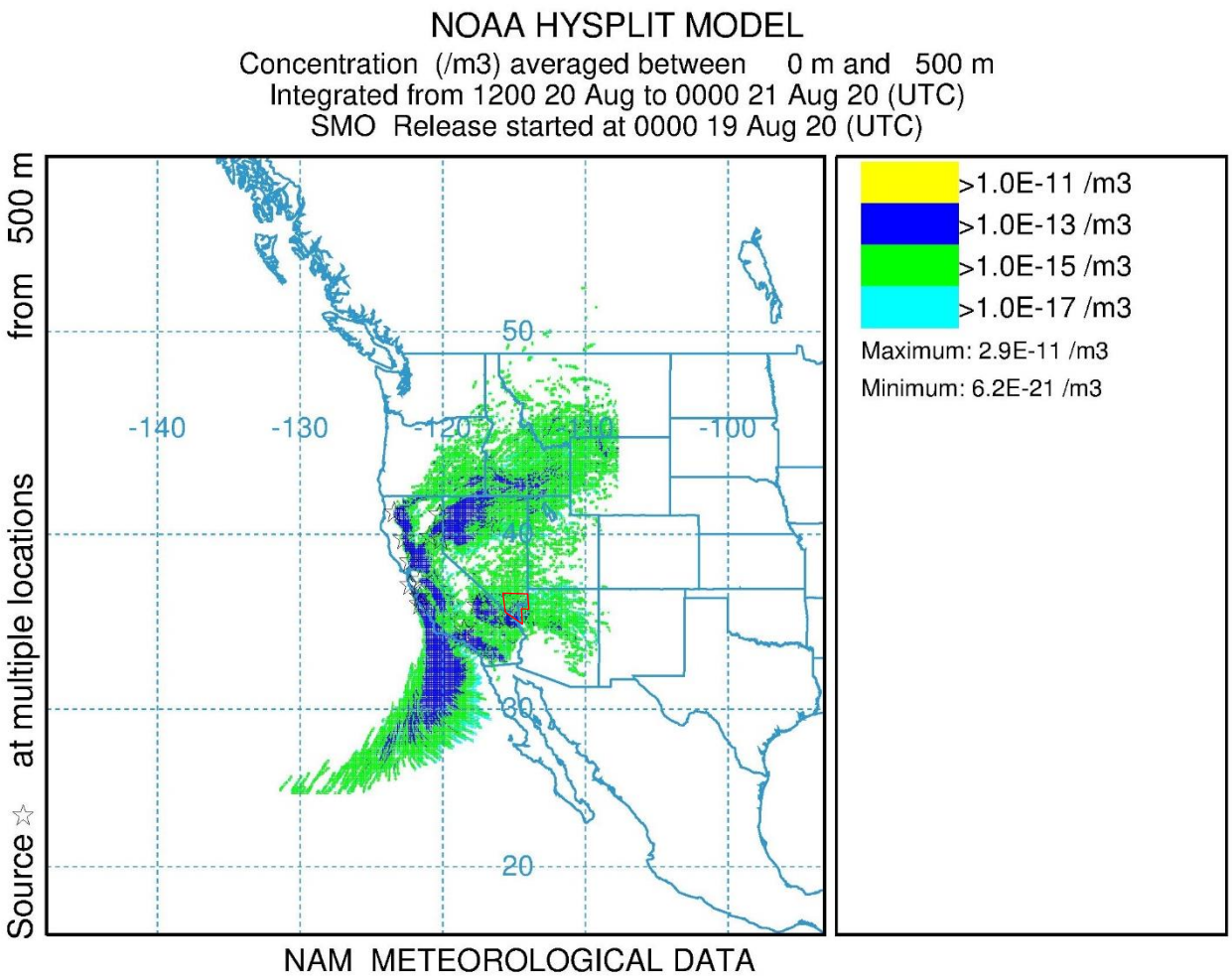

Figure 3-38. HYSPLIT forward dispersion modeling showing transport from all fires (shown as stars) burning on August 19, 2020. A 48-hour, NAM 12-km emissions and dispersion modeling of smoke tracer particles was initiated on August 19 at 00:00 UTC (4:00 p.m. PST on August 18) at 500 m above ground level. Hourly emission of tracers concluded on August 21 at 00:00 UTC (4:00 p.m. PST on August 20). The particulate smoke tracers shown here are integrated from August 20 at 12:00 UTC (4:00 a.m. PST on August 20) to August 21 at 00:00 UTC (4:00 p.m. PST on August 20) and from 0 to 500 m above ground level. The approximate outline of Clark County is shown in red.

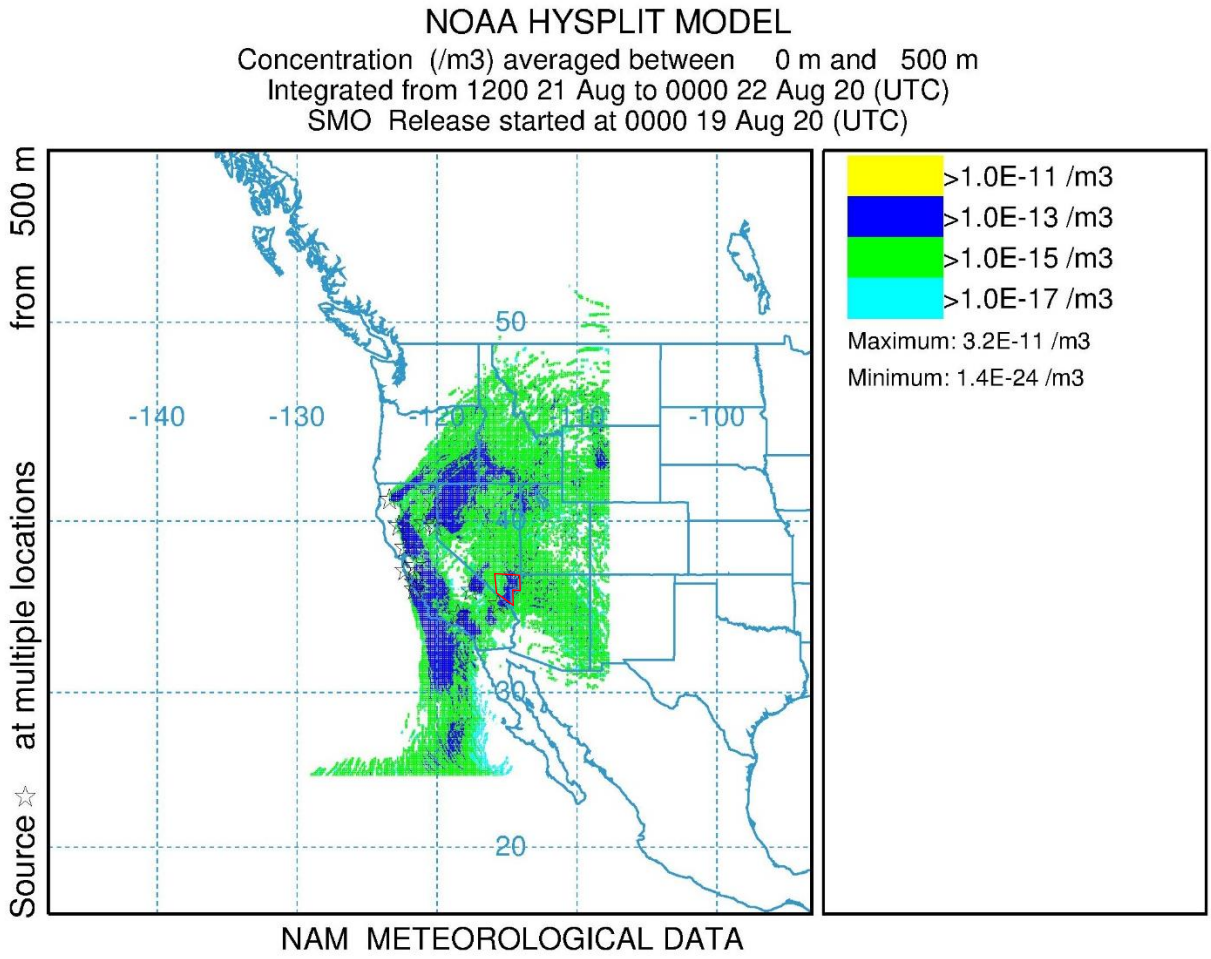

Figure 3-39. HYSPLIT forward dispersion modeling showing transport from all fires (shown as stars) burning on August 19, 2020. A 72-hour, NAM 12-km emissions and dispersion modeling of smoke tracer particles was initiated on August 19 at 00:00 UTC (4:00 p.m. PST on August 18) at 500 m above ground level. Hourly emission of tracers concluded on August 22 at 00:00 UTC (4:00 p.m. PST on August 21). The particulate smoke tracers shown here are integrated from August 21 at 12:00 UTC (4:00 a.m. PST on August 21) to August 22 at 00:00 UTC (4:00 p.m. PST on August 21) and from 0 to 500 m above ground level. The approximate outline of Clark County is shown in red.

3.1.4 Media Coverage and Ground Images

News, weather, and environmental organizations provided widespread coverage of the effects of smoky conditions on air quality in Clark County. On August 18, *8 News Now*, a local Las Vegas news organization, reported on the issuance of a smoke and ozone advisory by Clark County Department of Environment and Sustainability (DES) (https://www.8newsnow.com/news/local-news/air-quality-advisory-issued-for-tuesday-and-wednesday-due-to-wildfire-smoke/). The article cites a tweet

posted by Clark County DES (Figure 3-40) noting the Dome wildfire in Mojave National Preserve as the source of surface-level smoke expected for August 18 and August 19 (https://twitter.com/SustainClarkCty/status/1295781949731008512). In a follow up article on August 21, *8 News Now* reports that in addition to the fire in Mojave National Preserve, "hundreds of wildfires burning in California" contributed to the smoky conditions experienced in Clark County." (https://www.8newsnow.com/news/local-news/haze-hangs-over-las-vegas-valley/) The smoke advisory issued by Clark County DES on August 18, as well as the extensions issued on August 20 and 21, are provided in Appendix A. Additionally, 40 CFR 50.14(c)(1)(i) requires that air agencies must "notify the public promptly whenever an event occurs or is reasonably anticipated to occur which may result in the exceedance of an applicable air quality standard" in accordance with the mitigation requirement at 40 CFR 51.930(a)(1). Appendix A provides further details on Clark County Department of Environment and Sustainability's public notification for the potential exceptional event during August 18-21, 2020.

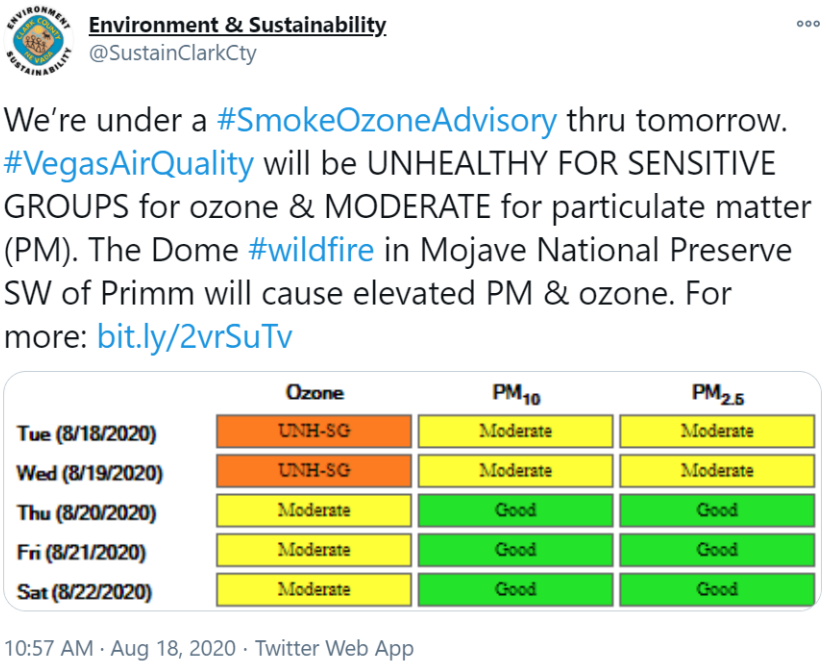

Figure 3-40. Tweet posted on August 18 by the Clark County DES reporting a smoke and ozone advisory in Clark County.

Wildfire smoke persisted through the original advisory, prompting the Clark County DES to extend the smoke and ozone advisory until August 23. KXNT Radio reported on this extension, writing "the Clark County Department of Environment and Sustainability (DES) is extending its advisory through Sunday for elevated levels of smoke and ozone due to the regional wildfires throughout the southwest U.S." (https://kxnt.radio.com/articles/press-release/county-extends-smoke-ozone-advisory-through-the-weekend) Similarly, on August 21 the Las Vegas Review Journal covered the

effects of wildfire smoke from numerous fires throughout the west (https://www.reviewjournal.com/local/weather/smoke-blots-out-las-vegas-sunrise-air-advisory-issued-through-weekend-2100432/). The extent of the smoke impact in Las Vegas is summarized well by the line, "shortly after sunrise, the sun was not visible in the Las Vegas sky because of extreme haze, smoke and ozone."

Ground images from the Clark County Department of Environment and Sustainability, Division of Air Quality's visibility cameras, located on the roof of the M Hotel in Las Vegas, clearly show the smoky conditions that persisted on from August 18 through August 21 (**Figures 3-41 through 3-44**). Each mosaic shows an image from one of the four event days as well as an image on a clear day (May 21, 2020) for comparison. When compared to images taken on a clear day, the event-day images show drastically reduced visibility and an opaque gray haze in every direction due to wildfire smoke, especially on August 21.

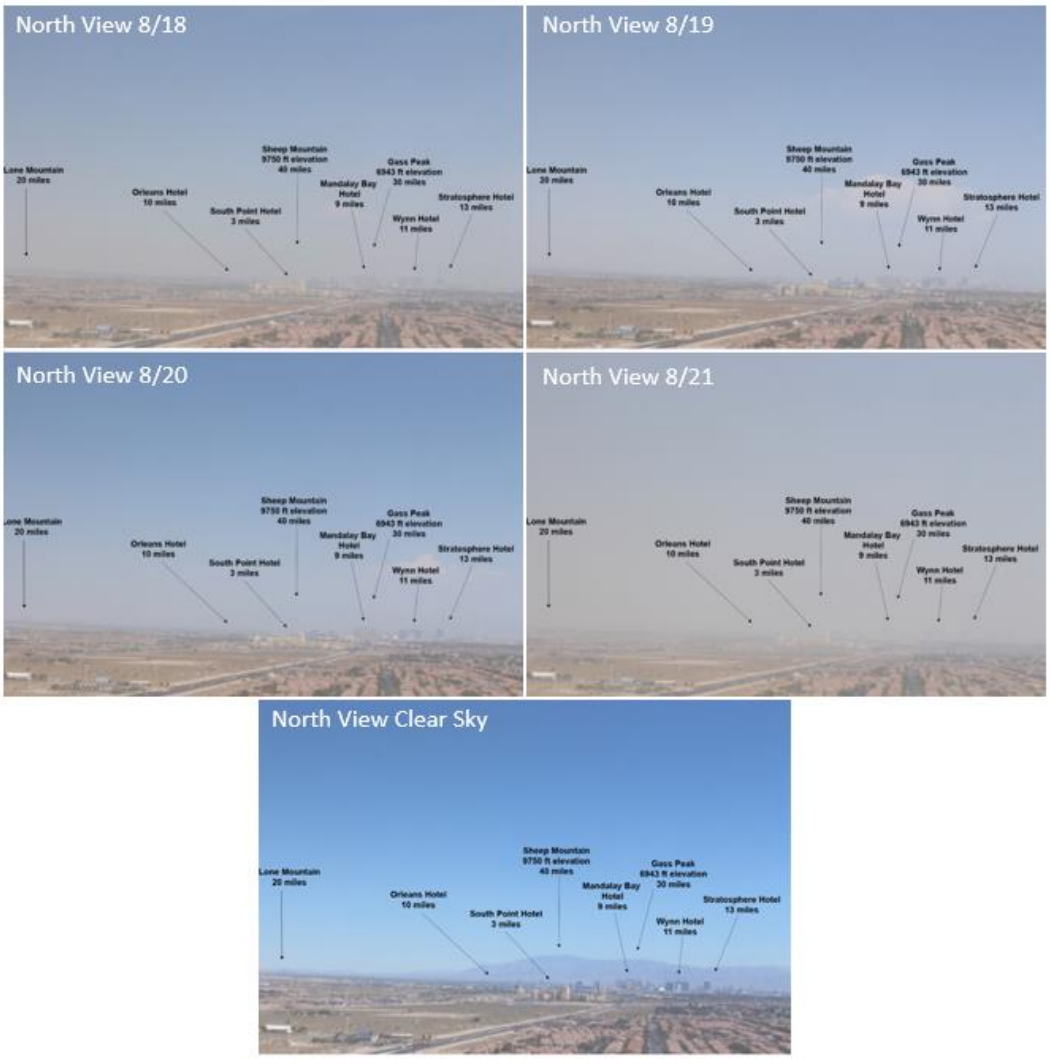

Figure 3-41. Clark County visibility images taken in the northern viewing direction. Images taken from webcams set up in Clark County are shown for the EE on August 18 through August 21 as well as on a clear day (May 21, 2020). Each image is labeled with landmarks.

Figure 3-42. Clark County visibility images taken in the northwestern viewing direction. Images taken from webcams set up in Clark County are shown for the EE on August 18 through August 21 as well as on a clear day (May 21, 2020). Each image is labeled with landmarks.

Figure 3-43. Clark County visibility images taken in the southern viewing direction. Images taken from webcams set up in Clark County are shown for the EE on August 18 through August 21 as well as on a clear day (May 21, 2020). Each image is labeled with landmarks.

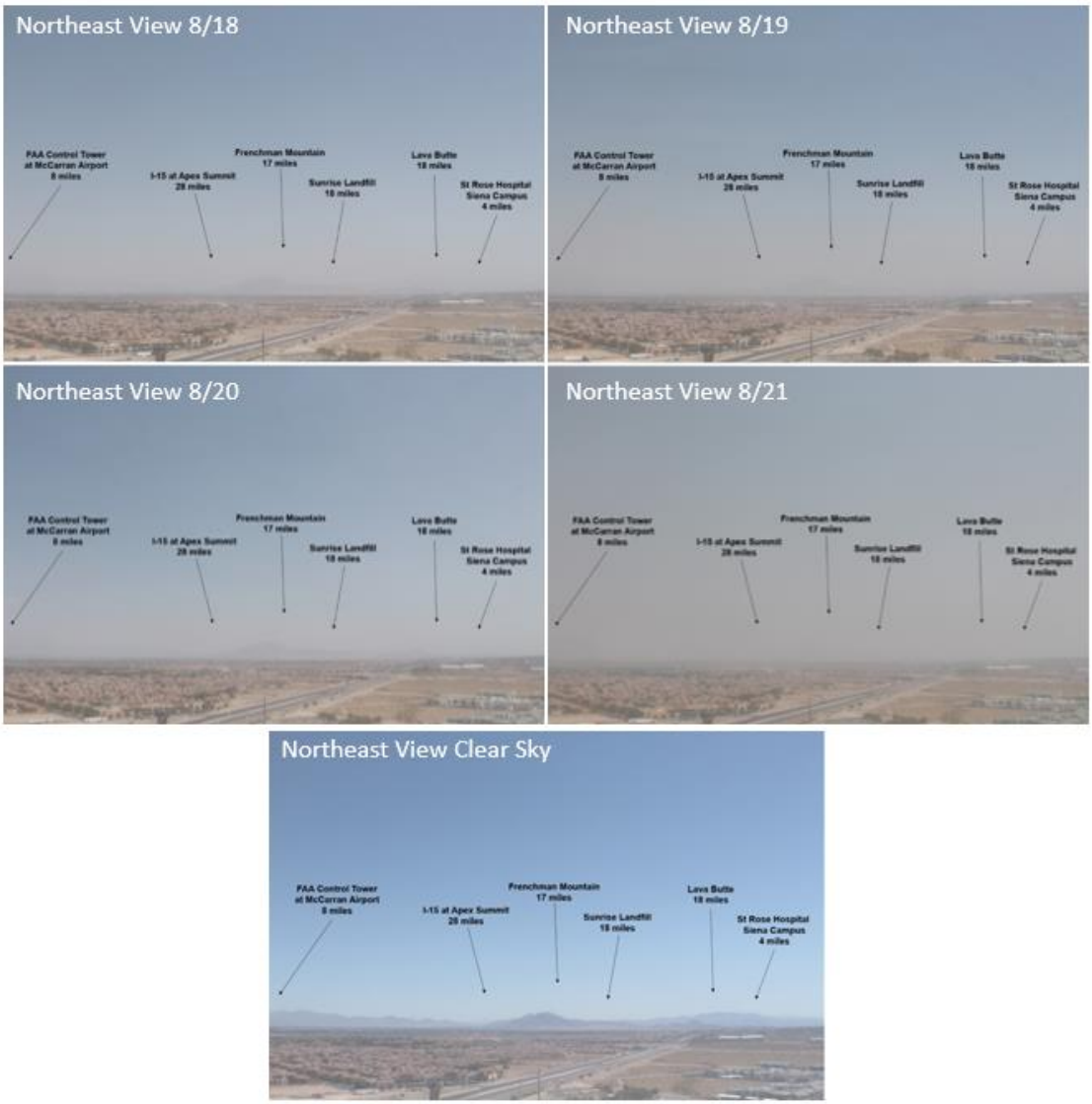

Figure 3-44. Clark County visibility images taken in the northeastern viewing direction. Images taken from webcams set up in Clark County are shown for the EE on August 18 through August 21 as well as on a clear day (May 21, 2020). Each image is labeled with landmarks.

3.2 Tier 2 Analyses

3.2.1 Key Factor #1: Q/d Analysis

The exceptional event guidance (U.S. Environmental Protection Agency, 2016) describes a method used to relate the quantity of smoke emissions and distance of the fire to an exceeding monitor. The resulting quantity, called Q/d, may be used to screen fires that meet a conservative threshold of air

quality impacts.[3] This section provides the results of the Q/d analyses for fires that were likely to have contributed to the August 18-21 ozone event in Clark County. Based on media coverage, transport analysis, and ground/satellite-based analyses in Section 3.1, multiple large complex, lightning-initiated wildfires in California (i.e., Red Salmon Complex, August Complex, LNU Lightning Complex, SCU Lightning Complex, CZU Lightning Complex, Lake Fire, Cold Springs Fire, River and Carmel fires, North Complex, Dolan Fire, North Range Fire, Dome Fire, and Loyalton Fire) contributed to smoky conditions and high ozone concentrations in Clark County, Nevada, on August 18-21, 2020.

Figure 3-45 shows multiple large California wildfires burning the vicinity of Clark County on August 18-21, 2020. Table 3-3 shows agency data available for all wildfires that are linked through back trajectories with the August 18-21 exceptional events (as of August 2021). Most of these fires started on wildland during a series of lightning storms that occurred in California during August 16-18, 2020.

- August Complex: https://inciweb.nwcg.gov/incident/6983/
- LNU Lightning Complex: https://inciweb.nwcg.gov/incident/7027/
- SCU Lightning Complex: https://www.fire.ca.gov/incidents/2020/8/18/scu-lightning-complex/
- CZU Lightning Complex: https://inciweb.nwcg.gov/incident/7028/
- Cold Springs Fire: https://inciweb.nwcg.gov/incident/7010/
- River Fire: https://inciweb.nwcg.gov/incident/7059/
- Carmel Fire: https://www.fire.ca.gov/incidents/2020/8/18/carmel-fire/
- North Complex: https://inciweb.nwcg.gov/incident/6997/
- Dolan Fire: https://inciweb.nwcg.gov/incident/7018/
- North Range Fire: https://www.visaliatimesdelta.com/story/news/2020/08/28/california-wildfire-naval-air-weapons-station-china-lake-fire-information/5657462002/
- Dome Fire: https://inciweb.nwcg.gov/incident/7000/

The Red Salmon Complex, Lake, and Loyalton fires began before August 16, 2020, but were also determined to be caused by lightning in predominately wildland areas.

- Red Salmon Complex: https://inciweb.nwcg.gov/incident/6891/
- Lake Fire: https://inciweb.nwcg.gov/incident/6953/
- Loyalton Fire: https://inciweb.nwcg.gov/incident/6975/

We provide the total acreage burned as of August 21, 2020, in Table 3-3 based on the available agency information. By August 21, 2020, these large wildfires had burned over 900,000 acres according to InciWeb and CalFire estimates. All of these fires were long-burning (September –

[3] Specifically, fires with a Q/d value meeting the 100 tons/km threshold may qualify for a Tier 2 demonstration of a clear causal relationship. However, this threshold is insufficient to identify all cases where ozone impacts from smoke may have occurred. Pages 16-17 of the guidance state "To determine an appropriate and conservative value for the Q/d threshold (below which the EPA recommends Tier 3 analyses for the clear causal relationship), the EPA conducted a review. The reviews and analyses did not conclude that particular ozone impacts will always occur above a particular value for Q/d. For this reason, a Q/d screening step alone is not sufficient to delineate conditions where sizable ozone impacts are likely to occur." (U.S. Environmental Protection Agency, 2016).

November 2020) due to restricted firefighting methods in wildland areas and fire-prone conditions in California.

Key factor #1 for a Tier 2 demonstration requires an analysis of wildfire smoke emissions from qualifying fires and the distance from each fire to the affected monitor or monitors. To identify qualifying fires, the guidance "recommends generating 24-hour back trajectories from the affected ozone monitoring site(s) beginning at each hour of these two or three dates" (U.S. Environmental Protection Agency, 2016). Three dates would be used only if the 8-hour averaging period for the daily maximum 8-hour ozone data include hours falling on two dates (i.e., the 8-hour average includes at least 11 p.m. and midnight on two distinct calendar days). For this demonstration, 24-hour HYSPLIT back trajectories were generated from the monitor location starting on each hour of the day of the exceedance.

The guidance states that "…fires that are close to any of these back trajectories" may be used to calculate Q/d (U.S. Environmental Protection Agency, 2016). To identify fires that fall near the HYSPLIT trajectories, trajectories were buffered by a distance of 25% of the distance traveled by the trajectory, which is consistent with uncertainty reported for HYSPLIT trajectory modeling (Draxler, 1991). **Figures 3-46 through 3-49** show the back trajectories and buffer of uncertainty from Clark County, Nevada, initiated on August 18-21. All fires falling within the uncertainty buffer of one or more trajectories were considered candidates for calculating Q/d.

To calculate Q/d for a qualifying fire, daily fire growth was identified using agency reports directly or news reports citing official sources. The daily area growth is first estimated by subtracting the previous day total area from the day's total area. This represents the new area burned on a given day and a lower limit to the total area burned on a given day. BlueSky Playground Version 3.0.1 (**https://tools.airfire.org/playground/v3/**) was used to estimate the daily emissions of NO_x and VOCs emissions associated with the daily growth in area burned for all 13 fires described in Table 3.3 on August 18-21. These emissions estimates underestimate the total daily emissions due to cases when the same area burns for multiple days that are not included in our emissions estimates. These daily emission estimates for NO_x and reactive VOCs (rVOCs) in tons are divided by the distance from each fire to impacted monitors. The fires' location—as reported in InciWeb or by CAL FIRE—was used to identify the distance to the impacted monitors and fuelbed type. Emissions calculations were based on very dry conditions.

EPA guidance recommends that an event may qualify for a Tier 2 demonstration if the Q/d value for a fire, or the aggregate Q/d across multiple fires, exceeds a conservative value of 100 tons/km. Daily Q/d results indicate that significant emissions of NO_x and rVOCs occurred from most of the candidate fires during the four exceedance days (**Tables 3-4 through 3-7**). However, due to the significant distance between the fire and the monitor location, the emissions were not large enough to reach the Q/d threshold of 100 tons/km for a Tier 2 demonstration, except for the CZU Lightning Complex Fire on August 19 with a Q/d value of 118 tons/km. Based on these results, it was determined that Tier 3 analyses were needed to demonstrate a clear causal relationship.

The Q/d analysis, as described in the ozone exceptional event guidance (U.S. Environmental Protection Agency, 2016) and presented here, would not reflect the impact of transport occurring over more than 24 hours prior to the first exceedance event on August 18. The trajectories in Section 3.1.3 show that transport from the California fires occurred over more than 24 hours. Because this demonstration includes wildfire smoke that was transported over multi-day timescales, we conducted an extended analysis to investigate emissions and the transport of smoke from fires over more than 24 hours. The results are presented in **Appendix B**. These analyses provide evidence that the identified fires emitted ozone precursors in the two days leading up to the August 18-21 exceedance events. Further, the trajectories provided here and in Section 3.1.3 show that these precursor emissions were likely to be transported to Clark County on the ozone exceedance event days.

The results of the Q/d analysis presented in this section, as well as the extended emissions transport assessment included in Appendix B, agree with and further strengthen the conceptual model and Tier 3 weight of evidence of a clear causal relationship between the identified wildfires smoke emissions and the monitored ozone exceedance identified in this demonstration.

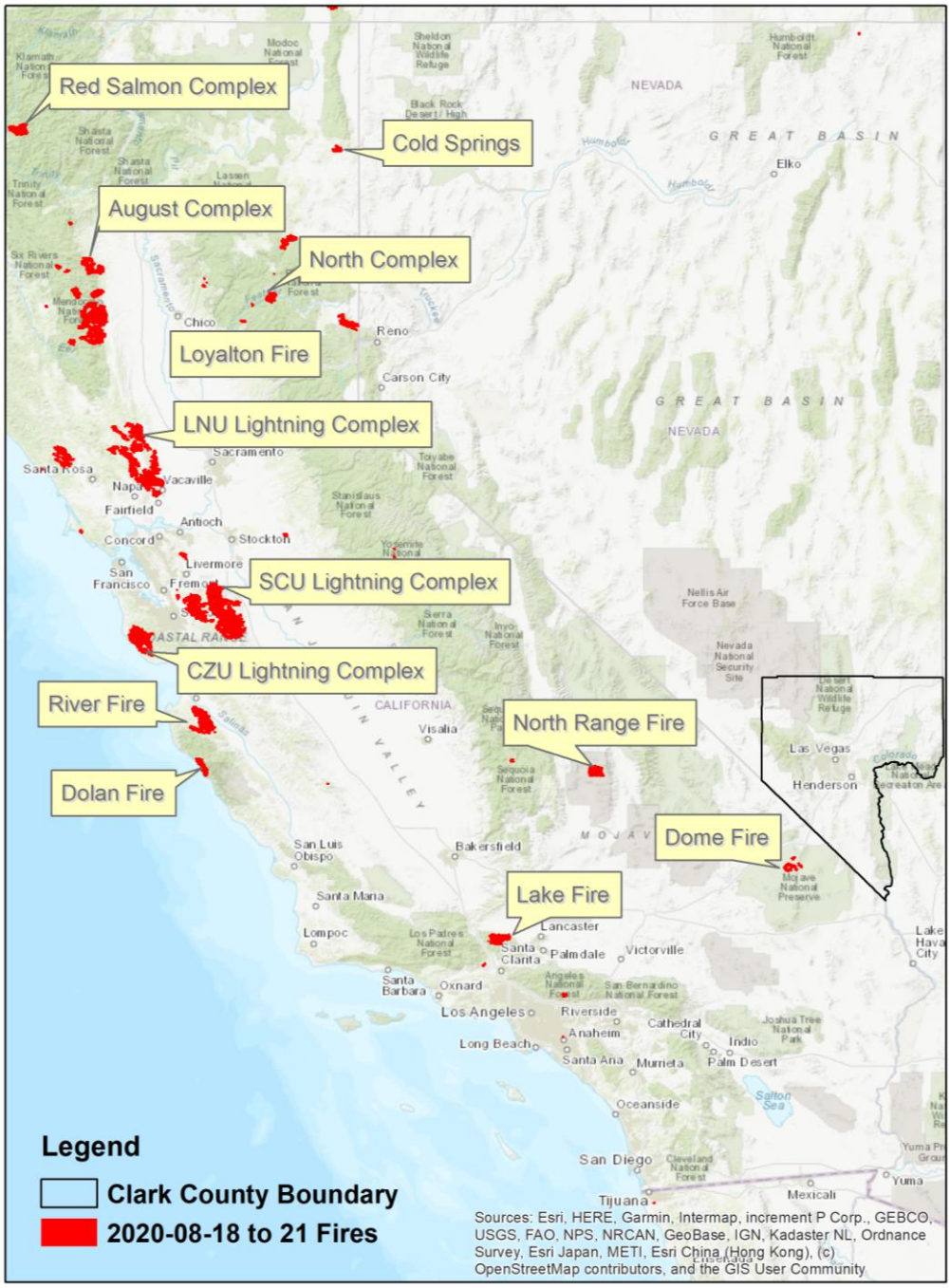

Figure 3-45. Large fires burning during August 18-21, 2020, in the vicinity of Clark County are shown in red. The Clark County boundary is shown in black.

Table 3-3. Fire data for the California fires associated with the August 18-21 EE. Information includes start/containment date, cause of the fire, the agency estimates of the area burned by the EE date (August 21, 2020), and the total reported acres burned. NA means a date has not officially been determined, while '*' means agency data was unavailable so MODIS fire hotspot estimates were used to calculate the burned area.

Fire Name	Start Date	Contained Date	Cause	Area Burned by EE Date (acres)	Total Area Burned (acres)
Red Salmon Complex	7/27/2020	11/17/2020	Lightning	18,566	144,698
August Complex	8/17/2020	11/15/2020	Lightning	>116,372	1,032,648
LNU Lightning Complex	8/17/2020	10/2/2020	Lightning	314,207	363,220
SCU Lightning Complex	8/16/2020	10/1/2020	Lightning	311,093*	396,624
CZU Lightning Complex	8/17/2020	9/22/2020	Lightning	63,000	86,509
Lake Fire	8/12/2020	9/28/2020	Lightning	30,763	31,089
Cold Springs	8/18/2020	9/14/2020	Lightning	7,282*	84,817
River and Carmel fires	8/16/2020	9/4/2020	Lightning	50,510	54,993
North Complex	8/17/2020	11/30/2020	Lightning	27,801	318,935
Dolan Fire	8/18/2020	12/30/2020	Unknown	14,000	124,924
North Range Fire	8/19/2020	Unknown	Lightning	50,000	~80,000
Dome Fire	8/16/2020	9/14/2020	Lightning	>21,000*	43,273
Loyalton Fire	8/14/2020	9/14/2020	Lightning	47,028	47,029

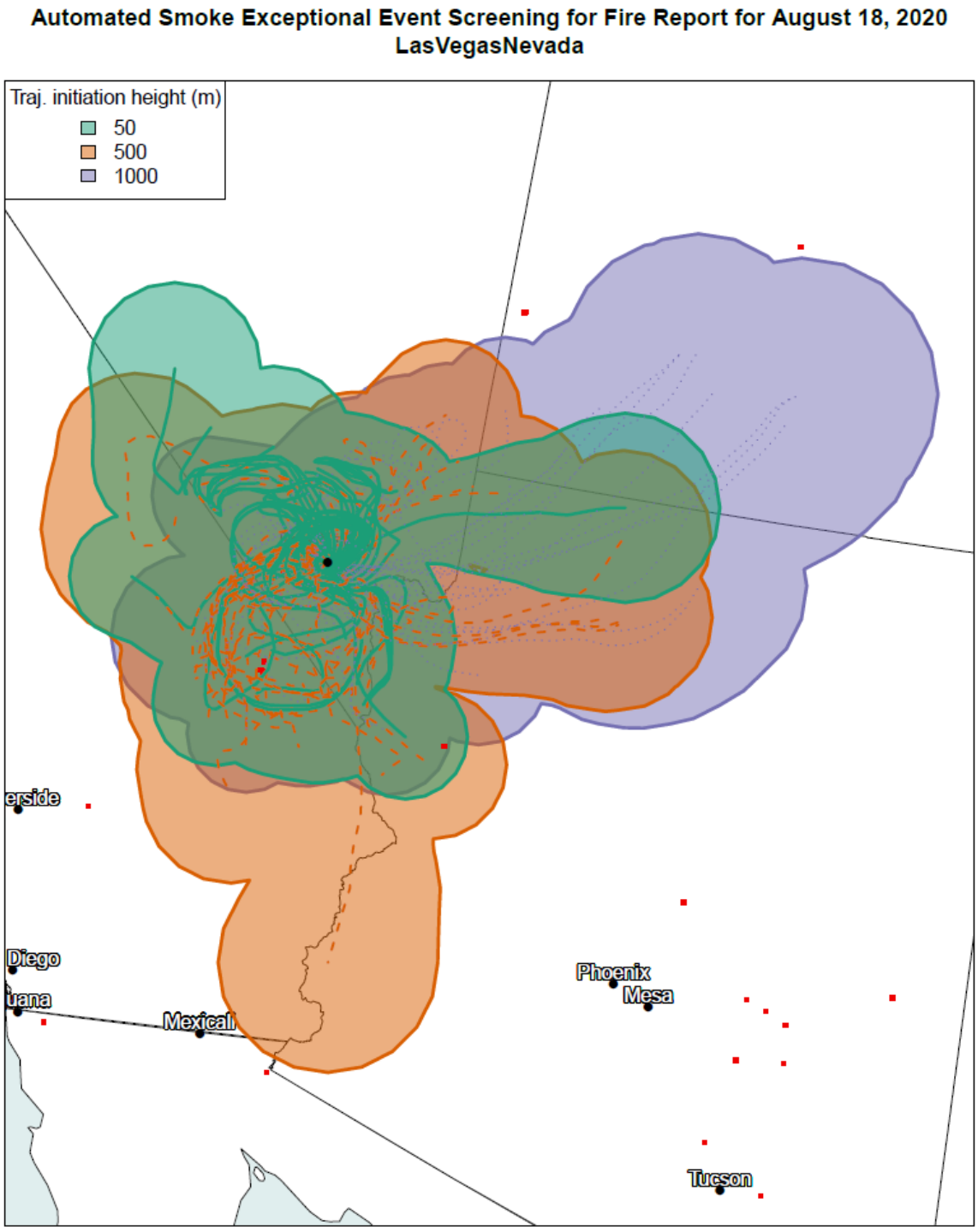

Figure 3-46. Q/d analysis for August 18, 2020. 24-hour back trajectories are shown as solid or dotted lines. The starting height of the back trajectory is indicated by the color. Uncertainty buffers, calculated as 25% of the distance traveled by the trajectory, are shown in colored polygons. Active fires on August 18 are shown as red squares. Fires falling within one or more uncertainty buffer(s) were considered candidates for calculation of individual or aggregate Q/d values.

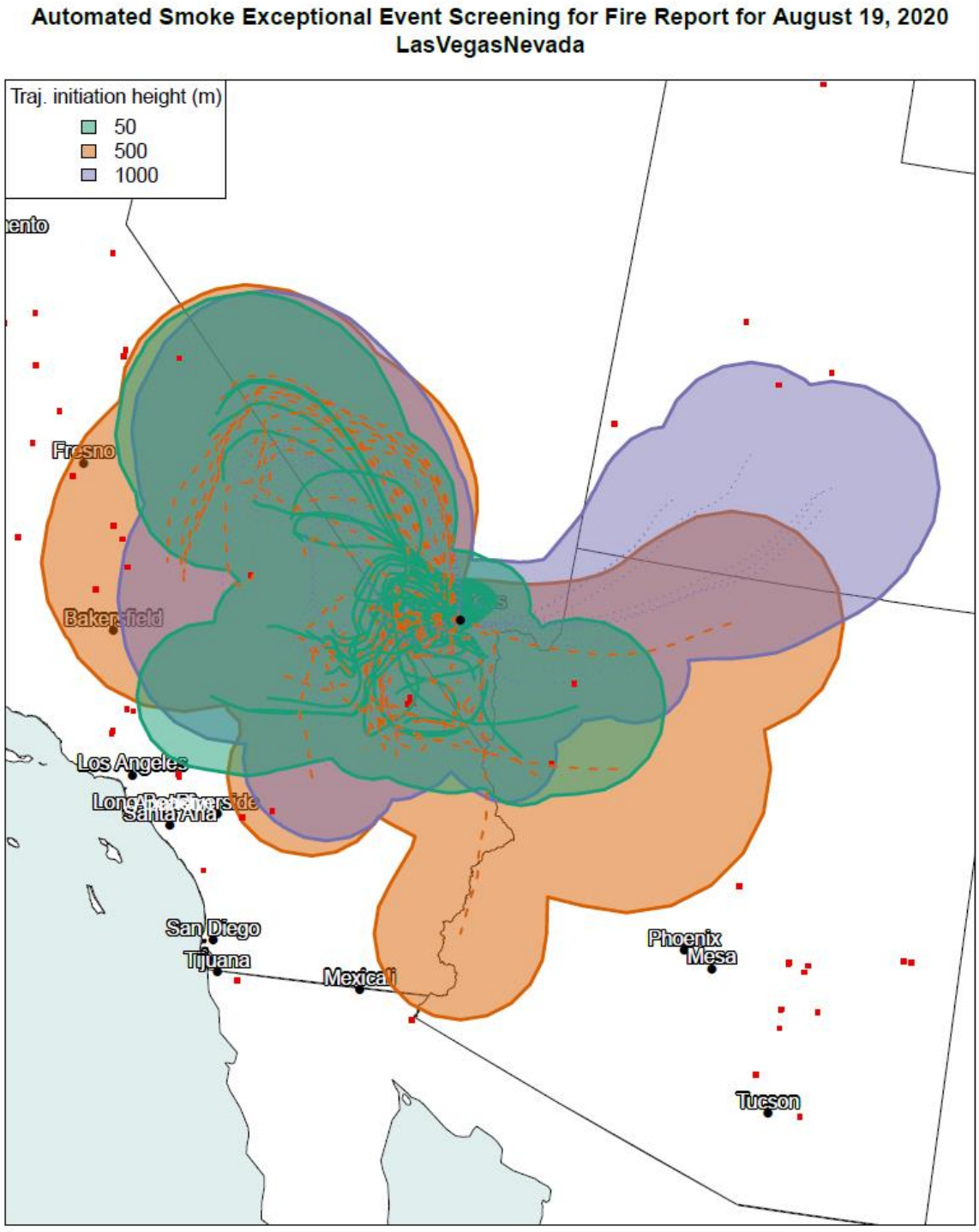

Figure 3-47. Q/d analysis for August 19, 2020. 24-hour back trajectories are shown as solid or dotted lines. The starting height of the back trajectory is indicated by the color. Uncertainty buffers, calculated as 25% of the distance traveled by the trajectory, are shown in colored polygons. Active fires on August 19 are shown as red squares. Fires falling within one or more uncertainty buffer(s) were considered candidates for calculation of individual or aggregate Q/d values.

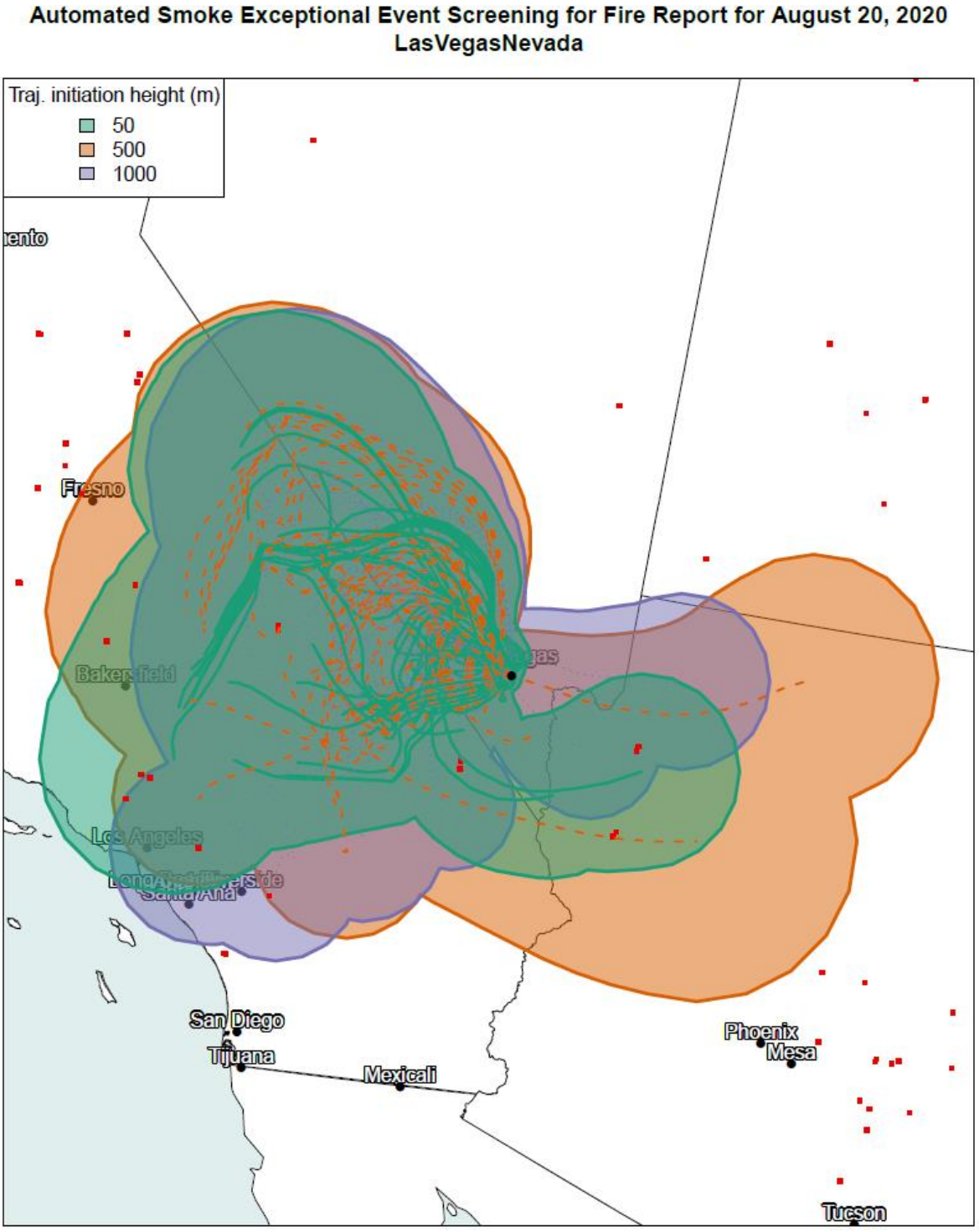

Figure 3-48. Q/d analysis for August 20, 2020. 24-hour back trajectories are shown as solid or dotted lines. The starting height of the back trajectory is indicated by the color. Uncertainty buffers, calculated as 25% of the distance traveled by the trajectory, are shown in colored polygons. Active fires on August 20 are shown as red squares. Fires falling within one or more uncertainty buffer(s) were considered candidates for calculation of individual or aggregate Q/d values.

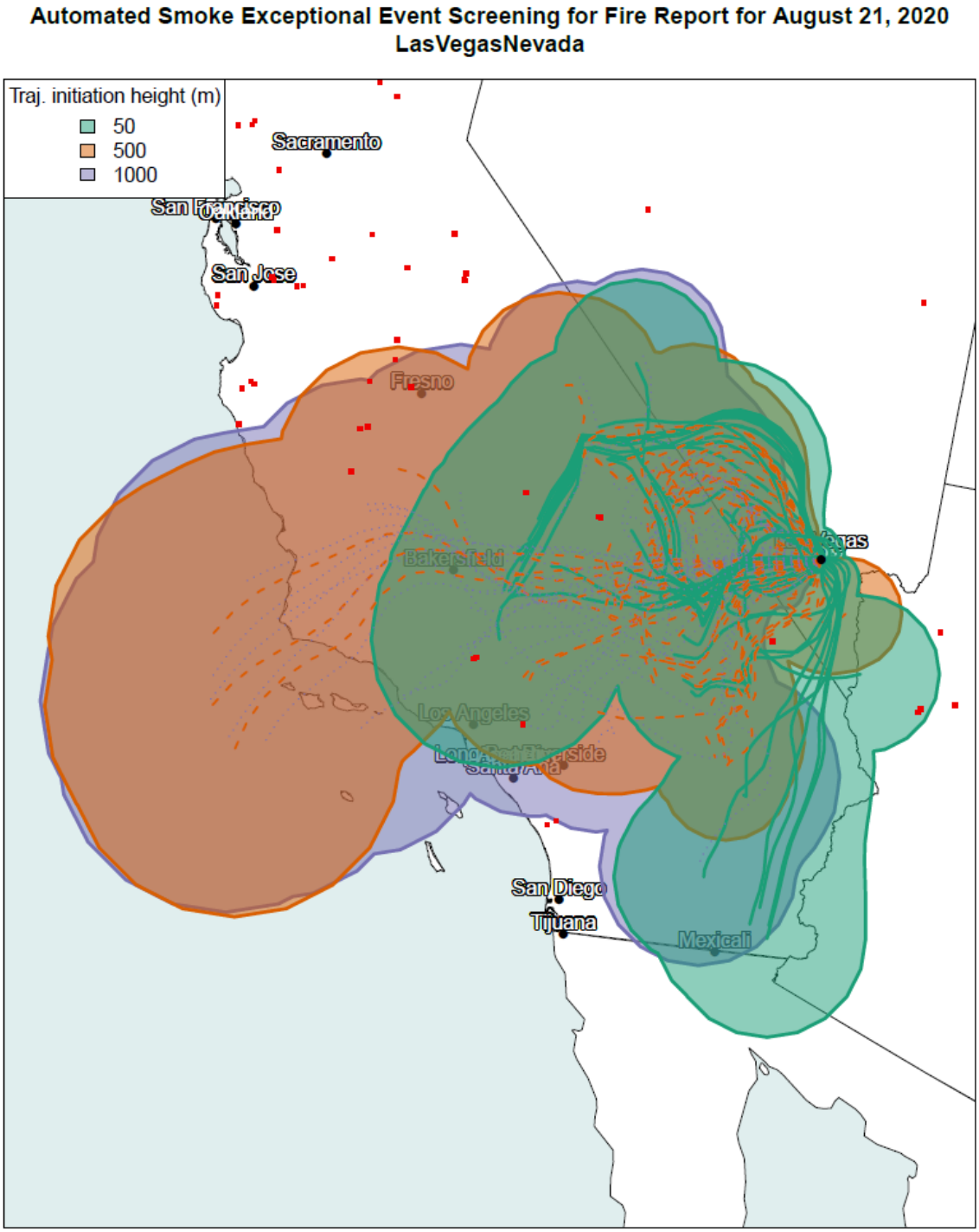

Figure 3-49. Q/d analysis for August 21, 2020. 24-hour back trajectories are shown as solid or dotted lines. The starting height of the back trajectory is indicated by the color. Uncertainty buffers, calculated as 25% of the distance traveled by the trajectory, are shown in colored polygons. Active fires on August 21 are shown as red squares. Fires falling within one or more uncertainty buffer(s) were considered candidates for calculation of individual or aggregate Q/d values.

Table 3-4. Daily growth, daily emissions associated with the daily growth in area burned, and Q/d for the fires with potential smoke contribution on August 18, 2020. Total area burned represents the cumulative area burned across the entire history of the fire up to and including August 18. Growth for all dates shown were obtained from agency estimates available from the Incident Information System (InciWeb) or satellite estimates of growth. Aggregate Q/d calculated for all fires shown is 28. Column "E (Tons)" represents the sum of NO_x and Reactive VOC emissions.

Fire Name	Total Area Burned (Acres)	Daily Growth (Acres)	NO_x (Tons)	VOCs (Tons)	Reactive VOCs (Tons)	E (Tons)	Distance (Km)	Q/d (Tons/km)	Fuel Loading	Fire Size Data Source
North Range Fire	NA	NA	NA	NA	NA	NA	NA	NA	Creosote bush shrubland	NA
Dome Fire	43,273	3,273	12.1	63.6	38	50	65	0.8	Creosote bush shrubland	https://inciweb.nwcg.gov/incident/7000/; MODIS hotspot estimate
Lake Fire	25,948	4,833	156.0	819.2	492	648	210	3.1	California live oak-blue oak woodland	https://inciweb.nwcg.gov/incident/6953/
Red Salmon Complex	15,497	368	11.88	344.59	207	219	910	0.2	Douglas fir madrone tanoak forest	https://inciweb.nwcg.gov/incident/6891/
August Complex Fire	3,025	2,200	45.11	1447.86	869	914	780	1.2	Jeffrey pine ponderosa pine Douglas fir California black oak forest	https://inciweb.nwcg.gov/incident/article/6983/53359/
LNU Lightning Complex Fire	46,000	34,000	766.4	5743.91	3,446	4,213	700	6.0	California live oak blue oak woodland	https://www.sfchronicle.com/california-wildfires/article/Whatever-anyone-can-spare-How-lightning-in-15538666.php
SCU Lightning Complex Fire	97,126	80,129	28.86	144.24	87	115	570	0.2	Wheatgrass cheatgrass grassland	MODIS hotspot estimate
Cold Springs Fire	NA	NA	NA	NA	NA	NA	NA	NA	Sagebrush shrubland	NA

Fire Name	Total Area Burned (Acres)	Daily Growth (Acres)	NO_x (Tons)	VOCs (Tons)	Reactive VOCs (Tons)	E (Tons)	Distance (Km)	Q/d (Tons/km)	Fuel Loading	Fire Size Data Source
River Fire	760	760	17.13	128.39	77	94	580	0.2	California live oak-blue oak woodland	MODIS hotspot estimate, total scaled by agency total burned area (correct bias)
Dolan Fire	NA	NA	NA	NA	NA	NA	NA	NA	California live oak-blue oak woodland	NA
North Complex Fire	4500	4500	162.92	6118.77	3671.262	3,834	670	5.7	Douglas fir sugar pine tanoak forest	https://inciweb.nwcg.gov/incident/article/6997/53414/
Loyalton Fire	46386	2239	53	1914.3	1148.58	1,202	590	2.0	Ponderosa pine Jeffrey pine forest	https://inciweb.nwcg.gov/incident/news/6975/
CZU Lightning Complex Fire	3488	3488	248	11655.6	6993.36	7,241	640	11	Redwood tanoak forest	https://inciweb.nwcg.gov/incident/7028/
Carmel Fire	NA	NA	NA	NA	NA	NA	NA	NA	California live oak blue oak woodland	NA

Table 3-5. Daily growth, daily emissions associated with the daily growth in area burned, and Q/d for the fires with potential smoke contribution on August 19, 2020. Total area burned represents the cumulative area burned across the entire history of the fire up to and including August 19. Growth for all dates shown were obtained from agency estimates available from the Incident Information System (InciWeb) or satellite estimates of growth. Aggregate Q/d calculated for all fires shown is 179. Column "E (Tons)" represents the sum of NO_x and Reactive VOC emissions.

Fire Name	Total Area Burned (Acres)	Daily Growth (Acres)	NO_x (Tons)	VOCs (Tons)	Reactive VOCs (Tons)	E (Tons)	Distance (Km)	Q/d (Tons/km)	Fuel Loading	Fire Size Data Source
North Range Fire	NA	NA	NA	NA	NA	NA	NA	NA	Creosote bush shrubland	NA
Dome Fire	Unknown	Unknown	NA	NA	NA	NA	NA	NA	Creosote bush shrubland	NA
Lake Fire	27,041	1,093	35.29	185.27	111	146	210	0.7	California live oak-blue oak woodland	https://goldrushcam.com/sierrasuntimes/index.php/news/local-news/24932-cal-fire-california-statewide-fire-summary-for-thursday-august-20-2020
Red Salmon Complex	16,255	758	24.47	709.79	426	450	910	0.5	Douglas fir madrone tanoak forest	https://inciweb.nwcg.gov/incident/6891/
August Complex Fire	65,030	62,005	1271.43	40806.55	24,484	25,755	780	33.0	Jeffrey pine ponderosa pine Douglas fir California black oak forest	https://inciweb.nwcg.gov/incident/article/6983/53467/
LNU Lightning Complex Fire	131,000	85,000	1916	14359.78	8,616	10,532	700	15.0	California live oak blue oak woodland	https://goldrushcam.com/sierrasuntimes/index.php/news/local-news/24932-cal-fire-california-statewide-fire-summary-for-thursday-august-20-2020

Fire Name	Total Area Burned (Acres)	Daily Growth (Acres)	NO_x (Tons)	VOCs (Tons)	Reactive VOCs (Tons)	E (Tons)	Distance (Km)	Q/d (Tons/km)	Fuel Loading	Fire Size Data Source
SCU Lightning Complex Fire	137,475	40,349	14.53	72.63	44	58	570	0.1	Wheatgrass cheatgrass grassland	https://goldrushcam.com/sierrasuntimes/index.php/news/local-news/24932-cal-fire-california-statewide-fire-summary-for-thursday-august-20-2020
Cold Springs Fire	6,306	6,306	20.84	109.5	66	87	700	0.1	Sagebrush shrubland	MODIS hotspot estimate
River Fire	33,653	32,893	741.45	5556.9	3,334	4,076	580	7.0	California live oak-blue oak woodland	https://goldrushcam.com/sierrasuntimes/index.php/news/local-news/24932-cal-fire-california-statewide-fire-summary-for-thursday-august-20-2020
Dolan Fire	2,500	NA	NA	NA	NA	NA	NA	NA	California live oak-blue oak woodland	https://goldrushcam.com/sierrasuntimes/index.php/news/local-news/24932-cal-fire-california-statewide-fire-summary-for-thursday-august-20-2020
North Complex Fire	8441	3941	142.68	5358.68	3215.208	3,358	670	5.0	Douglas fir sugar pine tanoak forest	https://goldrushcam.com/sierrasuntimes/index.php/news/local-news/24932-cal-fire-california-statewide-fire-summary-for-thursday-august-20-2020
Loyalton Fire	46386	0	0	0	0	0	590	0	Ponderosa pine Jeffrey pine forest	https://goldrushcam.com/sierrasuntimes/index.php/news/local-news/24932-cal-fire-california-statewide-fire-summary-for-thursday-august-20-2020
CZU Lightning Complex Fire	40000	36512	2596.07	122009.6	73205.73	75,802	640	118.4	Redwood tanoak forest	https://goldrushcam.com/sierrasuntimes/index.php/news/local-news/24932-cal-fire-california-statewide-fire-summary-for-thursday-august-20-2020
Carmel Fire	4285	4285	96.59	723.9	434.34	531	590	0.9	California live oak blue oak woodland	https://goldrushcam.com/sierrasuntimes/index.php/news/local-news/24932-cal-fire-california-statewide-fire-summary-for-thursday-august-20-2020

Table 3-6. Daily growth, daily emissions associated with the daily growth in area burned, and Q/d for the fires with potential smoke contribution on August 20, 2020. Total area burned represents the cumulative area burned across the entire history of the fire up to and including August 20. Growth for all dates shown were obtained from agency estimates available from the Incident Information System (InciWeb), satellite estimates of growth, or from news sources citing official reports. Aggregate Q/d calculated for all fires shown is 89. Column "E (Tons)" represents the sum of NO_x and Reactive VOC emissions.

Fire Name	Total Area Burned (Acres)	Daily Growth (Acres)	NO_x (Tons)	VOCs (Tons)	Reactive VOCs (Tons)	E (Tons)	Distance (Km)	Q/d (Tons/km)	Fuel Loading	Fire Size Data Source
North Range Fire	24,170	24,170	89.41	469.83	282	371	130	2.9	Creosote bush shrubland	MODIS hotspot estimate
Dome Fire	Unknown	Unknown	NA	NA	NA	NA	NA	NA	Creosote bush shrubland	NA
Lake Fire	27,841	800	25.83	135.61	81	107	210	0.5	California live oak-blue oak woodland	https://inciweb.nwcg.gov/incident/6953/
Red Salmon Complex	16,485	230	7.43	215.37	129	137	910	0.2	Douglas fir madrone tanoak forest	https://goldrushcam.com/sierrasuntimes/index.php/news/local-news/24946-cal-fire-california-statewide-fire-summary-for-friday-august-21-2020
August Complex Fire	116,372	51,342	1052.78	33789.04	20,273	21,326	780	27.3	Jeffrey pine ponderosa pine Douglas fir California black oak forest	https://inciweb.nwcg.gov/incident/article/6983/53484/
LNU Lightning Complex Fire	219,067	88,067	1985.13	14877.91	8,927	10,912	700	15.6	California live oak blue oak woodland	https://goldrushcam.com/sierrasuntimes/index.php/news/local-news/24946-cal-fire-california-statewide-fire-summary-for-friday-august-21-2020
SCU Lightning Complex Fire	229,968	92,493	33.31	166.49	100	133	570	0.2	Wheatgrass cheatgrass grassland	https://goldrushcam.com/sierrasuntimes/index.php/news/local-news/24946-cal-fire-california-statewide-fire-summary-for-friday-august-21-2020

Fire Name	Total Area Burned (Acres)	Daily Growth (Acres)	NO_x (Tons)	VOCs (Tons)	Reactive VOCs (Tons)	E (Tons)	Distance (Km)	Q/d (Tons/km)	Fuel Loading	Fire Size Data Source
Cold Springs Fire	7,283	977	3.23	16.97	10	13	700	0.0	Sagebrush shrubland	MODIS hotspot estimate
River Fire	39,464	5,811	130.99	981.7	589	720	580	1.2	California live oak-blue oak woodland	https://goldrushcam.com/sierrasuntimes/index.php/news/local-news/24946-cal-fire-california-statewide-fire-summary-for-friday-august-21-2020
Dolan Fire	8,500	6,000	135.25	1,013.63	608	743	580	1.3	California live oak-blue oak woodland	https://goldrushcam.com/sierrasuntimes/index.php/news/local-news/24946-cal-fire-california-statewide-fire-summary-for-friday-august-21-2020
North Complex Fire	1,6241	7,800	282.39	10,605.87	6,363.522	6,646	670	9.9	Douglas fir sugar pine tanoak forest	https://inciweb.nwcg.gov/incident/article/6997/53572/
Loyalton Fire	46,872	486	11.5	415.52	249.312	261	590	0.4	Ponderosa pine Jeffrey pine forest	https://goldrushcam.com/sierrasuntimes/index.php/news/local-news/24946-cal-fire-california-statewide-fire-summary-for-friday-august-21-2020
CZU Lightning Complex Fire	50,000	10,000	711.02	33,416.29	20,049.77	20,761	640	32	Redwood tanoak forest	https://goldrushcam.com/sierrasuntimes/index.php/news/local-news/24946-cal-fire-california-statewide-fire-summary-for-friday-august-21-2020
Carmel Fire	4,285	0	0	0	0	0	590	0	California live oak blue oak woodland	https://goldrushcam.com/sierrasuntimes/index.php/news/local-news/24946-cal-fire-california-statewide-fire-summary-for-friday-august-21-2020

Table 3-7. Daily growth, daily emissions associated with the daily growth in area burned, and Q/d for the fires with potential smoke contribution on August 21, 2020. Total area burned represents the cumulative area burned across the entire history of the fire up to and including August 21. Growth for all dates shown were obtained from agency estimates available from the Incident Information System (InciWeb), satellite estimates of growth, or from news sources citing official reports. Aggregate Q/d calculated for all fires shown is 80. Column "E (Tons)" represents the sum of NO_x and Reactive VOC emissions.

Fire Name	Total Area Burned (Acres)	Daily Growth (Acres)	NO_x (Tons)	VOCs (Tons)	Reactive VOCs (Tons)	E (Tons)	Distance (Km)	Q/d (Tons/ km)	Fuel Loading	Fire Size Data Source
North Range Fire	50,000	25,830	95.55	502.09	301	397	130	3.1	Creosote bush shrubland	https://www.ridgecrestca.com/news/20200822/blm-fire-at-naws-burns-50000-acres-0-containment
Dome Fire	Unknown	Unknown	NA	NA	NA	NA	65	NA	Creosote bush shrubland	NA
Lake Fire	30,763	2,922	94.34	495.3	297	392	210	1.9	California live oak-blue oak woodland	https://goldrushcam.com/sierrasuntimes/index.php/news/local-news/24964-cal-fire-california-statewide-fire-summary-for-saturday-morning-august-22-2020
Red Salmon Complex	18,566	2,081	67.19	1948.64	1,169	1,236	910	1.4	Douglas fir madrone tanoak forest	https://goldrushcam.com/sierrasuntimes/index.php/news/local-news/24964-cal-fire-california-statewide-fire-summary-for-saturday-morning-august-22-2020

Fire Name	Total Area Burned (Acres)	Daily Growth (Acres)	NO_x (Tons)	VOCs (Tons)	Reactive VOCs (Tons)	E (Tons)	Distance (Km)	Q/d (Tons/km)	Fuel Loading	Fire Size Data Source
August Complex Fire	>116372	Unknown	NA	NA	NA	NA	700	NA	Jeffrey pine ponderosa pine Douglas fir California black oak forest	NA
LNU Lightning Complex Fire	314,207	95,140	2144.57	16072.82	9,644	11,788	700	16.8	California live oak blue oak woodland	https://goldrushcam.com/sierrasuntimes/index.php/news/local-news/24964-cal-fire-california-statewide-fire-summary-for-saturday-morning-august-22-2020
SCU Lightning Complex Fire	291,968	62,000	22.33	111.6	67	89	570	0.2	Wheatgrass cheatgrass grassland	https://goldrushcam.com/sierrasuntimes/index.php/news/local-news/24964-cal-fire-california-statewide-fire-summary-for-saturday-morning-august-22-2020
Cold Springs Fire	7,283	0	0	0	0	0	700	0.0	Sagebrush shrubland	MODIS satellite data
River Fire	44,987	5,523	124.49	933.05	560	684	580	1.2	California live oak-blue oak woodland	https://goldrushcam.com/sierrasuntimes/index.php/news/local-news/24964-cal-fire-california-statewide-fire-summary-for-saturday-morning-august-22-2020
Dolan Fire	14,000	5,500	123.98	929.16	557	681	580	1.2	California live oak-blue oak woodland	https://goldrushcam.com/sierrasuntimes/index.php/news/local-news/24964-cal-fire-california-statewide-fire-summary-for-saturday-morning-august-22-2020
North Complex Fire	27801	11560	418.51	15718.44	9431.064	9,850	670	14.7	Douglas fir sugar pine tanoak forest	https://inciweb.nwcg.gov/incident/article/6997/53674/

Fire Name	Total Area Burned (Acres)	Daily Growth (Acres)	NO_x (Tons)	VOCs (Tons)	Reactive VOCs (Tons)	E (Tons)	Distance (Km)	Q/d (Tons/km)	Fuel Loading	Fire Size Data Source
Loyalton Fire	47028	156	3.69	133.38	80.028	84	590	0.142	Ponderosa pine Jeffrey pine forest	https://goldrushcam.com/sierrasuntimes/index.php/news/local-news/24964-cal-fire-california-statewide-fire-summary-for-saturday-morning-august-22-2020
CZU Lightning Complex Fire	63000	13000	924.33	43441.17	26064.7	26,989	640	42.2	Redwood tanoak forest	https://goldrushcam.com/sierrasuntimes/index.php/news/local-news/24964-cal-fire-california-statewide-fire-summary-for-saturday-morning-august-22-2020
Carmel Fire	5523	1238	27.91	209.15	125.49	153	590	0.26	California live oak blue oak woodland	https://goldrushcam.com/sierrasuntimes/index.php/news/local-news/24964-cal-fire-california-statewide-fire-summary-for-saturday-morning-august-22-2020

3.2.2 Key Factor #2: Comparison of Event Concentrations with Non-Event Concentrations

Another key factor in determining whether the August 18-21, 2020, exceedance event is exceptional is to compare event ozone concentrations with non-event concentrations via percentile and rank-order analysis. Table 3-8 shows August 18 through 21 ozone concentrations as a percentile in comparison with the last six years of data (with and without the other proposed 2018 and 2020 EE days included) at each site in Clark County. For the four monitoring sites (i.e., Paul Meyer, Walter Johnson, Joe Neal, and Green Valley) that show a NAAQS standard exceedance during the August 18-21 EE period, all of the exceedances are greater than or equal to the 97th percentile when compared to the last six years of data, even with the inclusion of all other proposed 2018 and 2020 EE days. Without the inclusion of the other EE days, the percentiles are higher at all monitoring sites showing August 18-21 MDA8 ozone concentrations at or above the 99th percentile except at Joe Neal on August 20. To confirm that the calculated percentiles are not biased by non-ozone season data, Table 3-9 shows the August 18 through 21 percentile ranks for all monitoring sites around Clark County in comparison with the last six years of ozone season (May to September) data. All monitoring sites show percentile ranks for August 18 above the 99th percentile (this was the highest ozone day during the EE–see Table 1-1 for more details). For the following days that include lower MDA8 ozone concentrations, all sites show a rank above the 95th percentile. When the other possible EE days are excluded, the percentile ranks increase for all sites on August 18 and 19 (above the 97th percentile on both days). On August 20, the rank for Joe Neal increases from the 95th to the 96th percentile. On August 21, the rank for Paul Meyer increases from the 96th to the 98th percentile. Although not all of the sites showed a >99th percentile rank for the entire EE time period compared with the last six ozone seasons, this analysis confirms that the August 18-21 EE included unusually high concentrations of ozone when compared with the last six years of data and the last six ozone seasons.

We also compared the rank-ordered concentrations at each site for 2020. As shown in Figures 2-3 through 2-6, 2020 ozone concentrations were not atypically low, which might bias our rank-ordered analysis for the August 18-21 EE. Tables 3-10 through 3-13 show the rank-ordered ozone concentrations for 2018 through 2020 and the design values for 2020, with the inclusion of proposed 2018 and 2020 EEs. For Joe Neal, only August 18 is ranked in the top five ozone days for 2020. However, without the other EE days included, August 18, 19, and 20 are ranked as the first, second, and third highest ozone days in 2020. For Paul Meyer, August 18 is ranked as the highest ozone day in 2020. When excluding other EE days, August 18, 19, and 21 are then ranked as first, third, and fifth highest ozone days in 2020. For Walter Johnson, August 18 is ranked as the highest ozone concentration for 2020. Without the other EE days, August 18 and 19 are ranked as the first and third highest ozone days in 2020. Finally, August 19 at the Green Valley monitoring site is ranked as the fourth highest ozone day on record in 2020. Without the other EE days included, August 19 becomes the second highest ozone day in 2020. When including all EE days, it's clear that August 18 is an extremely exceptional event with two sites showing this date as the highest ozone day in 2020. The

following days show decreasing ozone rankings (due to decreases in MDA8 ozone concentrations), however, this is likely due to a thicker smoke layer as the event progressed. During heavy smoke conditions, decreased solar radiation can suppress ozone production.

For further comparison with non-event ozone concentrations, **Table 3-14** shows 5-year (2015-2019) MDA8 ozone statistics for the week before and after August 18-21. This two-week window analysis shows that MDA8 ozone concentrations during the August 18-21 EE are well above the average and above the 95th percentile of the last five years of data at each affected monitoring site.
The percentile, rank-ordered analyses, and the two-week window analysis, indicate that all affected monitoring sites during August 18-21, 2020, showed unusually high ozone concentrations compared with non-event concentrations. This conclusion supports a key factor, suggesting that August 18-21 was an EE in Clark County, Nevada.

Table 3-8. Six-year percentile ozone. The August 18 through 21 EE ozone concentrations at each site are calculated as a percentile of the last six years, with and without other 2018 and 2020 EEs included in the historical record.

		Aug 18		Aug 19		Aug 20		Aug 21	
Site Name	AQS Site Code	6-Year Percentile	6-Year Percentile w/o EE Dates	6-Year Percentile	6-Year Percentile w/o EE Dates	6-Year Percentile	6-Year Percentile w/o EE Dates	6-Year Percentile	6-Year Percentile w/o EE Dates
Joe Neal	320030075	99.7	*99.8*	98.6	*99.0*	97.7	*98.4*		
Paul Meyer	320030043	100.	*100.*	99.3	*99.6*			98.3	*99.1*
Walter Johnson	320030071	100.	*100.*	99.1	*99.6*				
Green Valley	320030298			98.7	*99.3*				

Table 3-9. Six-year, ozone-season percentile ozone. The August 18 through 21 EE ozone concentrations at each site is calculated as a percentile of the last six years' ozone season (May-September), with and without other 2018 and 2020 EEs included in the historical record.

		Aug 18		Aug 19		Aug 20		Aug 21	
Site Name	AQS Site Code	6-Year Percentile	6-Year Percentile w/o EE Dates	6-Year Percentile	6-Year Percentile w/o EE Dates	6-Year Percentile	6-Year Percentile w/o EE Dates	6-Year Percentile	6-Year Percentile w/o EE Dates
Joe Neal	320030075	99.3	*99.6*	96.8	*97.8*	94.8	*96.3*		
Paul Meyer	320030043	100.	*100.*	98.5	*99.1*			96.2	*98.0*
Walter Johnson	320030071	99.9	*99.9*	98.0	*99.0*				
Green Valley	320030298			97.1	*98.5*				

Table 3-10. Site-specific ozone design values for the Joe Neal monitoring site. The top five highest ozone concentrations for 2018-2020 at Joe Neal are shown, and proposed EE days in 2018 and 2020 are included.

Joe Neal Rank	2018	2019	2020
Highest	80	74	81
Second Highest	78	70	78
Third Highest	76	69	78
Fourth Highest	76	68	78
Fifth Highest	74	67	76
Design Value		74	

Table 3-11. Site-specific ozone design values for the Paul Meyer monitoring site. The top five highest ozone concentrations for 2018-2020 at Paul Meyer are shown, and proposed EE days in 2018 and 2020 are included.

Paul Meyer Rank	2018	2019	2020
Highest	79	74	79
Second Highest	76	72	78
Third Highest	75	70	77
Fourth Highest	75	69	77
Fifth Highest	74	69	76
Design Value		73	

Table 3-12. Site-specific ozone design values for the Walter Johnson monitoring site. The top five highest ozone concentrations for 2018-2020 at Walter Johnson are shown, and proposed EE days in 2018 and 2020 are included.

Walter Johnson Rank	2018	2019	2020
Highest	79	77	82
Second Highest	77	69	82
Third Highest	77	69	78
Fourth Highest	76	68	77
Fifth Highest	76	68	75
Design Value		73	

Table 3-13. Site-specific ozone design values for the Green Valley monitoring site. The top five highest ozone concentrations for 2018-2020 at Green Valley are shown, and proposed EE days in 2018 and 2020 are included.

Green Valley Rank	2018	2019	2020
Highest	78	73	76
Second Highest	78	72	72
Third Highest	78	71	72
Fourth Highest	77	70	71
Fifth Highest	77	70	70
Design Value		72	

Table 3-14. Two-week non-event comparison. August 18-21, 2020, MDA8 ozone concentrations for each affected site are shown in the top row. Five-year (2015-2019) average MDA8 ozone statistics for August 4 through September 1 are shown for each affected site around Clark County to compare with the event ozone concentrations.

	Green Valley 320030298	Joe Neal 320030075	Paul Meyer 320030043	Walter Johnson 320030071
August 18		78	79	82
August 19	71	73	74	74
August 20		71		
August 21			71	
Mean	55	57	57	58
Median	54	57	57	57
Mode	56	52	53	57
St. Dev	7	8	8	8
Minimum	39	38	41	37
95 %ile	69	70	70	70
99 %ile	71	78	74	77
Maximum	73	80	79	82
Range	34	42	38	45
Count	114	113	114	114

3.2.3 Satellite Retrievals of Pollutant Concentrations

Satellite retrievals of pollutants associated with wildfire smoke, such as AOD, CO, and NO_x, can provide evidence that smoke was present at a monitoring site. We examined maps of Multi-Angle Implementation of Atmospheric Correction (MAIAC) AOD from the MODIS instrument onboard the Aqua and Terra satellites, CO retrievals from the Measurements of Pollution in the Troposphere (MOPITT) instrument onboard the Terra satellite, and NO_2 retrievals from the Ozone Monitoring Instrument (OMI). These maps provide evidence to support the transport of smoke from the fires in California, including from the Red Salmon Complex, August Complex, LNU Lightning Complex, SCU Lightning Complex, CZU Lightning Complex, Lake Fire, River and Carmel Fire, North Range Fire, and Dome Fire to Clark County, Nevada, as already demonstrated with visual imagery and trajectories in Sections 3.1 and 3.2. MODIS AOD measurements indicate the concentration of light-absorbing aerosols, including those emitted by wildfires, in the total atmospheric column. Between August 17 and August 21, AOD measurements show areas of widespread enhanced aerosols over the west and Midwestern United States, including California and Nevada (**Figure 3-50**). Areas of enhanced aerosols persisted over the fires in California and were transported to the Clark County area by August 18. MODIS AOD retrievals indicate increased aerosols in the Clark County area on August 18–August 21 (**Figure 3-51**).

CO measurements from MOPITT show a similar pattern of wildfire emission plume transport as seen in the MODIS AOD data noted above. The map shows enhanced CO stretching from California to Clark County on August 21 (**Figure 3-52**). On August 21, CO concentrations in areas of Clark County were up to approximately 2.75×10^{18} mol/cm^2. Unfortunately, CO measurements from MOPITT were unavailable over much of California and Nevada on August 18 and August 20. For completeness, the August 19 MOPITT retrieval is included in **Appendix C.** This image only shows Las Vegas from a limb-view and is not conclusive for the August 18-21 event. Furthermore, CO measurements from the Atmospheric Infrared Sounder (AIRS) satellite were unavailable from August 18-21.

We additionally examined OMI retrievals of tropospheric NO_2 (**Figure 3-53 through 3-55**). Over areas of dense, visible smoke and near actively burning fires, where significant smoke is present in the troposphere, OMI retrievals show an increase in measured NO_2. Elevated levels of NO_2 were especially pronounced over the LNU Lightning Complex in California on August 19.

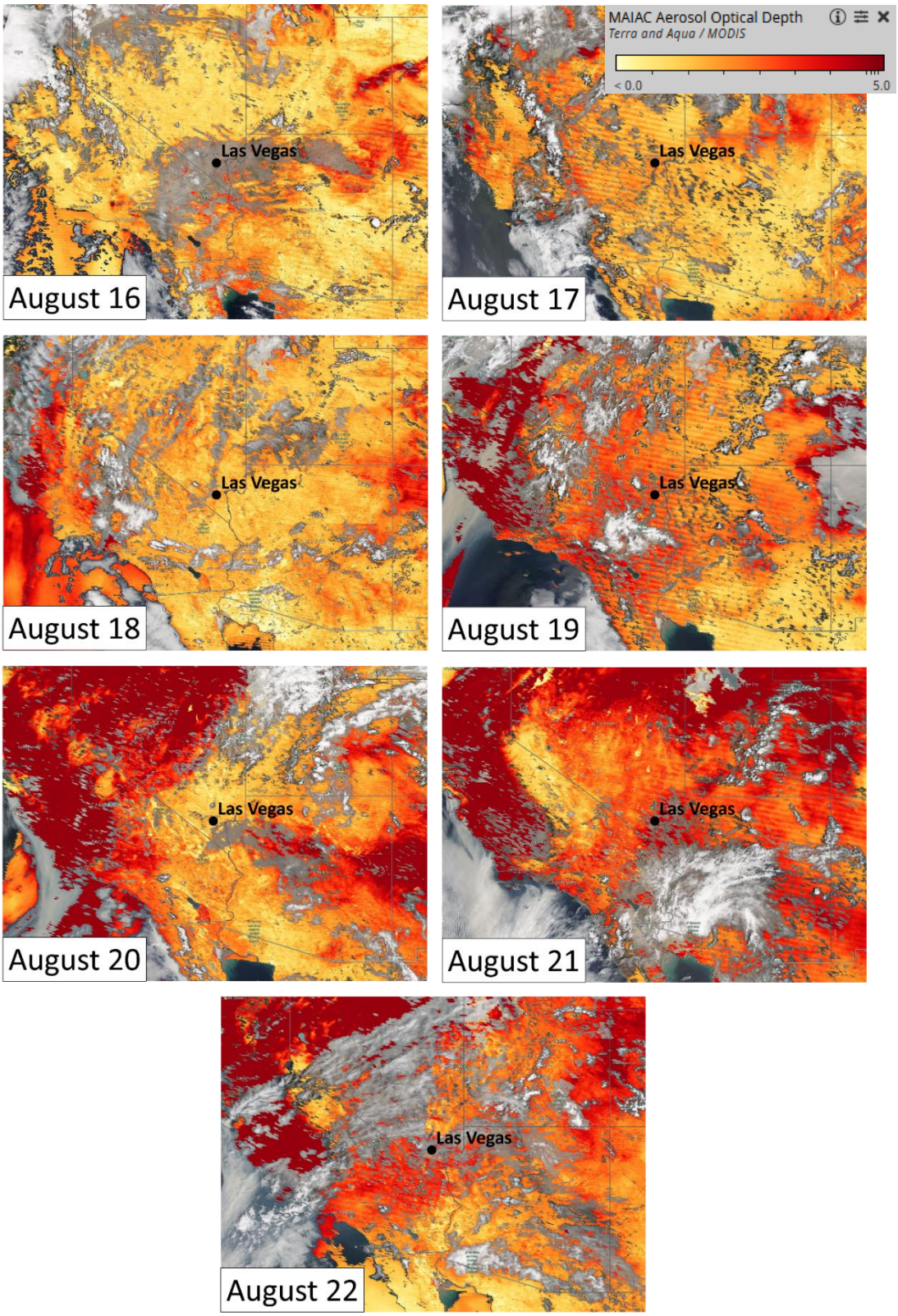

Figure 3-50. MAIAC MODIS Aqua/Terra combined AOD retrievals for the two days before the EE, during the EE on August 18-21, and the day after the EE are shown.

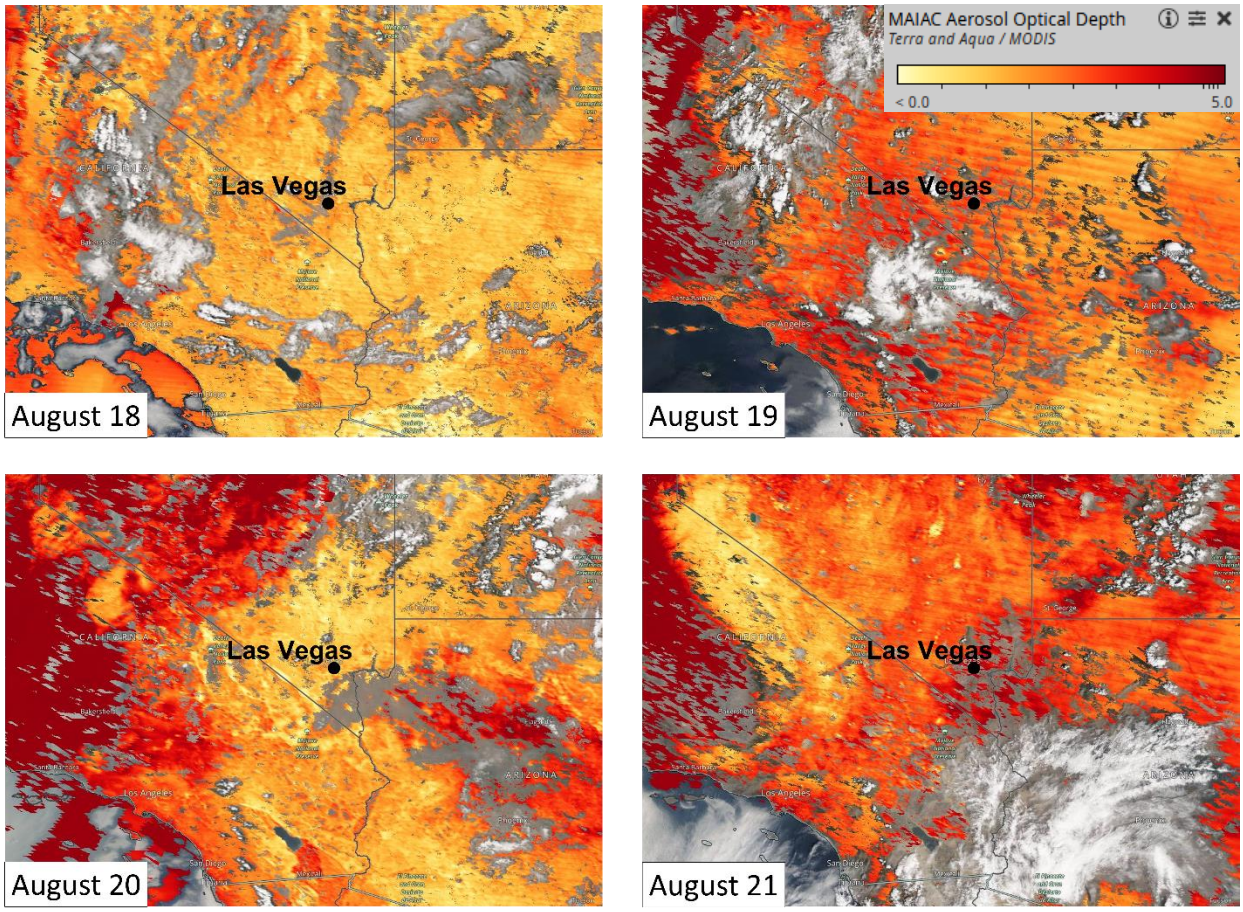

Figure 3-51 A zoomed-in view (over Clark County and southern California) of the MAIAC MODIS Aqua/Terra combined AOD retrieval during the EE on August 18-21, 2020.

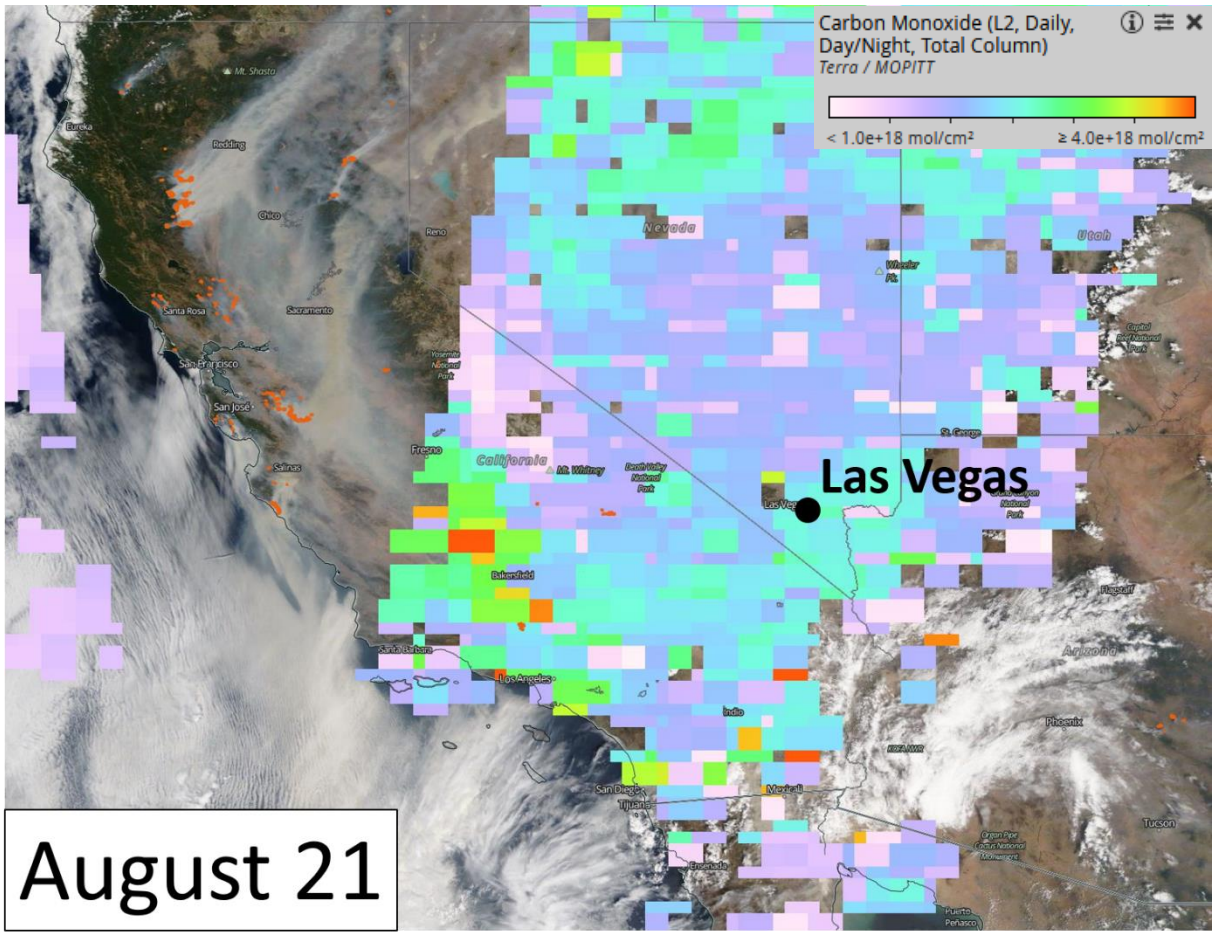

Figure 3-52. A zoomed-in view (over Clark County and the fires in California) of the Aqua MOPITT CO retrieval during the EE on August 21, 2020.

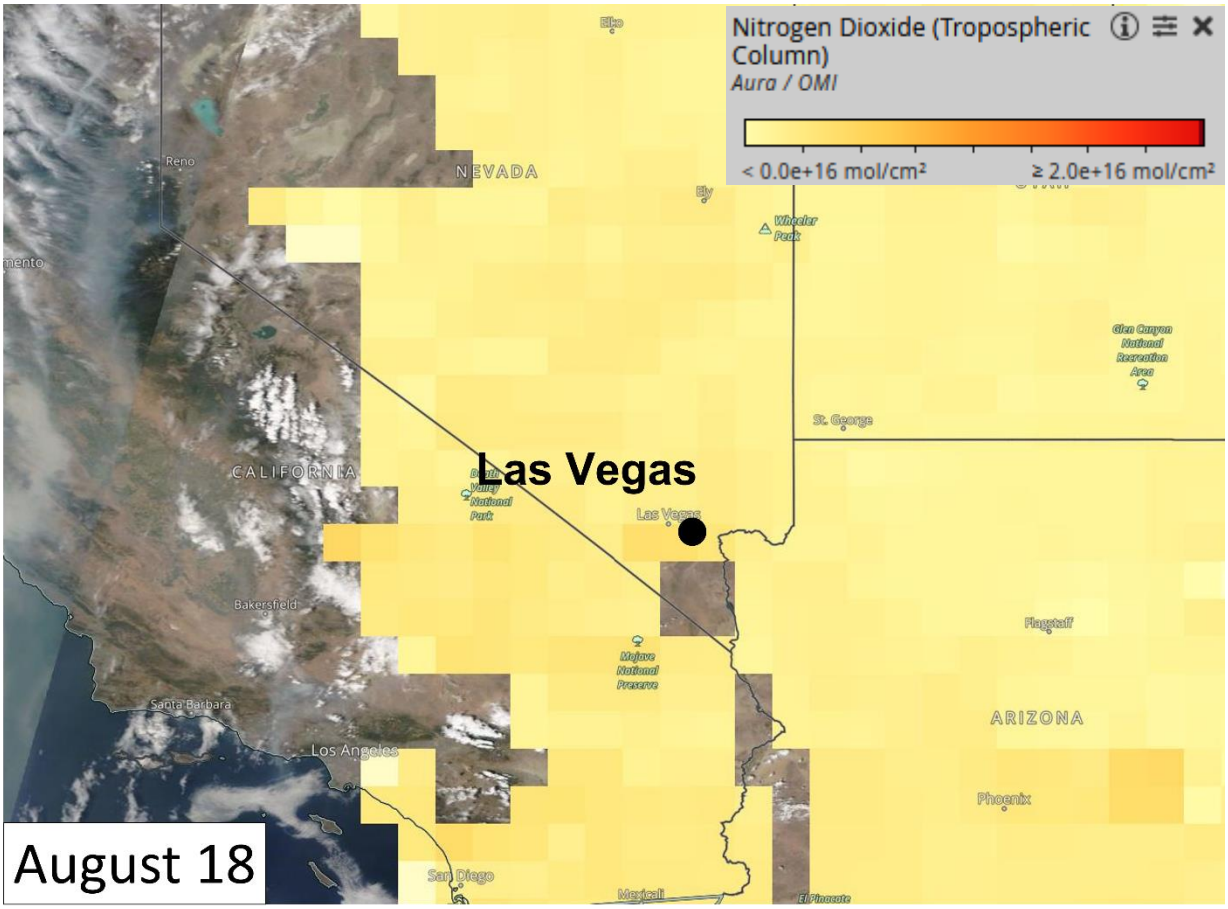

Figure 3-53. OMI Aura NO_2 retrieval for the EE on August 18, 2020.

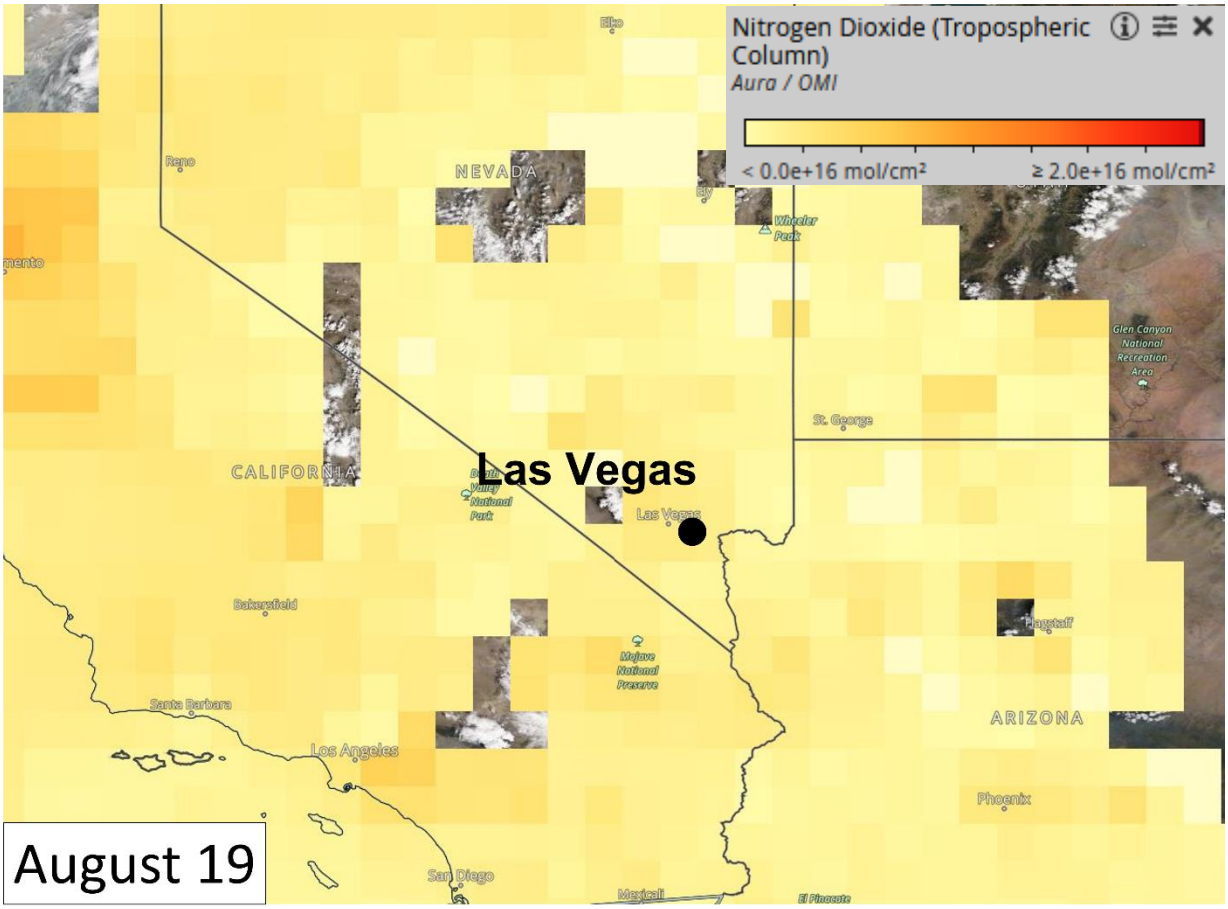

Figure 3-54. OMI Aura NO_2 retrieval for the EE on August 19, 2020.

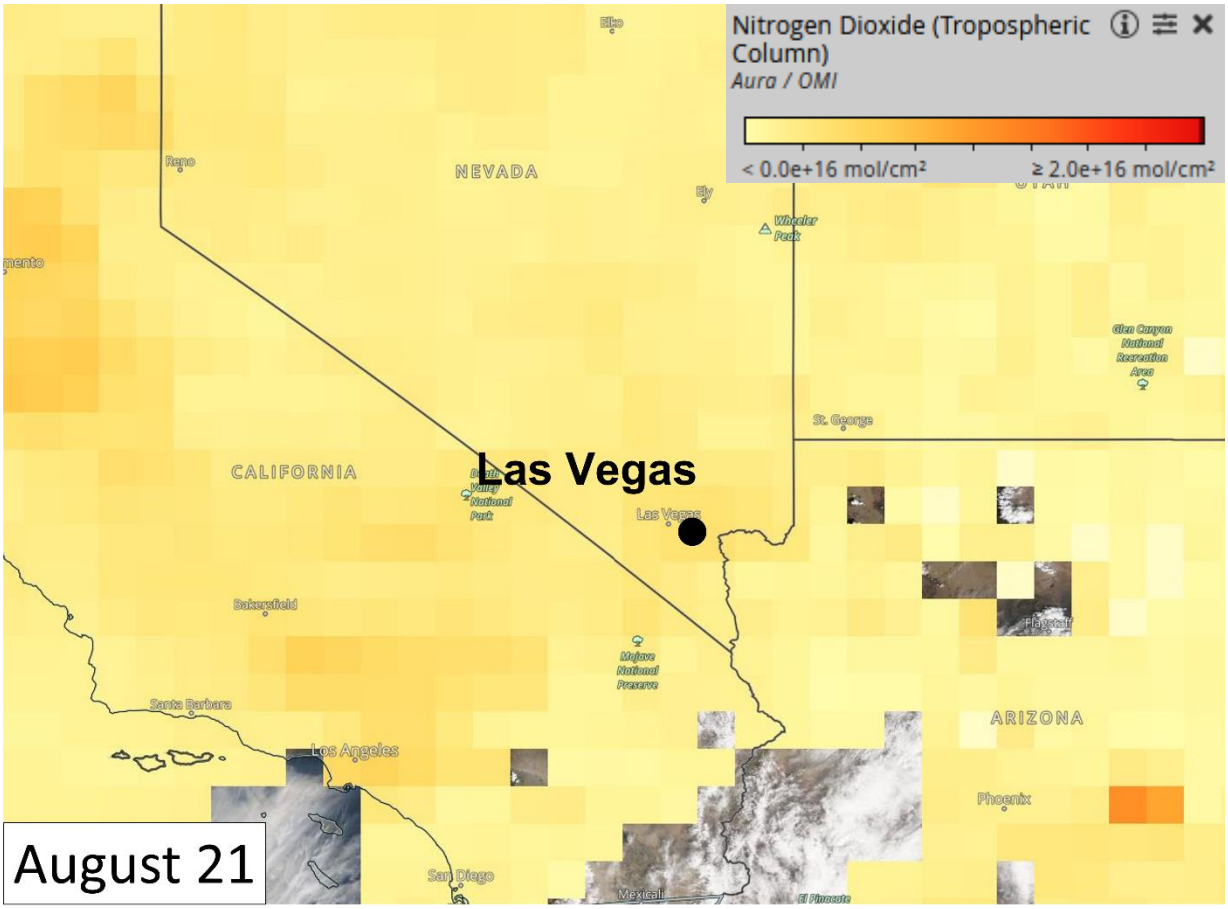

Figure 3-55. OMI Aura NO_2 retrieval for the EE on August 21, 2020.

3.2.4 Supporting Pollutant Trends and Diurnal Patterns

Ground measurements of wildfire plume components (e.g., $PM_{2.5}$, CO, NO_x, and VOCs) can be used to further demonstrate whether smoke impacted ground-level air quality if enhanced concentrations or unusual diurnal patterns are observed. We examined concentrations of $PM_{2.5}$, CO, NO, NO_2, and TNMOC measured at all exceedance sites as well as other nearby sites in Clark County. If $PM_{2.5}$, CO, NO_x, and VOCs were enhanced at the time the smoke plume arrived in Clark County, these measurements would provide additional supporting evidence of smoke impacts in Clark County.

Figure 3-56 shows an overall view of pollutants measured around Clark County in the week before and after the August 18-21 event. The peak daily concentration of $PM_{2.5}$ at exceedance-affected monitoring sites and nearby sites shows a steady increase starting on August 18 and peaking on August 21, coinciding with the elevated ozone on those days, compared to the weeks surrounding the event. After August 23, $PM_{2.5}$ returned to typical concentrations. The increased concentrations of $PM_{2.5}$ on event days provides support for the presence of an abnormal $PM_{2.5}$ source such as wildfire smoke at the surface. TNMOC, NO, and NO_2 do not show concentrations that are markedly different

in magnitude on event days compared to the weeks surrounding the event. The rest of this section examines temporal abnormalities and site-specific trends for each supporting pollutant. Because less than one season's worth of data is available for TNMOC, this pollutant is excluded from detailed examination below.

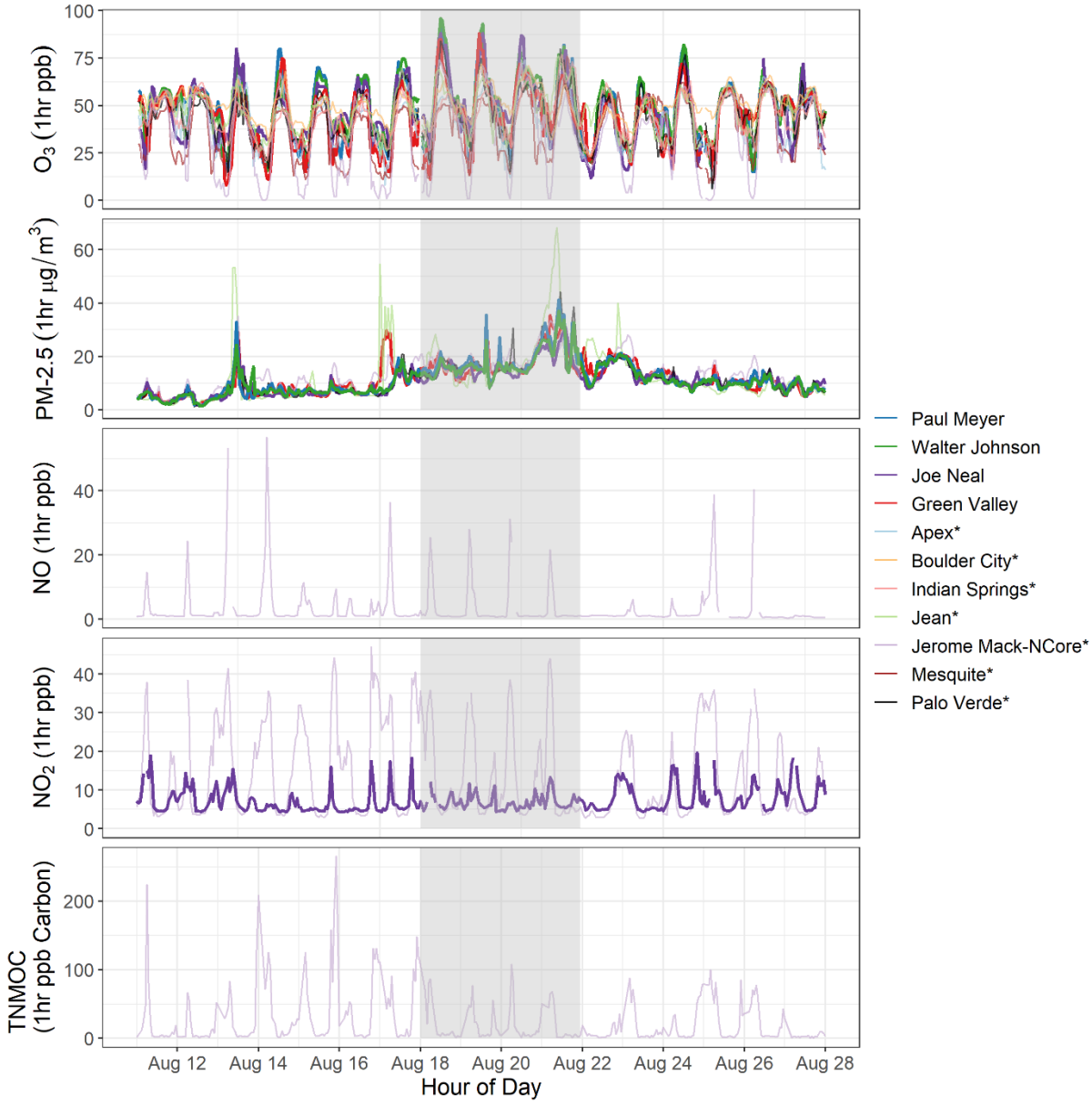

Figure 3-56. Hourly concentrations of ozone, $PM_{2.5}$, NO_x, and TNMOC. Colored lines represent sites in exceedance during the August 18-21 exceptional event. Gray lines represent supporting sites in Clark County. The gray bar represents August 18-21, 2020.

Unusual diurnal patterns of supporting measurements can provide evidence that smoke from multiple California wildfires impacted Clark County air quality during the August 18-21 exceptional event. Figure 3-57 shows the diurnal profile for ozone and $PM_{2.5}$ at multiple sites in Clark County for each day in the event period. Also plotted is the seasonal (May to September) average ozone and $PM_{2.5}$ at each site. Four years of $PM_{2.5}$ data are available from Paul Meyer, one year from Walter Johnson, three years from Joe Neal, and five years from Green Valley. On a typical day, the diurnal profile of ozone shows a peak around midday and an overnight trough, while the diurnal profile of $PM_{2.5}$ shows a slight dip during the early afternoon. In contrast, $PM_{2.5}$ on August 18, 19, and 21 showed a midday peak across sites. Additionally, the magnitude of $PM_{2.5}$ at each site is elevated well above each site's seasonal average $PM_{2.5}$ concentration for every day in the event period. Diurnal profiles of $PM_{10}/PM_{2.5}$ (Appendix D) show the relative contribution of PM_{10} was at or below average relative to $PM_{2.5}$ during the midday $PM_{2.5}$ enhancement, indicating that the contribution of dust to abnormalities in $PM_{2.5}$ concentration are minimal. The peak daytime ozone concentrations are elevated above the seasonal average peak concentration for every site and day in the event period. These deviations from average ozone and $PM_{2.5}$ trends support the evidence of smoke impacts on ozone concentrations at the surface during the event period.

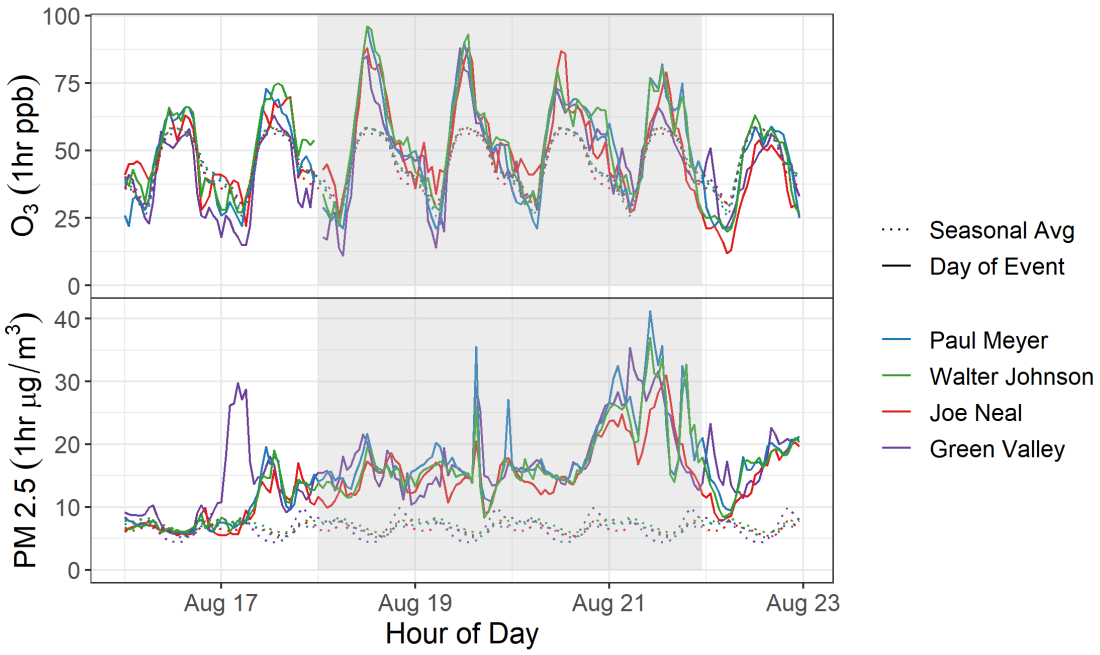

Figure 3-57. August 18-21 diurnal profile of ozone and $PM_{2.5}$ (solid lines), and the seasonal (May-Sept.) average (dotted lines) at sites in exceedance during the August 18-21, 2020, exceptional event. The gray shaded area highlights August 18-21, 2020.

Figures 3-58 through 3-61 further display the diurnal profile and average seasonal diurnal profile of ozone and $PM_{2.5}$ separated by event-affected monitoring site, along with the 5th to 95th percentiles of the seasonal diurnal profiles. These plots provide consistent evidence for the abnormal daytime

peaks in $PM_{2.5}$ at all sites and show concentrations of $PM_{2.5}$ on August 18-21 were above the 95th percentile on the evening of August 20 and the entire day on August 21.

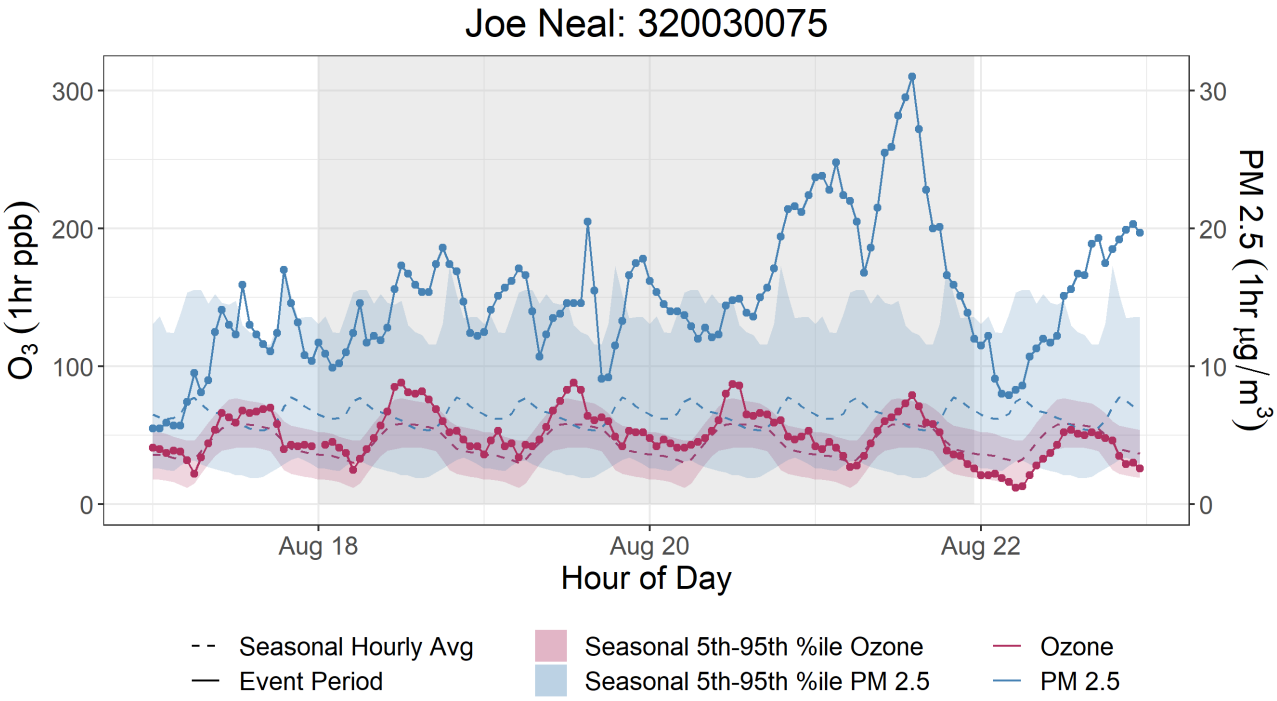

Figure 3-58. Diurnal profile of ozone (red) and $PM_{2.5}$ (blue) concentrations at Joe Neal, including concentrations during the August 18-21 exceptional event (solid lines) and the seasonal (May-Sept.) average (dotted lines). Shaded ribbons represent the 5-year 5th-95th percentile range. The gray shaded area highlights August 18-21, 2020.

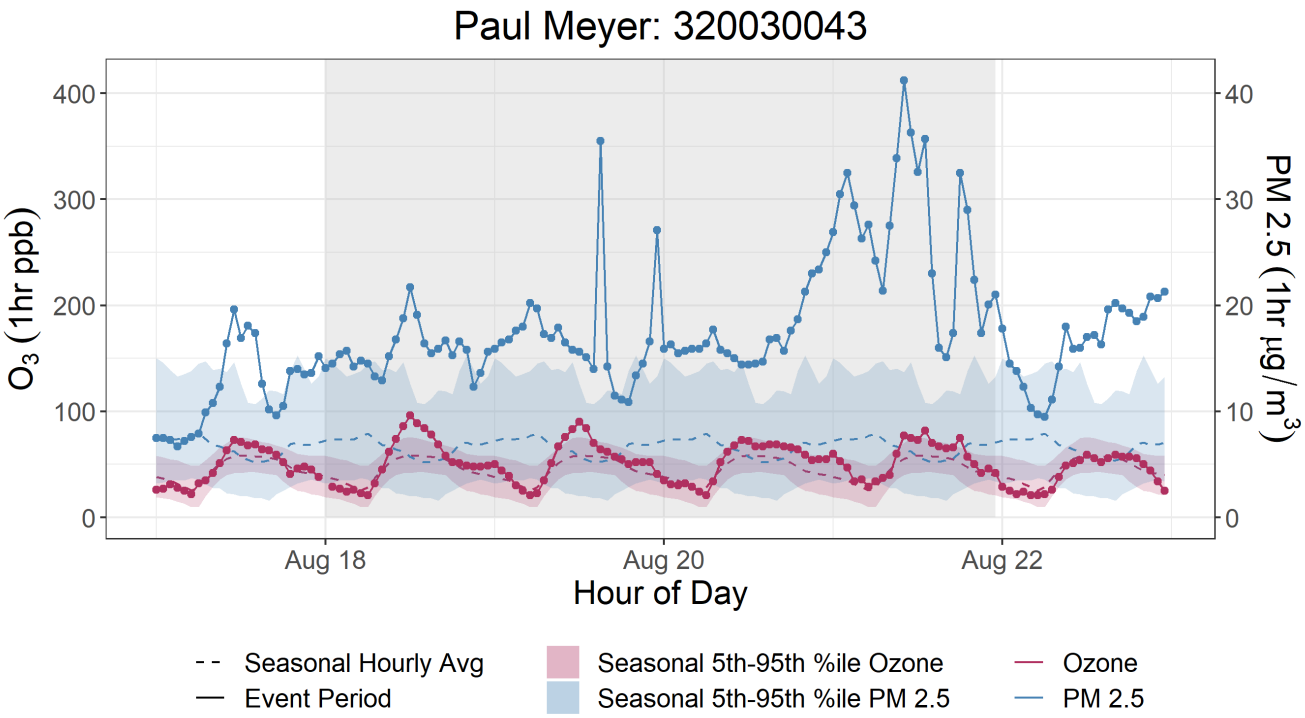

Figure 3-59. Diurnal profile of ozone (red) and $PM_{2.5}$ (blue) concentrations at Paul Meyer, including concentrations during the August 18-21 exceedance event (solid lines) and the seasonal (May-Sept.) average (dotted lines). Shaded ribbons represent the 5-year 5th-95th percentile range. The gray shaded area highlights August 18-21, 2020.

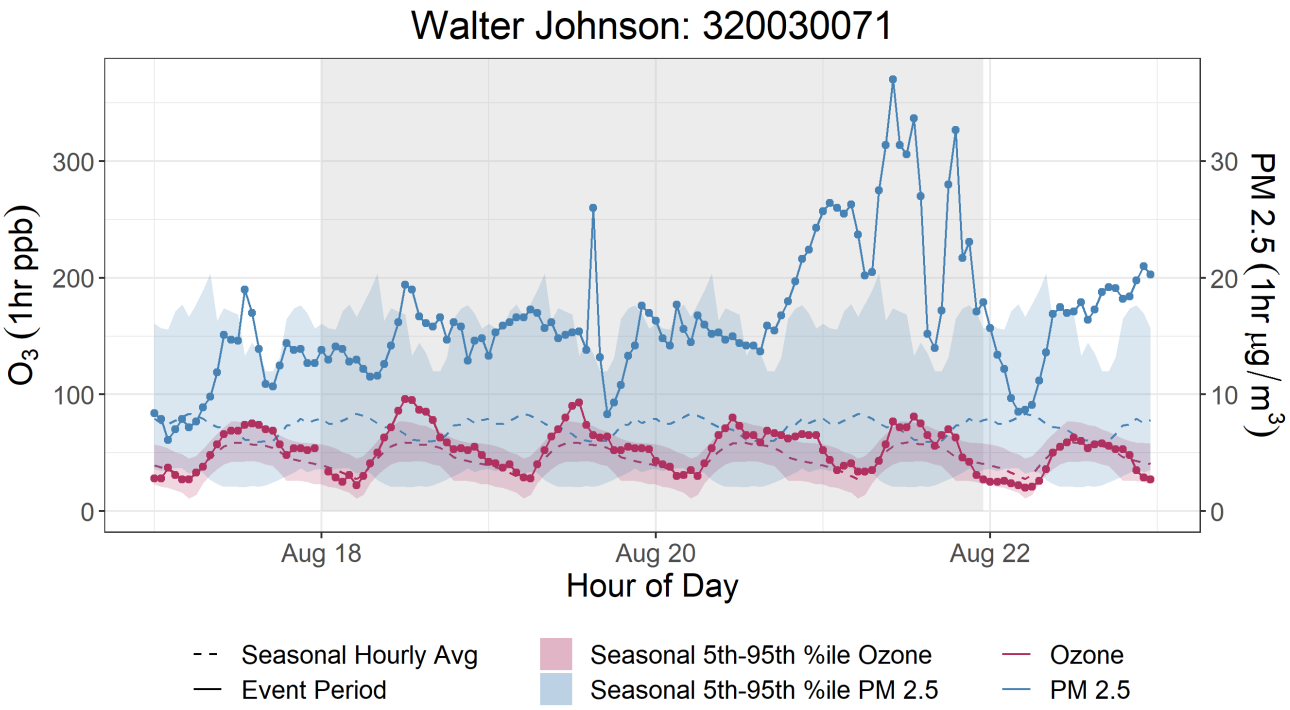

Figure 3-60. Diurnal profile of ozone (red) and $PM_{2.5}$ (blue) concentrations at Walter Johnson, including concentrations during the August 18-21 exceptional event (solid lines) and the seasonal (May-Sept.) average (dotted lines). Shaded ribbons represent the 5-year 5th-95th percentile range. The gray shaded area highlights August 18-21, 2020.

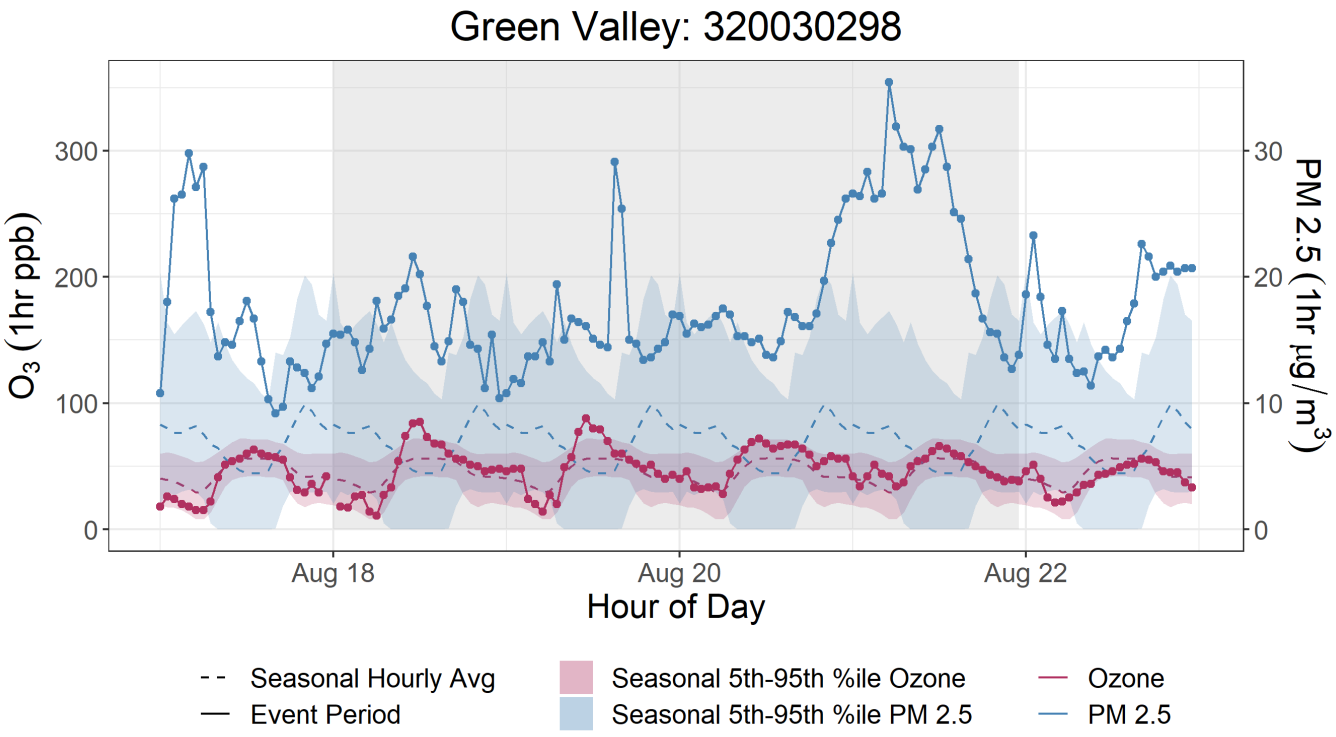

Figure 3-61. Diurnal profile of ozone (red) and $PM_{2.5}$ (blue) concentrations at Green Valley, including concentrations during the August 18-21 exceptional event (solid lines) and the seasonal (May-Sept.) average (dotted lines). Shaded ribbons represent the 5-year 5th-95th percentile range. The gray shaded area highlights August 18-21, 2020.

Diurnal profiles of ozone and CO on August 18-21 are included in Appendix D. CO data are available only for the Joe Neal and Green Valley event sites. CO concentrations reached magnitudes comparable to the 95th percentile value at each of these sites during the event period, but generally followed the expected diurnal pattern.

Concentrations of NO_x were examined for each day in the August 18-21 event in Clark County. NO data are available only at Jerome Mack (the NCore reference site), and NO_2 data are available only from Joe Neal and Jerome Mack. Available diurnal profiles of NO_x on August 18-21 are included in Appendix D. The daily NO_x trends did not deviate markedly from expected diurnal patterns during the event period, though peak concentrations of both NO and NO_2 at Jerome Mack were above average on each date.

The supporting pollutant trends and diurnal patterns, showing abnormal midday peaks in $PM_{2.5}$ and ozone concentrations outside of their normal seasonal or yearly historical averages, provide additional proof of smoke impacts on the Clark County area during the August 18-21, 2020, event. Wildfires can generate the precursors needed to create ozone, NO_x, and VOCs. While ozone concentrations can be suppressed very near a fire due to NO_x titration, downwind areas are likely to see an increase in ozone concentrations due to the presence of both precursor gases and sufficient

UV radiation (i.e., when an air mass leaves an area of very thick smoke that inhibited solar radiation) (Finlayson-Pitts and Pitts Jr, 1997; Jaffe et al., 2008; Bytnerowicz et al., 2010). Ozone precursors from wildfire smoke can also be transported a significant distance downwind, and if these compounds are mixed into an urban area (such as Las Vegas), the ozone concentrations produced can be significantly higher than they would be from either the smoke plume or the urban area alone (Jaffe et al., 2013; Wigder et al., 2013; Lu et al., 2016; Brey and Fischer, 2016). Since we find evidence of smoke impacts on August 18-21 in Clark County via supporting pollutant measurements and other analyses in Sections 3.1 and 3.2, we suggest that both the direct transport of ozone and the transport of ozone precursor gases likely caused the ozone exceedance.

Filter samples were also taken at the Jerome Mack (including a collocated sample) monitoring site in Clark County every three days during 2020. From these filter samples, concentrations of levoglucosan (a wildfire smoke tracer) were analyzed by the Desert Research Institute (DRI) via gas chromatography-mass spectroscopy (GC-MS). Levoglucosan is produced by the combustion of cellulose and is emitted during large wildfire events, which can then be transported downwind (Simoneit et al., 1999; Simoneit, 2002; Bhattarai et al., 2019). Levoglucosan has an atmospheric lifetime of one to four days before it is lost due to atmospheric oxidation and can therefore be used as a tracer of biomass burning (wildfires) far downwind from its source (Hoffmann et al., 2009; Hennigan et al., 2010; Bhattarai et al., 2019; Lai et al., 2014). In the Las Vegas region, residential wood combustion has historically not been a significant contributor to levoglucosan concentrations during the late summer time frame (Kimbrough et al., 2016). **Table 3-15** shows levoglucosan concentration, uncertainty, and positive/negative detection certainty on the days during and after the August 18-21 event. Because filter samples are only taken every three days, August 22 data are also used to characterize this event. Table 3-15 also shows the average levoglucosan concentration from 19 2018-2019 background days together with its standard deviation, and propagated uncertainty at the Jerome Mack site for comparison. On these background days, no ozone exceedance was observed, and fire/smoke influence was minimal according to HMS. For the August 18-21 event, after smoke from multiple, large complex wildfires in California reached Clark County on August 18, non-zero levoglucosan concentrations and a positive detection were seen. The 14 and 27 ng/m^3 detection of levoglucosan in Clark County at the Jerome Mack and the collocated measurement is significantly higher than the background average of 2±3 ng/m^3, providing certain evidence that wildfire smoke affected the area during the August 18-21 ozone exceedances.

Table 3-15. Levoglucosan concentrations at monitoring sites around Clark County, Nevada, before, during, and after the August 18-21 ozone event. Positive or negative detection is also shown.

Sample Date	Sampling Site	Levoglucosan (ng/m^3)	Levoglucosan Uncertainty (ng/m^3)	Levoglucosan Detected?
Background Days (2018-2019)	Jerome Mack	2±3	1	N/A
8/19/2020	Jerome Mack	14	2	Positive
	Collocated-Jerome Mack	14	2	Positive
8/22/2020	Jerome Mack	27	3	Positive

3.3 Tier 3 Analyses

3.3.1 Total Column and Meteorological Conditions

Satellite analyses and HYSPLIT trajectories shown in Section 3.1 provide strong evidence that smoke was present over Clark County at the times of the EEs from August 18–August 21, 2020. However, the visible true color, AOD, and CO satellite data do not provide information about the vertical distribution of visible or measured smoke components. We examined satellite-retrieved aerosol vertical profiles and ceilometer mixing height measurements to determine whether the smoke plume was present at or near the surface from August 18–August 21.

The Cloud-Aerosol Light Detection and Ranging (LIDAR) and Infrared Pathfinder Satellite Observation (CALIPSO) system is a remote sensing instrument mounted on the CloudSat satellite that provides vertical profile measurements of atmospheric aerosols and clouds. Detected aerosols are classified into marine, marine mixture, dust, dust mixture, clean/background, polluted continental, smoke, and volcanic aerosol types.

The most relevant CALIPSO aerosol retrievals over Clark County for the August 18–August 21 ozone events are available at approximately 2:40 p.m. LT on August 20 and at approximately 2:40 a.m. LT on August 22 (**Figures 3-62 and 3-64** for CALIPSO maps and **Figures 3-63 and 3-65** for visible satellite images with the CALIPSO track overlaid). The CALIPSO vertical profile captures information directly over Clark County during one day of the multiday ozone event and during the morning following the end of the multiday ozone event. Increased backscatter at 1,000 m to 4,000 m AGL provides evidence

of increased aerosols classified as smoke in the mixed layer over Clark County (Figures 3-66, 3-67, 3-68, and 3-69). The HYSPLIT trajectories shown in Section 3.1 provide evidence of smoke transport from the fires throughout California to Clark County, but do not provide information about the characteristics of aerosols in the vertical profile of the atmosphere over Clark County. Combining these two pieces of evidence, the CALIPSO aerosol retrieval provides evidence that enhanced aerosol concentrations were present in the vertical atmospheric column over Clark County on the afternoon of August 20 and the morning of August 22, while the HYSPLIT trajectories provide evidence of transport between the fires throughout California to Clark County. Together this evidence suggests that the smoke plume from the fires throughout California reached Clark County and likely affected air quality from August 18–August 21.

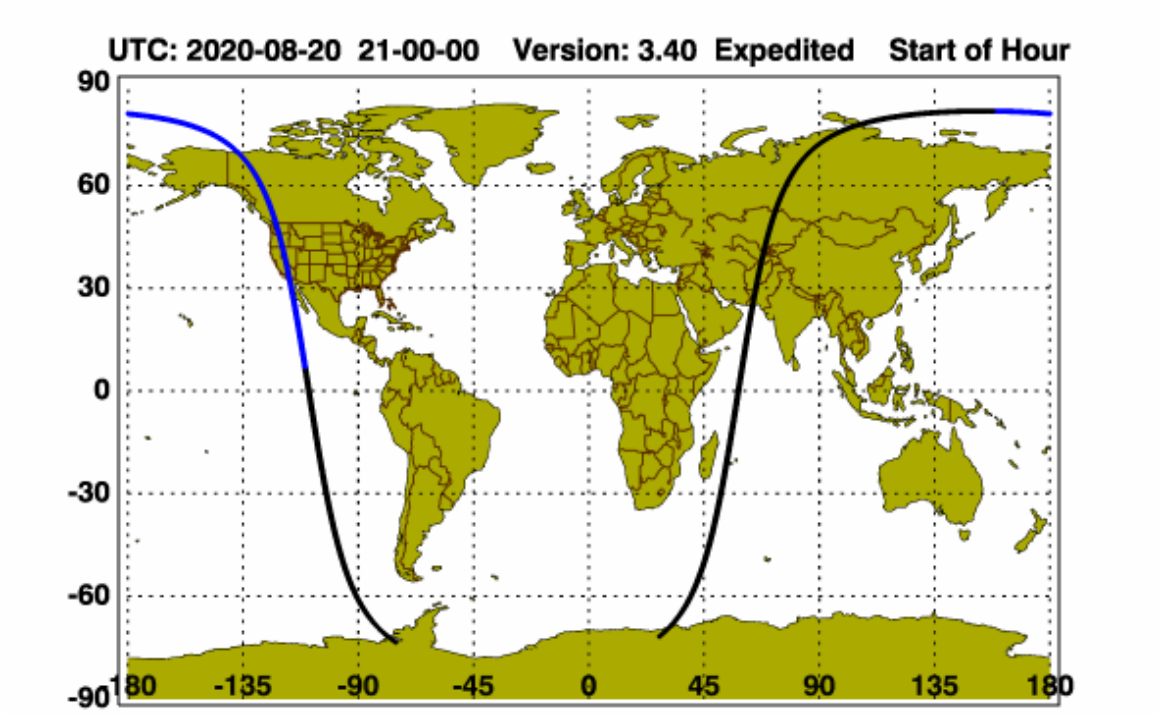

Figure 3-62. The CALIPSO retrieval path for August 20, 2020. This overpass was the closest to Clark County and the nearest in time to the EE date.

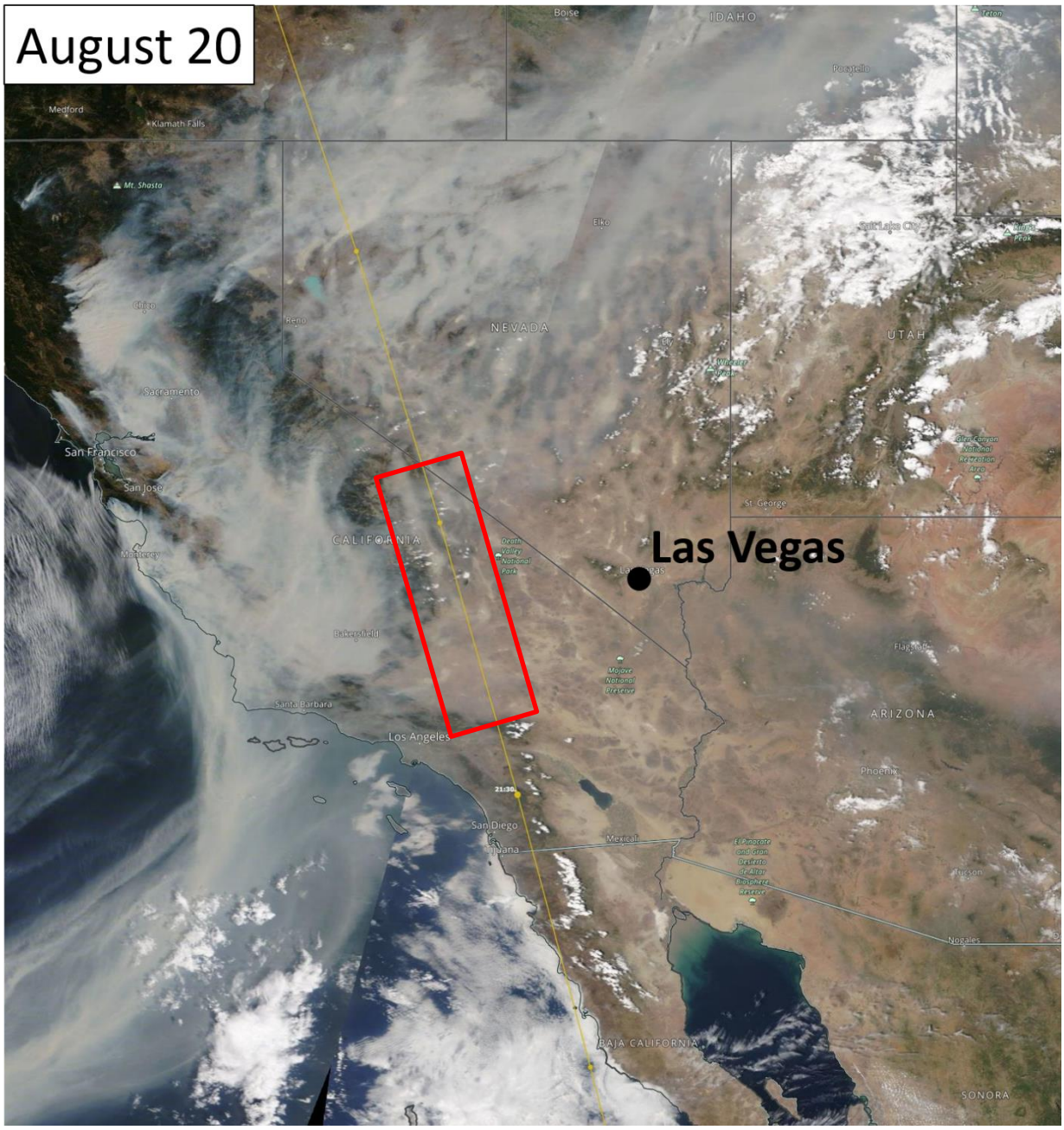

Figure 3-63. The CALIPSO retrieval path for August 20, 2020. This overpass was the closest to County and the nearest in time to the EE date.

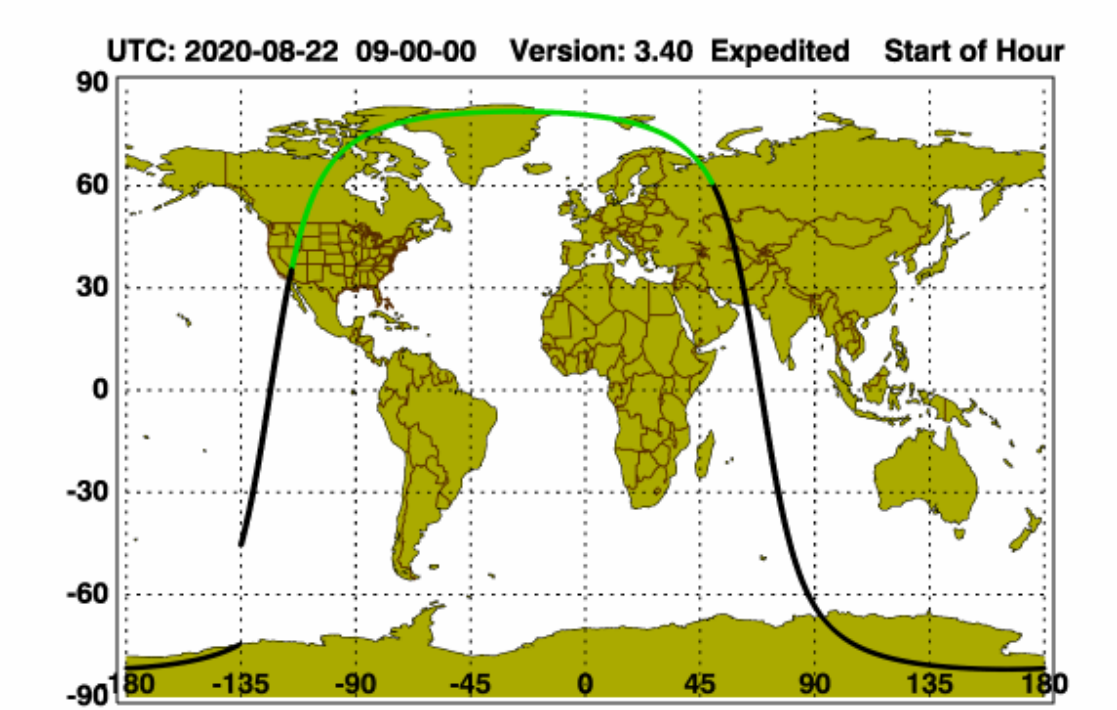

Figure 3-64. The CALIPSO retrieval path for August 22, 2020. This overpass was the closest to County and the nearest in time to the EE date.

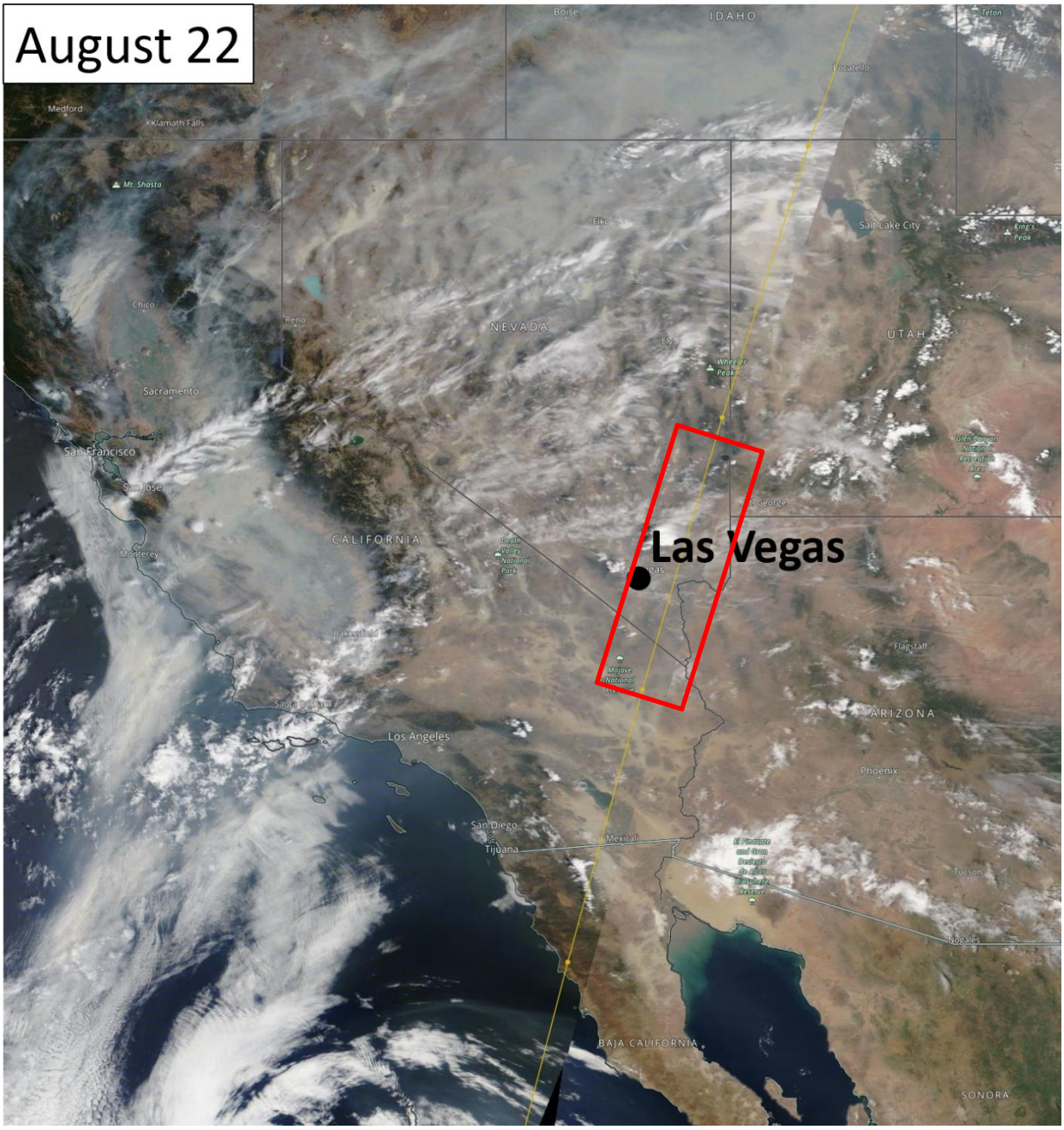

Figure 3-65. The CALIPSO retrieval path for August 22, 2020. This overpass was the closest to County and the nearest in time to the EE date.

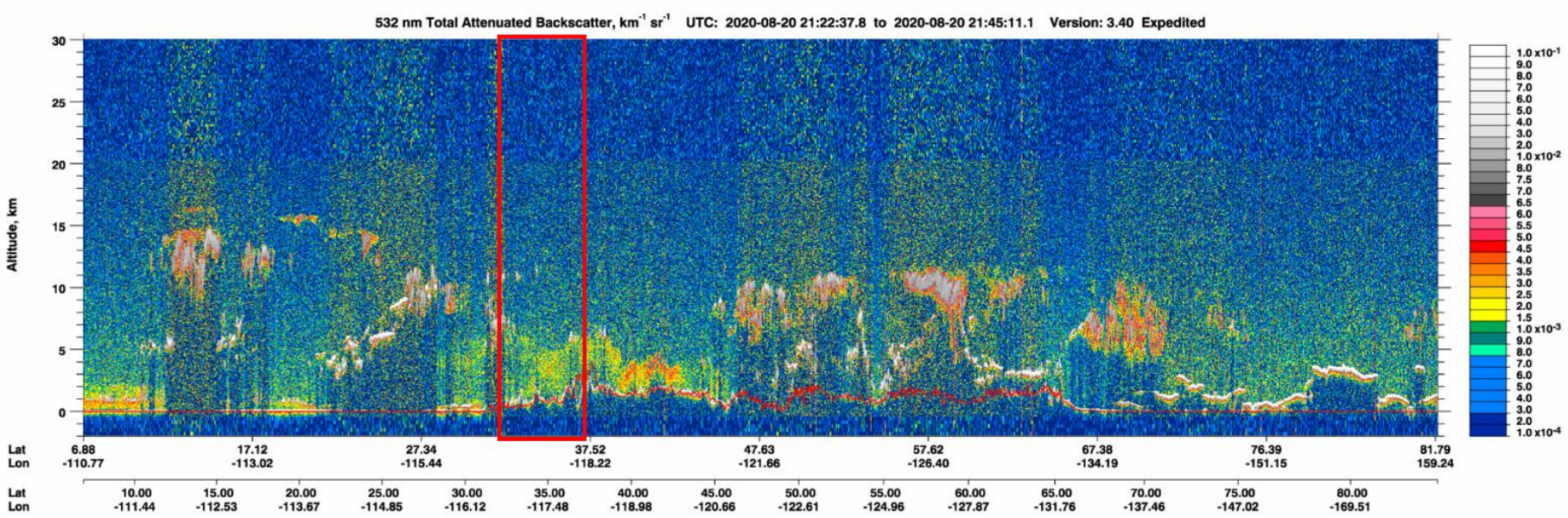

Figure 3-66. CALIPSO total column profile backscatter information for the August 20, 2020, overpass over Clark County, Nevada (approximate areas indicated by a red box).

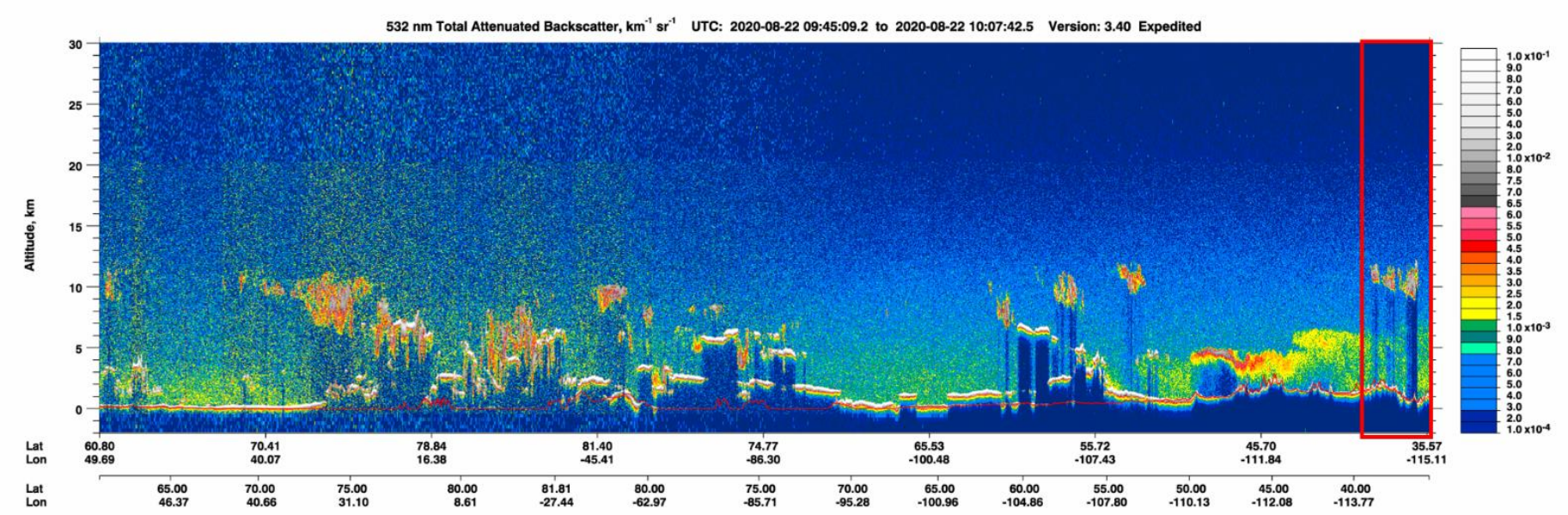

Figure 3-67. CALIPSO total column profile backscatter information for the August 22, 2020, overpass over Clark County (approximate areas indicated by a red box).

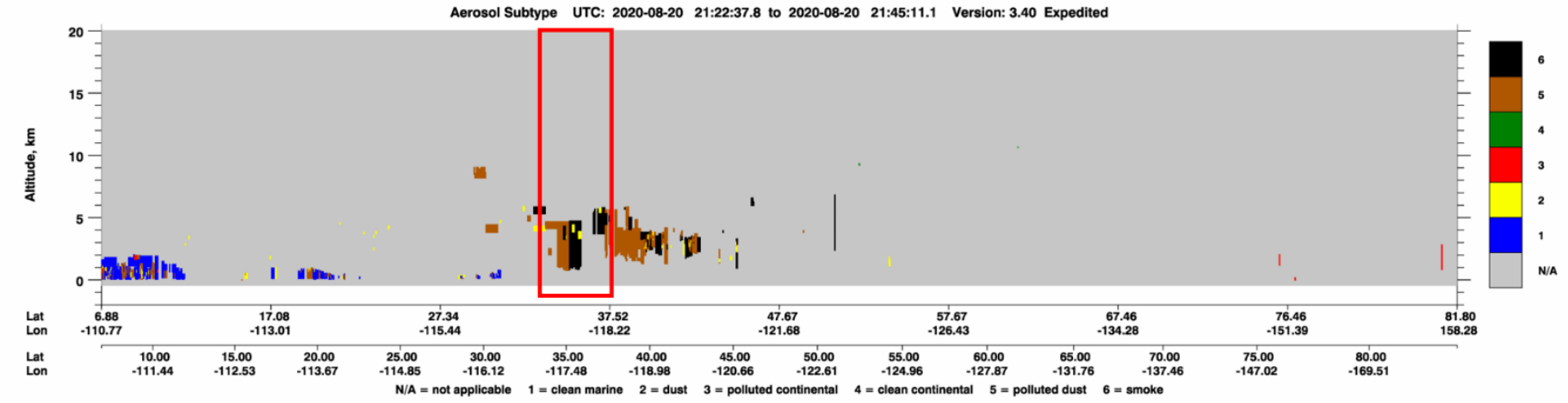

Figure 3-68. CALIPSO total column profile aerosol subtype information for the August 20, 2020, overpass over Clark County, Nevada (approximate areas indicated by a red box).

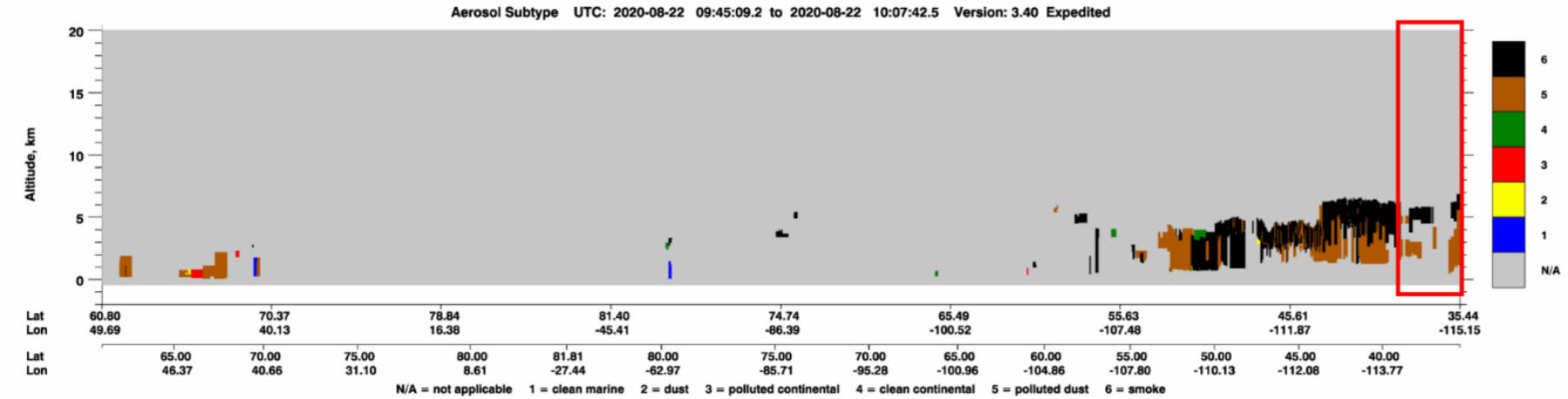

Figure 3-69. CALIPSO total column profile aerosol subtype information for the August 22, 2020, overpass over Clark County, Nevada (approximate areas indicated by a red box).

The mesoscale and local meteorological conditions from August 17–August 21 provide evidence of the transport of smoke from the fires throughout California to Clark County, Nevada, and subsequent vertical mixing of smoke from aloft to the surface. Upper-level wind barbs at 500 hPa over southern California and Nevada indicate a weak westerly and southwesterly wind direction on August 20 and August 21 causing smoke from the fires throughout California to move into Clark County (Figure 3-70).

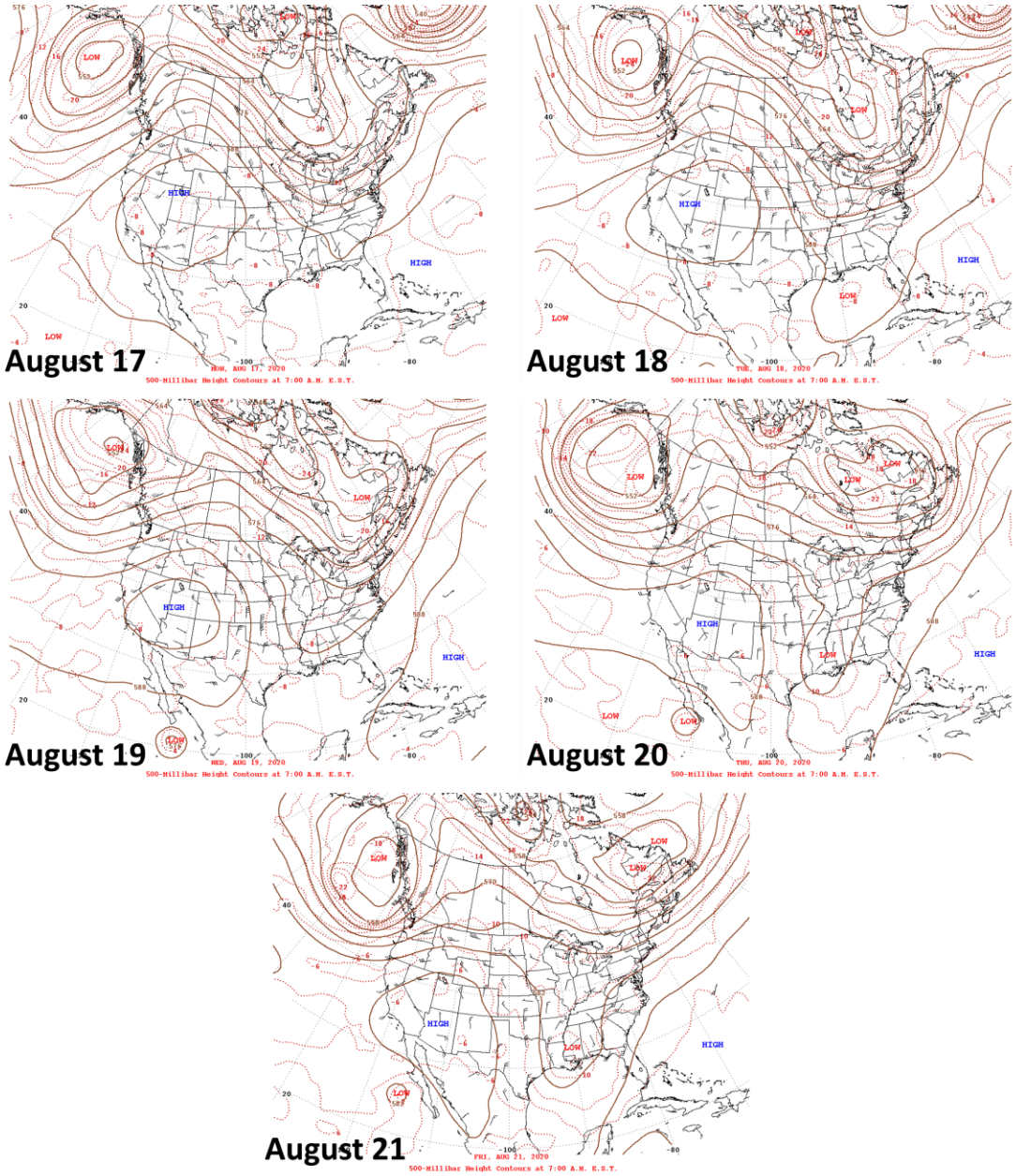

Figure 3-70. Daily upper-level meteorological maps for one day leading up to the EE and during the August 18-21 EE.

Local observations of mixing heights in the Las Vegas area from August 18–August 21 suggest that smoke was likely mixed into the lower levels of the atmosphere. Ceilometer data from the Jerome Mack site indicate mixing heights on August 18–August 21 between approximately 2,000 m and 3,000 m for several hours during each day (Figure 3-71). Furthermore, a surface low-pressure system was centered over the border of Nevada and California between August 18 and August 21. Low pressure at the surface is often associated with enhanced vertical mixing in the lower troposphere (Figure 3-72). Mixing height data from the ceilometer and the surface weather maps provide evidence of enhanced vertical mixing in the lower troposphere when smoke was present over Clark County.

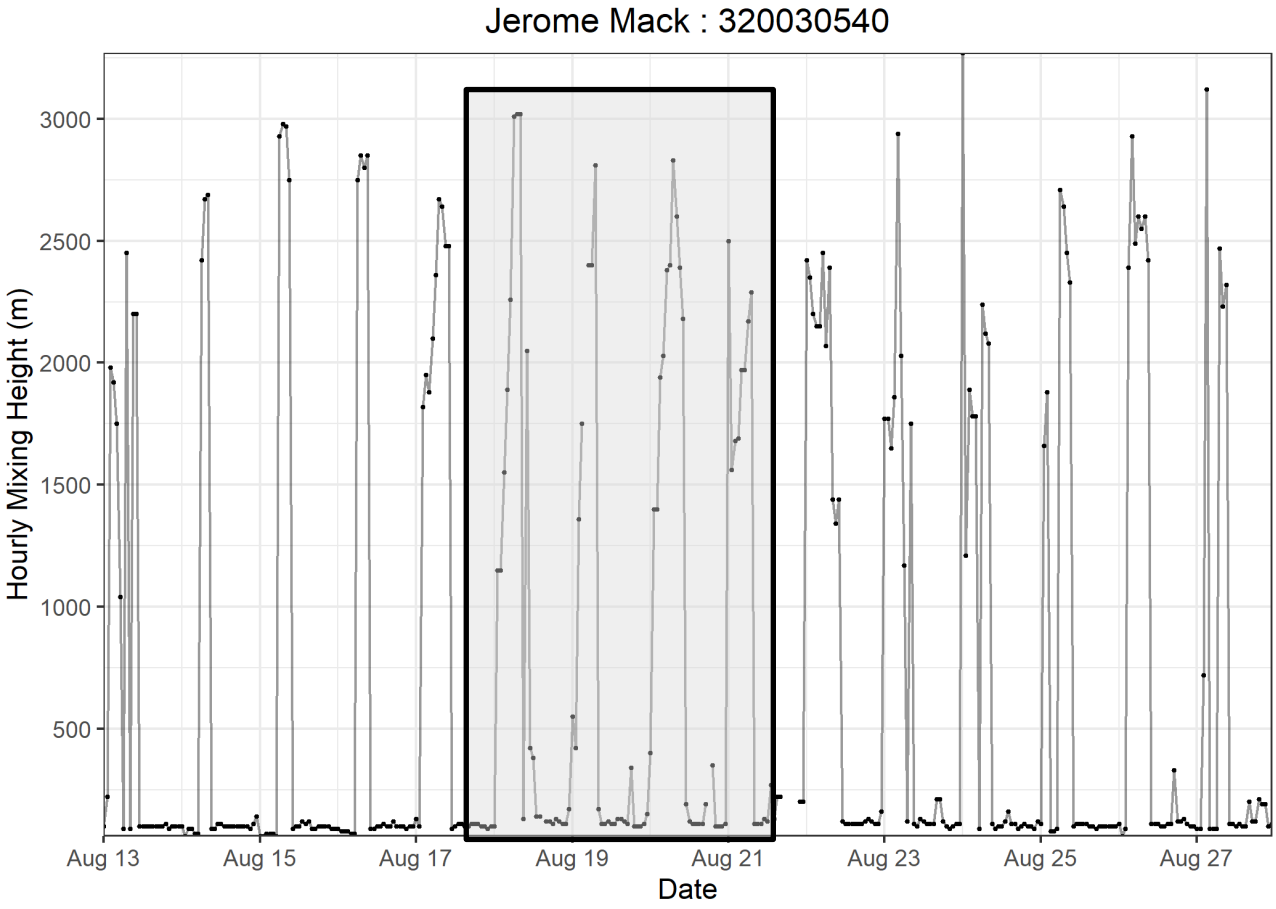

Figure 3-71. Time series of mixing heights taken from Jerome Mack (NCore Site) for two weeks before and after the August 18-21 EE. August 18-21 is highlighted in the grey box.

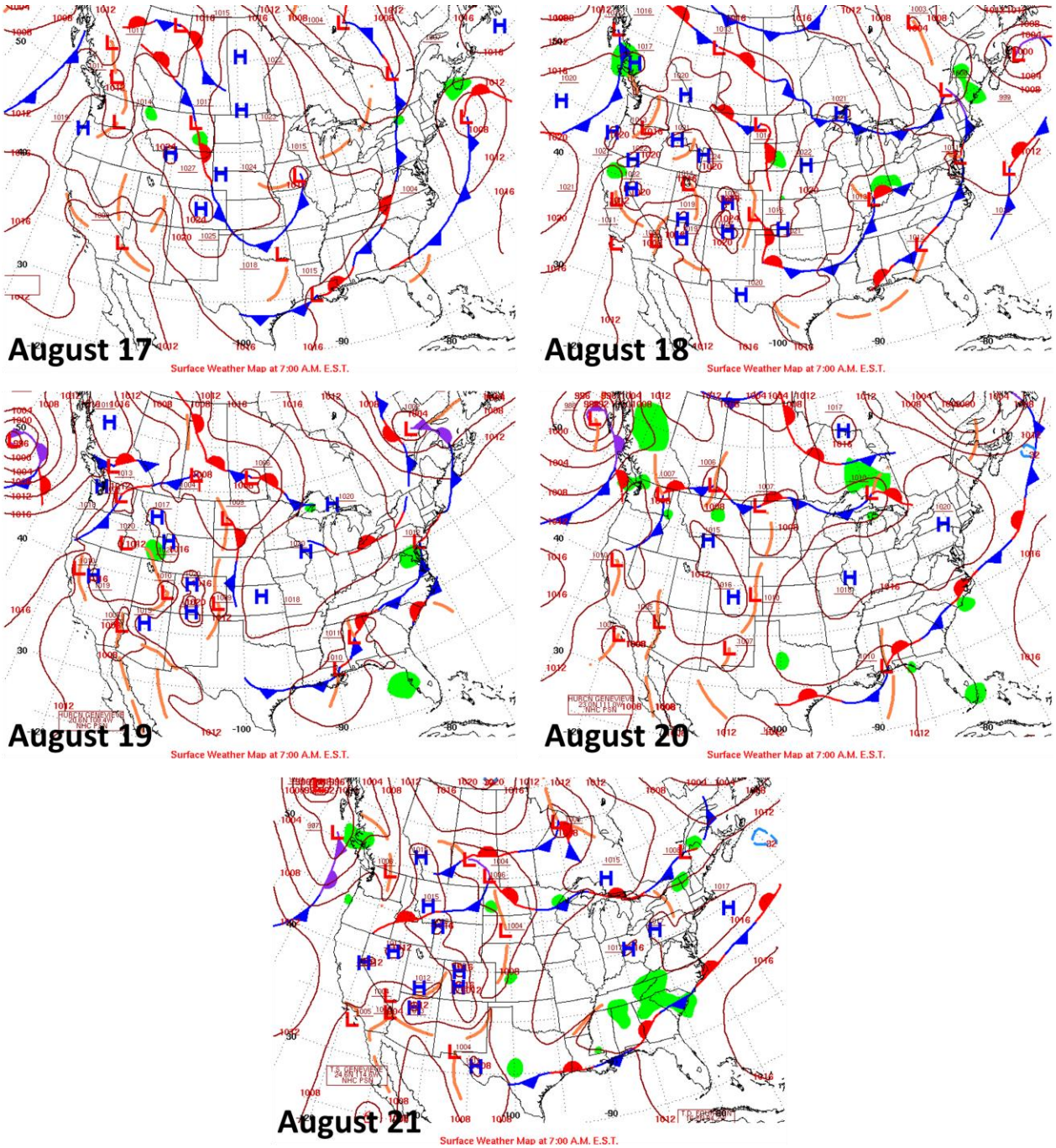

Figure 3-72. Daily surface meteorological maps for one day leading up to the EE and during the August 18-21 EE.

In addition to the ceilometer-based measurements of mixing heights, vertical temperature profiles (Skew-T diagrams) can also be used to estimate mixing heights (**Figures 3-73 through 3-75**). The vertical temperature profile at Las Vegas from August 18–August 21 shows that the vertical atmospheric profile was very dry in the lower troposphere—as shown by the wide space between the

temperature profile and the dewpoint profile—with wind shifting to a southwesterly direction by August 20. This indicates the potential for smoke transport in the lower levels of the atmosphere from the fires throughout California into Clark County. Enhanced vertical mixing from August 17–August 21 can be seen from a pronounced, very large mixed layer—as indicated by temperatures decreasing with height roughly along the dry adiabat up to at least 600 hPa—with associated warm temperatures and very dry air. The CALIPSO vertical profile of aerosols over Clark County in the afternoon of August 20 and the morning of August 22, the upper-level and surface weather maps, the ceilometer data, and the vertical temperature and wind profile suggest the existence of smoke within the mixed layer, the transport of smoke from the fires in California to Clark County in the free troposphere and mixed layer, and subsequent mixing to the surface in Clark County.

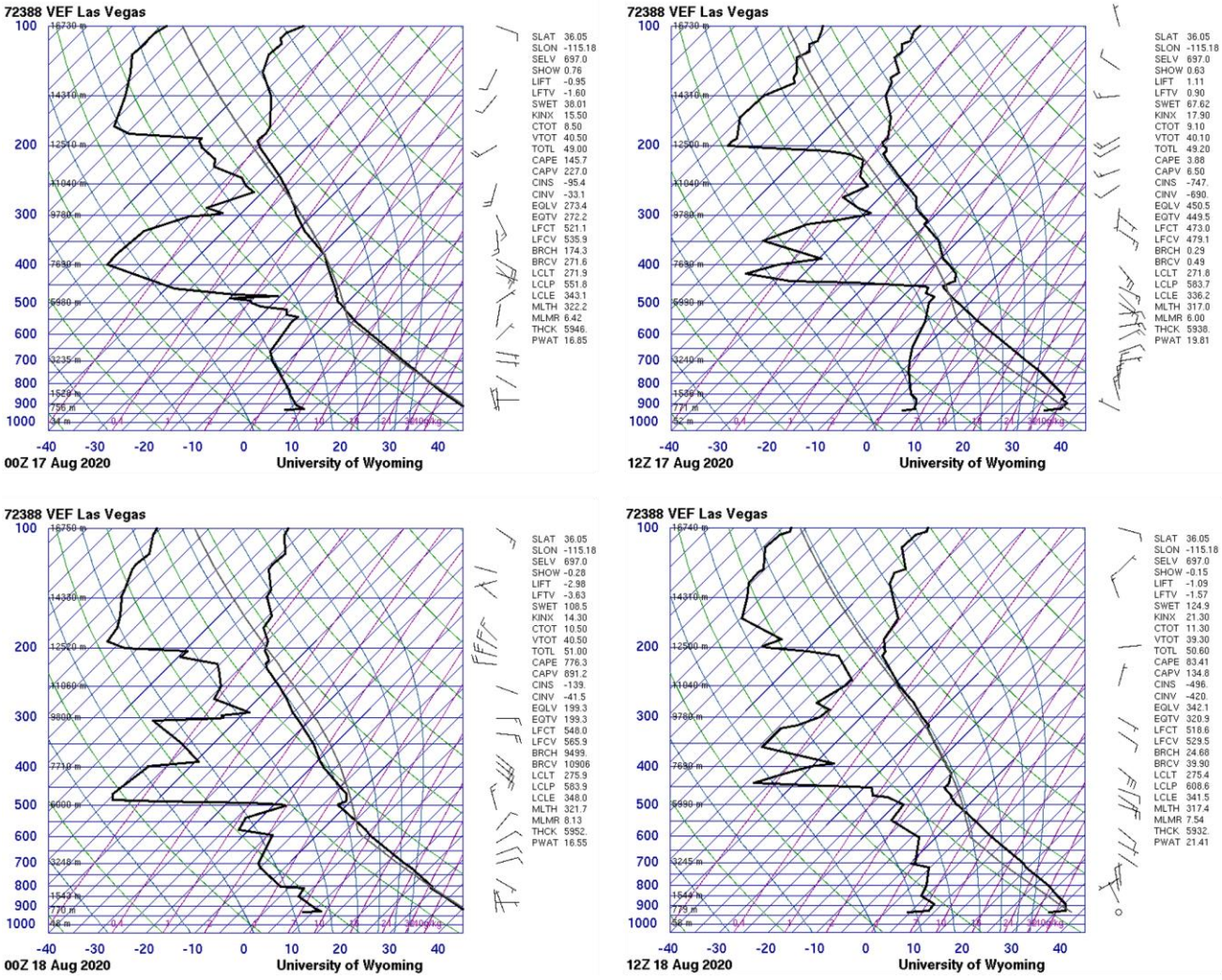

Figure 3-73. Skew-T diagrams from August 17-18, 2020, in Las Vegas, Nevada.

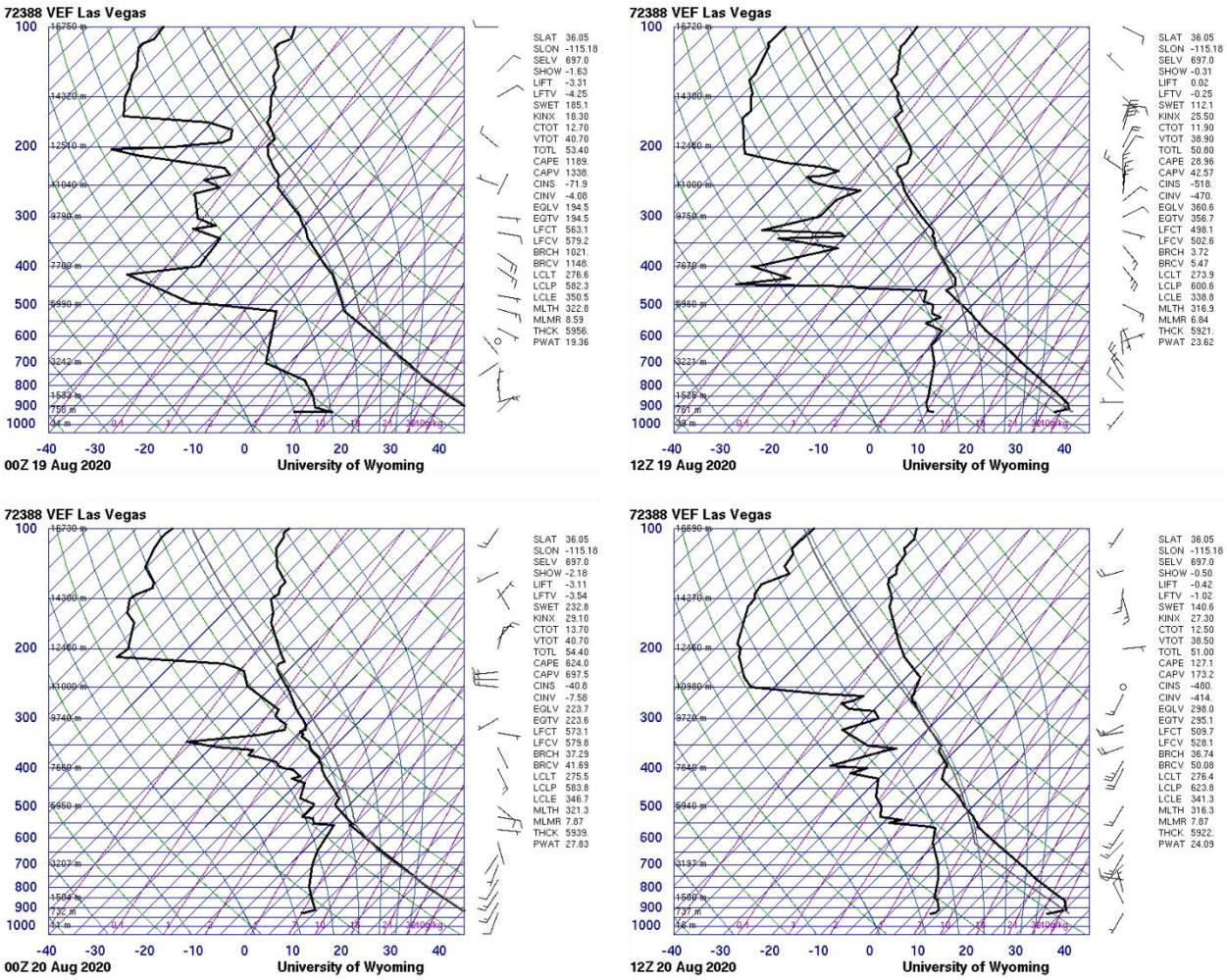

Figure 3-74. Skew-T diagrams from August 19-20, 2020, in Las Vegas, Nevada.

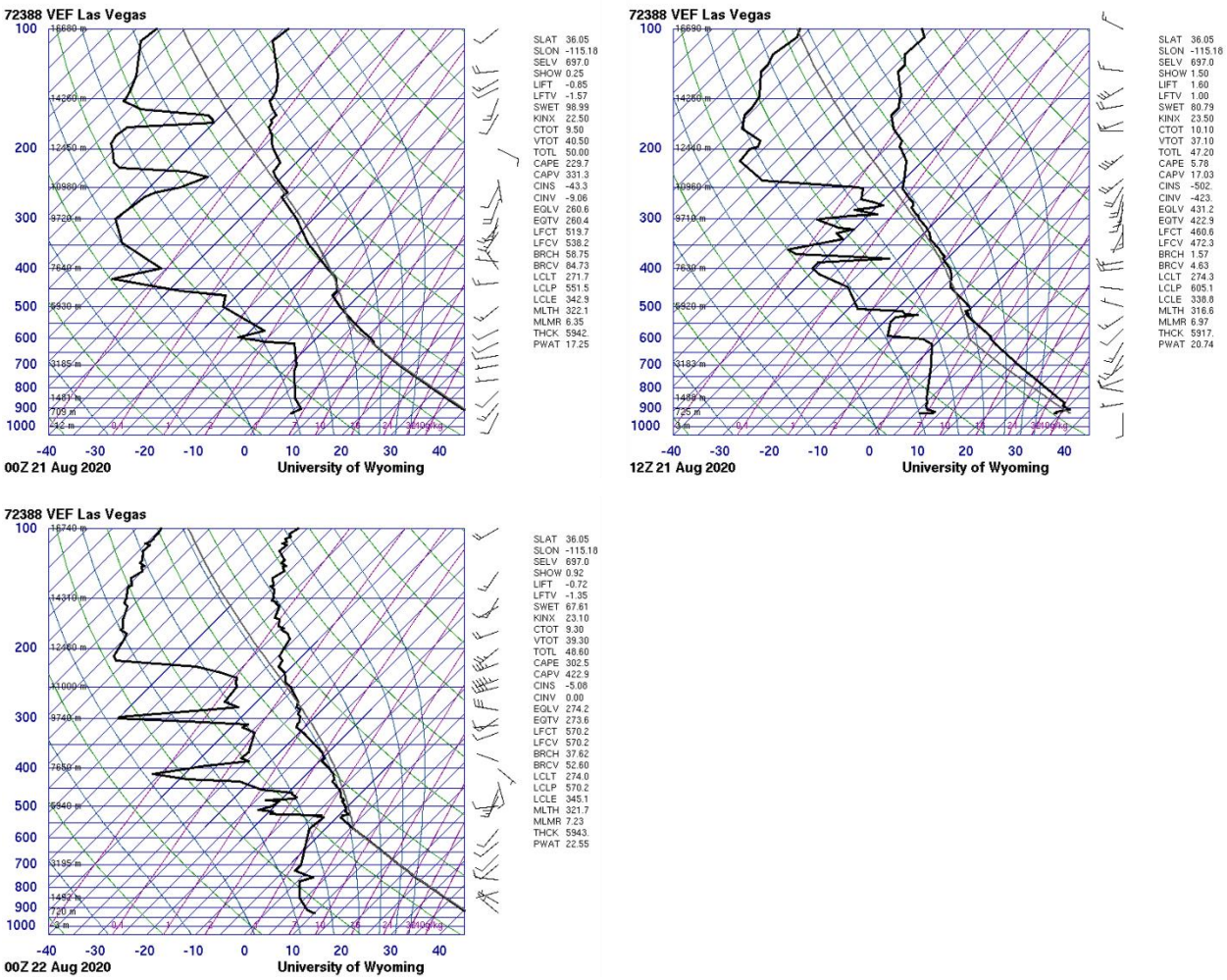

Figure 3-75. Skew-T diagrams from August 21-22, 2020, in Las Vegas, Nevada.

3.3.2 Matching Day Analysis

Ozone production and transport strongly depend on regional and local meteorological conditions. A comparison of ozone concentrations on suspected exceptional event days with non-event days that share similar meteorology can help identify periods when ozone production was affected by an atypical source. Given that similar meteorological days are likely to have similar ozone concentrations, noticeable differences in levels of ozone between the event date and meteorologically similar days can lend evidence to a clear causal relationship between a stratospheric intrusion and elevated ozone concentration.

Identify Meteorologically Similar Days

In order to identify the best matching meteorological days, both synoptic and local conditions were examined from ozone-season days (April 1 through September 30) between 2014 and 2020. Excluded from this set are days with suspected EEs in the 2018 and 2020 seasons, as well as dates within five days of the event date, to ensure that lingering effects of smoke transport or stratospheric intrusion did not appear in the data.

To best represent similar air transport, twice-daily HYSPLIT trajectories (initiated at 18:00 and 22:00 UTC) from Clark County for 2014-2020 were clustered by total spatial variance. The calculation, based on the difference between each point along a trajectory, provides seven distinct pathways of airflow into Clark County (see Section 3.3.3 for more details). The cluster that best represents the trajectory on the EE day was chosen, and ozone-season days within the cluster were then subset for regional meteorological comparison to the EE day.

For the meteorological comparison, a correlation score was assigned to each day from the cluster subset. The National Centers for Environmental Prediction (NCEP) reanalysis data were compiled for the ozone seasons in 2014-2020. Daily average wind speed, geopotential height, relative humidity, and temperature were considered at 1,000 mb and 500 mb. At the surface, daily average atmospheric pressure, maximum temperature, and minimum temperature were utilized. Pearson product-moment coefficient of linear correlation (pattern correlation) was calculated between the EE date and each cluster-subset ozone-season day in 2014-2020 for each parameter. The pattern correlation calculates the similarity between two mapped variables at corresponding grid locations within the domain. The statistic was calculated using a regional domain of 30°N-45°N latitude and 125°W-105°W longitude. The correlation score for each day was defined as the average pattern correlation of all parameters at each height level. The correlation scores were then ranked by the highest correlation for 1,000 mb, surface, and finally 500 mb. Dates within five days of the EE were removed from the similar day analysis to ensure the data are mutually exclusive. The 50 dates with the highest rank correlation scores were then chosen as candidate matching days for further analysis.

Local meteorological conditions for the subset of candidate matching days were then compared to conditions on each of August 18, 19, 20, and 21, and filtered to identify five or more days that best

matched each event date. Meteorological maps at the surface and 500 mb, along with local meteorological data describing temperature, wind, moisture, instability, mixing layer height, and cloud cover, were all examined. The data source for each parameter is summarized in Table 3-16.

Table 3-16. Local meteorological parameters and their data sources.

Meteorological Parameter	Data Source
Maximum daily temperature	Jerome Mack - NCore Monitoring Site
Average daily temperature	Jerome Mack - NCore Monitoring Site
Resultant daily wind direction	Jerome Mack - NCore Monitoring Site (calculated vector average)
Resultant daily wind speed	Jerome Mack - NCore Monitoring Site (calculated vector average)
Average daily wind speed	Jerome Mack - NCore Monitoring Site
Average daily relative humidity (RH)	Jerome Mack - NCore Monitoring Site
Precipitation	Jerome Mack - NCore Monitoring Site
Total daily global horizontal irradiance (GHI)	UNLV Measurement and Instrumentation Data Center (MIDC) in partnership with NREL (https://midcdmz.nrel.gov/apps/daily.pl?site=UNLV&start=20060318&yr=2021&mo=4&dy=29)
4:00 p.m. local standard time (LST) mixing layer mixing ratio	Upper air soundings from KVEF (http://weather.uwyo.edu/upperair/sounding.html)
4:00 p.m. LST lifted condensation level (LCL)	Upper air soundings from KVEF (http://weather.uwyo.edu/upperair/sounding.html)
4:00 p.m. LST convective available potential energy (CAPE)	Upper air soundings from KVEF (http://weather.uwyo.edu/upperair/sounding.html)
4:00 p.m. LST 1,000-500 mb thickness	Upper air soundings from KVEF (http://weather.uwyo.edu/upperair/sounding.html)
Daily surface meteorological map	NOAA's Weather Prediction Center Daily Weather Maps (https://www.wpc.ncep.noaa.gov/dailywxmap/index.html)
Daily 500 mb meteorological map	NOAA's Weather Prediction Center Daily Weather Maps (https://www.wpc.ncep.noaa.gov/dailywxmap/index.html)

Matching Day Analysis

The meteorological conditions between August 18-21, 2020, were very warm compared to average seasonal conditions. Table 3-17 displays the percentile ranking of each examined meteorological parameter at the Jerome Mack-NCore site among seven years of observations for the 30-day period surrounding each day in the event period (for example, August 3 through September 2 for the August 18 event date). The maximum temperature reached on August 18 and 19 was the highest on

record, as was the average temperature on August 20. Additionally, CAPE and 500-1,000 mb thickness were unusually high (94th and 100th percentile, respectively) on August 18. Measurement summaries over this 30-day period best represent the expected conditions on the event date. As is typical for Clark County during this period, there was no precipitation on any of the event dates.

Table 3-17. Percentile rank of meteorological parameters on each date within the event period, August 18-21, 2020, compared to the 30-day period surrounding each date over seven years. The percentile ranking of precipitation is marked NA because a vast majority of examined days recorded 0 inches. The percentile ranking of a directional degree value is irrelevant and has been marked NA.

Date	Max Temp (°F)	Avg Temp (°F)	Resultant Wind Direction (°)	Resultant Wind Speed (mph)	Avg Wind Speed (mph)	Avg RH (%)	Precip (in)	Total GHI (kWh/m^2)	Mixing Layer Mixing Ratio (g/kg)	LCL (mb)	CAPE (J/kg)	500-1,000 mb Thickness (m)
2020-08-18	100	98	NA	38	42	16	NA	21	78	40	94	100
2020-08-19	100	98	NA	26	27	26	NA	16	69	43	86	97
2020-08-20	98	100	NA	61	47	9	NA	36	43	20	70	97
2020-08-21	92	92	NA	79	78	58	NA	24	61	32	73	98

The subset of synoptically similar days identified according to the methodology above was further filtered based on parameters listed in Table 3-16 to match local meteorological conditions that existed on each event date. **Tables 3-18 through 3-21** show these best-matching days, as well as the MDA8 ozone concentration at each site that experienced an ozone exceedance on each date. Weather maps for each event date and each matching date listed in Tables 3-18 through 3-21 show highly consistent conditions, with a surface low-pressure system and an upper-level region of either low-gradient or relatively high pressure over Clark County. Most dates also had a surface high to the east. Surface and upper-level maps are included in **Appendix E**.

Table 3-18 shows the average MDA8 ozone concentration across the subset of days that are most meteorologically similar to the conditions that existed on August 18. Though CAPE on August 18 was very high, no precipitation was recorded, so this variable was matched less stringently than other meteorological variables. The expected range of ozone provided is defined by one standard deviation, a conservative estimate given the small sample size. The expected MDA8 ozone concentration, given similar meteorological conditions to those on August 18, 2020, is below the 70-ppb ozone standard at each site, ranging from 61 to 63 ppb. Further, the upper end of the provided range at each site does not exceed the ozone standard. None of the six meteorologically matching dates exceeds the 70-ppb ozone standard, and similar dates with higher photochemical potential than August 18 (lower wind speeds, higher average temperatures, or greater solar irradiance) did not exceed the ozone standard.

Similarly, Tables 3-19 through 3-21 show the average MDA8 ozone concentration across the days that are most meteorologically similar to the conditions that existed on August 19, 20, and 21, respectively. A small subset of matching days is excluded from this analysis, including June 23, 2015, July 7, 2017, and August 31, 2018, due to smoke influence. Detailed justification is provided in Appendix E. The expected MDA8 ozone concentrations, given similar meteorological conditions to those on each date, is below the 70-ppb ozone standard at each site, ranging from 58 to 61 ppb across event dates and sites. Further, the upper end of the provided range across all three dates at each site does not exceed the ozone standard. Only a single matching day across all event dates, June 16, 2017, exceeded the ozone standard. Little evidence of smoke, dust, or stratospheric intrusion exists on this date, so it was not excluded from the analysis. If meteorology were the sole cause of the ozone exceedances on August 18-21, 2020, we would expect to see similarly high ozone levels on each of the similar days listed in Tables 3-18 through 21. This similar day analysis shows that an ozone exceedance on any of the event dates (August 18-21) was unexpected based on meteorological conditions alone despite the high temperatures that persisted.

Table 3-18. Top matching meteorological days to August 18, 2020. PM, WJ, and JN refer to monitoring sites Paul Meyer, Walter Johnson, and Joe Neal, respectively. Average MDA8 ozone concentration of meteorologically similar days is shown plus-or-minus one standard deviation rounded to the nearest ppb.

Date	Max Temp (°F)	Avg Temp (°F)	Resultant Wind Direction (°)	Resultant Wind Speed (mph)	Avg Wind Speed (mph)	Avg RH (%)	Precip (in)	Total GHI (kWh/m^2)	Mixing Layer Mixing Ratio (g/kg)	LCL (mb)	CAPE (J/kg)	500-1,000 mb Thickness (m)	MDA8 Ozone Concentration (ppb)		
													PM	WJ	JN
2020-08-18	**115**	**102**	**194.63**	**1.89**	**3.22**	**10.33**	**0**	**6.54**	**8.59**	**582.32**	**1189.94**	**5956**	**79**	**82**	**78**
2017-08-29	111	97.08	238.06	1.5	2.24	19.17	0	5.91	8.15	627.53	143.55	5877	61	64	59
2018-08-01	110	101.38	211.63	0.48	3.72	19	0	7.28	10.51	629.32	1246.7	5927	66	68	68
2019-09-01	110	95.79	141.53	1.72	3.6	11.79	0	7.17	6.8	572.29	175.85	5910	60	61	57
2019-09-03	109	96.21	183.21	0.4	1.79	23.25	0	6.86	8.84	626.74	423.9	5879	58	62	67
2019-09-04	109	97.33	141.45	1.45	2.85	21.08	0.02	6.56	8.56	608.57	551.27	5903	59	60	62
2020-08-16	116	102.08	203.2	0.71	1.55	8.58	0	7.09	6.42	551.84	145.74	5946	63	63	60
Average MDA8 Ozone Concentration of Meteorologically Similar Days													**61 ± 3**	**63 ± 3**	**62 ± 4**

Table 3-19. Top matching meteorological days to August 19, 2020. PM, WJ, JN, and GV refer to monitoring sites Paul Meyer, Walter Johnson, and Joe Neal, and Green Valley, respectively. Average MDA8 ozone concentration of meteorologically similar days is shown plus-or-minus one standard deviation rounded to the nearest ppb.

Date	Max Temp (°F)	Avg Temp (°F)	Resultant Wind Direction (°)	Resultant Wind Speed (mph)	Avg Wind Speed (mph)	Avg RH (%)	Precip (in)	Total GHI (kWh/m^2)	Mixing Layer Mixing Ratio (g/kg)	LCL (mb)	CAPE (J/kg)	500-1,000 mb Thickness (m)	MDA8 Ozone Concentration (ppb)			
													PM	WJ	JN	GV
2020-08-19	**115**	**101.75**	**265.41**	**1.44**	**2.76**	**11.96**	**0**	**6.26**	**7.87**	**583.88**	**624**	**5939**	**74**	**74**	**73**	**71**
2017-07-06	116	103.08	265.63	0.63	2.39	10.38	0	8.31	7.48	572.65	862.13	5940	62	66	70	62
2017-07-10	106	96.33	293.08	1.18	4.75	23.58	0	4.98	9.51	657.31	261.61	5871	58	61	63	56
2017-08-29	111	97.08	238.06	1.5	2.24	19.17	0	5.91	8.15	627.53	143.55	5877	61	64	59	59
2018-06-04	109	94.54	213.73	2.25	3.77	7.71	0	8.62	4.89	545.03	230.82	5876	65	67	64	66
2019-07-13	112	99.42	222.49	2.14	3.1	16	0	8.38	7.05	578.47	278.7	5898	50	53	53	54
2019-07-26	107	97.75	264.15	1.97	4.4	24.42	0	7.44	8.74	626.25	131.4	5884	58	60	61	64
2019-08-04	111	100.38	217	2.88	4	10.83	0	7.45	8.21	597.62	712.16	5916	58	60	61	60
2019-09-05	105	95.29	204.99	1.36	2.92	24.38	0	5.07	8.94	638.8	320.54	5873	57	57	57	61
2020-07-11	113	102.17	215.86	3.04	4.1	9.04	0	7.71	7.71	583.92	233.94	5938	56	57	58	52
2020-07-12	114	104.88	217.59	4.34	5.09	7.71	0	8.38	7.48	570.3	238.23	5948	51	53	49	47
2020-08-16	116	102.08	203.2	0.71	1.55	8.58	0	7.09	6.42	551.84	145.74	5946	63	63	60	54
Average MDA8 Ozone Concentration of Meteorologically Similar Days													**58 ± 4**	**60 ± 5**	**60 ± 5**	**58 ± 5**

Table 3-20. Top matching meteorological days to August 20, 2020. JN refers to monitoring site Joe Neal. Average MDA8 ozone concentration of meteorologically similar days is shown plus-or-minus one standard deviation rounded to the nearest ppb.

Date	Max Temp (°F)	Avg Temp (°F)	Resultant Wind Direction (°)	Resultant Wind Speed (mph)	Avg Wind Speed (mph)	Avg RH (%)	Precip (in)	Total GHI (kWh/m^2)	Mixing Layer Mixing Ratio (g/kg)	LCL (mb)	CAPE (J/kg)	500-1,000 mb Thickness (m)	MDA8 Ozone Concentration (ppb)
													JN
2020-08-20	**113**	**102.54**	**215.66**	**2.88**	**3.42**	**9.25**	**0**	**6.95**	**6.35**	**551.58**	**229.74**	**5942**	**71**
2014-07-24	111	100.08	239.58	3.04	3.89	11.79	0	8.38	5	538.15	0	5938	53
2015-06-23	107	94.42	180.57	1.1	3.03	8	0	8.18	4.29	528.52	0	5890	64
2015-06-29	108	100.71	184.68	1.81	2.68	17.42	0	8.38	8.18	599.64	322.26	5924	57
2017-06-16	109	95.58	180.09	0.78	1.95	8	0	8.99	3.32	503.37	0	5892	74
2017-07-01	111	97.54	156.49	3.1	4.2	8.04	0	8.7	4.35	518.7	161.96	5906	67
2018-06-04	109	94.54	213.73	2.25	3.77	7.71	0	8.62	4.89	545.03	230.82	5876	64
2018-08-05	110	99.04	214.14	4.44	4.89	6.12	0	8.07	4.74	532.37	0	5921	68
2018-09-08	108	94.71	217.08	2.39	3.57	15.75	0	6.84	6.13	571.37	0	5898	52
2019-07-13	112	99.42	222.49	2.14	3.1	16	0	8.38	7.05	578.47	278.7	5898	53
2019-08-02	110	98.42	240.51	1.46	2.36	12.83	0	7.77	6.47	579.45	0	5904	59
2019-08-05	113	100.92	230.09	2.28	3.02	10.42	0	8	5.97	551.55	0	5931	61
2019-08-15	112	98.42	226.85	1.05	1.82	8.83	0	7.87	4.9	534.3	0	5899	63
2019-08-16	110	97.46	216.28	1.79	3.33	6.75	0	7.91	5.01	541.54	0	5904	70
2019-09-03	109	96.21	183.21	0.4	1.79	23.25	0	6.86	8.84	626.74	423.9	5879	67
2019-09-07	107	95.96	207.85	3.62	4.8	18.42	0	6.65	7.92	609.79	316.78	5886	65
2020-07-05	109	98.92	206.55	1.88	2.6	5.67	0	8.84	4.45	535.82	0	5895	52
2020-07-06	109	97.5	158.73	1.69	3.32	6.08	0	8.79	4.8	533.86	0	5912	60
2020-07-11	113	102.17	215.86	3.04	4.1	9.04	0	7.71	7.71	583.92	233.94	5938	58
2020-07-12	114	104.88	217.59	4.34	5.09	7.71	0	8.38	7.48	570.3	238.23	5948	49
Average MDA8 Ozone Concentration of Meteorologically Similar Days													**61 ± 7**

Table 3-21. Top matching meteorological days to August 21, 2020. PM refers to monitoring site Paul Meyer. Average MDA8 ozone concentration of meteorologically similar days is shown plus-or-minus one standard deviation rounded to the nearest ppb.

Date	Max Temp (°F)	Avg Temp (°F)	Resultant Wind Direction (°)	Resultant Wind Speed (mph)	Avg Wind Speed (mph)	Avg RH (%)	Precip (in)	Total GHI (kWh/m^2)	Mixing Layer Mixing Ratio (g/kg)	LCL (mb)	CAPE (J/kg)	500-1,000 mb Thickness (m)	MDA8 Ozone Concentration (ppb)
													PM
2020-08-21	**110**	**98.58**	**126.52**	**4.26**	**5.13**	**19.42**	**0**	**6.55**	**7.23**	**570.26**	**302.51**	**5943**	**71**
2015-08-15	108	94.17	193.77	1.83	2.49	31.79	0	7.58	7.01	581.81	58.67	5904	56
2017-07-01	111	97.54	156.49	3.1	4.2	8.04	0	8.7	4.35	518.7	161.96	5906	64
2017-07-29	107	97.46	110.72	4.1	4.7	24.75	0	8.09	8.83	624.5	581.29	5892	65
2018-06-13	110	96.83	194.1	2.27	3.59	8.71	0	8.78	4.16	520.26	41.57	5897	56
2018-07-07	110	101.12	172.56	1.87	3.31	18.33	0	4.97	8.35	608.71	271.66	5912	59
2018-07-28	113	102.83	174.82	3.39	4.78	16.12	0	7.92	8.71	597.79	608.21	5944	67
2018-07-29	108	97.29	142.43	4.51	5.8	28.96	0	6.04	9.77	657.56	262.61	5902	52
2018-08-15	105	93.75	166.34	3.32	4.77	26.58	0	6.15	8.26	649.84	81.33	5858	54
2019-07-12	109	98.71	153	0.78	3.3	14	0	6.3	7.24	594.58	372.34	5892	52
2019-07-30	107	98.79	146.94	7.7	7.87	16.96	0	7.61	8.73	614.11	520.36	5898	52
2019-08-01	106	94.67	138.2	1.42	2.33	28.42	0	8	9.3	640.56	575	5869	59
2019-08-13	108	95.62	129.54	1.08	2.17	13.08	0	7.89	6.09	578.83	124.03	5871	48
2019-09-01	110	95.79	141.53	1.72	3.6	11.79	0	7.17	6.8	572.29	175.85	5910	60
Average MDA8 Ozone Concentration of Meteorologically Similar Days													**57 ± 6**

These findings show that an external source of ozone contributed to the ozone exceedances between August 18-21, 2020. Our analysis expanded on methods shown in the EPA guidance and a previously concurred exceptional event to identify 6 to 19 days that are meteorologically similar to each of August 18, 19, 20, and 21, 2020 (Arizona Department of Environmental Quality, 2018). The expected MDA8 ozone concentration at each site is 10 or more parts per billion below the concentrations measured at each site on any of these four dates in 2020. Based on this evidence, it is unlikely that meteorology alone enhanced photochemical production of ozone enough to cause the exceedances on August 18-21, 2020. This validates the existence of an extrinsic ozone source on August 18-21, 2020.

3.3.3 GAM Statistical Modeling

Generalized additive models (GAM) are a type of statistical model that allows the user to predict a response based on linear and non-linear effects from multiple variables (Wood, 2017). These models tend to provide a more robust prediction than Eulerian photochemical models or simple comparisons of similar events (Simon et al., 2012; Jaffe et al., 2013; U.S. Environmental Protection Agency, 2016). Camalier et al. (2007) successfully used GAM modeling to predict ozone concentrations across the eastern United States using meteorological variables with r^2 values of up to 0.8. Additionally, previous concurred exceptional event demonstrations and associated literature, i.e., Sacramento Metropolitan Air Quality Management District (2011), Alvarado et al. (2015), Louisiana Department of Environmental Quality (2018), Arizona Department of Environmental Quality (2016), and Pernak et al. (2019) used GAM modeling to predict ozone events that exceed the NAAQS standards, some in EE cases. By comparing the GAM-predicted ozone values to the actual measured ozone concentrations (i.e., residuals), we can determine the effect of outside influences, such as wildfires or stratospheric intrusions, on ozone concentrations each day (Jaffe et al., 2004). High, positive residuals suggest a non-typical source of ozone in the area but cannot specifically identify a source. Gong et al. (2017) and McClure and Jaffe (2018) used GAM modeling, in addition to ground and satellite measurements of wildfire pollutants, to estimate the enhancement of ozone during wildfire smoke events. Similar to other concurred EE demonstrations, we used GAM modeling of meteorological and transport variables to estimate the MDA8 ozone concentrations at multiple sites across Clark County for 2014-2020. To estimate the effect of wildfire smoke on ozone concentrations, we can couple the GAM residual results (observed MDA8 ozone–GAM-predicted MDA8 ozone) with the other analyses to confirm that the non-typical enhancement of ozone is due to wildfires during August 18-21, 2020.

Using the same GAM methodology as prior concurred EE demonstrations and the studies mentioned above, we examined more than 30 meteorological and transport predictor variables, and through testing, compiled the 16 most important variables to estimate MDA8 ozone each day at eight monitoring sites across Clark County, Nevada (Paul Meyer, Walter Johnson, Joe Neal, Green Valley, Boulder City, Jean, Indian Springs, and Jerome Mack). As suggested by EPA guidance (U.S. Environmental Protection Agency, 2016), we used meteorological variables measured at each station

(the previous day's MDA8 ozone, daily min/max temperature, average temperature, temperature range, wind speed, wind direction, or pressure), if available (see Table 2-1). If meteorological variables were not available at a specific site, we supplemented the data with National Centers for Environmental Prediction (NCEP) reanalysis meteorological data to fill any data gaps. We also tested filling data gaps with Jerome Mack meteorological data and found results had no statistical difference. We used sounding data from KVEF (Las Vegas Airport) to provide vertical meteorological components; soundings are released at 00:00 and 12:00 UTC daily. Variables such as temperature, relative humidity, wind speed, and wind direction were averaged over the first 1,000 m above the surface to provide near-surface, vertical meteorological parameters. Other sounding variables, such as Convective Available Potential Energy (CAPE), Lifting Condensation Level (LCL) pressure, mixing layer potential temperature, mixed layer mixing ratio, and 500-1,000 hPa thickness provided additional meteorological information about the vertical column above Clark County. We also initiated HYSPLIT GDAS 1°x1° 24-hour back trajectories from downtown Las Vegas (36.173° N, -115.155° W, 500 m AGL) at 18:00 and 22:00 UTC (10:00 a.m. and 2:00 p.m. local standard time) each day to provide information on morning and afternoon transport during critical ozone production hours. We clustered the twice-per-day back trajectories from 2014-2020 into seven clusters. **Figure 3-76** shows the clusters, percentage of trajectories per cluster, and heights of each trajectory cluster. We identified a general source region for each cluster: (1) Northwest U.S., (2) Stagnant Las Vegas, (3) Central California, (4) Long-Range Transport, (5) Northern California, (6) Southern California, and (7) Baja Mexico. Within the GAM, we use the cluster value to provide a factor for the distance traveled by each back trajectory. Additionally, day of year (DOY) was used in the GAM to provide information on season and weekly processes. The year (2014, 2015, etc.) was used a factor for the DOY parameter to distinguish interannual variability.

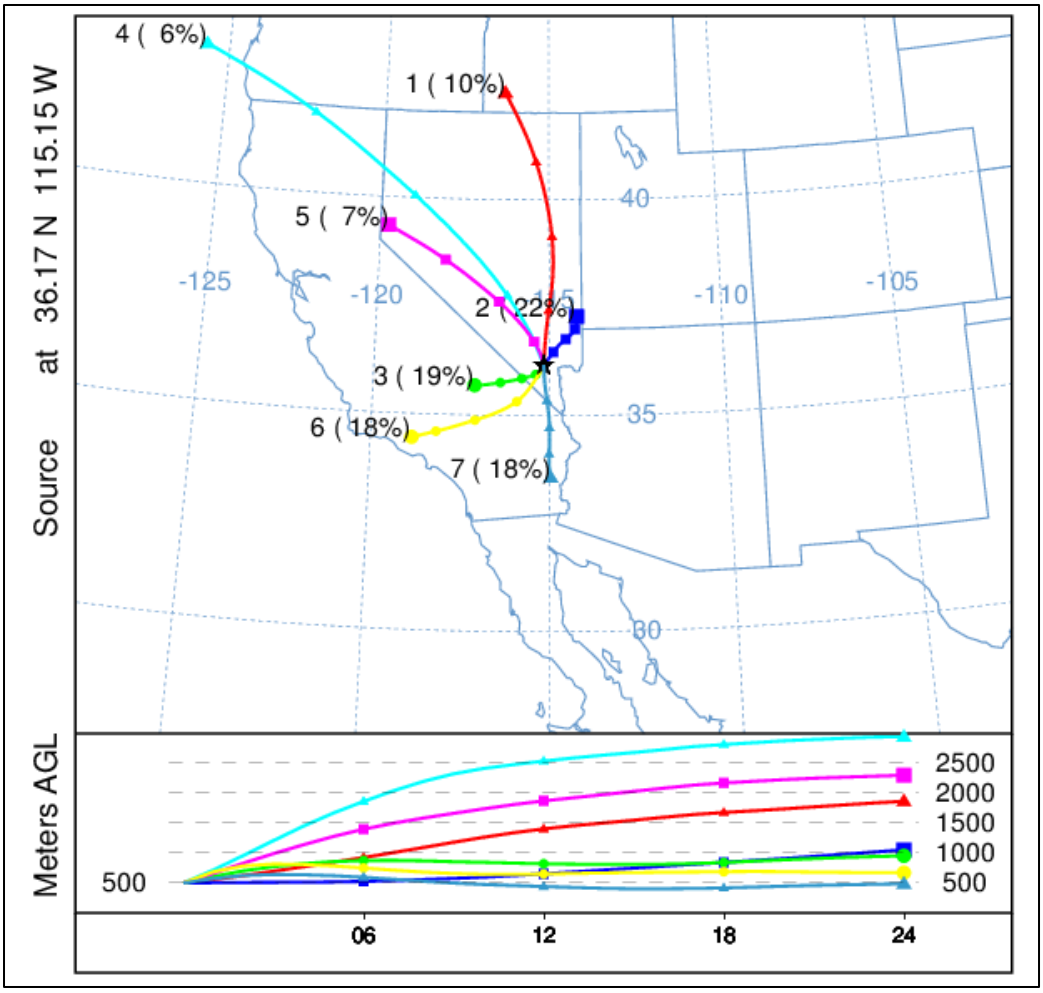

Figure 3-76. Clusters for 2014-2020 back trajectories. Seven unique clusters were identified for the twice daily (18:00 and 22:00 UTC) back-trajectories for 2014-2020 initiated in the middle of the Las Vegas Valley. The percentage of trajectories per cluster is shown next to the cluster number, and the height of each cluster is shown below the map.

Once all the meteorological and transport variables were compiled, we inserted them into the GAM equation to predict MDA8 ozone:

$$g(MDA8\ O_{3,i}) = f_1(V1_i) + f_2(V2_i) + f_3(V3_i) + \cdots + residual_i$$

where f_i are fit functions calculated from penalized cubic regression splines of observations (allowing non-linearity in the fit), Vi are the variables, and i is the daily observation. All variables were given a cubic spline basis except for wind direction, which used a cyclic cubic regression spline basis. For DOY and back trajectory distances, we used year factors (i.e., 2014-2020) and cluster factors (i.e., 1-7) to distinguish interannual variability and source region differences. The factors provide a different smooth function for each category (Wood, 2017). For example, the GAM smooth of DOY for 2014 can

be different than 2015, 2016, etc. In order to optimize the GAM, we first must adjust knots or remove any variables that are over-fitting or under-performing. We used the "mgcv" R package to summarize and check each variable for each monitoring site (Wood, 2020). A single GAM equation (using the same variables) was used for each monitoring site for consistency. During the initial optimization process, we removed the proposed 2018 and 2020 EE days from the dataset. We also ran 10 cross-validation tests by randomly splitting data 80/20 between training/testing for each monitoring site to ensure consistent results. All cross-validation tests showed statistically similar results with no large deviations for different data splits. We used data from each site during the April -September ozone seasons for 2014 through 2020, which is consistent with other papers modeling urban ozone (e.g., Pernak et al., 2019; McClure and Jaffe, 2018; Solberg et al., 2019; Solberg et al., 2018) and ozone concentrations during the periods with exceptional events are within the representative range of ozone in the GAM model.

Table 3-22 shows the variables used in the GAM and their F-value. The F-value suggests how important each variable is (higher value = more important) when predicting MDA8 ozone. Any bolded F-values had a statistically significant correlation ($p < 0.05$). R^2, the positive 95th quantile of residuals, and normalized mean square residual values for each monitoring site are listed at the bottom of the table.

Table 3-22. GAM variable results. F-values per parameter used in the GAM model are shown for each site. Units and data sources for each parameter in the GAM model are shown on the right of the table. The 95th quantile, R^2, and normalized mean square residual information are shown at the bottom of the table.

Parameters	Paul Meyer	Walter Johnson	Joe Neal	Green Valley	Jerome Mack	Boulder City	Jean	Indian Springs	Unit	Source
Day of Year (DOY) factored by Year (2014-2020)	**8.11**	**7.09**	**7.65**	**11.8**	**7.94**	**7.11**	**8.68**	**7.53**	--	--
Previous Day MDA8 Ozone	**37.9**	**22.7**	**41.5**	**18.1**	**27.9**	**31.3**	**105.5**	**123.8**	ppb	Monitor Data
Average Daily Temperature	1.92	**2.90**	**4.80**	0.05	1.83	2.13	0.12	1.83	K	Monitor Data/NCEP Reanalysis
Maximum Daily Temperature	1.37	**2.74**	**2.48**	0.16	0.38	0.02	1.30	1.52	K	
Temperature Range (TMax - TMin)	**4.12**	2.13	1.38	1.74	1.77	1.51	0.50	0.54	K	
Average Daily Pressure	**5.54**	**6.42**	**6.74**	**4.64**	**2.94**	0.22	2.17	0.24	hPa	
Average Daily Wind Speed	**11.1**	**5.03**	**7.49**	**5.02**	**15.3**	0.07	0.49	2.19	knots	
Average Daily Wind Direction	0.47	**1.04**	0.24	**1.35**	**2.43**	0.69	0.11	**2.48**	deg	
18 UTC HYSPLIT Distance factored by Cluster	1.70	1.82	1.69	0.92	2.52	2.97	1.66	1.03	km	HYSPLIT Back-Trajectories
22 UTC HYSPLIT Distance factored by Cluster	1.03	0.74	1.47	1.47	1.20	1.26	1.19	0.50	km	
00 UTC Convective Available Potential Energy	3.50	0.13	0.37	1.17	1.16	0.57	**5.71**	**6.49**	J/kg	Sounding Data
00 UTC Lifting Condensation Level Pressure	1.36	**2.78**	2.29	2.41	**3.76**	0.38	1.43	0.38	hPa	
00 UTC Mixing Layer Potential Temperature	0.65	0.79	1.72	0.10	1.23	0.97	1.09	2.53	K	
00 UTC Mixed Layer Mixing Ratio	**2.10**	**2.76**	**2.85**	**3.09**	**3.07**	**2.42**	0.69	1.04	g/kg	
00 UTC 500-1000 hPa Thickness	**2.91**	0.43	1.70	1.60	1.69	**4.11**	**2.18**	1.83	m	
12 UTC 1km Average Relative Humidity	**12.4**	**14.6**	**17.8**	**21.3**	**37.5**	**26.0**	**11.1**	2.18	%	
95th Quantile of Positive Residuals (ppb)	10	10	10	10	9	9	9	10		
R^2	0.55	0.58	0.60	0.58	0.61	0.58	0.57	0.55		
Normalized Mean Square Residual	3.6E-06	7.3E-04	6.1E-05	1.3E-04	3.1E-05	1.3E-04	1.2E-04	1.5E-04		

Table 3-23 provides GAM residual and fit results for all sites for the ozone seasons of 2014 through 2020. Overall, the residuals are low for all data points, and similarly low for all non-EE days. However, the 2018 and 2020 EE day residuals are significantly higher than the non-EE day results, meaning there are large, atypical influences on these days. Figure 3-77 shows non-EE vs EE median residuals with the 95th confidence intervals denoted as notches in the boxplots. We show the data in both ways to provide specific values, as well as illustrate the difference in non-EE vs EE residuals. Since the 95th confidence intervals for median EE residuals are above and do not overlap with those for non-EE residuals at any site in Clark County, we can state that the median residuals are higher and statistically different ($p<0.025$). The R^2 for each site ranged between 0.55 and 0.61, suggesting a good fit for each monitoring site, and similar to the results in prior studies and EE demonstrations mentioned previously (r^2 range of 0.4-0.8). We also provide the positive 95th quantile MDA8 ozone concentration, which is used to estimate a "No Fire" MDA8 ozone value based on the EPA guidance (U.S. Environmental Protection Agency, 2016). We also provide the median residuals (and confidence interval) for all non-EE days with observed MDA8 at or above 60 ppb; this threshold was needed to build a sufficient sample size with a representative distribution, and derive the median and 95% confidence interval. It should be noted that four out of the seven years modeled by the GAM were high wildfire years, and these values likely include a significant amount of wildfire days. We were not able to systematically remove wildfire influence by subsetting the Clark County ozone data based on HMS smoke, HMS smoke and $PM_{2.5}$ concentrations, and low wildfire years. These methods produced a significant number of false positives and negatives, and yielded datasets that were still affected by wildfire smoke. Therefore, these values should be considered an upper estimate of residuals for high ozone days. We see that the median residuals for 2018 and 2020 EE days are significantly higher than those on non-EE high observed ozone days since their confidence intervals do not overlap (or are comparable for the Jerome Mack station). The non-EE day residuals on days where observed MDA8 was at or above 60 ppb were determined to be normally distributed with a slight positive skew (median skewness = 0.39).

Table 3-23. Overall, 2014-2020 GAM median residuals and 95% confidence interval range in square brackets for each site modeled. Sample size is shown in parentheses below the residual statistics. For sample sizes of less than ten, we include a range of residuals in square brackets instead of the 95% confidence interval. Residual results are split by non-EE days and the 2018 and 2020 EE days. R^2 for each site is also shown along with the positive 95th quantile result.

Site Name	All Residuals (ppb)	Non-EE Day Residuals (ppb)	2018 & 2020 EE Day Residuals (ppb)	R^2	Positive 95th Quantile (ppb)	Non-EE Day Residuals when MDA8 ≥ 60 ppb (ppb)
Boulder City	0.22 [-0.04, 0.48] (1,132)	0.22 [-0.04, 0.48] (1,130)	12.05 [10.38-13.72] (2)	0.58	9	4.05 [3.55, 4.55] (200)
Green Valley	0.17 [-0.15, 0.48] (948)	0.10 [-0.21, 0.41] (934)	7.38 [5.40, 9.36] (14)	0.58	10	3.76 [3.28, 4.23] (271)
Indian Springs	0.13 [-0.18, 0.44] (1,014)	0.08 [-0.22, 0.38] (1,010)	12.30 [9.37-17.19] (4)	0.55	10	4.79 [4.26, 5.32] (201)
Jean	0.21 [-0.06, 0.48] (1,149)	0.20 [-0.07, 0.47] (1,146)	12.57 [9.59-13.90] (3)	0.57	9	3.40 [2.94, 3.85] (290)
Jerome Mack	0.09 [-0.19, 0.36] (1,152)	0.05 [-0.22, 0.32] (1,141)	6.83 [4.21, 9.45] (11)	0.61	9	3.83 [3.32, 4.33] (242)
Joe Neal	0.23 [-0.08, 0.54] (1,113)	0.17 [-0.13, 0.47] (1,097)	7.77 [5.79, 9.75] (16)	0.60	10	3.32 [2.92, 3.71] (377)
Paul Meyer	0.21 [-0.08, 0.50] (1,159)	0.10 [-0.19, 0.39] (1,137)	8.11 [6.34, 9.88] (22)	0.55	10	3.58 [3.19, 3.97] (388)
Walter Johnson	0.27 [-0.03, 0.57] (1,163)	0.19 [-0.10, 0.48] (1,141)	7.16 [5.11, 9.21] (22)	0.58	10	3.53 [3.13, 3.93] (379)

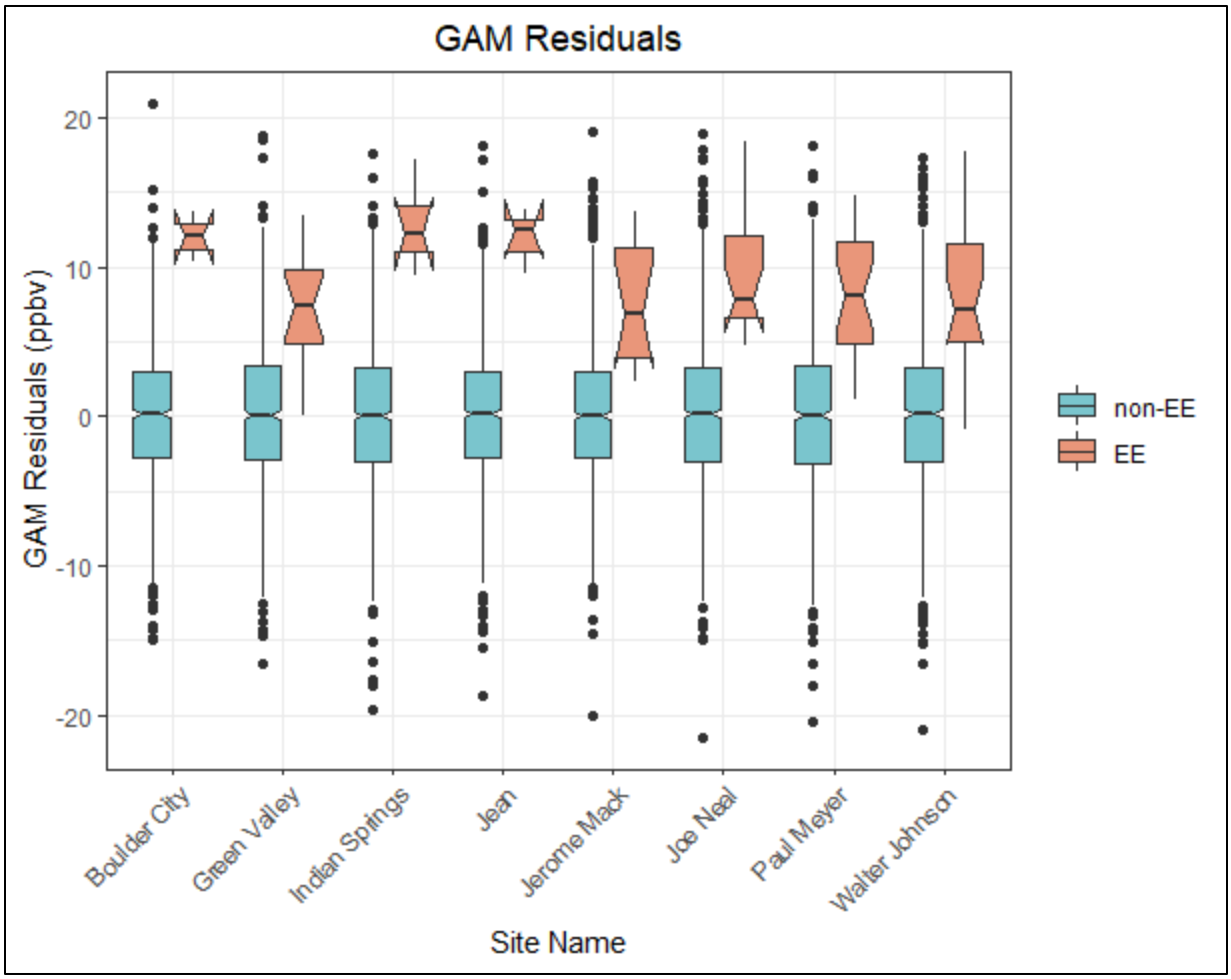

Figure 3-77. Exceptional event vs. non-exceptional event residuals. Non-exceptional events (non-EE in blue) and exceptional events (EE in orange) residuals are shown for each site modeled in Clark County. The notches for each box represent the 95th confidence interval. This figure illustrates the information in Table 3-23.

Overall, the GAM results show low bias and consistently significantly higher residuals on EE days compared with non-EE days. We also evaluated the GAM performance on verified high ozone, non-smoke days by looking at specific case studies. This was done to assess whether high-ozone days, such as the EE days, have a consistent bias that is not evident in the overall or high ozone day GAM performance. Out of the seven years used in the GAM model, four were high wildfire years in California (2015, 2017, 2018, and 2020). Since summer winds in Clark County are typically out of California (44% of trajectories originate in California according to the cluster analysis [not including transport through California in the Baja Mexico cluster]), wildfire smoke is likely to affect a large portion of summer days and influence ozone concentrations in Clark County. We identified specific case studies where most monitoring sites in Clark County had an MDA8 ozone concentration greater than or equal to 60 ppb and had no wildfire influence; "no wildfire influence" was determined by

inspecting HMS smoke plumes and HYSPLIT back trajectories for each day and confirming no smoke was over, near, or transported to Clark County. We found one to two examples from each year used in the GAM modeling, and required that at least half of the case study days needed to include an exceedance of the ozone NAAQS. **Table 3-24** shows the results of these case studies. Most case study days, including NAAQS exceedance days, show positive and negative residuals even when median ozone is greater than or equal to 65 ppb in Clark County, similar to the results for the entire multi-year dataset. GAM residuals on non-EE days when MDA8 is at or above 60 ppb have a median of 3.69 [95% confidence interval: 3.47, 3.88] (see Table 3-16). The high ozone, non-smoke case study days all show median residuals within or below the confidence interval of the high ozone residuals (from Table 3-16), meaning that the GAM model is able to accurately predict high ozone, non-smoke days within a reasonable range of error. Two additional factors indicate the GAM has good performance on normal, high ozone days: (1) the median residuals for the case studies are mostly lower than the 95% confidence interval of high ozone residuals (i.e., includes non-EE wildfire days), and (2) the case study days were verified as non-smoke days, Thus, residuals above the 95th confidence interval of the median residuals, such as those on the EE days, are statistically higher than on days with comparable high ozone concentrations, and not biased high because of the high ozone concentrations on these days.

Table 3-24. GAM high ozone, non-smoke case study results. Median GAM residuals for ten days in 2014-2020 are shown where most monitoring sites had MDA8 ozone concentrations of 60 ppb or greater. Sites used to calculate the MDA8 and GAM residual median/range are listed in the Clark County AQS Site Number column by site number.

Date	Clark County AQS Site Number	Median (Range) of Observed MDA8 Ozone (ppb)	Median (Range) GAM Residual (ppb)
5/17/2014	0601, 0075, 1019, 0540, 0043, 0071	66 (64-71)	1.66 (-0.53-4.28)
6/4/2014	0601, 0075, 0540, 1019, 0043, 0071	69 (66-72)	3.46 (1.70-4.80)
6/3/2015	1019, 0043, 0075, 0540, 7772, 0601, 0071	71 (65-72)	3.01 (-0.34-5.77)
6/20/2015	0601, 0298, 7772, 1019, 0540, 0075, 0043, 0071	65 (63-70)	1.40 (-6.20-5.28)
6/3/2016	0298, 1019, 0075, 0540, 0043, 0071	65 (63-71)	3.89 (1.89-5.26)
7/28/2016	0075, 0071, 0298, 0540, 0043	70 (63-72)	0.24 (-5.95-3.67)
6/17/2017	0601, 0075, 0071, 1019, 0540, 0298, 0043	66 (63-72)	1.85 (-1.94-7.01)
6/4/2018	0601, 0298, 7772, 1019, 0540, 0075, 0043, 0071	65 (60-67)	3.06 (-0.91-3.60)
5/5/2019	0601, 0298, 7772, 1019, 0540, 0075, 0043, 0071	65 (62-67)	1.28 (-2.00-3.42)
5/15/2020	0298, 0043, 0075, 0071	63 (63-65)	1.52 (1.09-3.49)

We also evaluate the bias of GAM residuals versus predicted MDA8 ozone concentrations in Figure 3-78. Residuals (i.e., observed ozone minus GAM-predicted MDA8 ozone) should be independent of the GAM-predicted ozone value, meaning that the difference between the actual ozone concentration on a given day and the GAM output should be due to outside influences and not well described by meteorological or seasonal values (i.e., variables used in the GAM prediction). Therefore, in a well-fit model, positive and negative residuals should be evenly distributed across all

GAM-predicted ozone concentrations and on average zero. In Figure 3-78, we see daily GAM residuals at all eight monitoring sites in Clark County from 2014-2020, the residuals are evenly distributed across all GAM-predicted ozone concentrations, with no pattern or bias at high or low MDA8 fit concentrations. This evaluation of bias in the model is consistent with established literature and other EE demonstrations (Gong et al., 2018; McVey et al., 2018; Texas Commission on Environmental Quality, 2021; Pernak et al., 2019), and indicate a well-fit model. In **Figure 3-79**, we also provide a histogram of the residuals at each monitoring site modeled in Clark County. This analysis shows that residuals at each site are distributed normally around a median near zero, and none of the distributions shows significant tails at high or low residuals (median skew = 0.05 with 95% confidence interval [-0.03, 0.12]). This analysis of error in the model and our results are consistent with previously concurred EE demonstrations (Arizona Department of Environmental Quality, 2016) and previous literature (Jaffe et al., 2013; Alvarado et al., 2015; Gong et al., 2017; McClure and Jaffe, 2018; Pernak et al., 2019). **Appendix F** provides GAM residual analysis from the concurred ADEQ and submitted TCEQ demonstrations that compare well with our GAM residual results. Based on these analysis methods, bias in the model is low throughout the range of MDA8 prediction values and confirms that the GAM can be used to predict MDA8 ozone concentrations in Clark County.

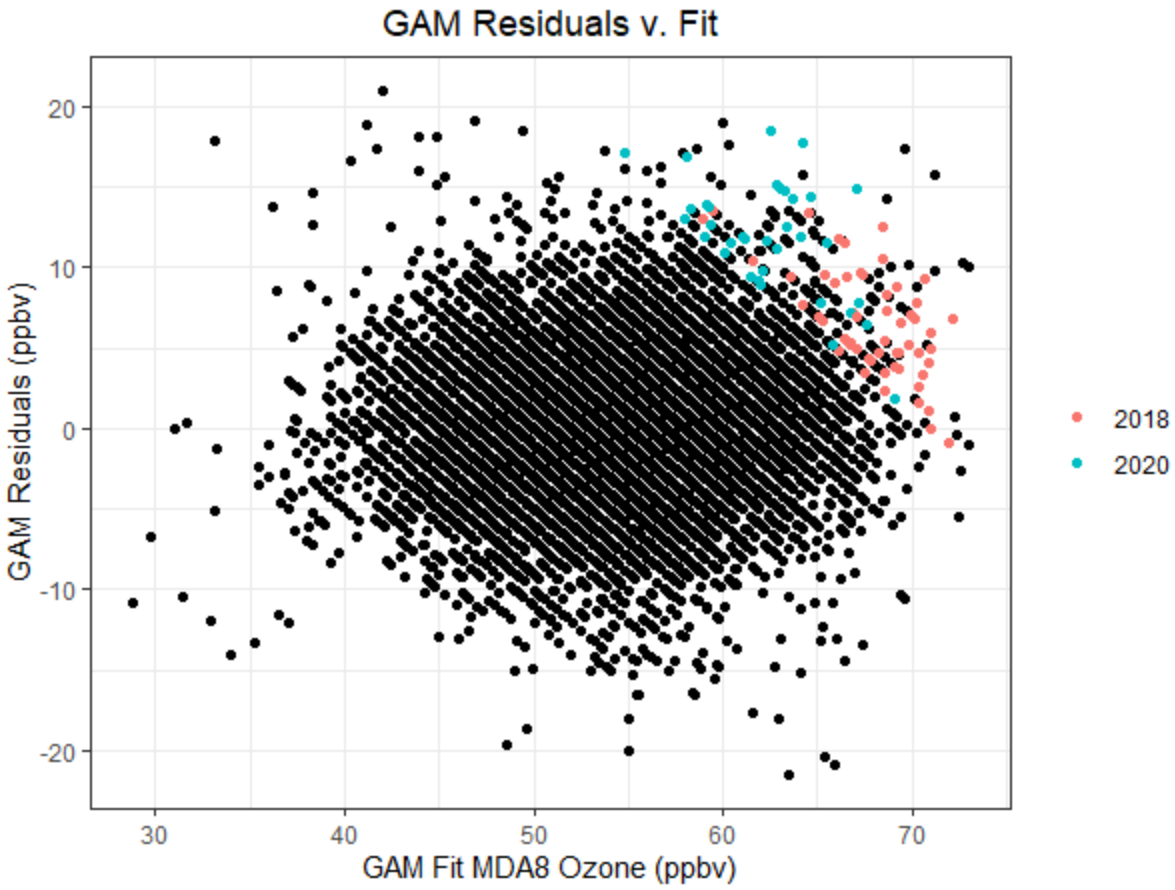

Figure 3-78. Daily GAM residuals for 2014-2020 vs GAM Fit (Predicted) MDA8 Ozone values. 2018 and 2020 exceptional events residuals are shown in red and blue.

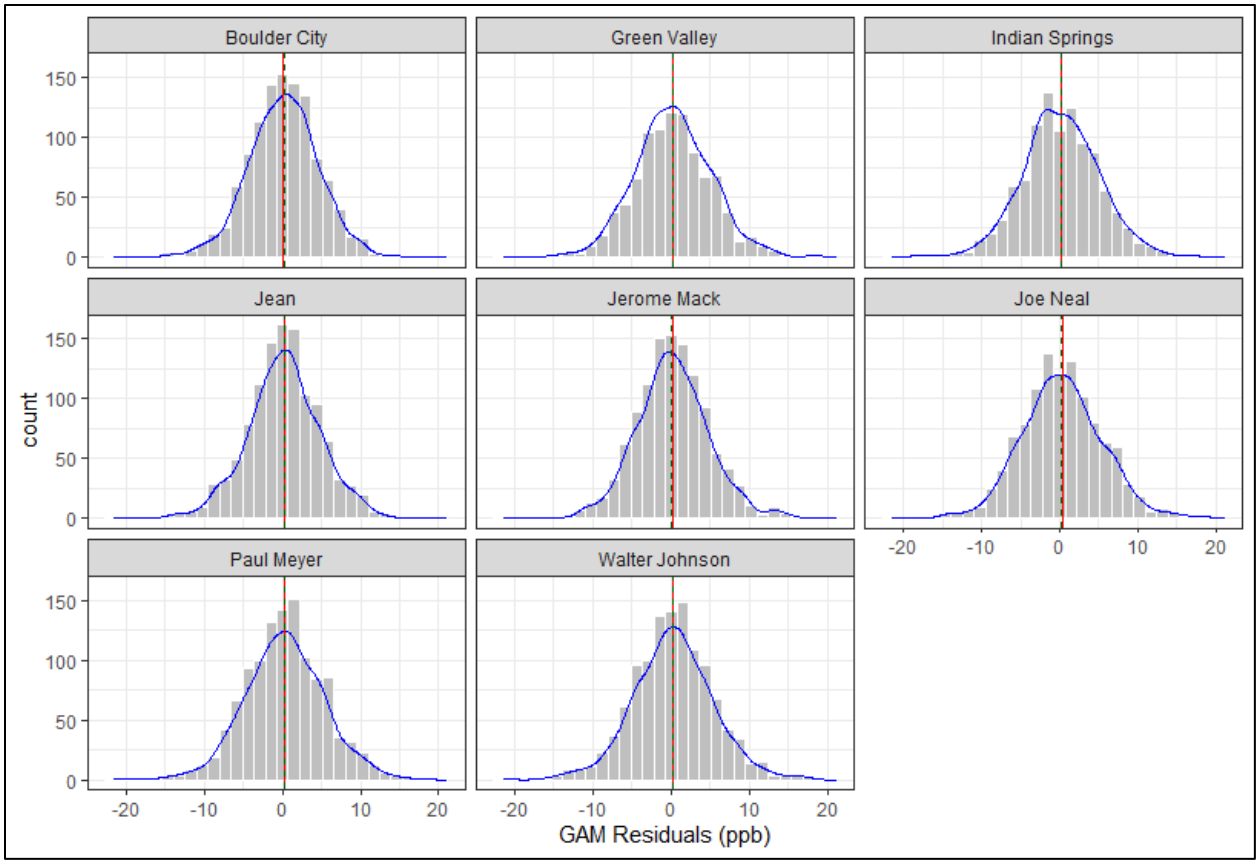

Figure 3-79. Histogram of GAM residuals at all modeled Clark County monitoring sites. The red line indicates the mean and the green dashed line indicates the median. The blue line provides the density distribution.

Within the GAM model, we include HYSPLIT 24-hour distance values, which are factored by cluster, to provide source region and stagnation information into the algorithm. A major upwind pollution source for Las Vegas is the Los Angeles Basin (see the Southern California cluster), which is around 400 km away. Since the GAM model uses source region and distance traveled information to help predict daily MDA8 ozone concentrations, contributions from LA should be accounted for in the algorithm. Based on this, we can assess whether GAM residuals on LA-source region days were significantly different from other source regions. In **Figures 3-80 and 3-81**, we subset the GAM results by removing any potential EE days. From these results, we find that both morning (18:00 UTC) and afternoon (22:00 UTC) trajectory data have similar distributions for all clusters. The notches in the box plots (representing the 95th confidence interval) provide an estimate of statistical difference, and show that the median of residuals is near zero for all clusters. The Northwest U.S. cluster at 18:00 UTC shows slightly negative residuals, while the Long-Range Transport cluster shows slightly positive residuals for both 18:00 and 22:00 UTC. The Southern California cluster shows a median residual of around zero for both 18:00 and 22:00 UTC trajectories, with significant overlap between the 95th confidence intervals of most other clusters (not statistically different). Additionally, the number of data points per cluster (bottom of each figure) corresponds well with transport from California being

dominant for the April through September time frame. Overall, this analysis provides evidence that even when the Los Angeles Basin (Southern California cluster) is upwind of Las Vegas, the GAM model performs well (low median residuals), and the results are statistically similar to most of the other clusters. This implies that when residuals are large, the Los Angeles Basin's influence is unlikely to be the only contributor to enhancements in MDA8 ozone.

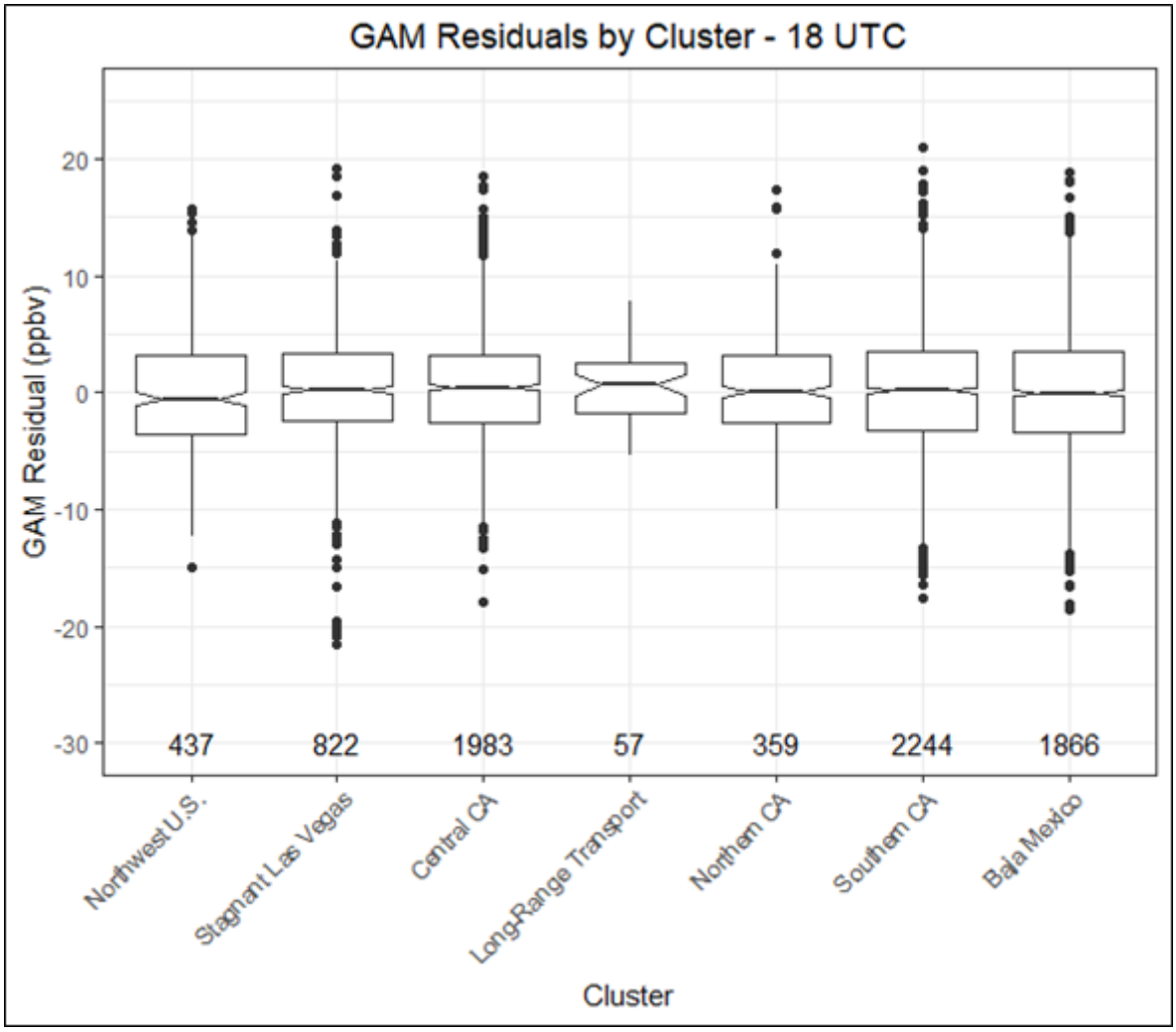

Figure 3-80. GAM cluster residual results for 18:00 UTC. The cluster is determined by grouping 24-hour back trajectories from Las Vegas based on their path. Clusters were created by using back trajectory results from Clark County between 2014 and 2020 (EE days were removed).

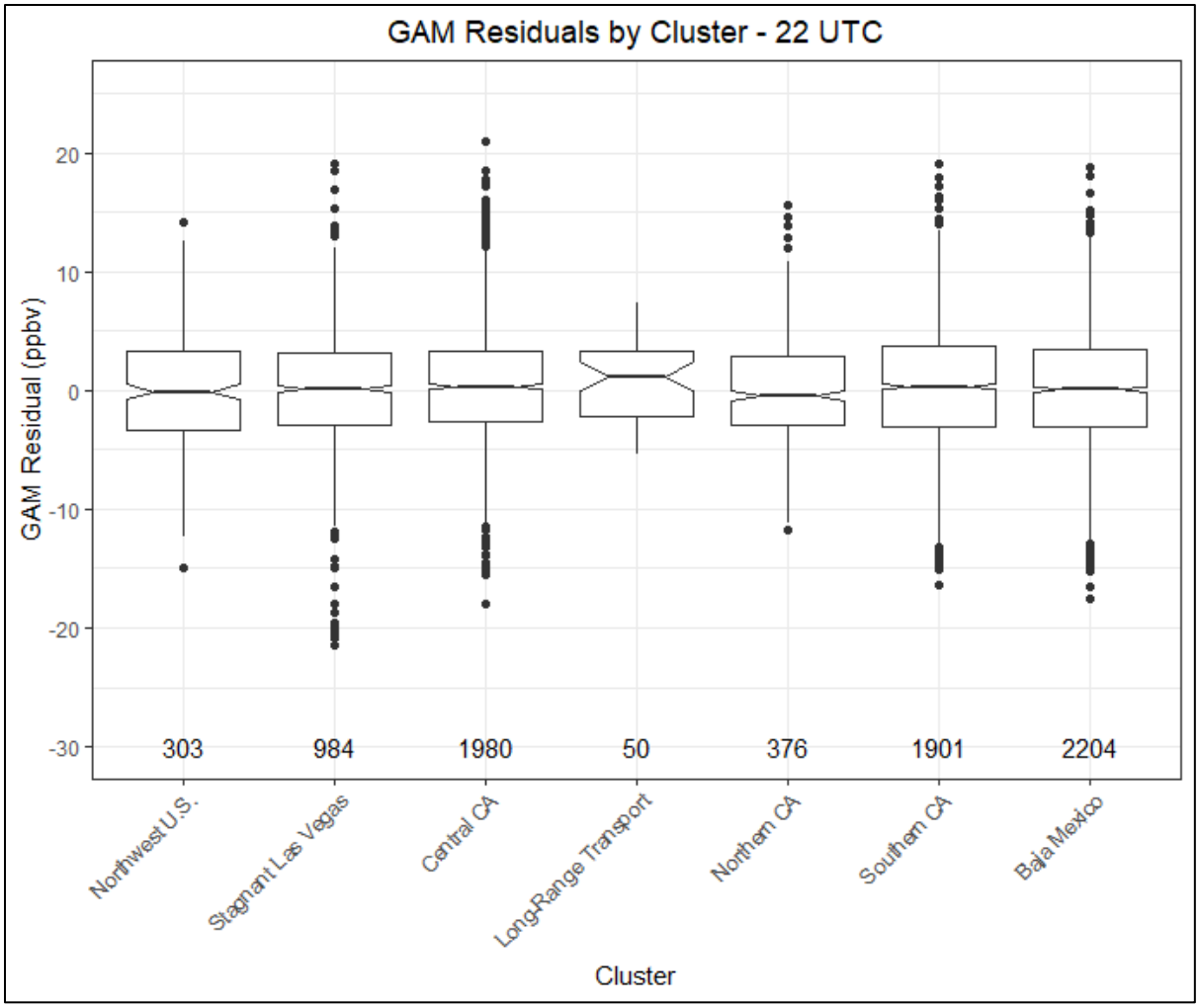

Figure 3-81. GAM cluster residual results for 22:00 UTC. The cluster is determined by grouping 24-hour back trajectories from Las Vegas based on their path. Clusters were created by using back trajectory results from Clark County between 2014 and 2020 (EE days were removed).

Mobile emissions sources decreased throughout the U.S. after COVID restrictions went into place in March 2020. Based on emission inventories from Las Vegas, on-road emissions make up a significant portion of the NO_x emissions inventory (see Section 2.3 for more details). Based on traffic data from the Nevada Department of Transportation, on-road traffic in Clark County in 2020 was significantly different than 2019 through early to mid-June (depending on the area where traffic volume was measured; see Appendix G for more details). Figure 3-82 provides a scatter plot of MDA8 ozone observed versus GAM fit for all eight monitoring sites, separated by year. The linear regression fit, slope, and intercept do not show large difference between 2020 and other modeled years. Figure 3-83 provides a more in-depth look at the most heavily affected months due to COVID restrictions and traffic changes (April – May 2020). The 95th confidence interval (shown as a notch in the box plots) show overlap between 2020 and most other years (except 2015 and 2016). The May 6, 9, and 28 EE days are included in the 2020 box. This analysis shows that there was not a statistically

different GAM response in 2020 compared with other years; this is confirmed in the COVID analysis section (Appendix G), where we show that MDA8 ozone during April – May 2020 in Las Vegas was not statistically different from previous years. While the reduction in traffic emissions due to COVID restrictions did not affect the August 18-21 event, we thought it was important to address the effects of COVID restrictions on the 2020 GAM results. Overall, ozone in Clark County did not change significantly and, similarly, GAM results were not significantly affected.

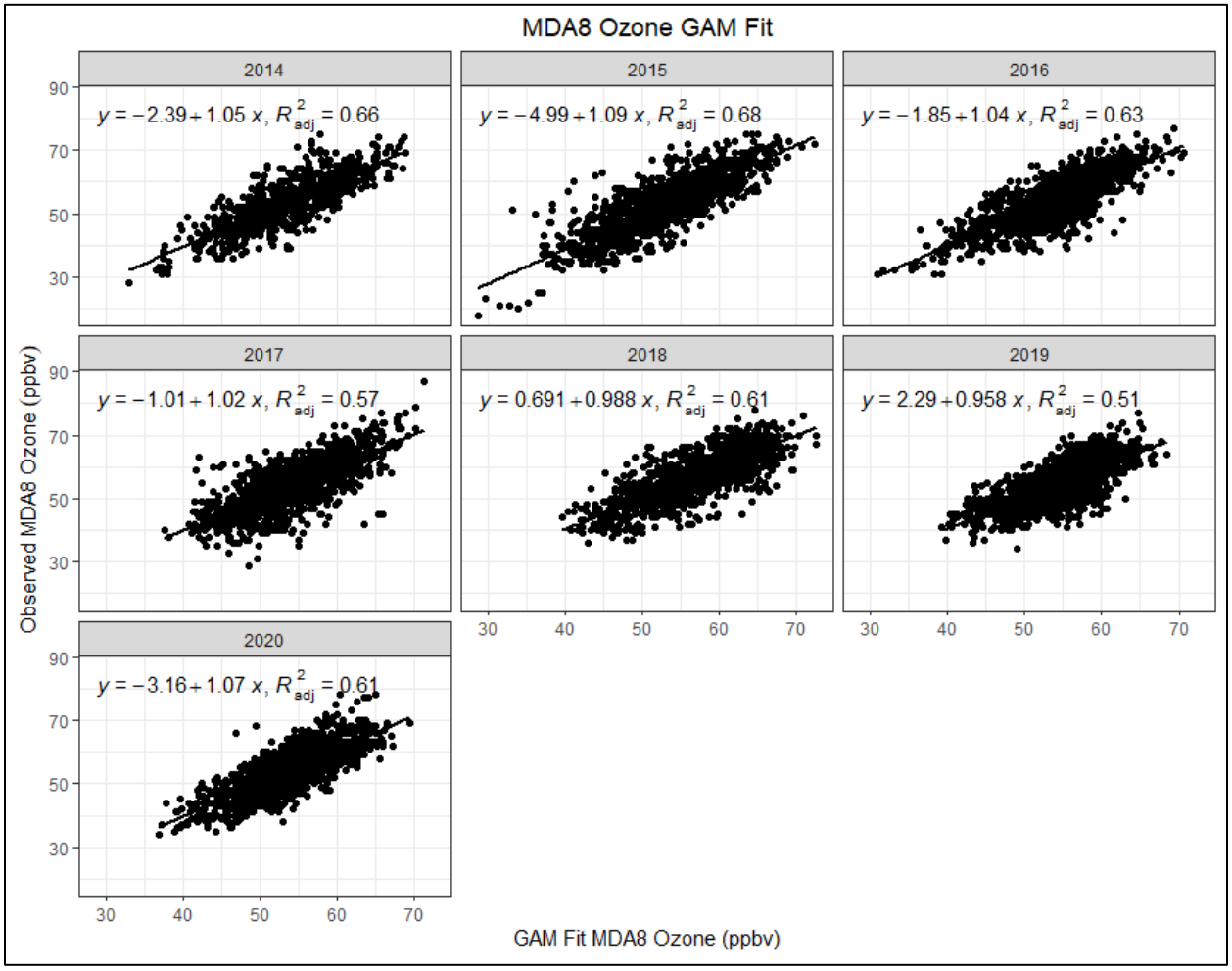

Figure 3-82. Observed MDA8 ozone vs. GAM fit ozone by year. The relationship between observed MDA8 ozone and GAM fit ozone at all eight modeled monitoring sites in Clark County is broken out by year, with linear regression and fit statistics shown (slope, intercept, and r^2). EE days are not included in the regression equations.

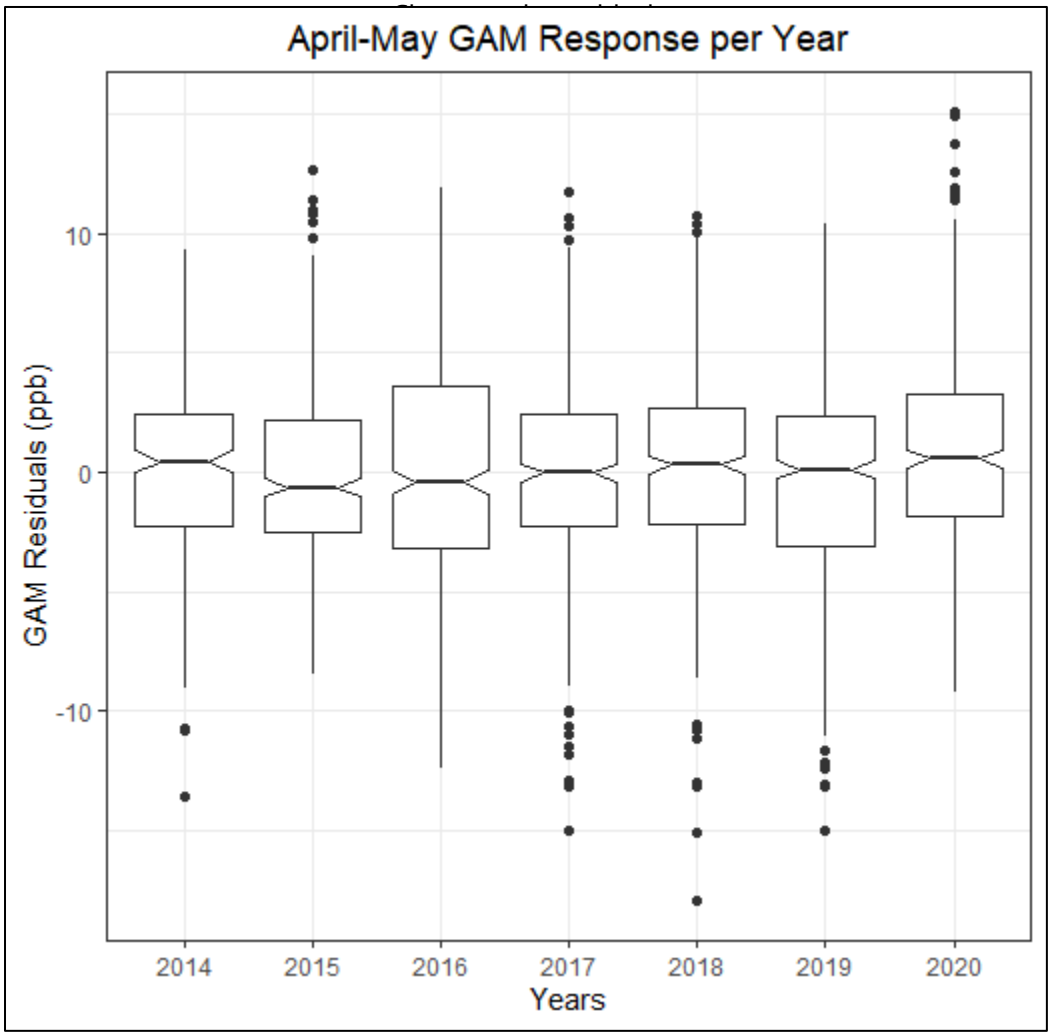

Figure 3-83. April–May Interannual GAM Response. April–May residuals per year from 2014–2020 are plotted for all eight modeled monitoring sites in Clark County. The potential EE days of May 6, 9, and 28 are included.

Figure 3-84 provides the observed MDA8 ozone versus GAM Fit MDA8 from 2014 through 2020 for the sites affected during August 18-21 (Green Valley, Joe Neal, Paul Meyer, and Walter Johnson). We marked the possible 2020 (red), 2018 (blue), and other (purple) EE days to show that observed MDA8 ozone on these days is higher than those predicted by the GAM. The other (purple) points are from 2014–2016 and are suspected wildfire events, as indicated in EPA AQS record. We also highlight the August 18-21, 2020, EE days as a large red triangle in each figure. Linear regression statistics (slope, intercept, and r^2) are also provided for context. All linear regressions show a slope near unity, and a low intercept value (around 3-4 ppb) with a good fit r^2 value.

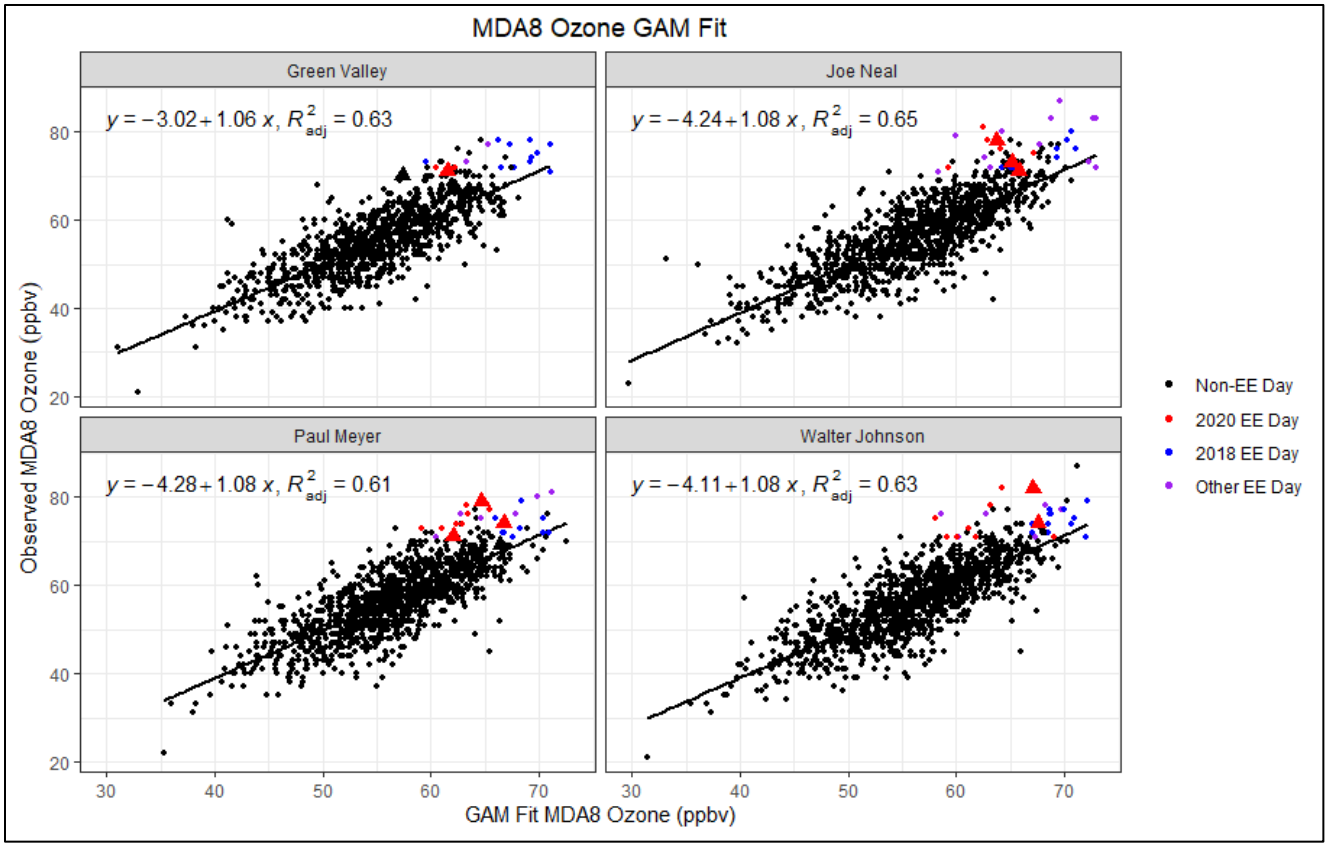

Figure 3-84. GAM MDA8 Fit versus Observed MDA8 ozone data from 2014 through 2020 for the EE affected sites during August 18-21, 2020. Black circles indicate data not associated with the 2018 or 2020 EE days, red circles indicate 2020 EE days, blue circles indicate 2018 EE days, and purple circles indicate 2014-2016 EE days. August 18-21 points are shown as a red triangle. The black line is the linear regression of the data, and statistics (equation and r^2 value) are shown in the top of each sub-figure.

Table 3-25 provides the GAM results for August 18-21, 2020, at each monitoring site affected by the exceptional event. GAM residuals show a modeled wildfire impact between 6 and 15 ppb for all monitoring sites, with MDA8 GAM prediction values well below the 0.070 ppm standard. EPA guidance requires a further level of investigation; by adding the GAM MDA8 prediction value and the positive 95th quantile of residuals, we calculated the "No Fire" MDA8 ozone value. The difference between the observed and "No Fire" MDA8 ozone value (-4 to 5 ppb) is a conservative estimate of the influence of wildfire smoke at each site. Due to the large number of wildfires affecting Clark County during the 7-year modeling period, we also calculate the "No Fire" and minimum predicted fire influence given the 75th percentile (0 to 10 ppb). This provides a range of minimum smoke enhancement (-4 to 10 ppb). The actual enhancement due to wildfire smoke likely lies between the minimum smoke enhancement estimate and the GAM residual. The reason for lower predicted fire influence on the later days of the event is likely due to a combination of previous day's MDA8 ozone being used as a predictor in the GAM model (artificially adding smoke influence to the model) and

heavy smoke inhibiting ozone formation. Previous studies and concurred exceptional event demonstrations show and discuss the limitations of the 95th positive percentile evaluation (Miller et al., 2014; Arizona Department of Environmental Quality, 2016). Additionally, production of ozone is an extremely complex process that can only be predicted by meteorological variables in a GAM model with a 50%-80% correlation based on previously cited papers (our GAM model shows a 55%-61% correlation). In our case, this leaves exceptional events, wildfire influence during high wildfires years, stratospheric intrusions, non-normal emissions, non-normal meteorology, etc., which make up the other 39%-45%. Due to the large number of high wildfire years used in the GAM model, we assert that the minimum predicted fire influence value (as determined by the positive 95th quantile) should not be used as strict guideline for actual fire influence. Based on the values from the GAM model, we see a significant, non-typical enhancement in MDA8 ozone concentrations at the affected Clark County monitoring sites during the August 18-21, 2020, event.

Table 3-25. August 18-21 GAM results and residuals for each site. The GAM residual is the difference between observed MDA8 ozone and the GAM Prediction. We also estimate the minimum predicted fire influence based on the positive 95th quantile and GAM prediction value.

Date	Site Name	MDA8 O_3 Concentration[a] (ppm)	MDA8 GAM Prediction[b] (ppm)	GAM Residual (ppm)	Positive 75^{th}-95^{th} Quantile[c] (ppm)	"No Fire" MDA8[b+c] (ppm)	Minimum Predicted Fire Influence[a-(b+c)] (ppm)
8/18/2020	Paul Meyer	0.079	0.064	0.015	0.005-0.010	0.069-0.074	0.005-0.010
	Walter Johnson	0.082	0.067	0.015	0.005-0.010	0.072-0.077	0.005-0.010
	Joe Neal	0.078	0.063	0.015	0.006-0.010	0.069-0.073	0.005-0.009
8/19/2020	Paul Meyer	0.074	0.066	0.008	0.005-0.010	0.071-0.076	-0.002-0.003
	Walter Johnson	0.074	0.067	0.007	0.005-0.010	0.072-0.077	-0.003-0.002
	Joe Neal	0.073	0.065	0.008	0.006-0.010	0.071-0.075	-0.002-0.002
	Green Valley	0.071	0.061	0.010	0.005-0.010	0.066-0.071	0.000-0.005
8/20/2020	Joe Neal	0.071	0.065	0.006	0.006-0.010	0.071-0.075	-0.004-0.000
8/21/2020	Paul Meyer	0.071	0.062	0.009	0.005-0.010	0.067-0.072	-0.001-0.004

Finally, Figure 3-85 shows a 2-week time series of observed MDA8 ozone values across Clark County and the GAM prediction values at those sites. The August 18-21, 2020, event shows a large gap between observed MDA8 ozone and the GAM-predicted values. Outside of the possible exceptional event days, the GAM prediction values are very close to the observed values, suggesting that immediately before and after the event, we are able to accurately predict typical fluctuations in ozone on non-event days.

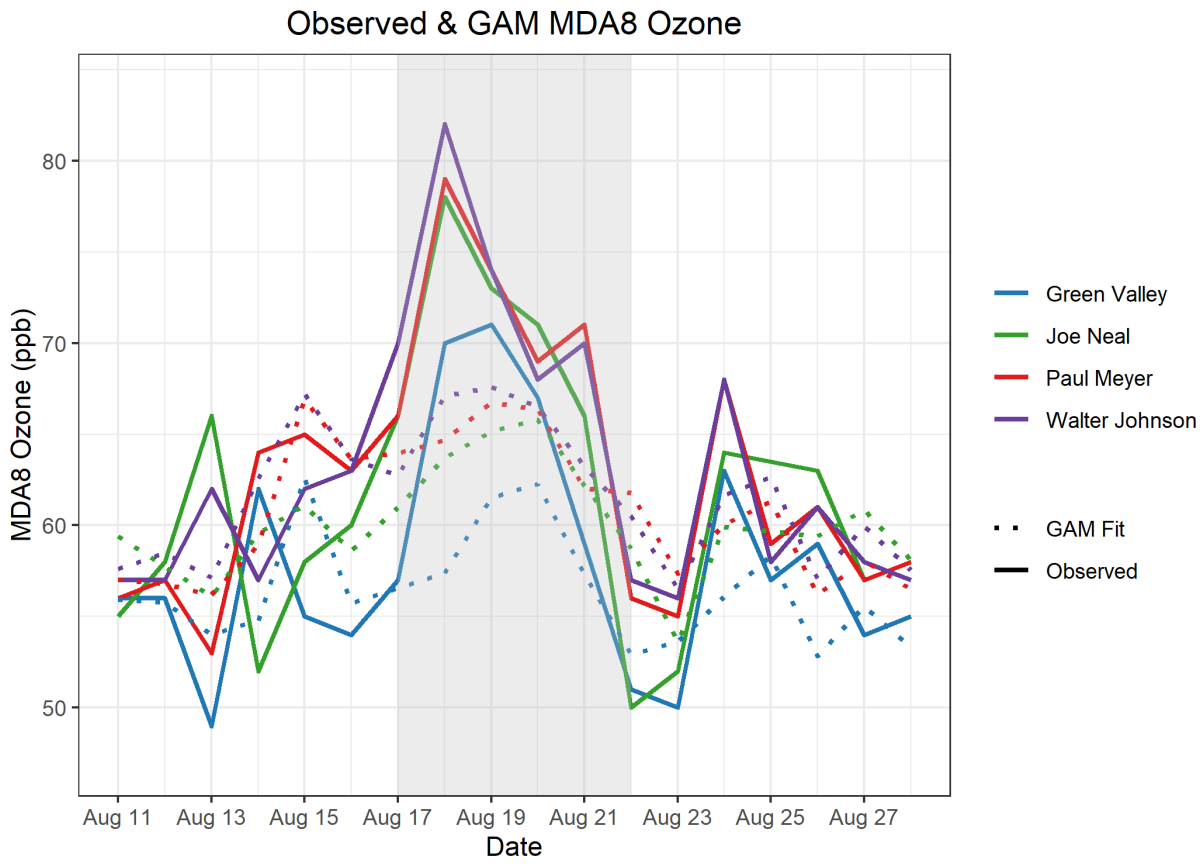

Figure 3-85. GAM time series showing observed MDA8 ozone for two weeks before and after the August 18-21 EE (solid lines). The GAM MDA8 ozone fit value is also shown for two weeks before and after September 2 (dotted line).

Overall, the GAM evidence clearly demonstrates that a non-typical source of ozone significantly impacted concentrations all EE-affected Clark County sites on August 18-21, 2020. Coupled with wildfire smoke evidence from all other tiers of analyses, we can conclude by weight of evidence that the enhancement in ozone concentration was due to smoke from the large complex, lightning-initiated wildfires in California that was transported to Clark County, Nevada.

3.4 Clear Causal Relationship Conclusions

The analyses conducted in this report support the impact of smoke from the large complex, lightning-initiated wildfires in California on ozone concentrations in Clark County, Nevada, during August 18-21, 2020. We find that:

1. Visible satellite imagery, news articles, and back trajectories support the conclusion of smoke transport from the wildfires in California to Clark County.
2. A large mixing layer, aerosols in the vertical profile, back trajectories starting near the fires and ending at the surface in Clark County, and surface enhancements of wildfire-related pollutants (i.e., levoglucosan and $PM_{2.5}$) in Clark County support the conclusion that smoke was mixed down to the surface in Clark County.
3. Comparisons with non-event concentrations, meteorologically similar matching day analysis, and GAM statistical modeling support the conclusion that the ozone concentrations seen in Clark County were significantly above typical summer concentrations for the meteorological conditions on the day.

The analyses presented in this report fulfill the requirements for a Tier 3 EE demonstration, and all conclusions for each type of analysis are summarized in Table 3-26. The effect of the wildfires in California on Clark County caused ozone exceedances at the Paul Meyer, Walter Johnson, Joe Neal, and Green Valley monitoring stations. Based on the evidence shown that the lightning-initiated wildfires in California were natural events and unlikely to recur, as well as the clear causal relationship between the wildfires and the monitored exceedances, we conclude that the ozone exceedance event during August 18-21, 2020, in Clark County was not reasonably controllable or preventable.

Table 3-26. Results for each tier analysis for the September 2 EE.

Tier	Requirements	Finding
1	• Comparison of fire-influenced exceedance with historical concentrations • Key factor: Evidence that fire and monitor meet one of the following criteria: — Seasonality differs from typical season, or — Ozone concentrations are 5-10 ppb higher than non-event related concentrations • Evidence of transport of fire emissions to monitor: — Trajectories of fire emissions (reaching ground level), or — Satellite Images and supporting evidence from surface measurements — Media coverage and photographic evidence of smoke	• The August 18-21, 2020, ozone exceedance event occurred during a typical ozone season, but event concentrations were significantly higher than non-event concentrations. • Trajectories, satellite images, media coverage, and ground images support smoke transport from the California wildfires into Clark County.
2	• All Tier 1 requirements • Key Factor #1: Fire emissions and distance of fires • Key Factor #2: Comparison of the event-related ozone concentration with non-event-related high ozone concentrations (high percentile rank over five years/seasons) — Annual and seasonal comparison • Evidence that fire emissions affected the monitor (at least one of the following): — Visibility impacts — Changes in supporting measurements — Satellite enhancements of fire-related species (i.e., NOx, CO, AOD, etc.) — Fire-related enhancement ratios and/or tracer species — Differences in spatial/temporal patterns	• Q/d values for the California fires were well below 100. • Ozone concentrations at all sites showed high percentile rank over the past five years and ozone seasons. • Surface concentrations of supporting pollutants ($PM_{2.5}$ and CO) show enhanced concentrations and changes in typical diurnal profiles, consistent with smoke. • Satellite measurements also show enhanced levels of fire-related species. • Levoglucosan, a wildfire tracer, showed a positive detection during this event.
3	• All Tier 2 requirements • Evidence of fire emissions effects on monitor: — Multiple analyses from those listed for Tier 2 • Evidence of fire emissions transport to the monitor: — Trajectory or satellite plume analysis, and — Additional discussion of meteorological conditions • Additional evidence such as: — Comparison to ozone concentrations on matching (meteorologically similar) days — Statistical regression modeling — Photochemical modeling of smoke contributions to ozone concentrations	• Meteorology patterns during this event show transport from California wildfires to Clark County. • Vertical profiles show vertical mixing and transport to the surface as well as smoke-identified aerosol in the column. • Meteorologically similar day analysis shows that average MDA8 ozone across similar days was well below the ozone NAAQS and 10 ppb lower than the August 18-21 exceedance at all affected sites. • GAM statistical modeling predicts ozone concentrations lower than observed, suggesting an impact from non-typical sources on ozone concentrations in Clark County during this event.

4. Natural Event Unlikely to Recur

A wildfire is defined in 40 CFR 50.1(n) as "any fire started by an unplanned ignition caused by lightning; volcanoes; other acts of nature; unauthorized activity; or accidental, human-caused actions, or a prescribed fire that has developed into a wildfire. A wildfire that predominantly occurs on wildland is a natural event." Furthermore, a "wildland" is "an area in which human activity and development are essentially non-existent, except for roads, railroads, power lines, and similar transportation facilities. Structures, if any, are widely scattered." 40 CFR 50.1(o). As shown in Table 3-3, each fire that contributed to this event was caused by lightning (except one where the cause is unknown), and therefore meets the definition of wildfire. Based on the documentation provided in Section 3.2.1 of this submittal, each fire predominately took place on wildlands designated as National Forests, as seen in Figure 3-45. Therefore, under 40 CFR §50.1, the fires listed in Table 3-3 can be classified as natural events that are unlikely to recur. Accordingly, the Clark County Department of Environment and Sustainability has shown in this submittal that smoke from California wildfires, which led to an ozone exceedance in Clark County of August 18-21, 2020, may be considered for treatment as an EE.

5. Not Reasonably Controllable or Preventable

As shown by the documentation provided in Section 3.2.1 of this submittal, each wildfire listed in Table 3-3 burned predominantly on wildland. The Exceptional Events rule stated in 40 CFR 50.1(j) indicates that a wildfire that occurs on wildland is not reasonably controllable or preventable. Previous sections of this report have shown that each fire referenced in this report was a wildfire that occurred on wildland. The InciWeb report for each fire indicates that these wildfires burned across vast areas in generally inaccessible land, limiting firefighting efforts in each event (https://inciweb.nwcg.gov/). The Clark County Department of Environment and Sustainability is not aware of any evidence clearly demonstrating that prevention or control efforts beyond those made would have been reasonable. Therefore, the emissions that caused exceedances at monitors in Clark County on August 18-21 are neither reasonably controllable or preventable.

6. Public Comment

This exceptional event demonstration will undergo a 30-day public comment period concurrent with EPA's review beginning September 3, 2021. A copy of the public notice, along with any comments received and responses to those comments, will be submitted to EPA after the comment period has closed, consistent with the requirements of 40 CFR 50.14(c)(3)(v). **Appendix H** contains documentation of the public comment process.

7. Conclusions and Recommendations

The analyses conducted in this report support the conclusion that smoke from multiple large complex, lightning-initiated wildfires in California impacted ozone concentrations in Clark County, Nevada, during August 18-21, 2020. This EE demonstration has provided the following elements required by the EPA guidance for wildfire EEs (U.S. Environmental Protection Agency, 2016):

1. A narrative conceptual model that describes the wildfires in California and how the emissions from these wildfires led to ozone exceedances downwind in Clark County (Sections 1 and 2).
2. A clear causal relationship between the California wildfires and the August 18-21 exceedances through ground and satellite-based measurements, trajectories, emission modeling, comparison with non-event concentrations, vertical profile analysis, and statistical modeling (Section 3).
3. Event ozone concentrations at or above the 99th percentile when compared with the last six years of observations at each site and among the four highest ozone days at each site (excluding other 2018 and 2020 EE events–Section 3).
4. The California wildfires were determined to be caused by lighting and began in wildland areas where they grew rapidly and quickly beyond firefighting controls, classifying this event as unlikely to recur (Section 4).
5. Demonstration that the transport of emissions from the wildfires in California to Clark County was neither reasonably controllable or preventable (Section 5).
6. This demonstration went through the public comment process via Clark County's Department of Environment and Sustainability (Section 6).

The major conclusions and supporting analyses found in this report are:

1. Visible satellite imagery, news articles, and back trajectories support the conclusion of smoke transport from the wildfires in California to Clark County.
2. A large mixing layer, aerosols in the vertical profile, back trajectories starting near the fires and ending at the surface in Clark County, and surface enhancements of wildfire-related pollutants (i.e., levoglucosan and $PM_{2.5}$) in Clark County support the conclusion that smoke was mixed down to the surface in Clark County.
3. Comparisons with non-event concentrations, meteorologically similar matching day analysis, and GAM statistical modeling support the conclusion that the ozone concentrations seen in Clark County were significantly above typical summer concentrations for the meteorological conditions on the day.

The analyses presented in this report fulfill the requirements for a Tier 3 EE demonstration, and all conclusions for each type of analysis are summarized in Table 3-26. The effect of the California

wildfires on Clark County caused ozone exceedances at the Paul Meyer, Walter Johnson, Joe Neal, and Green Valley monitoring stations. Based on the evidence shown that the California wildfires were natural events and unlikely to recur, as well as the clear causal relationship between the wildfire event and the monitored exceedances, we conclude that the ozone exceedance event during August 18-21, 2020, in Clark County was not reasonably controllable or preventable.

8. References

Alvarado M., Lonsdale C., Mountain M., and Hegarty J. (2015) Investigating the impact of meteorology on O_3 and $PM_{2.5}$ trends, background levels, and NAAQS exceedances. Final report prepared for the Texas Commission on Environmental Quality, Austin, TX, by Atmospheric and Environmental Research, Inc., Lexington, MA, August 31.

Arizona Department of Environmental Quality (2016) State of Arizona exceptional event documentation for wildfire-caused ozone exceedances on June 20, 2015 in the Maricopa nonattainment area. Final report, September. Available at https://static.azdeq.gov/pn/1609_ee_report.pdf.

Arizona Department of Environmental Quality (2018) State of Arizona exceptional event documentation for wildfire-caused ozone exceedances on July 7, 2017 in the Maricopa Nonattainment Area. Final report, May. Available at https://static.azdeq.gov/pn/Ozone_2017ExceptionalEvent.pdf.

Bhattarai H., Saikawa E., Wan X., Zhu H., Ram K., Gao S., Kang S., Zhang Q., Zhang Y., Wu G., Wang X., Kawamura K., Fu P., and Cong Z. (2019) Levoglucosan as a tracer of biomass burning: recent progress and perspectives. *Atmospheric Research*, 220, 20-33, doi: 10.1016/j.atmosres.2019.01.004. Available at http://www.sciencedirect.com/science/article/pii/S0169809518311098.

Brey S.J. and Fischer E.V. (2016) Smoke in the city: how often and where does smoke impact summertime ozone in the United States? *Environ. Sci. Technol.*, 50(3), 1288-1294, doi: 10.1021/acs.est.5b05218, 2016/02/02.

Bytnerowicz A., Cayan D., Riggan P., Schilling S., Dawson P., Tyree M., Wolden L., Tissell R., and Preisler H. (2010) Analysis of the effects of combustion emissions and Santa Ana winds on ambient ozone during the October 2007 southern California wildfires. *Atmos. Environ.*, 44, 678-687, doi: 10.1016/j.atmosenv.2009.11.014.

Camalier L., Cox W., and Dolwick P. (2007) The effects of meteorology on ozone in urban areas and their use in assessing ozone trends. *Atmos. Environ.*, 41, 7127-7137, doi: 10.1016/j.atmosenv.2007.04.061.

Clark County Department of Air Quality (2019) Ozone Advance program progress report update. August.

Clark County Department of Environment and Sustainability (2020) Revision to the Nevada state implementation plan for the 2015 Ozone NAAQS: emissions inventory and emissions statement requirements. September. Available at https://files.clarkcountynv.gov/clarknv/Environmental%20Sustainability/SIP%20Related%20Documents/O3/20200901_2015_O3%20EI-ES_SIP_FINAL.pdf?t=1617690564073&t=1617690564073.

Draxler R.R. (1991) The accuracy of rrajectories during ANATEX calculated using dynamic model analyses versus rawinsonde observations. *Journal of Applied Meteorology*, 30, 1446-1467, doi: 10.1175/1520-0450(1991)030<1446:TAOTDA>2.0.CO;2, February 25. Available at https://journals.ametsoc.org/doi/abs/10.1175/1520-0450%281991%29030%3C1446%3ATAOTDA%3E2.0.CO%3B2.

Finlayson-Pitts B.J. and Pitts Jr J.N. (1997) Tropospheric air pollution: Ozone, airborne toxics, polycyclic aromatic hydrocarbons, and particles. *Science*, 276, 1045-1051, (5315).

Gong X., Kaulfus A., Nair U., and Jaffe D.A. (2017) Quantifying O_3 impacts in urban areas due to wildfires using a generalized additive model. *Environ. Sci. Technol.*, 51(22), 13216-13223, doi: 10.1021/acs.est.7b03130.

Gong X., Hong S., and Jaffe D.A. (2018) Ozone in China: spatial distribution and leading meteorological factors controlling O_3 in 16 Chinese cities. *Aerosol and Air Quality Research*, 18(9), 2287-2300. Available at http://dx.doi.org/10.4209/aaqr.2017.10.0368.

Hennigan C.J., Sullivan A.P., Collett J.L., Jr., and Robinson A.L. (2010) Levoglucosan stability in biomass burning particles exposed to hydroxyl radicals. *Geophysical Research Letters*, 37(L09806), doi: 10.1029/2010GL043088. Available at https://www.firescience.gov/projects/09-1-03-1/project/09-1-03-1_hennigan_etal_grl_2010.pdf.

Hoffmann D., Tilgner A., Iinuma Y., and Herrmann H. (2009) Atmospheric stability of levoglucosan: a detailed laboratory and modeling study. *Environ. Sci. Technol.*, 44, 694–699.

Jaffe D., Chand D., Hafner W., Westerling A., and Spracklen D. (2008) Influence of fires on O_3 concentrations in the western U.S. *Environ. Sci. Technol.*, 42(16), 5885-5891, doi: 10.1021/es800084k.

Jaffe D.A., Bertschi I., Jaegle L., Novelli P., Reid J.S., Tanimoto H., Vingarzan R., and Westphal D.L. (2004) Long-range transport of Siberian biomass burning emissions and impact on surface ozone in western North America. *Geophys. Res. Let.*, 31(L16106).

Jaffe D.A., Wigder N., Downey N., Pfister G., Boynard A., and Reid S.B. (2013) Impact of wildfires on ozone exceptional events in the western U.S. *Environ. Sci. Technol.*, 47(19), 11065-11072, doi: 10.1021/es402164f, October 1. Available at http://pubs.acs.org/doi/abs/10.1021/es402164f.

Kimbrough S., Hays M., Preston B., Vallero D.A., and Hagler G.S.W. (2016) Episodic impacts from California wildfires identified in Las Vegas near-road air quality monitoring. *Environ. Sci. Technol.*, 50(1), 18-24. Available at https://doi.org/10.1021/acs.est.5b05038.

Lai C., Liu Y., Ma J., Ma Q., and He H. (2014) Degradation kinetics of levoglucosan initiated by hydroxyl radical under different environmental conditions. *Atmospheric Environment*, 91, 32-39, doi: 10.1016/j.atmosenv.2014.03.054, 2014/07/01/. Available at http://www.sciencedirect.com/science/article/pii/S1352231014002398.

Langford A.O., Senff C.J., Alvarez R.J., Brioude J., Cooper O.R., Holloway J.S., Lin M.Y., Marchbanks R.D., Pierce R.B., Sandberg S.P., Weickmann A.M., and Williams E.J. (2015) An overview of the 2013 Las Vegas Ozone Study (LVOS): impact of stratospheric intrusions and long-range transport on surface air quality. *Atmospheric Environment*, 109, 305-322, doi: 10.1016/j.atmosenv.2014.08.040, 2015/05/01/. Available at http://www.sciencedirect.com/science/article/pii/S1352231014006426.

Louisiana Department of Environmental Quality (2018) Louisiana exceptional event of September 14, 2017: analysis of atmospheric processes associated with the ozone exceedance and supporting data. Report submitted to the U.S. EPA Region 6, Dallas, TX, March. Available at

https://www.epa.gov/sites/production/files/2018-08/documents/ldeq_ee_demonstration_final_w_appendices.pdf.

Lu X., Zhang L., Yue X., Zhang J., Jaffe D., Stohl A., Zhao Y., and Shao J. (2016) Wildfire influences on the variability and trend of summer surface ozone in the mountainous western United States. *Atmospheric Chemistry & Physics*, 16, 14687-14702, doi: 10.5194/acp-16-14687-2016.

McClure C.D. and Jaffe D.A. (2018) Investigation of high ozone events due to wildfire smoke in an urban area. *Atmospheric Environment*, 194, 146-157, doi: 10.1016/j.atmosenv.2018.09.021, 2018/12/01/. Available at http://www.sciencedirect.com/science/article/pii/S1352231018306137.

McVey A., Pernak R., Hegarty J., and Alvarado M. (2018) El Paso ozone and $PM_{2.5}$ background and totals trend analysis. Final report prepared for the Texas Commission on Environmental Quality, Austin, Texas, by Atmospheric and Environmental Research, Inc., Lexington, MA, June. Available at https://www.tceq.texas.gov/assets/public/implementation/air/am/contracts/reports/da/582188176307-20180629-aer-ElPasoOzonePMBackgroundTotalsTrends.pdf.

Miller D., DeWinter J., and Reid S. (2014) Documentation of data portal and case study to support analysis of fire impacts on ground-level ozone concentrations. Technical memorandum prepared for the U.S. Environmental Protection Agency, Research Triangle Park, NC by Sonoma Technology, Inc., Petaluma, CA, STI-910507-6062, September 5.

National Weather Service Forecast Office (2020) Las Vegas, NV: general climatic summary. Available at https://www.wrh.noaa.gov/vef/lassum.php.

Pernak R., Alvarado M., Lonsdale C., Mountain M., Hegarty J., and Nehrkorn T. (2019) Forecasting surface O_3 in Texas urban areas using random forest and generalized additive models. *Aerosol and Air Quality Research*, 19, 2815-2826, doi: 10.4209/aaqr.2018.12.0464.

Sacramento Metropolitan Air Quality Management District (2011) Exceptional events demonstration for 1-hour ozone exceedances in the Sacramento regional nonattainment area due to 2008 wildfires. Report to the U.S. Environmental Protection Agency, March 30.

Simon H., Baker K.R., and Phillips S. (2012) Compilation and interpretation of photochemical model performance statistics published between 2006 and 2012. *Atmos. Environ.*, 61, 124-139, doi: 10.1016/j.atmosenv.2012.07.012.

Simoneit B.R.T., Schauer J.J., Nolte C.G., Oros D.R., Elias V.O., Fraser M.P., Rogge W.F., and Cass G.R. (1999) Levoglucosan, a tracer for cellulose in biomass burning and atmospheric particles. *Atmos. Environ.*, 33, 173-182.

Simoneit B.R.T. (2002) Biomass burning - a review of organic tracers for smoke from incomplete combustion. *Applied Geochemistry*, 17, 129-162.

Solberg S., Walker S.-E., Schneider P., Guerreiro C., and Colette A. (2018) Discounting the effect of meteorology on trends in surface ozone: development of statistical tools. Technical paper by the European Topic Centre on Air Pollution and Climate Change Mitigation, Bilthoven, the Netherlands, ETC/ACM Technical Paper 2017/15, August. Available at

https://www.eionet.europa.eu/etcs/etc-atni/products/etc-atni-reports/etcacm_tp_2017_15_discount_meteo_on_o3_trends.

Solberg S., Walker S.-E., Guerreiro C., and Colette A. (2019) Statistical modelling for long-term trends of pollutants: use of a GAM model for the assessment of measurements of O_3, NO_2 and PM. Report by the European Topic Centre on Air pollution, transport, noise and industrial pollution, Kjeller, Norway, ETC/ATNI 2019/14, December. Available at https://www.eionet.europa.eu/etcs/etc-atni/products/etc-atni-reports/etc-atni-report-14-2019-statistical-modelling-for-long-term-trends-of-pollutants-use-of-a-gam-model-for-the-assessment-of-measurements-of-o3-no2-and-pm-1.

Texas Commission on Environmental Quality (2021) Dallas-Fort Worth area exceptional event demonstration for ozone on August 16, 17, and 21, 2020. April. Available at https://www.tceq.texas.gov/assets/public/airquality/airmod/docs/ozoneExceptionalEvent/2020-DFW-EE-Ozone.pdf.

U.S. Census Bureau (2010) State & County QuickFacts. Available at http://quickfacts.census.gov/qfd/states/.html.

U.S. Environmental Protection Agency (2016) Guidance on the preparation of exceptional events demonstrations for wildfire events that may influence ozone concentrations. Final report, September. Available at www.epa.gov/sites/production/files/2016-09/documents/exceptional_events_guidance_9-16-16_final.pdf.

U.S. Environmental Protection Agency (2020) Green Book: 8-hour ozone (2015) area information. Available at https://www.epa.gov/green-book/green-book-8-hour-ozone-2015-area-information.

Wigder N.L., Jaffe D.A., and Saketa F.A. (2013) Ozone and particulate matter enhancements from regional wildfires observed at Mount Bachelor during 2004–2011. *Atmos. Environ.*, 75, 24-31, doi: 10.1016/j.atmosenv.2013.04.026, August. Available at http://www.sciencedirect.com/science/article/pii/S1352231013002719.

Wood S. (2020) Mixed GAM computation vehicle with automatic smoothness estimation. Available at https://cran.r-project.org/web/packages/mgcv/mgcv.pdf.

Wood S.N. (2017) *Generalized additive models: an introduction with R*, 2nd edition, CRC Press, Boca Raton, FL.

Zhang L., Lin M., Langford A.O., Horowitz L.W., Senff C.J., Klovenski E., Wang Y., Alvarez R.J., II, Petropavlovskikh I., Cullis P., Sterling C.W., Peischl J., Ryerson T.B., Brown S.S., Decker Z.C.J., Kirgis G., and Conley S. (2020) Characterizing sources of high surface ozone events in the southwestern US with intensive field measurements and two global models. *Atmospheric Chemistry & Physics*, 20, 10379-10400, doi: 10.5194/acp-20-10379-2020. Available at https://acp.copernicus.org/articles/20/10379/2020/acp-20-10379-2020.pdf.